UNIVERSITY OF SOUTHAMPTON

A MODEL OF INTEGRATIVE FEEDBACK AND HOMEOSTASIS IN LIPID BIOSYNTHESIS

JASON BEARD B.Sc. (Hons)

THESIS SUBMITTED FOR THE DEGREE OF DOCTOR OF PHILOSOPHY

FACULTY OF SCIENCE

DEPARTMENT OF CHEMISTRY

MARCH 2003

UNIVERSITY OF SOUTHAMPTON

ABSTRACT

FACULTY OF SCIENCE

CHEMISTRY

Doctor of Philosophy

A MODEL OF INTEGRATIVE FEEDBACK AND HOMEOSTASIS IN LIPID BIOSYNTHESIS

by Jason Beard

Cell membranes exhibit a high degree of species complexity, arising from lipid headgroup and hydrocarbon chain diversity. It has long been known that these lipid species are under control, but the processes that drive this control remain elusive. Recently, it was reported that CTP:phosphocholine cytidylyltransferase (CCT), an extrinsic membrane protein that catalyses a rate-limiting step in the synthesis of phosophatidylcholine (PC) lipids, is controlled by the elastic energy stored in the membranes with which it associates (Attard, GS *et al* (2000) Proc. Natl. Acad. Sci. USA 97, 9032-9036), a property also known as the membrane torque tension (MTT). Furthermore, the literature on the lipid requirements of the enzymes of phospholipid biosynthesis suggests that control by the MTT may be a general characteristic of these networks. This has led to the proposal that the property under homeostatic control is the MTT. This could ensure maintenance of the membrane integrity and provide a mechanism for a non-specific physical integrative feedback signal.

In order to test this hypothesis, a model of the membrane biosynthesis network of eukaryotic cells has been developed to predict the effects of the enzymes of phospholipid biosynthesis on the MTT and to correlate this with the reported lipid dependence. The predicted locations of these feedback points are in excellent agreement with experimental observations of lipid activation. The model is also used to investigate the effects of introducing integrative feedback, based on the MTT, at various points in the network. It is found that feedback at the CCT reaction dramatically increases robustness. Furthermore, only a few feedback loops are necessary to produce a highly robust network.

Contents

List of Figures

List of Tables

List of Equations

Acknowledgements

Firstly, I must thank my supervisor George Attard for his committed assistance, enthusiasm and seemingly unending patience with me.

I would like to thank all of the Attard group, past and present, particularly Matt Cheetham for his useful discussions, suggestions and proof reading. Thanks must also go to Marcus (for the 14 mile walk to the Golden Gate Bridge and the philosophical input), Toby (for not dismantling my computer) and John & Alan (for my basement lab apprenticeship).

Thanks to Tara (for understanding that 3 months can easily become 3 years) to John & Rich (for the F-Block hospitality and the Blackberry Terrace years) and to Kristian (for providing an excuse to watch rubbish TV). Also to Jason, Geoff and Dave (for constantly reminding me that there is more to life than being a student: caffeine, alcohol and curry as far as I can tell).

Finally, I am indebted to my parents, without whose unconditional support none of this would have been possible.

Abbreviations

ζ (zeta)	Critical Packing Parameter
λ (lambda)	The Torque Parameter (a proxy for the torque tension)
σ (sigma)	The Modulation Coefficient (for enzyme activity with feedback)
τ (tau)	Bilayer Stress
ATL	Anti Tumour Lipid
ATP	Adenosine triphosphate
c_1, c_2	Coefficients of σ
CCT	CTP:phosphocholine Cytidylyltransferase EC 2.7.7.15
c_{ij}	Stoichiometric Coefficient
CL	Cardiolipin
CMC	Critical Micelle Concentration
CNR	Custom Numerical Routine
CPP	Critical Packing Parameter
CPT	Choline phosphotransferase EC 2.7.8.2
CTP	Cytidine Triphosphate
DAG	Diacylglycerol
DGK	Diacylglyerol kinase
DNA	Deoxyribonucleic Acid
DOPC	Dioleoylphosphatidylcholine
DOPE	Dioleoylphosphatidylethanolamine
EC	Enzyme Commision numbers assigned by IUPAC-IUBMB
ECT	CTP:ethanolamine cytidylyltransferase EC 2.7.7.14
EPT	Ethanolamine phosphotransferase EC 2.7.8.1
ER	Endoplasmic Reticulum
ET-18-OMe	1-O-octadecyl-2-O-methyl-rac-glycerol-3-phosphocholine
g3p	Glycerol-3-phosphate
g3pACT	Glycerol-3-phosphate acyltransferase EC 2.3.1.15
GUI	Graphical User Interface
H_I	Normal topology Hexagonal phase
H_{II}	Inverse topology Hexagonal phase
IUB	International Union of Biochemistry
IUPAC	International Union of Pure and Applied Chemistry
J(R1)	Flux through reaction 1
k(R1)	Rate coefficient for reaction 1
LPA	Lyosphosphatidic acid
LPC	Lysophosphatidylcholine
LPE	Lysophosphatidylethanolamine
LPS	Lysophosphatidylserine
L_α	Lamellar Phase

MCA	Metabolic Control Analysis
MTT	Membrane Torque Tension
N_{enz}	Number of enzymes
N_{met}	Number of metabolites
ODE	Ordinary Differential Equation
PA	Phosphatidic acid
PAP	PA phosphohydrolase EC 3.1.3.4
PC	Phosphatidylcholine
PE	Phosphatidylethanolamine
PEMT	Phosphatidylethanolamine N-methyltransferase EC 2.1.1.17
PG	Phosphatidylglycerol
PI	Phosphatidylinositol
PIP	Phosphatidylinositol 4-phosphate
PIP_2	Phosphatidylinositol 4,5-biphosphate
PKC	Protein Kinase C EC 2.7.1.37
PLA_2	Phospholipase A_2 EC 3.1.1.15
PLC	Phospholipase C EC 3.1.4.3
PLD	Phospholipase D EC 3.1.4.4
PS	Phosphatidylserine
PSD	Phospatidylserine decarboxylase EC 4.1.1.65
PSS I	Phosphatidylserine synthase I
PSS II	Phosphatidylserine synthase II EC 2.7.8.8
Px, LPx	PC or PE or PS etc, LPC or LPE or LPS etc.
R1	Reaction 1
R1(λ-)	Reaction 1 acts to decrease the torque parameter.
R1(I)	Inverse Feedback applied at reaction 1
R1(N)	Normal Feedback applied at reaction 1
R1(TL+)	Reaction 1 acts to increase the total lipid
REF	Row-Echelon Form (of a matrix)
RER	Rough Endoplasmic Reticulum
RREF	Reduced Row-Echelon Form (of a matrix)
S_i	Name/concentration of a variable metabolite
SM	Sphingomyelin
StN	Stoichiometric Network
Total Lipid	Total concentration of lipid species
TSS	Target Steady State
type 0 lipid	Favouring lamellar phase
type I lipid	Favouring positive spontaneous curvature (away from water)
type II lipid	Favouring negative spontaneous curvature (towards water)
X_i	Name/concentration of a clamped metabolite

Homeostasis in Biomembranes

1

Contents

1.1 Cell Membranes

Cell membranes, often referred to as biomembranes, are some of the most commonly occurring structures in both animal and plant cells. Examples include the plasma membrane that surrounds the cell, forming a part of the cell wall and constituting a barrier between the intra and extra cellular regions. The nucleus, mitochondria and Golgi apparatus are all surrounded by biomembranes that separate these specialised organelles from the cytosolic environment. The endoplasmic reticulum (ER) is a membrane that acts as the principal site of phospholipid biosynthesis. A schematic of a cell is shown in figure 1.01 (Roberts 1976, p.18) with details of the membrane and the endoplasmic reticulum.

Biomembranes can be thought of as complex amphiphilic mixtures. They are primarily bilayer structures, with localised areas of more complex aggregate geometries. Cell membranes are characterized by a high degree of species complexity that arises from a combination of lipid headgroup diversity and hydrocarbon chain variation; some of the main phospholipid species are shown by headgroup classification in figure 1.02. Further details of phospholipid nomenclature may be found in the literature (Silvius 1993). Biological membranes contain many different lipids (phospholipids and glycolipids) as well as steroids such as cholesterol and other hydrophobic and amphiphilic molecules, including proteins. Embedded into the cell membrane are proteins of two varieties: Peripheral or extrinsic proteins

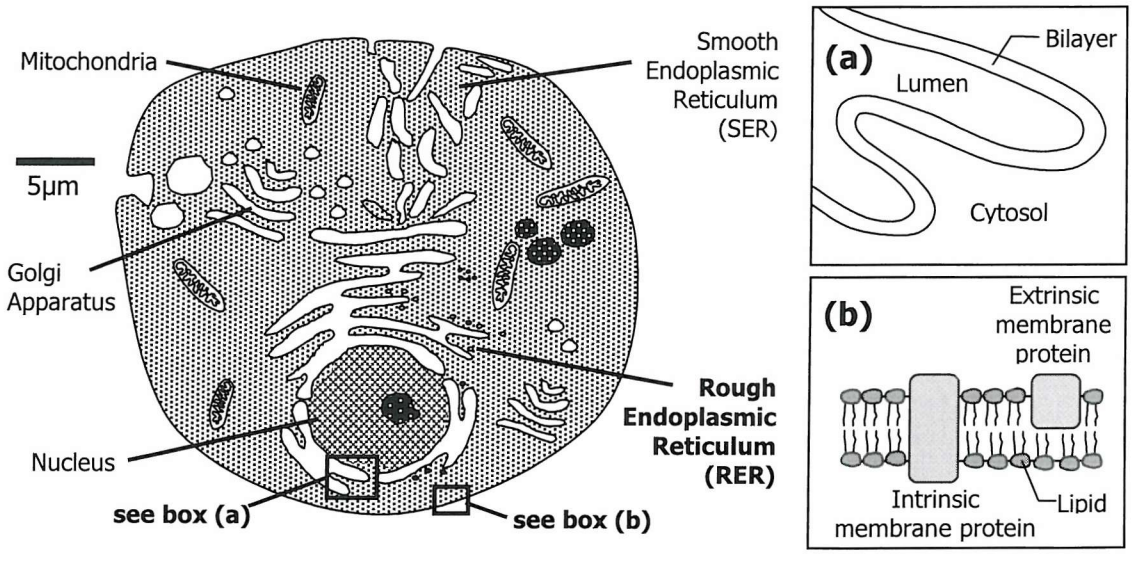

Figure 1.01: Schematic diagram of a generalised eukaryotic cell: with details showing
(a) The bilayer structure of the endoplasmic reticulum.
(b) Intrinsic (membrane spanning) and extrinsic (membrane associated) proteins.

are attached to only one membrane surface, integral or intrinsic proteins span the lipid bilayer.

The membrane lipids are present in diverse proportions in different biomembranes (Karp 1984, p.145). The difference in lipid composition of individual biomembranes suggests that the function of the membrane is related to its composition. Crucially, cell membranes contain a mixture of lipids which, when isolated, are found not to form bilayer phases (Cullis *et al.* 1996; Tate *et al.* 1991; Yeagle 1989). Phosphatidyl-ethanolamines, for example, are present as one of the major lipid components in biomembranes, but are type II lipids and therefore when isolated form H_{II} phases. Additionally, several membrane lipids present at very low concentrations are integral components of intracellular signalling pathways. Furthermore, studies have shown that the distribution of lipids and proteins in the cell membrane is asymmetric (Lodish 1979; Rothman & Lenard 1977). There is therefore evidence of a high degree of control over membrane lipid composition, including effects on cell division and survival (Kent 1997). It has been known for many years that many of the lipid species are under control but the functional parameters that drive this control have remained elusive. Questions that arise include, what mechanisms are responsible for the control of membrane lipid composition and, more specifically, what is the homeostatically controlled property of membranes? Candidates for this include lipid composition, total lipid content or some other factor relating to composition.

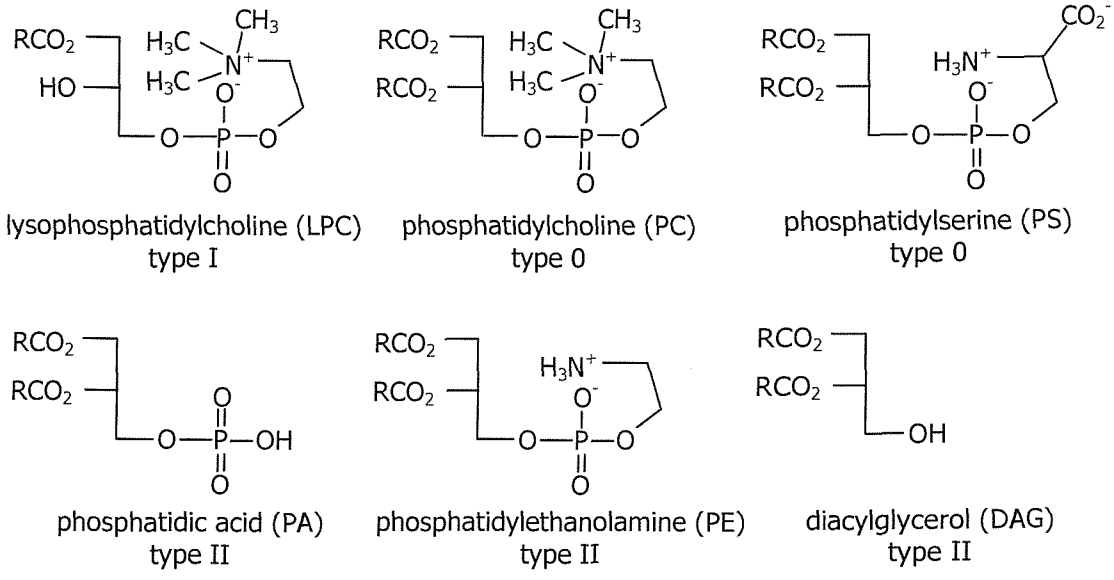

Figure 1.02: Phospholipids of eukaryotic biomembranes and their amphiphile classifications.

1.2 CCT and Phospholipid Biosynthesis

The membrane proteins responsible for lipid biosynthesis represent important machinery in the control of membrane composition. Examination of phospholipid biosynthetic enzyme regulation can therefore lead to clues about the mechanisms that ensure the observed homeostasis in the membrane.

Recently, it was reported that CTP:phosphocholine cytidylyltransferase (CCT), an important enzyme in phospholipid biosynthesis, is modulated by the elastic energy stored in the membrane with which it associates (Attard *et al.* 2000). The origins of the stored elastic energy are discussed later (in section 1.4). Here the importance of CCT in lipid biosynthesis is examined. CCT is an extrinsic membrane protein that mediates a reaction regarded as the rate-limiting step of the CDP-choline pathway for PC biosynthesis.

1.2.1 The CDP-choline pathway

In mammals the CDP-choline pathway is the predominant pathway for PC biosynthesis (Kent 1995); in most mammalian cells the CDP-choline pathway is the exclusive route of PC production. Bacteria produce PC exclusively by methylation of phosphatidylethanolamine (PE), using phosphatidylethanolamine N-methyltransferase (PEMT). However, in mammals significant amounts of PC are synthesized from PE only in liver cells (Kent 1997). There is also evidence that PEMT cannot substitute for the CDP-choline pathway (Waite & Vance 2000).

The synthesis of PC is significant as it is the major lipid constituent of cell membranes, representing about 50% of total phospholipids (Tronchere *et al.* 1994). PC is important not only as the most abundant membrane phospholipid, but also as the precursor to the other major phospholipid constituents including phosphatidyl-ethanolamine (PE) and phosphatidylserine (PS). Thus, regulation of PC biosynthesis plays a significant role in the accumulation of membrane phospholipids, which is critical for the production of new membrane during the S phase of the cell cycle (Jackowski 1994). Control of this pathway has a major influence on the membrane. Yet while the phospholipid biosynthesis pathways have been known for decades, their regulation is an area of considerable debate.

1.2.2 The Role of CCT

CCT catalyses the addition of cytidine triphosphate (CTP) to phosphocholine (Pcho), producing CDP-choline (CDPcho). This then reacts with diacylglycerol (DAG) to form phosphatidylcholine (PC), as shown in figure 1.03. The CCT mediated reaction has been recognized for 20 years as the rate limiting and regulatory step of the CDP-choline pathway (Kent 1995) (Feldman *et al.* 1978).

The activity of CCT is modulated by its interaction with lipid bilayers (Kent 1997). CCT has long been known to reside in two distinct intracellular pools: soluble and membrane associated (Jamil *et al.* 1993). The membrane bound form is mainly associated with the rough endoplasmic reticulum (RER) of cells, where the majority of phospholipid biosynthesis occurs. Studies have shown that the soluble pool is a reservoir of inactive enzyme; CCT activity is therefore thought to be modulated, both in vitro and in vivo, by reversible membrane association and concomitant activation of pre-existing enzyme (Bladergroen *et al.* 1998). CCT binds to membranes through a section of 11 amino acid residues. Model peptide studies show that, upon binding to a membrane, the conformation of this section changes from a random coil to an amphipathic helical structure (Dunne *et al.* 1996). This results in a conformation change causing increased activity through increased affinity for the CDP-choline substrate.

Attard *et al.* have proposed a model in which the translocation of CCT to the membrane is driven by relief of the stored elastic energy that is achieved (Attard *et al.* 2000). The remainder of this chapter looks at the origins of stored elastic energy in bilayers before returning to examine the significance and implications of its role in the regulation of phospholipid biosynthesis through the modulation of CCT activity and the hypothesis that emerges regarding the importance of the stored elastic energy in the control of the composition of cell membranes.

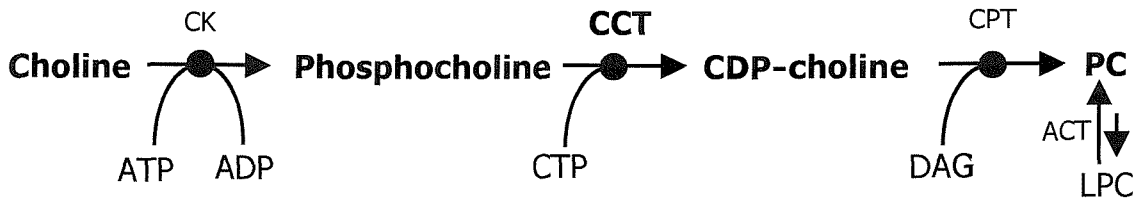

Figure 1.03: The CDP-choline pathway for the biosynthesis of PC.
CK = choline kinase, CCT = CTP: phosphocholine cytidylyltransferase, CPT = CDP-choline:1,2-diacylglycerol cholinephosphotransferase, ACT = Lyso-PC acyltransferase.

1.3 Aggregation and the Origin of Stored Elastic Energy

Despite the apparently overwhelming complexity of cell membranes, their structure may be rationalised, at least qualitatively, using the models of amphiphile aggregation that follow. The details of lipid polymorphism and discussion of spontaneous curvature outlined here provide an understanding of the origins of the stored elastic energy.

1.3.1 Amphiphilic Properties of Phospholipids

Phospholipids contain both hydrophobic and hydrophilic moieties as shown in figure 1.04. This property causes lipids to exhibit amphipathic behaviour. When an amphiphile is mixed with water, three types of behaviour can be observed. At low concentrations, the amphiphiles exist as a solution of monomers. As the concentration is increased, these monomers aggregate into micelles. The concentration at which this occurs is known as the critical micelle concentration (CMC). As the concentration of the amphiphile in water increases further, the micelles increase in number and size. Eventually it is favourable for micelles to fuse and the amphiphiles exhibit lyotropic liquid crystal phase behaviour. The next section examines the causes of micelle formation. This is followed by a discussion of the lyotropic liquid crystal phases, aggregate curvature and phase sequences.

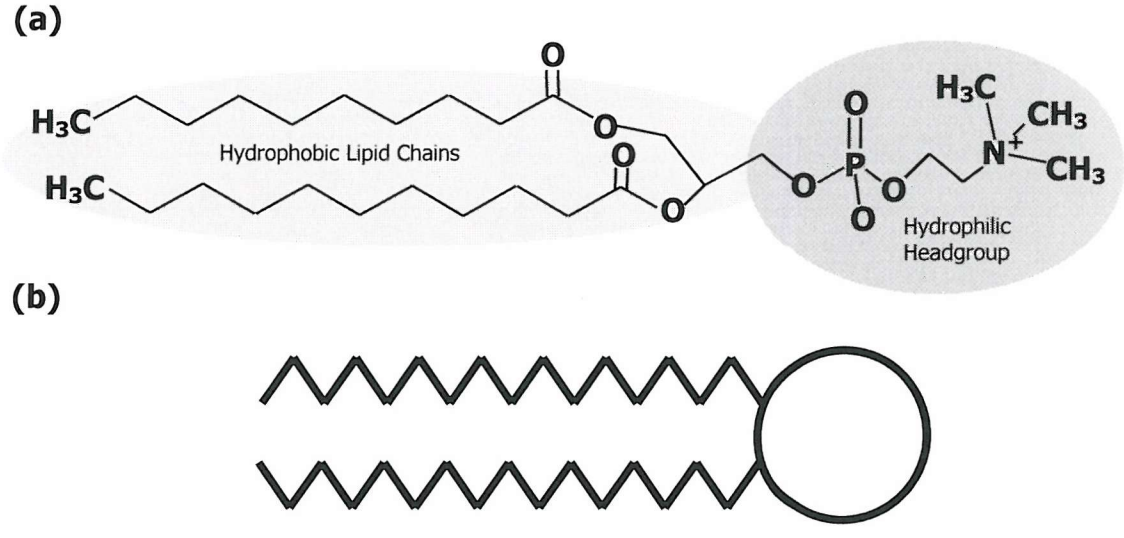

Figure 1.04: The basic structure (a) and schematic representation (b) of a phospholipid. The molecule is a phosphatidylcholine lipid with a hydrophilic choline headgroup and two hydrophobic hydrocarbon chains.

1.3.2 Hydrophobic Effects - Micelles

Micelles are aggregate structures of lipids, see figure 1.05, which are formed at concentrations above the CMC. Micelle formation minimises the energetically unfavourable contact between the hydrophobic areas of the amphiphile and water.

The origin of the hydrophobic effect is essentially entropic. The enthalpy of formation (ΔH) of micelles is an endothermic process of roughly 1 kJ per mol of lipid (Atkins 1994, p973). The change in Gibbs free energy ($\Delta G = \Delta H - T\Delta S$) for any spontaneous process must be negative. Micelles form readily at concentrations above the CMC, so the entropic effects must dominate and the entropic contribution ($T\Delta S$) must be positive, i.e. there must be a net increase in disorder upon aggregation. Indeed, the entropy of formation of micelles has been determined experimentally as ~140 J K^{-1} mol^{-1}. This seemingly counter-intuitive decrease in order upon aggregation is easily understood by examining what happens to the bulk solution.

Understanding the origin of the net increase in disorder brought about by micelle formation requires consideration of the structures formed by water surrounding hydrocarbon. When amphiphiles are present in solution as monomers, water surrounds the hydrocarbon chains and forms an ordered clathrate cage. In this arrangement, each water molecule is hydrogen bonded to four neighbouring water molecules. In bulk water, there is less hydrogen bonding, therefore the clathrate structure is a more ordered state. The formation of micelles results in a net increase in disorder, due to the loss of the solvation shells surrounding the hydrocarbon chains. This entropic consideration is the origin of the hydrophobic effect, which drives the aggregation of hydrophobic groups in biological systems (Israelachvili 1992, p.341-365).

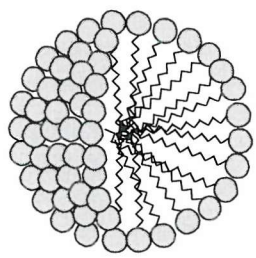

Figure 1.05: Normal topology micelles.
The micelle is a spherical structure with the hydrophilic headgroups facing the aqueous domain.

1.3.3 Lyotropic Liquid Crystal Phases – Lipid Polymorphism

Further increase in the amphiphile concentration produces greater numbers of and larger micelles. At even higher amphiphile concentrations other aggregate geometries dominate, these are the *lyotropic liquid crystal phases* (liquid crystals come in two basic classifications: *thermotropic* and *lyotropic*: the phase transitions of thermotropic liquid crystals depend on temperature, while those of lyotropic liquid crystals depend on both temperature and concentration). The transition to a lyotropic liquid crystal phase occurs because, as the concentration of micelles in solution increases, the spacing between the micelles decreases. Eventually, it is energetically favourable for the micelles to fuse to form a lyotropic liquid crystal phase.

There are four main types of lyotropic liquid crystal phase morphology; these are the micellar cubic, hexagonal, bicontinuous cubic and lamellar phases shown in figure 1.06. The fluid lamellar phase, or bilayer phase, is recognisable as similar to the structure of biological membranes.

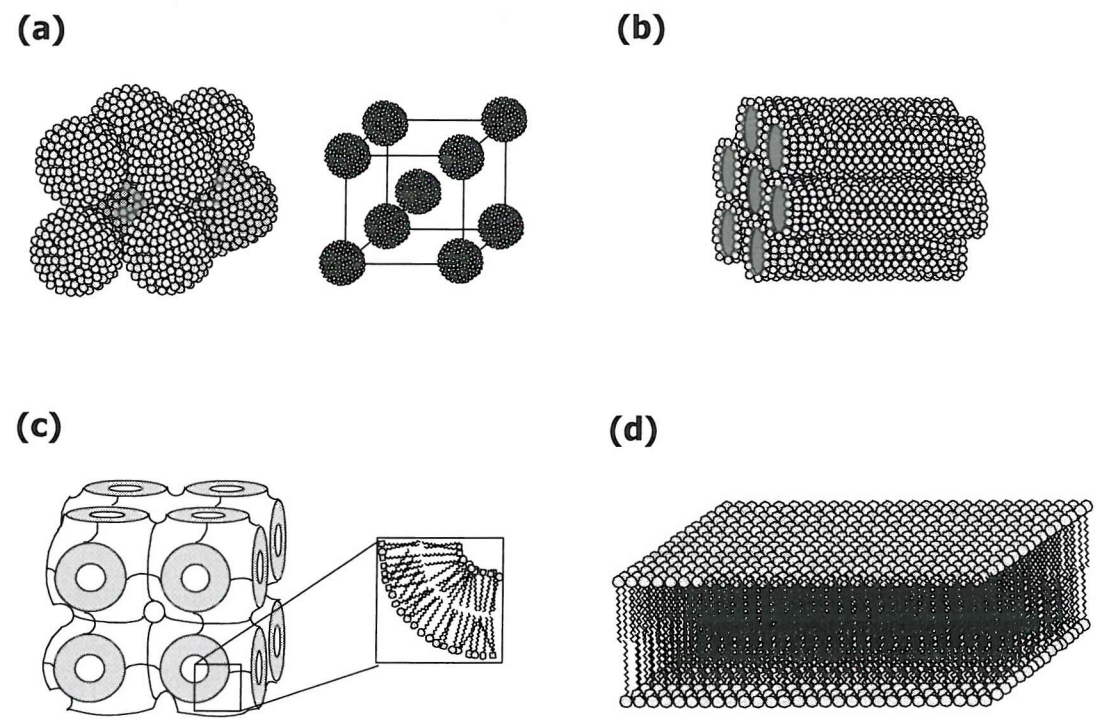

Figure 1.06: Lyotropic liquid crystal phases.
(a) Micellar Cubic, I_1. **(b)** Hexagonal, H. **(c)** Bicontinuous Cubic. **(d)** Lamellar, L_α.

A. Curvature of the aggregate

As the concentration of amphiphile is increased, a phase sequence that characterises the amphiphile is observed; the phase sequence depends on the properties of the amphiphile and its micelles, since different micellar shapes aggregate to form different lyotropic liquid crystal phases. Normal topology spherical micelles, for example, form a micellar cubic phase (I_1), forming the hexagonal phase (H) at higher concentrations.

The type of micelles and the sequences can be rationalised by considering the curvature of the aggregate as defined in figure 1.07. The diagram shows the two radii of curvature R_1 and R_2, the principal curvatures (equations 1.01 and 1.02) and the definition of the Gaussian curvature and the mean curvature (equations 1.03 and 1.04). For the discussion of lyotropic liquid crystal phase sequences, the mean curvature is most useful.

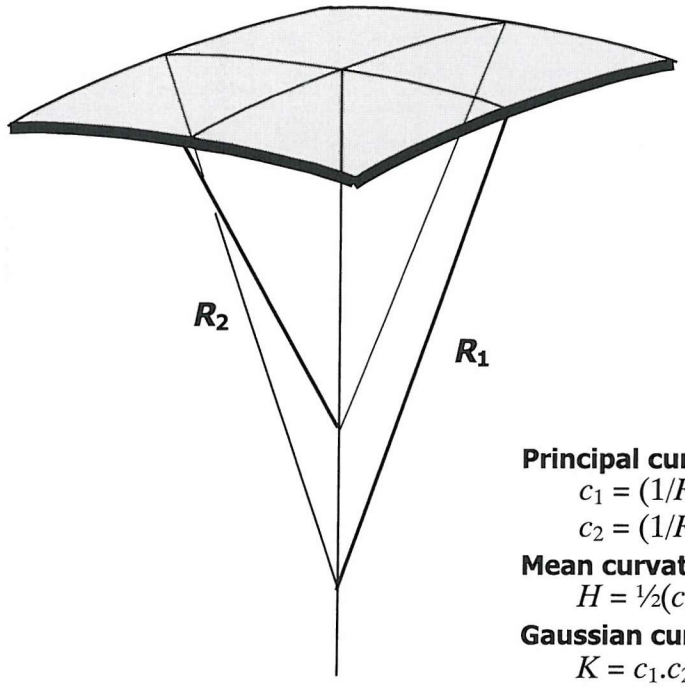

Principal curvatures:

$c_1 = (1/R_1)$ equation 1.01

$c_2 = (1/R_2)$ equation 1.02

Mean curvature (*H*):

$H = \frac{1}{2}(c_1+c_2)$ equation 1.03

Gaussian curvature (*K*):

$K = c_1.c_2$ equation 1.04

Figure 1.07: The principal radii of curvature R_1 and R_2 and the definitions of the principal, mean and Gaussian curvatures.

B. Lyotropic liquid crystal phase sequence

As the concentration of amphiphile is increased, different aggregate geometries are observed. The geometries of these aggregates are characterised by their different mean curvature (H). For positive mean curvature, the aggregation is described as *normal topology*, whilst for negative mean curvature aggregation is described as *inverse topology*.

The lyotropic liquid crystal phase sequence exhibited by an amphiphile can be predicted qualitatively from the mean curvature of its micelles. Figure 1.08 summarises the phase sequences for different mean curvatures. For an amphiphile that forms normal topology spherical micelles ($H = 1 / R$), the phase sequence exhibited upon increasing temperature will be:

spherical micelle $L_1^{(s)}$ → micellar cubic I_1 → hexagonal H → fluid lamellar L_α.

Whilst an amphiphile that forms vesicles ($H = 0$) will exhibit the phase sequence:

vesicular micelle $L_1^{(v)}$ → fluid lamellar L_α → inverse hexagonal H_{II}.

The particular importance of the fluid lamellar to inverse hexagonal phase transition as the origin of the stored elastic energy will be discussed after an examination of the models used to classify amphiphiles based on the lyotropic phases they favour.

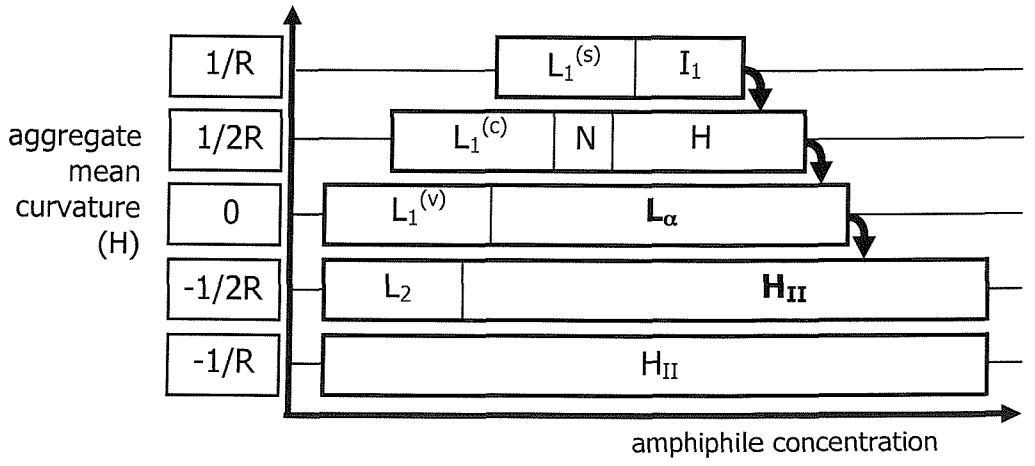

Figure 1.08: Schematic diagram showing the influence of the aggregate mean curvature and amphiphile concentration on the lyotropic liquid crystal phase sequence.
$L_1^{(s)}$ = spherical micellar solution, $L_1^{(c)}$ cylindrical micellar solution, I_1 = micellar cubic, N = nematic phase, H = normal hexagonal phase, $L_1^{(v)}$ = vesicular micellar solution, L_α = lamellar phase, L_2= inverse micellar solution and H_{II} = inverse hexagonal phase.

1.3.4 Models of Aggregation

As has been shown, phospholipids are amphiphilic species that form aggregates with varied topologies in aqueous solution. These structures are characterised by their spontaneous curvatures, which may be successfully explained by considering the geometry of, and forces between the monomers that make up the aggregates. The models presented here provide a basis for understanding the relationship between the characteristics of the constituent lipids and the spontaneous curvature. The two models to be discussed are the *critical packing parameter model* and the *lateral stress profile model.*

A. Critical Packing Parameter model

The *critical packing parameter*, which describes the shape of a monomer, can be used to semi-quantitatively predict the micelle morphology formed by an amphiphile. The critical packing parameter (ζ, zeta) is defined in equation 1.05 where v is the cylindrical volume, a_0 is the headgroup cross sectional area and l_c is the length of the hydrocarbon chain (in the all trans position) (Israelachvili 1992, p.367-394).

$$\zeta = v/a_0 l_c \qquad \text{equation 1.05}$$

The values of v and l_c may be estimated from equations 1.06 and 1.07, where n is the number of carbon atoms in the hydrocarbon chain.

$$v = (27.4 + 26.9n) \times 10^3 \text{ nm}^3 \qquad \text{equation 1.06}$$

$$l_c = (0.154 + 0.1265n) \text{ nm} \qquad \text{equation 1.07}$$

The critical packing parameter (ζ) is used to describe the micelle shapes formed as detailed in figure 1.09. For $\zeta = 1/3$ the molecule is considered conical, and spherical micelles are easily formed. If $\zeta = 3/1$ then the molecule is considered inversely conical, i.e. the hydrocarbon cross-section is larger than that of the headgroup. Here the formation of inverse micelles may be assumed.

The critical packing parameter model can be used to qualitatively predict the micellar geometries that an amphiphile will form (Eibl 1984; Hoffmann 1984). The method is not however quantitative; a_0 can vary with concentration, ionic strength and hydration.

For the scope of this work, the critical packing parameter model introduces the idea of 'shape', as illustrated in figure 1.09, which is a convenient way to describe and rationalise the behaviour of amphiphiles.

Shape	Critical Packing Parameter (ζ)	Structure Formed
	$\zeta < 1/3$	 Spherical Micelles
	$1/3 < \zeta < 1/2$	 Cylindrical Micelles
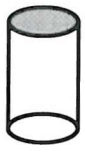	$1/2 < \zeta \leq 1$	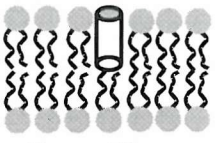 Planar Bilayers
	$\zeta > 1$	 Inverse Micelles

Figure 1.09: **The relationship of the critical packing parameter (ζ) to amphiphile shape and aggregate geometry.** The third column shows how the amphiphiles pack into the aggregates formed.

B. Lateral Stress Profile model

An alternative method for the rationalisation of lyotropic liquid crystal phase behaviour is the lateral stress model. The lateral stress model considers the forces between the monomers in an aggregate, rather than predicting aggregation using basic geometric considerations as in the critical packing parameter model.

The forces that act within a bilayer may be considered. On crossing from the aqueous domain into the headgroup region and through the hydrocarbon domains of a phospholipid bilayer, the lateral pressure varies depending on the distance from the water/hydrocarbon interface. The net headgroup interaction is a combination of attractive forces including hydrogen bonding and bridging ions, and repulsive forces such as steric and electrostatic interactions. The net tail interaction is also determined by the balance of attractive forces and repulsive steric effects. The forces are shown schematically in figure 1.10 (a) (Booth *et al.* 1997).

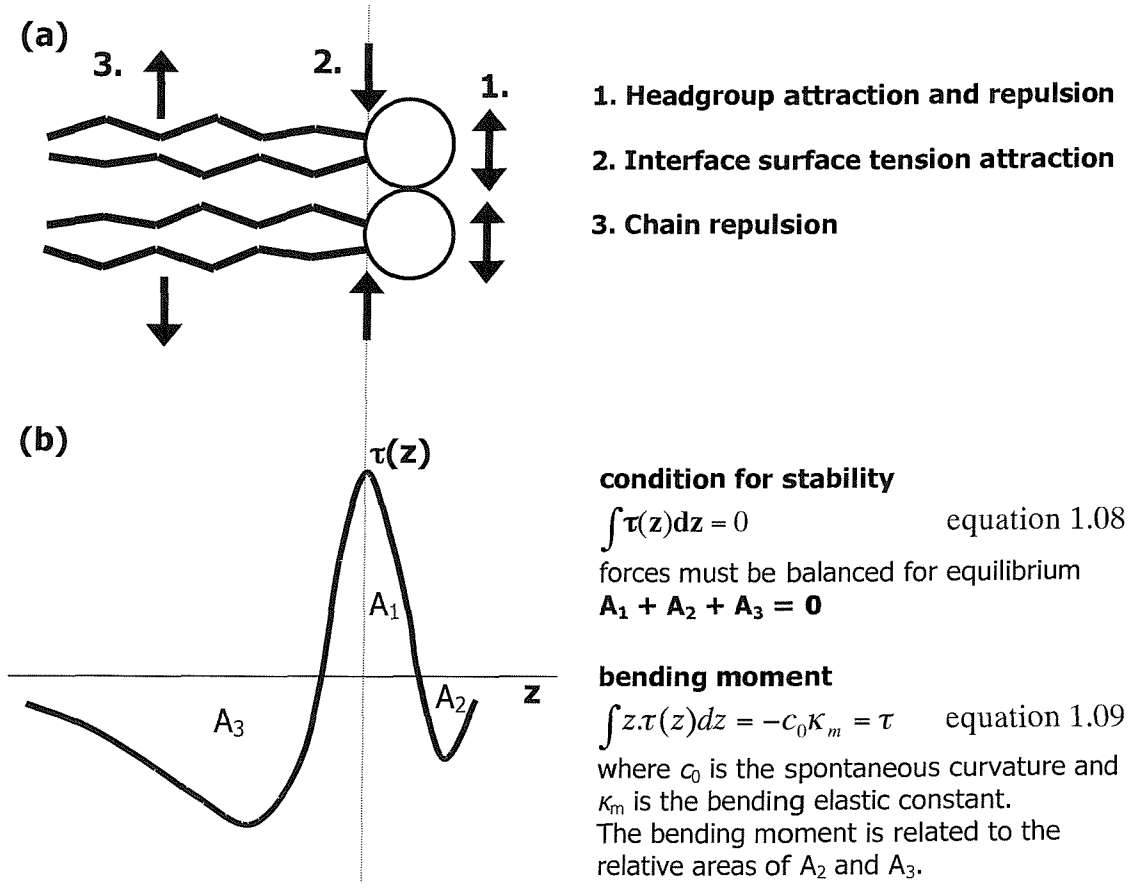

Figure 1.10. The lateral stress profile model:
(a) The forces between amphiphiles in a monolayer.
(b) An example lateral stress profile.

The lateral stress treatment models amphiphiles in a theoretical monolayer. Stress (τ) is equal to the negative pressure (–P). The lateral stress profile of an amphiphile in a monolayer is given by plotting the stress against the distance from the interface (z). An example is shown in the figure 1.10 (b). Examining the profile, three domains are apparent (A_1, A_2 and A_3). The stress profile may be rationalised by considering the forces in each region.

At the interface (A_1), there is a net negative pressure, which acts to minimise the area of the interface. Since the stress is the negative of pressure, the lateral stress at this interface is positive. In the headgroup region (A_2), electrostatic or steric repulsion push the headgroups apart, resulting in a positive pressure or negative stress. In some lipids, hydrogen bonding between headgroups can lead to a dramatic reduction in lateral stress. In the hydrocarbon domain (A_3), steric interactions between neighbouring chains push them apart and lead to a negative lateral stress.

The sum of the three areas must equal zero, this is the condition for stability as defined in equation 1.08. Of more interest is the bending moment (proportional to the spontaneous mean curvature), given by equation 1.09. This is in a simple way related to the relative areas of A_2 and A_3, the forces at the headgroup and within the hydrocarbon domain. Broadly speaking, if the areas A_2 and A_3 are equal in magnitude the leaflets of the aggregate have no tendency to bend. Unequal stresses lead to a desire to curve, either towards the aqueous domain producing an inverse topology phase or away from the aqueous domain producing a normal topology phase. The lyotropic liquid crystal phase sequences are thus determined by the stress profiles, which are dependent on the nature of the headgroup and the hydrocarbon chain characteristics.

The lateral stress method is, of course, dependent upon the measurement or calculation of the forces that determine the lateral stress profile. Computer simulations, which model the intermolecular interactions using statistical thermodynamics, can be used to supplement measurements (Israelachvili 1992, p.367-394). These details are beyond the scope of this work and the detailed thermodynamics of the lateral stress model may be found in the literature (Seddon 1996; Seddon 1990); here the model is presented since it helps rationalise the relationship between microscopic structure and the macroscopic phases observed.

C. Classification of amphiphiles into types

Predictions from the two models for the phase behaviour of amphiphiles have led to a simple classification system for amphiphiles. Lipids may be characterised as type I, type 0 or type II, as shown in figure 1.11. Type I amphiphiles favour normal topology phases and typically have a single hydrocarbon chain and a bulky headgroup. Type 0 amphiphiles are bilayer favouring and usually have two hydrocarbon chains and a large headgroup. Type II amphiphiles favour inverse topology phases and often have unsaturated chains and a small headgroup.

Monomer Shape	Amphiphile Classification	Examples
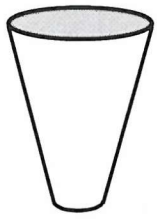	**Type I** Normal topology phases	Typically amphiphiles with a single alkyl chain and a large headgroup, e.g. lysophosphatidylcholine 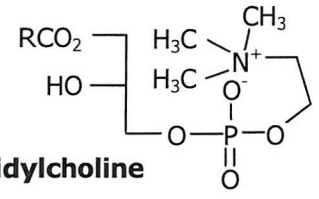 **lysophosphatidylcholine**
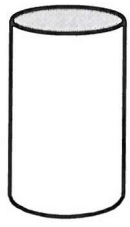	**Type 0** Bilayer phases	Typically amphiphiles with two alkyl chains (saturated) and a large headgroup, e.g. phosphatidylcholine 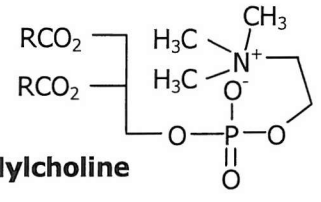 **phosphatidylcholine**
	**Type II** Inverse topology phases	Typically amphiphiles with two alkyl chains (often unsaturated) and a less bulky headgroup. e.g. phosphatidylethanolamine 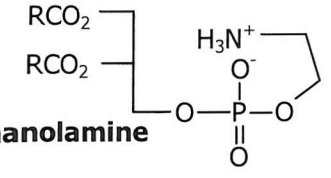 **phosphatidylethanolamine**

Figure 1.11: Amphiphile classification and details of typical structures.

1.3.5 Spontaneous Curvature

Figure 1.12 shows theoretical monolayers of type 0, type I and type II amphiphiles adopting their spontaneous curvatures (Seddon 1996). Positive curvature is defined as being away from water and negative curvature as towards the aqueous region. With the information on how amphiphiles prefer to curve, their accommodation into bilayers may now be considered.

1.3.6 The L_α to H_{II} Phase Transition

The discussion now focuses on the bilayer phase, as this is the relevant phase for considering cell membranes. The next aggregate in the phase sequence (see figure 1.08) is the H_{II} phase. Understanding the physics of mixed bilayers requires an understanding of the L_α to H_{II} phase transition. The L_α to H_{II} phase transition can be brought about by increasing the temperature. As the temperature is raised the increase in conformational disorder of the chains results in an increase in chain volume. An amphiphile may be type 0 at low temperatures, however at higher temperatures the increase in volume of the hydrocarbon chain may make it type II (with bilayers of mixed amphiphiles, changes in the mean hydrocarbon volume can also be brought about by varying the concentration of each amphiphile). At a given temperature, bilayers of amphiphiles with these properties will undergo a phase transition to the H_{II} phase. This phase transition occurs because, at this temperature, the total free energy of the H_{II} phase becomes lower than that for the L_α phase. However, prior to the phase transition, the increasing hydrocarbon splay must be accommodated in the bilayer arrangement.

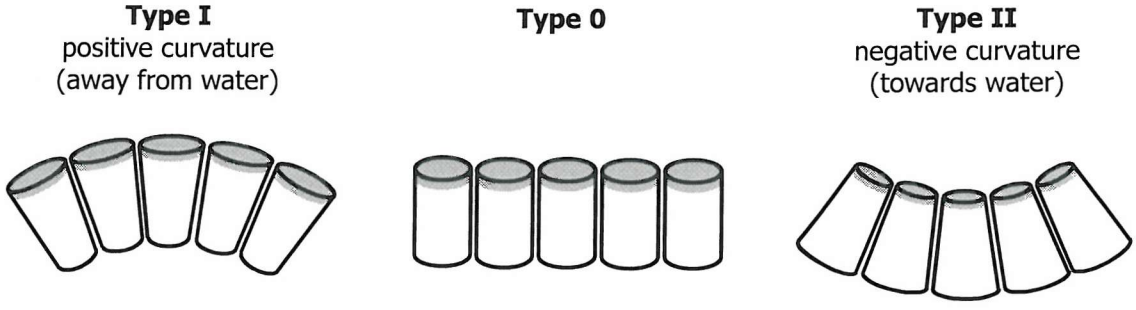

Figure 1.12: Spontaneous curvature.
The arrangements represent theoretical monolayers adopting their spontaneous curvatures.
The cylinders represent the shape of lipid molecules, with the headgroups shown by the shaded ends.

1.3.7 Frustration of Curvature – Membrane Torque Tension

Non-bilayer lipids may be accommodated within a bilayer prior to the L_α to H_{II} phase transition. The individual leaflets will have some desire to curve but not sufficient to induce the L_α to H_{II} phase transition. Therefore, the amphiphiles remain in the bilayer phase. If the monolayers were to adopt their spontaneous mean curvatures, there would exist a void in the hydrocarbon interior as shown in figure 1.13. Of course, this is precluded by the high-energy cost involved. The bilayer arrangement therefore constrains the monolayers to lie flat; the spontaneous curvature is frustrated, and the amphiphiles are accommodated by changes in the bilayer that affect the elasticity of the bilayer.

Changes in bilayer elasticity are rationalised by examining the adjustments to a bilayer that are necessary to equalise the cross-sectional areas of the headgroup and tail to allow the monomers to pack into the flat bilayer. For type II amphiphiles the tail area must be decreased, or the headgroup area increased. The effective headgroup cross-section of a type II amphiphile in a bilayer can be increased by stretching the bilayer. This decreases the chain repulsion and increases headgroup spacing, allowing more hydration and, in effect, increases the headgroup cross-section.

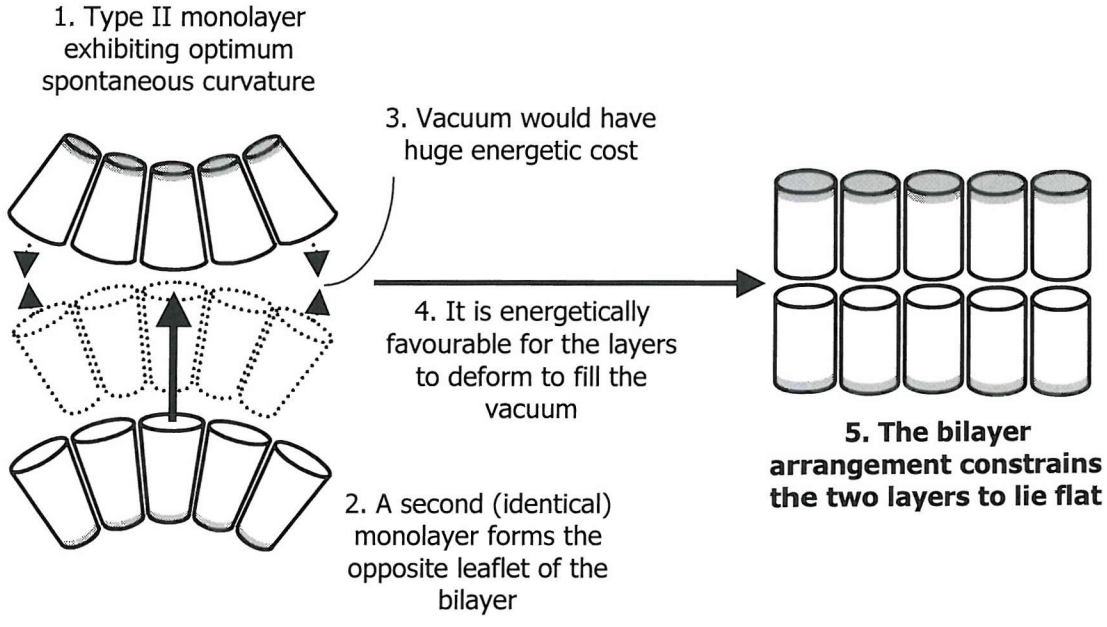

Figure 1.13: Frustration of curvature.
The bilayer arrangement constrains the two layers to lie flat.

For an ideal bilayer composed solely of type 0 amphiphiles, the torque tension is zero; there is no desire for curvature. In a frustrated bilayer, the desire for curvature results in a torque within the membrane. The stored elastic energy in a bilayer that is constrained to remain flat is therefore often called the *bilayer torque tension*, or the *membrane torque tension* (MTT) when discussing cell membranes. The bilayer torque tension is proportional to the spontaneous curvature of its constituent monolayers. However, it is also dependent on the mean curvature rigidity of the bilayer, which resists the spontaneous mean curvature. The relationship is shown in equation 1.10, where τ is the torque tension, κ_m is the mean curvature bending rigidity and c_o is the spontaneous curvature.

$$\tau = -\kappa_m.c_o \qquad \text{equation 1.10}$$

1.3.8 A Model System: Binary Mixtures of DOPC and DOPE

Examination of binary mixtures of PC and PE allows consideration of two of the main membrane phospholipids in more detail. PC and PE are species central to the model developed in this work. Discussion of this model system also serves to summarise the ideas presented so far.

The headgroup structures of dioleoylphosphatidylcholine (DOPC) and dioleoylphosphatidylethanolamine (DOPE) were shown in figure 1.02. When DOPC is mixed with water, it forms a lamellar (type 0) phase. In contrast, when DOPE is mixed with water, it forms an inverse hexagonal (type II) phase. The lateral stress profile can be used to account for these dramatic differences in the liquid crystalline behaviour of DOPC and DOPE. These two phospholipids are both two chain zwitterionic species but they differ in the cationic part of the headgroup: DOPC has a NMe_3^+ group and DOPE has a NH_3^+ group. The difference between these headgroups is the reason for the difference in the lateral stress profiles. The hydrogens of the NH_3^+ moiety of DOPE headgroups form hydrogen bonds to phosphate groups on neighbouring molecules. For DOPC with its NMe_3^+ group, there is no headgroup hydrogen bonding. In DOPE, the attractive hydrogen bonding interactions cause a reduction of lateral stress in the headgroup region, favouring negative spontaneous curvature, and resulting in the formation of an inverse hexagonal phase.

A model for cell membranes must consider systems that are in the lamellar phase, but contain lipids which when isolated form inverse topology structures. This situation can be illustrated by considering simple binary mixtures of DOPC and DOPE. As was stated in section 1.3.6, with bilayers of mixed amphiphiles changes in the stored curvature elastic stress can be brought about by varying the concentration of each amphiphile. Bilayer structures formed by DOPC (vesicles and lamellar phases) are of relatively low rigidity, with minimal stored elastic energy due to the small spontaneous curvature of DOPC. Addition of DOPE to DOPC changes the spontaneous curvature of each leaflet to more negative values; the addition of DOPE increases the desire of each leaflet to curve away from the other. These changes are summarised in figure 1.14. However, the desire of the leaflets to bend is frustrated by the presence of the opposing leaflet. This constraint means that the increase in spontaneous curvature, due to the change in the lipid composition, leads to an increase in the bilayer torque tension. An increase in the layer rigidity and thickness also occurs. Above a certain concentration, the strain on the layer will make it energetically favourable for the bilayer structure to breakdown. A phase transition to the H_{II} phase will occur, however this is not believed to occur in biomembranes under physiological conditions.

The DOPC + DOPE mixture described above is a good simple model for the membranes of the endoplasmic reticulum since cell membranes contain a mixture of lipids, which when isolated are found not to form bilayer phases. The situation in a membrane of the endoplasmic reticulum is of course much more complex than that in a model system. Nevertheless, the same basic arguments about lipid composition and spontaneous curvature that have been outlined above can be applied.

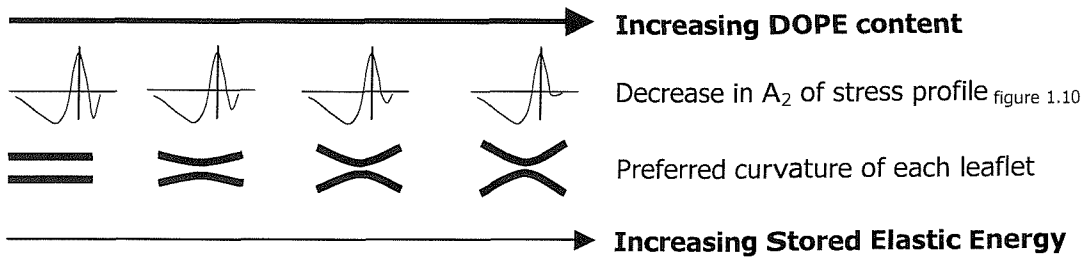

Figure 1.14: Effects on the spontaneous curvature of the addition of DOPE to DOPC bilayers. (stress profiles and preferred curvatures not to scale).

1.4 The Regulation of CCT Activity

Having examined the origins of the stored elastic energy, the discussion now returns to the regulation of CCT activity. First, the literature on CCT regulation is briefly reviewed for studies that have looked at the factors that may activate CCT. A model for the activation of CCT being driven by the stored elastic energy of the bilayer to which it partitions is then presented. Anti-tumour lipids (ATLs) are then discussed, as their method of action is believed to involve cell membrane targeted disruption of the CDP-choline pathway at the CCT reaction.

1.4.1 Previous Explanations of CCT Regulation

There have been many attempts to elucidate how the lipid composition of biomembranes modulates the binding of CCT and therefore its activity. Explanations have included hydrophobic and electrostatic interaction with phospholipids in the membrane and the alteration of phospholipid headgroup packing.

The alteration of headgroup packing theory (Cornell 1991b) relates the enzyme activity to the physical structure of the membrane according to the phospholipid headgroups. Crucially however, this does not explain inhibition by lysoPC, or it synthetic analogues (Boggs *et al.* 1995b), which share the same headgroup as PC.

Electrostatic interaction has also been suggested as the factor that determines the binding of CCT to membranes (Arnold & Cornell 1996; Cornell 1991a); anionic phospholipids in the membrane would be expected to attract cationic amino acid residues present in the amphipathic helix of CCT. However, this explanation does not account for the modulation of CCT activity by neutral lipids like DAG, which have minimal electrostatic effect on the membrane. DAG and lyso-PC are however of significance when examining the stored elastic energy.

The next section looks at a model for the modulation of CCT activity through translocation driven by the stored elastic energy. This model does not exclude that other factors, such as electrostatics, may make a contribution but simply explains how membrane torque tension can influence the binding and activity of CCT.

1.4.2 Model for CCT Regulation by the Stored Elastic Energy

Examination of the lipid structures reveals that the lipids that activate CCT are type II amphiphiles whilst the lipids that deactivate CCT are type I. The observation that type II lipids activate CCT has been pointed out previously (Jamil *et al.* 1993), however the physical origins of this have remained unclear. Attard *et al.* have shown that CCT activity is directly correlated with the membrane torque tension and presented a model for the activation of CCT by translocation to the membrane driven by the release of the stored elastic energy.

Figure 1.15 (overleaf) shows the dependence of binding of CCT on the torque tension of a monolayer. In (1) a monolayer of lipids with negative spontaneous curvature (represented by shading) is forced into a flat conformation as a leaflet of a bilayer (2) with a resultant increase in stored elastic energy (shown by darker shading). The partitioning of the amphipathic helical domain of CCT into the monolayer (3) allows the surrounding molecules to splay; the partitioning is driven by the release of the stored elastic energy. In (4) a different monolayer, with reduced negative spontaneous curvature, is forced flat (5), this conformation has a lower torque tension than (2). In (6) the tension relieved upon binding of CCT is less than (3) and fewer CCT molecules partition to the membrane.

The above explains the activation of CCT by type II lipids; deactivation by type I lipids occurs as the type I lipids reduce the membrane torque tension; there is then less driving force available for binding of CCT to the membrane. CCT present in the membrane is released by addition of type I amphiphiles, since they will partition readily and the release of the stored elastic energy facilitates the disassociation of CCT. The stored elastic energy model thus accounts for the reduction of CCT binding and activity by type I lipids. Therefore, the curvature elastic stress hypothesis explains both positive and negative regulation of CCT (Lykidis & Jackowski 2001), in contrast to previously proposed mechanisms that addressed only the stimulation of CCT by lipids (Arnold & Cornell 1996; Cornell 1991b).

The next section looks at anti tumour lipids as their action has been linked to disruption of CCT activity. They are of interest as part of the inspiration for this work and the discussion reinforces some of the points made so far.

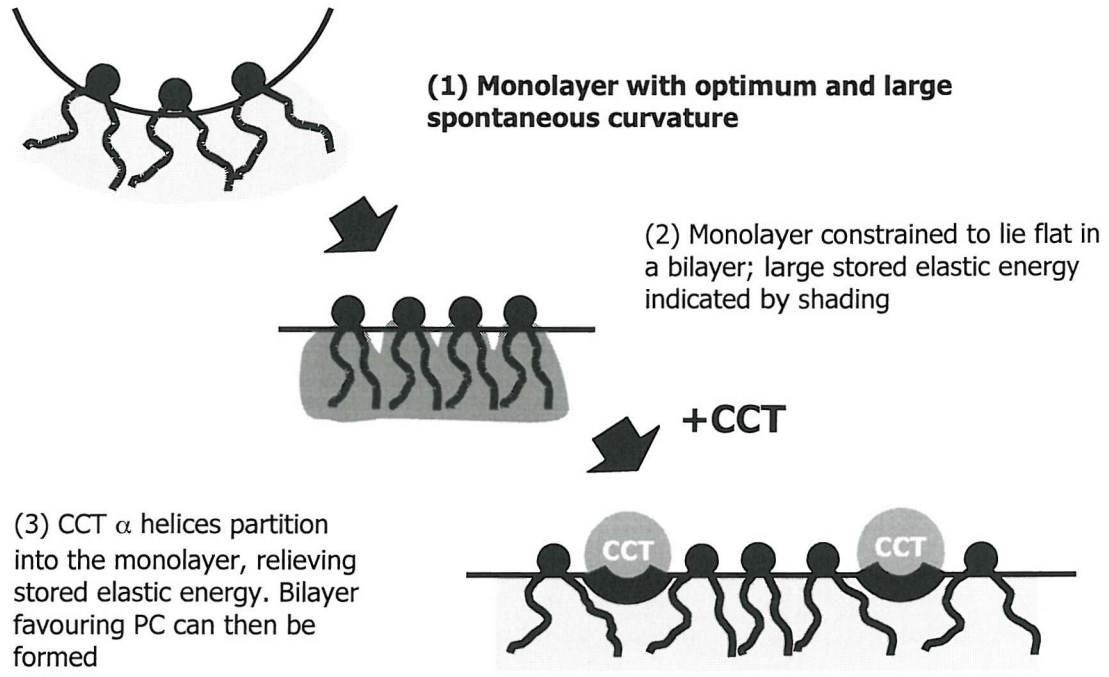

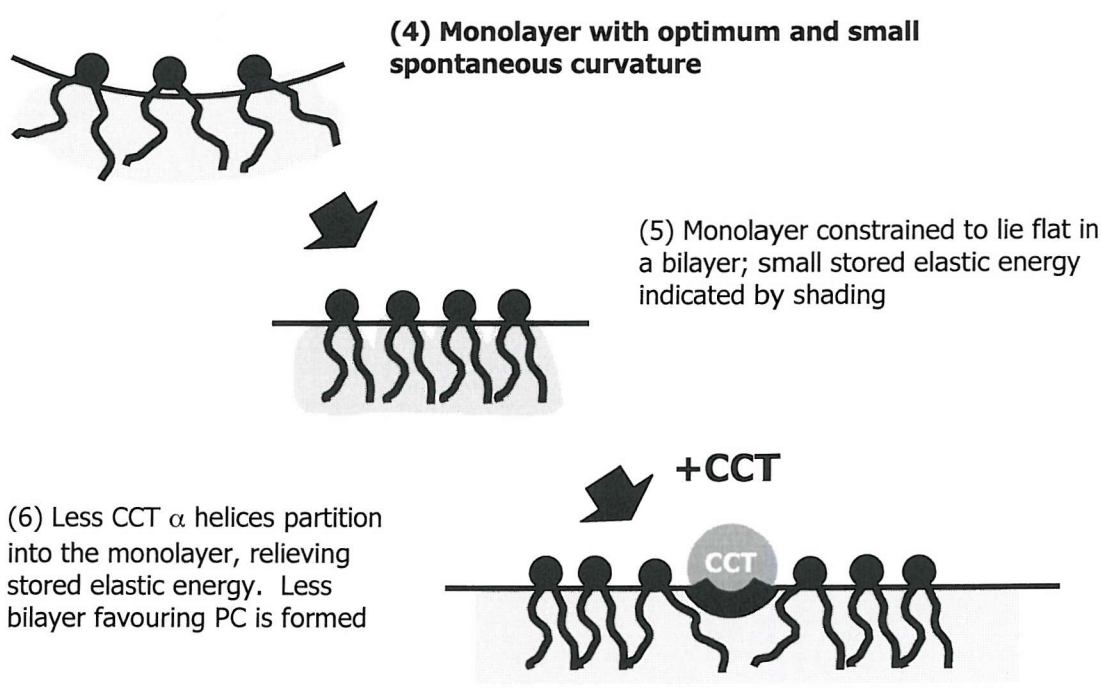

Figure 1.15: Model for the modulation of CCT by type I and II lipids (Attard *et al.* 2000)

1.4.3 Anti Tumour Lipids

Cancer is one of the most common terminal diseases in humans and its treatment is a huge area of scientific and medical research. In the developed world, one person in five dies from cancer and The World Health Organisation has estimated that the disease kills six million people each year (Rennie & Rusting 1996). The statistics show that the treatment of cancer is far from a routine procedure.

Synthetic anti tumour lipids (ATLs), also known as ether lipids, have emerged as effective agents in model systems and are currently undergoing clinical trials. There is significant interest in them since their mode of action appears to differ from that of the current DNA-interactive agents (Boggs *et al.* 1995b). ATLs appear to inhibit cell growth by blocking lipid synthesis. As will be described later, their site of action (Lohmeyer & Workman 1995) appears to be at the rough endoplasmic reticulum (RER). The effect of exposing cancer cells to ATLs is to arrest their growth (cytostasis), which is followed by cell death (apoptosis). Although ATLs are detergent molecules, the concentrations at which they are therapeutically active are significantly lower (by about two orders of magnitude) than those which lead to direct lysis of cells by detergent effects. Over the past four years, it has been shown that ATLs block CCT. Recently it was found that cytostatic activity is a general property of type I amphiphiles and this activity is not dependent on the detailed chemical structure of the headgroups. The unifying lipid type and the influence on a membrane bound protein suggest an importance of the ideas of membrane torque tension from the previous section. To understand how ether lipids act, and why they are important, it is essential to be aware of how tumours occur, grow and are treated.

A. Tumour formation

The human body is constructed from around 10^{13} cells, which are interdependent and regulate each others proliferation. Cells will typically only undergo cell division when appropriate, by following signals from their neighbours. A cancer cell, in contrast, operates independently of its neighbours and its proliferation is consequentially unchecked. There are many different cancers, but there are fundamental similarities in the development of all cancers; the unregulated proliferation, leading to tumour development is the strongest common motif. Tumour formation can result from the mutation of just one cell (Karp 1984). DNA in

the cells' genes contains the information required to build proteins that perform precise biological tasks. Mutations in the DNA result in the construction of altered proteins. The resultant deviation from regular protein activity may be sufficient to cause the cell to behave very differently. Gene types responsible for triggering and inhibiting cell growth are known to give rise to cancer when mutated, reflecting the importance of altered cell growth to the development of cancer. Mutated cells must also become disconnected from their neighbours and overcome the internal apoptosis mechanisms, which are designed to cause defective cells to self-terminate. If just one mutated cell goes unchecked by these controls, it can multiply rapidly and result in a tumour. Tumour advancement can disrupt organs and precipitate metastasis (the formation of secondary tumours in other locations), ultimately causing death.

B. Limitations of existing cancer treatments

Cancer in metastasis must be treated with a chemotherapy that does not require knowledge of the location of every cancerous cell. An ideal chemotherapeutic would target the disease without harm to the host. However, current drugs are not specific to cancer cells. The aim of treatment is to destroy the malignant cells with minimal effect on healthy cells, by careful dose control. The success of this exploits the fact that division of healthy cells is slow compared to cancer cells. Cell division is controlled by the cell cycle as shown in figure 1.16 (Jackowski 1996). The cycle is the same for healthy and tumour cells, but for cancer cells the period is much shorter. Conventional chemotherapeutics act directly on the DNA of cells causing cell destruction as the cell cycle is disrupted. Due to their rapid division, malignant cells are more vulnerable to chemotherapeutics.

C. Action and selectivity of ether lipids

DNA replication is not the only target for anticancer drugs. Targeting of the plasma membrane is a relatively new area of interest: in the late 1970's a class of compounds known as ether lipids were used as therapeutic agents (Berdel 1990). These compounds differ from existing therapies since they appear to act at the cell membrane. The biological properties of ether lipids were first exposed in the early 1960's when they were synthesised as analogues of lysophosphatidylcholine (lysoPC or LPC). Ether lipids were screened for activity against a range of diseases and some were found to selectively destroy human leukaemic cells (Westphal 1987).

The action and selectivity of ether lipids for cancer cells has not been fully explained. It has however been determined that partitioning into the plasma membrane is the initial method of ether lipid uptake. At high concentrations of 1-O-octadecyl-2-O-methyl-*rac*-glycerol-3-phosphocholine (ET-18-OME), leukaemic cells show significant plasma membrane damage (Noseda *et al.* 1989) confirming the cell membrane as the target (cytolytic action is prevented with ether lipid concentrations below its CMC). With regard to the selectivity for malignant cells, it is generally accepted that the different membrane composition of cancer cells is an important factor. The alteration of membrane cholesterol content has been shown to modulate ether lipid cytotoxicity, leading to the view that physical membrane properties like fluidity and permeability may determine the sensitivity to ether lipids (Principe & Braquet 1995). In addition, transformed cells typically exhibit amplified rates of PC metabolism placing an increased demand on the PC biosynthetic pathway and making the cells more sensitive to the inhibition of the CDP-choline pathway (Lykidis & Jackowski 2001).

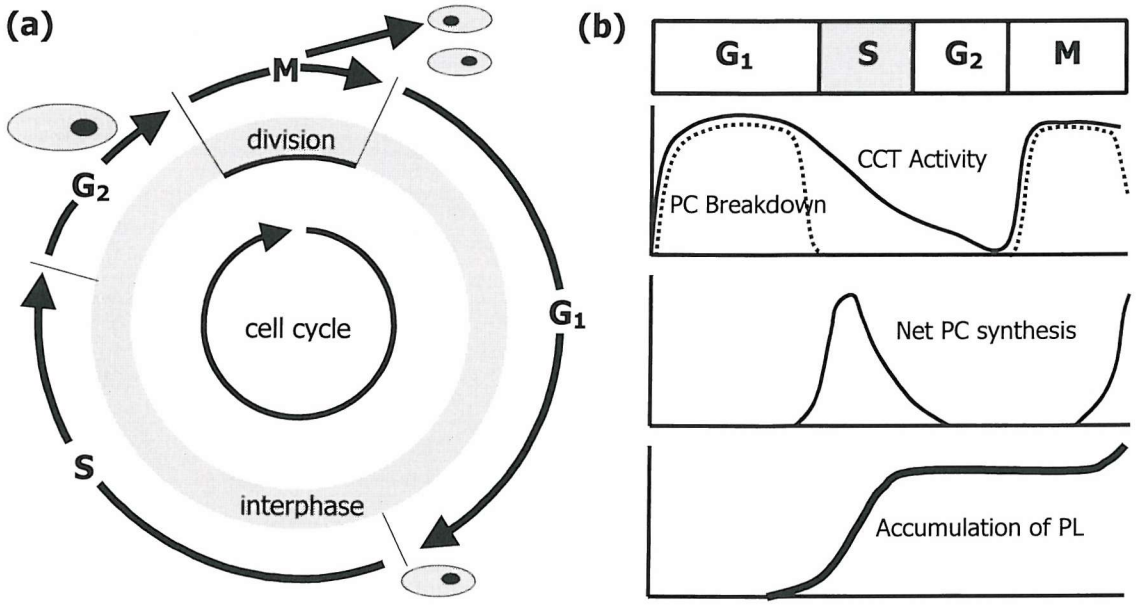

Figure 1.16: The cell cycle.
(a) A schematic diagram. M is mitosis (cell division), G_1 is the first gap phase, S is the synthesis phase where DNA replication occurs, finally G_2 is the second gap phase. When a cell is not dividing it is in the interphase: composed of the G_1, S, and G_2 phases and normally comprising 90% of the cell cycle period. Here preparations are made for division, this involves the replication of DNA and the doubling of lipid mass. The period of the eukaryotic cell cycle varies over several orders of magnitude between cell types, ranging from 8 hours to more than a year.
(b) Periodic Events in Phospholipid Metabolism. A schematic representation of the periodic changes in CT activity and PC degradation, which results in net membrane biogenesis in S phase.

At low ether lipid concentrations, it appears that cytotoxicity results from cytostasis. The precise mechanism that results in cytostasis is unknown. The range of structures that are cytotoxic is large, precluding any conventional receptor mediated mechanism. One key feature of all cytotoxic ether lipid analogues is that they are all type I amphiphiles. It has been postulated that the cytotoxicity of ether lipids is a direct result of this type I amphiphilic behaviour; studies have suggested that the more type I an amphiphile is the greater its cytotoxicity (Dymond 2001 and also; Wan 1997).

D. Anti tumour lipids deactivate CCT

There is much experimental evidence that the cytostatic action of ATLs can be attributed to the disruption of the CDP-choline pathway through the deactivation of CCT. CCT is widely regarded as the rate limiting step in the synthesis of PC. Observations of reduced levels of PC have been made in cells as a result of addition of ET-18-OMe (Modolell *et al.* 1979). Further studies have found that ET-18-OMe blocks choline incorporation into PC (Herrmann 1985; Vogler *et al.* 1985; Zhou & Arthur 1995). In addition, supplementation of exogenous lysoPC eliminates the cytotoxicity of ether lipids (Boggs *et al.* 1995a). LysoPC can be converted to PC by acylation, removing the dependence on the CDP-choline route. This suggests that the CDP-choline pathway is key to the cytotoxity of ether lipids, and this pathway is limited by CCT.

The model for CCT activation presented in figure 1.15 (p.1.23) provides an explanation for the action of ATLs. Indeed, a dramatic effect of type I amphiphiles on CCT activity has been observed (Attard *et al.* 2000). The partitioning of ATLs relieves the membrane torque tension, facilitating the dissociation of CCT from the endoplasmic reticulum, thus inhibiting CCT activity and disrupting this critical step in PC biosynthesis. Production of phospholipid prior to division is required to provide adequate membrane surface to create daughter cells. In order to proliferate, cells must double their phospholipid mass (Jackowski 1994; Jackowski 1996). Deficiency in PC prevents the cell from progressing through the cell cycle and dividing, resulting in cytostasis and ultimately cell death (apoptosis).

1.5 Homeostatic Control of Curvature Elastic Stress

This section looks at the significance of the observation that the stored elastic energy can influence the incorporation into biomembranes of an important class of amphipathic molecules: membrane proteins and, more specifically, membrane associated biosynthetic enzymes. First, the evidence for a link between membrane composition and function is examined. This is followed by a discussion of the significance of the observation that a number of membrane proteins appear to be affected by the stored elastic energy within membranes. Finally, the consequences of these effects when considering the enzymes involved in lipid biosynthesis are considered.

1.5.1 The Link between Membrane Composition and Function

The variation of lipid composition between specific biomembranes suggests the function of a membrane may be related to its composition. The presence of non-bilayer forming lipids in cell membranes implies an importance of stored elastic energy, which will be available to act as a driving force in a bilayer containing such lipids. This indicates that the function of a membrane may be dependent upon its composition through modulation of the membrane torque tension. It has been hypothesised that cell membranes homeostatically fine-tune their lipid content to preserve an optimum range of stored elastic energy (Gruner 1985), and that this provides the connection between membrane composition and function. Membranes could maintain optimum membrane torque tension through simple adjustment of their type II lipid content. However, regulation is likely to be a complex process involving control that encompasses the many species that influence the intrinsic membrane curvature.

If cells maintain the stored elastic energy in their membranes, how does the stored elastic energy modify membrane function? As mentioned previously, physical properties like headgroup spacing and hydration would change. In addition, alteration in the packing of hydrocarbon chains would affect diffusion and partitioning into the membrane. Other lipid associated cell functions directly dependent on membrane composition, e.g. endocytosis, could also be influenced by regulation of the membrane spontaneous curvature. However, the effects of the

stored elastic energy upon amphipathic proteins associated with or embedded into cell membranes are of particular importance; it is postulated that the modulation of integral and peripheral membrane protein activity by the membrane torque tension is a general phenomenon.

1.5.2 Generality of MTT Modulation of Membrane Protein Activity

Gruner reported that curvature stress is highly regulated in the natural membrane, indicative of its importance in the optimal functioning of membrane associated proteins (Gruner 1985). Direct correlation between membrane protein activity and lipid composition (which conforms to the type I/O and type II classification) has been shown in experimental studies of various enzymes.

Protein kinase C (PKC) is a protein involved in cellular signalling; although PKC activity is dependent on diacylglycerol (DAG) through a receptor-mediated mechanism, the activity of PKC has been shown to be dependent on lipid composition in synthetic vesicles (Slater *et al.* 1994; Stubbs & Slater 1996). The conformation of proteins can also be affected; the rate-determining step in the folding of bacteriorhodopsin, an integral membrane protein, is governed by vesicle composition (Curran *et al.* 1999). Gramicidin A dimerises to form a functioning channel through a bilayer, and this process has been observed to be disrupted by changes in lipid composition in synthetic vesicles (Lundbaek 1997). These findings are consistent with the membrane stress being important in the mechanisms of a wide array of membrane associated and membrane bound enzymes.

In general, the activities of these proteins are dependent upon the surrounding lipid composition. Synthetic vesicles such as the DOPC/PE mixtures, described in section 1.3.8, containing different types of lipids also confer activity. Therefore, it is generally accepted that, rather than a receptor mediated protein activation by individual lipid components, a physical property conferred by the bilayer as a whole is activating the protein. It is thought that membrane torque tension, and the resultant forces within a bilayer, directly affect membrane protein structure and function. The next section examines how the stored elastic energy in a cell membrane may act as a feedback regulation signal upon the enzymes responsible for maintaining the membrane: the enzymes of phospholipid biosynthesis.

1.5.3 The Significance of Regulation of Lipid Biosynthetic Enzymes

If protein activity is modulated by the membrane, an area of real interest is where the proteins build the membrane that modulates them. This is the case for CCT and the other membrane-associated proteins of lipid biosynthesis. Of course, the presence of all proteins, like any other amphipathic molecule, will influence the membrane (Killian & deKruijff 1986) but the biosynthetic enzymes have a special role. These proteins potentially complete a control loop, as shown in figure 1.17, and this can be understood by examining the effect of CCT.

CCT synthesises components of the RER, and the composition of the RER modulates CCT activity; this forms a framework for a feedback loop. CCT is driven to its active form in membranes by high membrane torque tension and the result is the reduction of membrane torque tension through the production of bilayer favouring PC. Since CCT is active only in the membrane form, greater quantities of PC lipids will be synthesised when there is higher membrane torque tension, giving greater relief. It can be seen that the proposed model appears to provide the cell with a method to maintain homeostatic control over its membrane composition through negative feedback loops. This echoes a fundamental principle of metabolic regulation: feedback regulation of biosynthesis by the end product (Jamil *et al.* 1990). Eukaryotic cells might therefore use membrane torque tension as a feedback signal to regulate phospholipid synthesis.

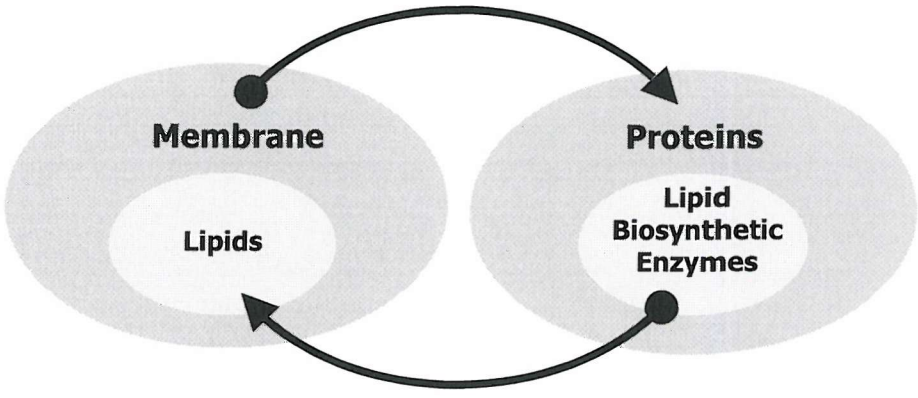

Figure 1.17: The completion of the control loop by the lipid biosynthetic enzymes.
The indirect effect of the proteins as normal amphipathic molecules is neglected (i.e. the proteins are constituents of the membrane but are shown separately here to emphasise the interactions).

1.5.4 Multiple Feedback Loops?

CCT is not the only enzyme involved in lipid biosynthesis that is modulated by membrane composition. Studies of the literature reveal that the activity of many enzymes involved in phospholipid synthesis is dependent on the composition of their associated membranes. CCT is of primary interest since regulation of the CDP-choline pathway is widely believed to occur through the CCT step in the pathway (Jamil *et al.* 1993). PC is both the main lipid component and a vital precursor to other lipid species. Cells convert PC lipids into other membrane components such as PA, PS and DAG, and these in turn are precursors to other species including PE.

The conversion of PC into the other lipid species is mediated by proteins including phospholipase A_2 (PLA_2), phospholipase C (PLC), phospholipase D (PLD) and diacylglycerol kinase (DGK). There is evidence that these membrane associated biosynthetic enzymes have activities that are dependent upon the membrane lipid composition and that this dependence may conform to the type II / type I/0 classification (these studies are examined later in a validation of this work). The evidence to date suggests multiple feedback loops exist between the membrane and the biosynthetic proteins. This is shown in figure 1.18. These effects on enzyme activity suggest membrane composition can therefore be successfully monitored and maintained by membrane curvature elastic stress acting as a feedback signal.

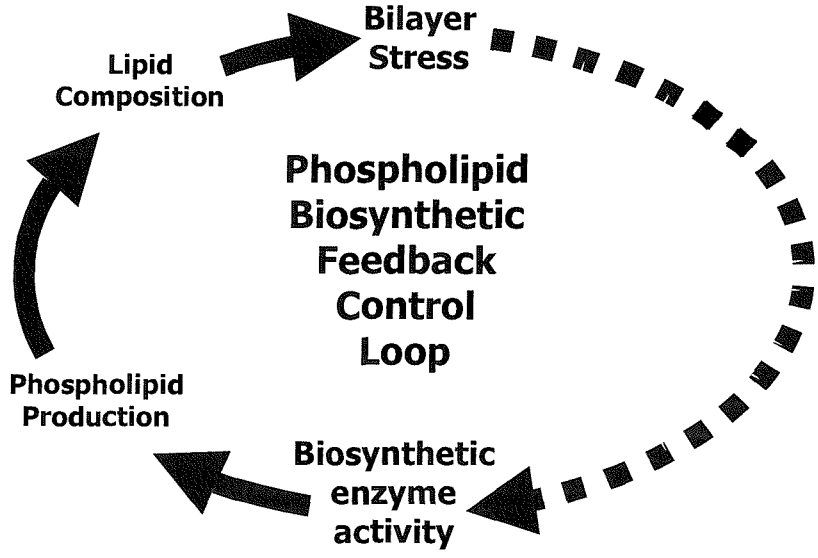

Figure 1.18: Hypothesis diagram. The figure shows the feedback control loop (shown by arrows) completed by the dependence of the enzyme activity on the bilayer stress (shown by the dotted arrow).

1.5.5 Working Hypothesis that MTT is under Homeostatic Control

The evidence presented so far is consistent with the hypothesis that the membrane torque tension is the homeostatically conserved property in biomembranes. Our general postulate is that membrane-bending rigidity acts as a transducer or an integrator of cell signals, and acts as a signal in its own right, through its dependence on lipid composition and influence over enzyme activation. It is important to emphasise that the mechanism is an example of integrative feedback that is carried as a purely physical signal, and should be distinguished from conventional ligand receptor type feedback.

It has been discussed how the stored elastic energy controls the enzymes of lipid biosynthesis, the machinery of the cell membrane. This control is clearly not just important for the synthesis of lipids, because the modulation of protein activity is seen for a wide range of types of enzymes (see section 1.5.2). The effect on so many processes suggests that it is critical that the stored elastic energy is controlled. This seems reasonable, as the cell membrane will be involved in a wide range of cellular events. It seems appropriate that cells should use the torque tension to regulate lipid biosynthesis, because the maintenance of the torque tension within a critical range of values ensures that the membrane bilayer does not undergo a phase transition into a porous state. It is also reasonable that the cell should use a non-specific physical signal for this purpose, because this is the simplest and most robust means of ensuring membrane integrity.

1.5.6 Purpose of Study: A Model of the CDP:choline Pathway

The nature of the hypothesis to be tested necessitates an analysis of the operation of the system as a whole. For example, when considering how CCT controls the pathway, it is natural to look at how CCT might control the production of PC. This alone involves an analysis beyond the local reaction. A dominant tendency in biochemistry has been to focus on individual processes, which can be studied in isolation. Whilst this is a necessary process that can yield important information and improve understanding of a systems mechanisms, exclusive concentration upon artificially isolated components and aspects of system behaviour can lead to oversimplification and the loss of important system controls. In particular, the

integration of signals and the proposed feedback mechanism cannot be considered in terms of isolated reactions.

In this work, the aim was to look specifically at how membrane stress effects can be implemented in a model, based on knowledge of the structure of the metabolic network for lipid synthesis and the spontaneous curvature of the lipids of the membrane. Specifically, we postulate that the observed modulation of enzyme activity is the manifestation of the control of membrane torque tension. The main aim of this work was to use the model to test this. It was important to gain a deeper understanding of the pathway, so a central part of the work was the construction of a model of phospholipid biosynthesis. The model that has been set up can be used to investigate the effects of the enzymes of lipid biosynthesis upon the stored elastic energy. The model can also be used to investigate the type of stabilisation that would emerge from the feedback regime proposed.

To test the arguments that the modulation seen for CCT may be general, and that its purpose is to control the MTT, it was important to determine the extent to which the other phospholipid biosynthetic proteins may be controlled by the stored elastic energy. This was achieved by sensitivity analysis of the model and correlation with experimental evidence. The predictions of each enzyme's effect on the MTT can be used, by comparison with the literature, to verify if the observed lipid sensitivities are consistent with the predicted feedback loops, as figure 1.19. This would suggest the modulation of enzyme activity is acting to maintain the stored elastic energy and would be a key piece of evidence consistent with the hypothesis that membrane torque tension is the homeostatically controlled property in biomembranes.

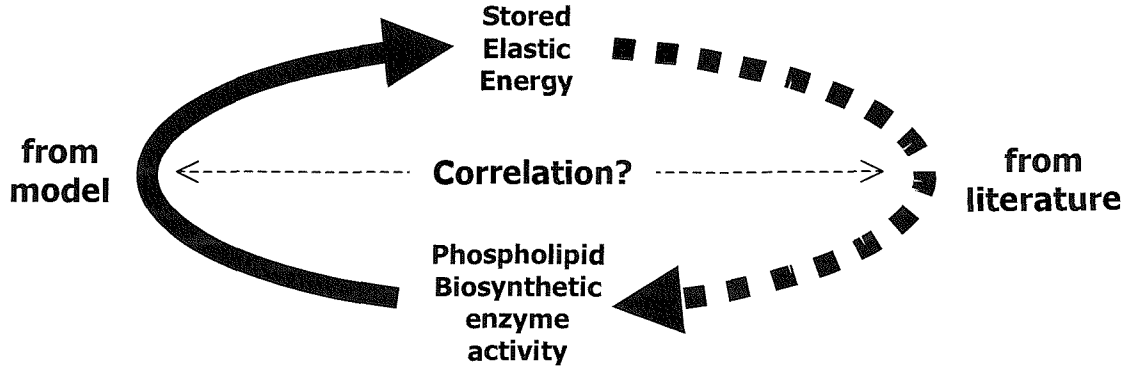

Figure 1.19: Testing the hypothesis.
Is the effect of the enzyme on the MTT predicted by the model consistent with the literature reports of enzyme modulation by phospholipids, such that the MTT would be homeostatically controlled?

1.6 References

Arnold RS & Cornell RB (1996)
Lipid Regulation of CTP: Electrostatic, Hydrophobic, and Synergistic Interactions of Anionic Phospholipids and Diacylglycerol.
Biochemistry **35**: 9917-9924.

Atkins PW (1994) *Physical Chemistry*
Fifth edition. Oxford University Press.

Attard GS, Smith WS, Templer RH, Hunt AN & Jackowski S (2000)
Modulation of CTP:phosphocholine cytidylyltransferase by membrane curvature elastic stress.
Proc. Natl. Acad. Sci. USA **97**: 9032-9036.

Berdel WE (1990)
Ether lipids and derivatives as investigational anticancer drugs.
Onkologie **13**: 245-250.

Bladergroen BA, Wensing T, Van Golde LMG & Geelen MJH (1998)
Reversible translocation of CTP:phosphocholine cytidylyltransferase from cytosol to membranes in the adult bovine liver around parturition.
Biochim. Biophys. Acta **1391**: 233-240.

Boggs KP, Rock CO & Jackowski S (1995a)
LysoPC attentuates the cytotoxic effects of ET-18-OMe.
J. Biol. Chem. **270**: 11612-11618.

Boggs KP, Rock CO & Jackowski S (1995b)
Lysophosphatidylcholine and 1-O-Octadecyl-2-O-Methyl-rac-Glycero-3-Phosphocholine Inhibit the CDP-Choline Pathway of Phosphatidylcholine Synthesis at the CTP Step.
J. Biol. Chem. **270**: 7757-7764.

Booth PJ, Riley ML, Flitsch SL, Templer RH, Farooq A, Curran AR, Chadborn N & Wright P (1997)
Evidence that bilayer bending rigidity affects membrane protein folding.
Biochemistry **36**: 197-203.

Cornell RB (1991a)
Regulation of CTP:Phosphocholine Cytidylyltransferase by Lipids. 1. Negative Surface Charge Dependence for Activation.
Biochemistry **30**: 5873-5880.

Cornell RB (1991b)
Regulation of CTP:Phosphocholine Cytidylyltransferase by Lipids. 2. Surface Curvature, Acyl Chain Length, and Lipid-Phase Dependence for activation.
Biochemistry **30**: 5881-5888.

Cullis PR, Fenske DB & Hope MJ (1996) *Physical Properties and Functional Roles of Lipids in Membranes*, p.1-33.
In *Biochemistry of Lipids, Lipoproteins and Membranes*
Edited by D. E. Vance & J. E. Vance. Elsevier Science.

Curran AR, Templer RH & Booth PJ (1999)
Modulation of Folding and Assembly of the Membrane Protein Bacteriorhodopsin by Intermolecular Forces within the Lipid Bilayer.
Biochemistry **38**: 9328-9336.

Dunne SJ, Cornell RB, Johnson JE, Glover NR & Tracey AS (1996)
Structure of the Membrane Binding Domain of CTP:Phosphocholine Cytidylyltransferase.
Biochemistry **35**: 11975-11984.

Dymond MK (2001)
An Investigation into the Mechanism of Action of Amphiphiles with Cytotoxic Properties
Ph.D. Thesis University of Southampton.

Eibl H (1984)
Phospholipids as Functional Constituents of Biomembranes.
Angewandte Chemie **23**: 257-238.

Feldman DA, Kovac CR, Dranginis PL & Weinhold PA (1978)
The role of Phosphatidylglycerol in the Activation of CTP:Phosphocholine Cytidylyltransferase from Rat Lung.
J. Biol. Chem. **253**: 4980-4986.

Gruner SM (1985)
Intrinisic curvature hypothesis for the biomembrane lipid composition. A role for nonbilayer lipids.
Proc. Nat. Acad. Sci. USA **82**: 3665-3669.

Herrmann D (1985)
Changes in cellular lipid synthesis of normal and neoplastic cells during cytolysis induced by alkyl lysophospholipid analogues.
J. Natl. Cancer Inst. **75**: 423-430.

Hoffmann H (1984)
From micellar solutions to liquid crystal phases.
Ber. Bunsenges. Phys. Chem. **88**: 1078-1093.

Israelachvili J (1992) *Intermolecular and Surface Forces*
Second edition. San Diego: Academic Press Inc.

Jackowski S (1994)
Co-ordination of membrane phospholipid synthesis with the cell cycle.
J. Biol. Chem. **269**: 3858-3867.

Jackowski S (1996)
Cell Cycle Regulation of Membrane Phospholipid Metabolism.
J. Biol. Chem. **271**: 20219-20222.

Jamil H, Hatch GM & Vance DE (1993)
Evidence that binding of CTP:phosphocholine cytidylyltransferase to membranes in rat hepatocytes is modulated by the ratio of bilayer- to non-bilayer-forming lipids.
Biochem. J. **291**: 419-427.

Jamil H, Yao Z & Vance DE (1990)

Feedback regulation of CTP:phosphocholine cytidylyltransferase Translocation between Cytosol and Endoplasmic Reticulum by Phosphatidylcholine.
J. Biol. Chem. **265**: 4332-4339.

Karp G (1984) *Cell Biology*
Second edition. McGraw-Hill.

Kent C (1995)
Eukaryotic Phospholipid Biosynthesis.
Annu. Rev. Biochem. **64**: 315-343.

Kent C (1997)
CTP:phosphocholine cytidylyltransferase.
Biochim. Biophys. Acta **1348**: 79-90.

Killian JA & deKruijff B (1986)
The Influence of Proteins and Peptides on the Phase Properties of Lipids.
Chem. Phys. Lipids **40**: 259-284.

Lodish HFR, J.E. (1979)
The Assembly of Cell Membranes.
Scientific American **240**: 38-53.

Lohmeyer M & Workman P (1995)
Growth arrest vs direct cytotoxicity and the importance of molecular structure for the in vitro anti-tumour activity of ether lipids.
Br J Cancer **72**: 277-286.

Lundbaek JA, Maer, A.M. Andersen, O.S. (1997)
Lipid Bilayer Electrostatic Energy, Curvature Stress, and Assembly of Gramicidin Channels.
Biochemistry **36**: 5695-5701.

Lykidis A & Jackowski S (2001)
Regulation of Mammalian Cell Membrane Biosynthesis.
Prog. Nucleic Acid Re. **65**: 361-393.

Modolell M, Andreesen R, Pahlke W, Brugger U & Munder P (1979)
Disturbance of phospholipid metabolism during the selective destruction of tumor cells induced by alkyl-lysophospholipids.
Cancer Res. **39**: 4681-4686.

Noseda A, Ehite JG, Godwin PL, Jerome WG & Modest EJ (1989)
Membrane Damage in Leukemic Cells Induced by Ether and Ester Lipid: An Electron Microscopy Study.
Experimental and Molecular Pathology **50**: 69-83.

Principe P & Braquet P (1995)
Advances in ether phospholipids treatment of cancer.
Crit. Rev. Oncol. Hematol. **18**: 155-178.

Rennie J & Rusting R (1996)
Making Headway Against Cancer.
Sci. Am. **275**: 29-30.

Roberts MBV (1976) *Biology: A Functional Approach*
Second edition. Nelson.

Rothman JE & Lenard J (1977)
Membrane Asymmetry.
Science **195**: 743-753.

Seddon J (1996)
Lyotropic Phase Behaviour of Biological Amphiphiles.
Ber. Bunsenges. Phys. Chem. **100**: 300-393.

Seddon JM (1990)
Structure of the inverted hexagonal (HII) phase, and non-lamellar phase transitions of lipids.
Biochemica et Biophysica Acta **1031**: 1-69.

Silvius JR (1993) *Structure and Nomenclature*, p.1-22.
In *Phospholipids Handbook*
Edited by G. Cevc. New York: Marcel Dekker.

Slater SJ, Kelly MB, Taddeo FJ, Ho C, Rubin E & Stubbs CD (1994)
The Modulation of Protein Kinase C Activity by Membrane Lipid Bilayer Structure.
J. Biol. Chem. **269**: 4866-4871.

Stubbs CD & Slater SJ (1996)
The effects of non-lamellar forming lipids on membrane protein-lipid interactions.
Chem. Phys. Lipids **81**: 185-195.

Tate MW, Eikenberry EF, Turner DC, Shyamsunder E & Gruner SM (1991)
Nonbilayer Phases of Membrane Lipids.
Chem. Phys. Lipids **57**: 147-164.

Tronchere H, Record M, Terce F & Chap H (1994)
Phosphatidylcholine Cycle and regulation of phosphatidylcholine biosynthesis by enzyme translocation.
Biochim. Biophys. Acta **1212**: 137-151.

Vogler V, Whigham E, Bennett W & Olson A (1985)
Effect of alkyl-lysophospholipids on phosphatidylcholine biosynthesis in leukemic cell lines.
Exp. Hematol. **13**: 629-633.

Waite KA & Vance DE (2000)
Why Expression of Phosphatidylethanolamine *N*-Methyltransferase Does Not Rescue Chinese Hamster Ovary Cells That Have an Impaired CDP-Choline Pathway.
J. Biol. Chem. **275**: 21197-21202.

Wan JW (1997)
Novel Ether Lipids as Antineoplastic Agents
Ph.D. Thesis University of Southampton.

Westphal O (1987)
Ether Lipids in Oncology-Welcoming Address.

Lipids **22**: 787-788.

Yeagle PL (1989)
Lipid regulation of cell membrane structure and function.
FASEB J. **3**: 1833-1842.

Zhou X & Arthur G (1995)
Effect of 1-O-octadecyl-2-O-methyl-glycerophosphocholine on phosphatidylcholine and phosphatidylethanolamine synthesis in MCF-7 and A549 cells and its relationship to inhibition of cell proliferation.
Eur. J. Biochem. **232**: 881-888.

Modelling Biochemical Networks 2

Contents

2.1 Introduction

This chapter is intended as an introduction to the techniques of kinetic modelling, particularly those techniques applied to the modelling of biochemical pathways. Firstly, the methods used to model the kinetics of reaction systems are examined. The particular challenges associated with the stoichiometric networks seen in metabolic pathways are then detailed. Finally, the important concepts of robustness and connectivity are introduced. These topics are intended to provide a framework for understanding the development of the model outlined in chapter 3.

2.1.1 Principles of Modelling

The 'scientific method', first described by Francis Bacon, consists of four steps. The first is an observation of the real system in operation. This is followed by the formulation of a hypothesis to explain how the system works. Prediction of the system's behaviour on the basis of the hypothesis is then possible, followed finally by performance of experiments to test the validity of the hypothesis.

Modelling is simply a tool for scientists to use, and the procedures used follow the steps detailed above. Modelling studies of reaction systems all focus on obtaining a basic description of the individual reactions of the system, and the rate of each reaction. In most studies, this information is obtained by an iterative, inductive process: after carrying out experiments and analysing the results, a mechanism is deduced and a model is derived from it. New experiments can then be performed to test and refine the mechanism and model.

The optimum model can be used not only to describe the experimental results, but also to predict behaviour of the system under conditions that have not been studied explicitly. Understanding the mechanism of a chemical reaction also allows comparison of different systems to gain deeper insight into their reactivity and the underlying processes which control the outcome of a reaction. This approach is extremely powerful and, over the years, great effort has been put into both gaining mechanistic information for reacting systems, and developing mathematical models for them. These vary from treatments to produce rate laws for single reactions, to models that simulate complex reaction systems.

2.2 Methods of Modelling

Kinetic models fall into two general categories: algebraic expressions, or *rate laws*, derived from the mechanistic steps describing the reaction, and numerical simulations of a reaction system using a computer.

2.2.1 Algebraic Methods

A rate law is an equation obtained by analysing a reaction mechanism. In general, coupled differential equations are written for the time dependence of each chemical species and approximations are made to combine and simplify them. Ideally, the final expression involves only measurable or controllable concentrations for comparison with experimental data. A simple example is the Michaelis-Menten rate equation (this is discussed in section 2.2.2).

First, the *integral method* (Atkins 1994, p.869; Pilling & Seakins 1996, p.9) for rate laws is illustrated. The technique and some of its associated problems will be shown by considering some relevant simple models and their analytical solutions.

A. Example 1: single step

For a single first order reaction, A → Products, the rate law can be written in the following way

$$da/dt = -ka \quad \text{where } a = [A]_t, \text{ the concentration of A at time } t$$

This is the easiest situation to use an analytical solution. Integrating:

$$a = a_0\exp(-kt) \therefore \ln(a_0/a)=kt \quad \text{where } a_0 \text{ is the initial concentration of A.}$$

a may be found directly, at any given time t, from a_0 and k.

B. Example 2: consecutive reactions

Metabolic networks at their simplest are constructed from consecutive reactions, here the simplest case is examined, two consecutive reactions as a closed system.

$$A \xrightarrow[k_1]{} B \xrightarrow[k_2]{} C$$

$da/dt = -v_1 = -k_1a$ $\quad db/dt = v_1 - v_2 = k_1a - k_2b$

$dc/dt = v_2 = k_2b$ $\quad$ also $da/dt + db/dt + dc/dt = 0$ (material balance)

The first equation (da/dt) may be solved, as for example 1, since it is a simple first order differential equation:

$a = a_0\exp(-k_1t)$ $\quad$ here k_1 is the *time constant* for this reaction.

Substituting this into the second equation gives:

$db/dt = k_1a_0\exp(-k_1t) - k_2b$

This equation is less simple to solve, requiring an integrating factor. If only A is present initially, the solution is:

$b = a_0k_1/(k_2 - k_1)\{\exp(-k_1t) - \exp(-k_2t)\}$

Finally, material balance gives the concentration of C:

$c = a_0 - a - b$

C. Example 3: parallel reactions

Here it is illustrated how parallel competing reactions (branches in a pathway) complicate matters further.

$A \rightarrow B$ $\quad k_1$

$A \rightarrow C$ $\quad k_2$

It might be supposed that the products B and C would be formed with different time constants dependent on k_1 and k_2 respectively, but this is not the case. The relative yields of B and C will however be determined by the relative magnitudes of the rate constants.

$da/dt = -(k_1 + k_2)a$

$\therefore$ $\quad a = a_0\exp\{-(k_1 + k_2)t\}$

also $\quad db/dt = k_1a$, substituting for a:

$db/dt = k_1a_0\exp\{-(k_1 + k_2)t\}$

This can be integrated to give:

$$b = \{k_1a/(k_1 + k_2)\}[1 - \exp\{-(k_1 + k_2)t\}]$$

Finally, a similar expression can be found for c:

$$c = \{k_2a/(k_1 + k_2)\}[1 - \exp\{-(k_1 + k_2)t\}]$$

Note the time constant for the exponential growth of B and C is $(k_1 + k_2)$ the same as that for the decay of A. However, the yields of B and C, b_∞ and c_∞, are dependent on the relative magnitudes of the rate constants k_1 and k_2.

$$b_\infty = k_1a_0/(k_1 + k_2)$$
$$c_\infty = k_2a_0/(k_1 + k_2)$$

D. Example 4: bimolecular reactions

Despite the complexities introduced so far, all the steps have only involved one substrate. When the order of the reaction is higher, the integrated rate law is further complicated, as shown in table 2.01 for two bimolecular reactions: A + A → P and A + B → P (Pilling & Seakins 1996).

	Order	da/dt	kt
A → P	1	$-ka$	$\ln(a_0/a)$ as shown in example 1
A + A → P	2	$-ka^2$	$(1/a) - (1/a_0)$
A + B → P	2	$-kab$	$(b_0 - a_0)^{-1}\ln[(a_0b)/(b_0a)]$

Table 2.01: Differential and integral forms of rate equations.

It is apparent that the integral method becomes increasingly complicated as the number of steps are increased. Any realistic metabolic model will include more than one reaction, with multiple substrates and parallel and consecutive reactions also likely to be present. Furthermore, steps which have reaction equations like those in table 2.01 will in reality incorporate many elementary steps. When the aim is to obtain a rate law for such a system, it is necessary to make approximations.

2.2.2 The Steady State Approximation

The most common method used to obtain a rate law is to apply the *steady state approximation* to the coupled differential equations obtained from the reaction mechanism. Transient reaction intermediates are assumed to have very small, stable concentrations. This allows the time derivative of their concentrations to be set equal to zero, and the concentrations of those species are expressed in terms of stable reactants and products only.

Use of the steady-state approximation can place restrictions on the experimental conditions used to study a particular chemical reaction. For example, a vast excess of a reagent may be necessary, or only a small extent of reaction might be allowed. For many chemical reactions, such limitations do not present difficulties and, if steady-state conditions truly exist, allow valuable mechanistic information to be obtained.

A. The Michaelis-Menten equation

The Michaelis-Menten equation is based on a steady state treatment of the following reaction scheme:

$$\mathrm{E} + \mathrm{S} \underset{k_{-1}}{\overset{k_1}{\rightleftharpoons}} \mathrm{ES} \xrightarrow{k_2} \mathrm{E} + \mathrm{P}$$

where E = free enzyme, S = substrate,
ES = enzyme substrate complex, P = product.

Applying the steady state approximation to the intermediate complex:

$$\frac{d[\mathrm{ES}]}{dt} = k_1[\mathrm{E}][\mathrm{S}] - (k_{-1} + k_2)[\mathrm{ES}] = 0$$

Rearranging:

$$[\mathrm{ES}] = \frac{k_1}{k_{-1} + k_2}[\mathrm{E}][\mathrm{S}]$$

$$v = \frac{k_1 k_2}{k_{-1} + k_2}[\mathrm{E}][\mathrm{S}]$$

but, $[E] = [E]_0 - [ES]$, therefore:

$$K_m[ES] = \left([E]_0[S] - [ES][S]\right)$$

where the Michaelis Constant $K_m = \frac{k_{-1} + k_2}{k_1}$

Rearranging:

$$[ES] = \frac{[E]_0[S]}{K_m + [S]}$$

Giving:

$$v = k_2 \frac{[E]_0[S]}{K_m + [S]}$$

Given that $V_m = k_2[E]_0$:

$$v = V_m \frac{[S]}{K_m + [S]}$$

This is the irreversible Michaelis-Menten rate equation. A similar treatment can be performed for a two substrate reaction giving:

$$v = V_m \frac{[A][B]}{k_A k_B + k_B[A] + k_A[B] + [A][B]}$$

The Michaelis-Menten model, perhaps the most valuable quantitative model in biochemistry, illustrates that a model need not be universally valid, or free of all defects to be useful as there are many conditions where it does not apply (Garfinkel 1981). The next section examines the methods used when the steady state approximation cannot be applied, and the techniques used in these situations.

2.2.3 Computer Simulations

There are numerous classes of reactions that cannot be treated analytically. They include:

1. Reactions whose mechanisms are too complicated to yield a rate law.
2. Reactions whose rate laws are too complex to be tested experimentally.
3. Reactions that never attain steady state under the experimental conditions of interest.
4. Reactions in which limitations like excess reagents or small extent of reaction are inconvenient or result in loss of important information.
5. Reactions in which physical conditions such as temperature and volume are not constant.

These complications clearly present problems when a model is dealing with a system of reactions, rather than an individual reaction. Any realistic metabolic model will be described by a set of non-linear equations for which there is no analytical solution (Hofmeyr 1986). For such systems, where approximations are not appropriate, kinetic modelling is best performed numerically by a computer.

Numerical simulation of chemical reactions is a powerful tool to complement experiments. Unlike algebraic rate laws, which are often highly simplified, simulations allow detailed models to be developed and tested as data accumulate. They also provide a means of evaluating various hypotheses for further experimental investigation. The ability to carry out reliable "what if" simulations can be particularly valuable in studies of very complex systems, such as metabolic pathways.

By far the most common method used is the *deterministic approach*, in which the time-dependence of species concentrations is written as a set of coupled differential equations that are then integrated. A deterministic model presumes that a reaction system is sufficiently well understood that the complete time-dependent behaviour of the system is contained in the solutions to the differential equations. This method works well for many systems

2.2.4 Numerical Integration

Using the processing power of computers, mechanisms involving hundreds of reactions and many species can be rapidly integrated giving the concentrations of reactants as a function of time. A brief indication of how this may be achieved follows to illustrate the general principle.

A. An illustration of the technique

Consider the first order reaction

$$A \rightarrow B$$

Using this simple example facilitates integration of the rate equation, allowing a comparison of the integral and numerical techniques. The integral method is shown first. Integrating equation 2.01 gives the result in equation 2.02.

$$\frac{d[A]}{dt} = k[A] \qquad \text{equation 2.01}$$

$$\int \frac{1}{[A]} . d[A] = \int k . dt$$

$$[A] = [A]_0 . e^{-kt} \qquad \text{equation 2.02}$$

The numerical technique involves evaluating the concentration at some time, $t + dt$, given its concentration at time t, $[A]_t$. This is achieved using an expression of the form shown in eqution 2.03 where Φ is a function, which depends on the rate coefficients and the concentrations at time t.

$$[A]_{t+dt} = [A]_t + \Phi . dt \qquad \text{equation 2.03}$$

The numerical technique is concerned with the evaluation of Φ.

The form of Φ may be determined by use of the analytical solution:

$$[A]_{t+dt} = [A]_t . e^{-k.dt}$$

this can be expanded as a series:

$$[A]_{t+dt} = [A]_t.[1 - k.dt + (\tfrac{1}{2}.k.dt)^2 + \ldots \ldots .]$$

multiplying out:

$$[A]_{t+dt} = [A]_t - k.[A]_t.dt + [A]_t(\tfrac{1}{2}.k.dt)^2 + \ldots \ldots .$$

for small dt (where the third and higher terms are insignificant)

$$\Phi = -k.[A]_t \qquad \text{equation 2.04}$$

It should be noted that Φ has been shown to be equal to the 'instantaneous rate' at time t, $k.[A]_t$. This type of integration is known as an explicit method. Incrementing the concentration of A involves simply subtracting $k.[A]_t.dt$: a simple procedure which can be rapidly repeated to track the time evolution of the concentration of A.

B. Problems with numerical solutions: Stiffness

In the previous example, the approximation amounts to keeping dt small with respect to the rate gradient. With systems that are more complex in nature, a problem arises. For example:

$$\begin{array}{ccccc} A & \xrightarrow{k_{15}} & B & \xrightarrow{k_{16}} & C \end{array} \qquad k_{15} >> k_{16}$$

This is the situation where the steady state approximation applies. It might be assumed that at large times, where the concentration of B changes very little, the numerical integration routine could move on to larger timesteps.

However, this produces large errors. The numerical integration becomes unstable and the solutions may show oscillatory behaviour. When the kinetics are determined by processes occurring with very different timescales the differential equations produced are known as *'stiff coupled differential equations'* (Heinrich *et al.* 1977) and are difficult to solve efficiently using numerical techniques. However, more efficient, so-called implicit numerical techniques have been devised (Gear 1971; Stoer & Bulirsh 1980).

C. The power of simulation: Sensitivity Analysis

The quality of the results of simulation are only as accurate as the input data, namely the kinetic constants for each reaction. In order to improve the results it is necessary to know which reactions are the most important. Once these have been identified, investigations can focus on these reactions and the corresponding rate constants may be measured, remeasured or refined.

Sensitivity Analysis is a method often chosen to investigate a reaction mechanism. The method involves varying each of the individual rate constants by a set amount, in each case noting the effect on the system, for example changes in concentrations or fluxes of species. The most sensitive reactions in the system will cause the largest changes in the system.

When looking at the effect of the rate coefficient k_j on the production of one particular species y_i, the *sensitivity coefficient* S_{ij} is as defined in equation 2.05.

$$S_{ij} = dy_i(t)/dk_j(t_0) \qquad \text{equation 2.05}$$

This can provide information on the dominant mechanisms occurring in a complex system. It is often more practical to perform sensitivity analysis with a model than to perform the corresponding experiments (Garfinkel 1981). The method relies on use of computational power to investigate the behaviour of the system, repeating simulations while varying the parameter of interest.

D. Further analysis: Metabolic Control Analysis

Metabolic Control Analysis (MCA) is a formalised method of sensitivity analysis of fluxes and metabolite concentrations. MCA is used to study the relative control exerted by each step on the system's variables (fluxes and metabolite concentrations). This control is measured by applying a perturbation to the step being studied and then measuring the effect on the variable of interest after the system has settled to a new steady state. The details of MCA (Cascante *et al.* 1996; Fell 1992) will not be discussed here. However, two useful results of MCA were useful in determining how to experiment with the model developed:

A *control coefficient* is a relative measure of how much a perturbation on a parameter (for example, a rate coefficient) affects a system variable (for example, the fluxes or metabolite concentrations). Control coefficients are analogous to 'sensitivities'; they are global properties and in metabolic systems, control is a systemic property, dependent on all of the system's elements.

The *elasticity coefficients* are defined as the ratio of relative change in local rate to the relative change in one parameter (normally the concentration of an effector). Each enzyme has as many elasticity coefficients as the number of parameters (eg substrates, products or modifiers) that affect it. For example, one says *there is a substrate elasticity of 2* if the rate of a reaction increases by 6% when the substrate concentration increases by 3%. Unlike control coefficients, elasticity coefficients are not systemic properties but rather measure how isolated enzymes are sensitive to changes in their parameters. This emphasises the similarity of elasticity coefficients and 'order of reaction', however it should be noted that elasticities are rarely integers and vary with the conditions.

Although these quantitative measures are not used directly here, the concepts form the framework for the methods used in this work to investigate the systems responses. The method of sensitivity analysis is returned to, in the discussion of the experiments performed on the model, in chapter 4. Moving to a system of reactions, there are many more factors to consider. The kinetics remain the same, but with a complex pathway the modeller must address the structure of the stoichiometric network.

2.3 Modelling Metabolic Pathways

This section will examine in more detail the methods and concepts that are used when performing modelling of metabolic pathways. A significant amount of research into these procedures was necessary to develop our model. The material covered in this chapter is often taken for granted in the literature, however much of it is not obvious to the non-specialist. A review here will serve to facilitate understanding of the development of the model, described in the next chapter. Many of the concepts and examples are based on the work of Hofmeyr (Hofmeyr 1986). Some of the problems were encountered and solved independently but where there is overlap, the expressions and language from this paper have been used for consistency.

After examining the mathematical representation of metabolic networks, this section details the metabolic elements and the basic network structures that can be formed from these elements. Examples are used to illustrate the key features of each network structure. The discussion then moves to focus on finding the parameters of the system by solving the stoichiometric equations for the flux relationships. These methods are also illustrated with example network structures and a discussion of the influence of each structure on the solution. Finally, the links between 'connectivity' and the 'robustness' and 'efficiency' of pathways is briefly explored.

2.3.1 Mathematical Representation of the Stoichiometric Network

The two elements essential to the description of a biochemical network are the stoichiometric reactions (the network structure) and an algebraic expression for the rate of each reaction (the kinetics). To these may be added constraints on groups of metabolites, known as moiety conservation (this is explained in the example covered in section 2.3.6 D).

In this first section, the network structure is considered. This section will first define some of the terms used to describe networks and represent them mathematically, before looking at how complex metabolic structures can be thought of as constructed from a few simple building blocks.

A. The stoichiometric equations

The network structure can be represented by writing an equation for each metabolite. For a system with n_{met} metabolites and n_{enz} enzyme reactions, there are n_{met} equations of the form in equation 2.06, where S_i is the concentration of the metabolite.

$$\frac{dS_i}{dt} = \sum_{j=1}^{n_{enz}} c_{ij} v_j \qquad \text{equation 2.06}$$

B. The stoichiometric coefficients

c_{ij} is an integer called the *stoichiometric coefficient*, which specifies the number of molecules of metabolite S_i participating in the stoichiometric equation of reaction j. The sign is positive if the metabolite S_i is a product of reaction j, negative if a substrate and zero if the metabolite does not participate in the reaction.

C. The stoichiometric matrix

The set of stoichiometric equations may be represented as a matrix. The *stoichiometric matrix* is a convenient representation of the information contained in the stoichiometric equations. The matrix has n_{met} rows, each representing a metabolite, and n_{enz} columns, each representing a reaction. The stoichiometric coefficients are then the entries in this matrix. Examples, which illustrate the construction of stoichiometric networks, can be found later in this chapter.

D. The balance equations

At the steady state, the metabolite concentrations are time invariant; the total rate of production of each metabolite is balanced by the total rate of consumption, giving a zero net rate of change of concentration. The stoichiometric equations are equated to zero to give a set of nmet *balance equations* of the form shown in equation 2.07.

$$\frac{dS_i}{dt} = \sum_{j=1}^{n_{enz}} c_{ij} v_j = 0 \qquad \text{for } i = 1,2,\ldots.,n_{met} \qquad \text{equation 2.07}$$

These equations may be written in matrix form and, with extra information, can be used to find the steady state fluxes. This will be illustrated with examples in section 2.3.7. However, before this is possible a discussion of the stoichiometry of metabolic networks, and the elements from which the networks are built, is required.

2.3.2 Metabolic Elements

The construction and solution of metabolic pathways requires a detailed understanding of the stoichiometry of network structures and the elements from which they are constructed.

In all metabolic pathways, two or more enzyme-catalysed reactions are linked by common metabolites with the product of one enzyme being the substrate of another. There are two types of link (Hofmeyr 1995):

> In a Type 1 linkage, the second enzyme converts the linking metabolite to a new metabolite, see figure 2.01 (a). This is the type of reaction seen in ordinary linear chains.
>
> In a Type 2 linkage, the second enzyme reverses the action of the first enzyme (with respect to the linking metabolite) as shown in figure 2.01 (b). The second reaction is a distinct reaction catalysed by a different enzyme. This is a feature of reactions coupled by the interconversion of different forms of cofactors, e.g. ATP/ADP.

The combination of these two types of linkage lead to a number of *metabolic structures,* which are now discussed.

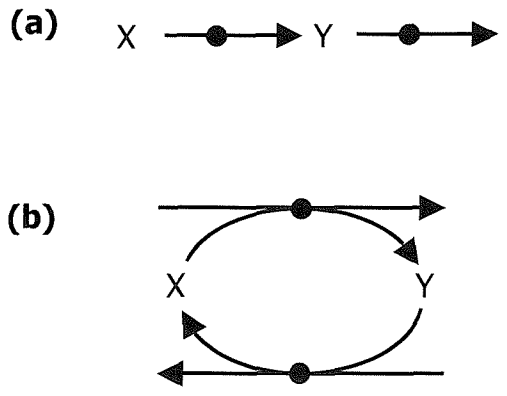

Figure 2.01: Basic metabolic elements:
(a) Type 1 linkage: the second enzyme converts the linking metabolite to a new metabolite.
(b) Type 2 linkage: the second enzyme reverses the action of the first enzyme.

2.3.3 Metabolic Structures

The two types of link detailed in section 2.3.2 can be combined to form four basic structures. The four simple structures are shown in figure 2.02. These structures are the building blocks for all metabolic pathways. The four structures are: a chain, a branch, a loop and a cycle. These structures are considered briefly, before looking at the methods used to build pathways constructed from them.

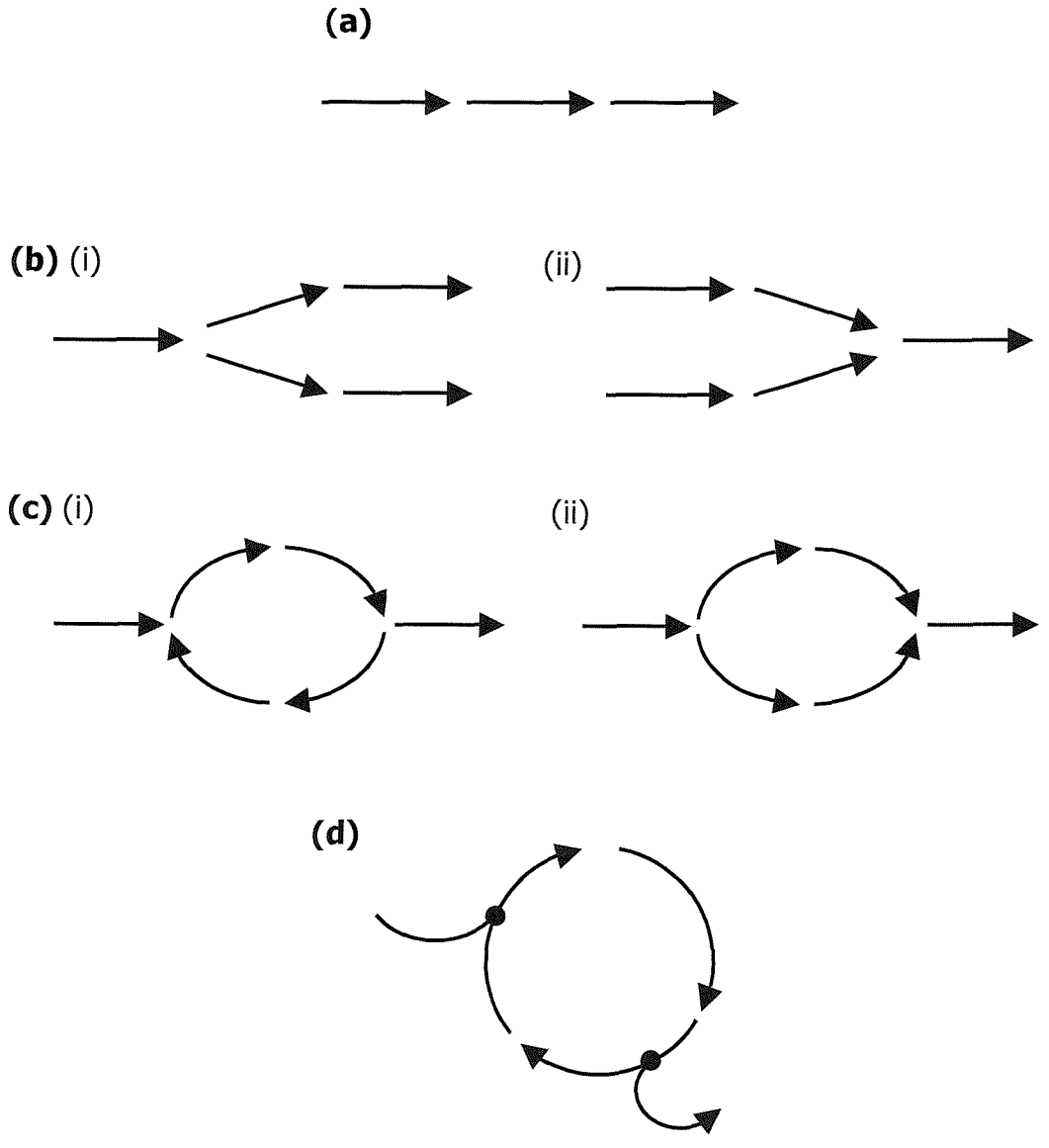

Figure 2.02: Metabolic structures constructed from the metabolic elements:
(a) Linear chain.
(b) Branched chains (diverging (i) and converging (ii)).
(c) Loops (opposed branches (i) and parallel reconverging branches (ii)).
(d) Cycle (incorporates type II linkage).

A. Linear chains

Linear chains consist of a series of consecutive type 1 linkages, as shown in figure 2.02 (a). Isolated, a linear chain is the simplest metabolic pathway structure; at steady state each reaction has the same flux, since for each metabolite to have a time-invariant concentration the rate of consumption must equal rate of production.

B. Branched chains

Branches arise when one intermediate is metabolised by two enzymes and each commits the metabolite to a different product. Figure 2.02 (b) shows a branch with diverging fluxes (i). Reversing the branches gives a converging branch as shown in (ii). Importantly, branching gives rise to more than one steady state flux. The sum of the entry fluxes at a branch point must equal that of the exit fluxes at steady state. This will be examined in the examples that follow.

C. Loops

Strictly, loops are simply branches that reconverge. However, they are important enough to be commented on separately. Two examples are shown in figure 2.02 (c). Flow can be opposed (i) or parallel (ii). The simplest forms of loops are reactions catalysed by two isozymes (parallel) or the futile loop where two enzymes catalyse opposite directions of the same transformation (opposed e.g. kinase/phosphatase loops). At steady state, the sum of the branch fluxes equals the entry and exit fluxes.

D. Cycles

The structures above are all constructed from a number of type 1 linkages, i.e. single substrate, single product reactions. However, many metabolic reactions have multiple substrates and products and these can give rise to cycles (cycles with single substrate reactions would be closed with no entry and exit points and would therefore be of no metabolic significance). The simplest cycle is the type 2 linkage itself, as shown in figure 2.01. The most important consequence of cycles is that the total concentration of members of the cycles is constant in the absence of true branches in the cycle (true branches are the type in figure 2.02 (b), not the entry and exit reactions of the cycle seen in (d)). This is known as *moiety conservation* and is an important way in which the stoichiometry of the network can act to limit the networks behaviour (this is detailed in section 2.3.6).

2.3.4 Open Systems: Clamping Metabolites

When constructing systems from the elements above, it must be remembered that an essential feature of biological systems is that they are open. A biological system can interact with its environment through the exchange of mass and energy. It is therefore vital to understand how to define a system as open. For a model of a metabolic pathway to be open, there must be fluxes into and out of the system. These fluxes are referred to as source and sink fluxes respectively. Their effect is to provide the system with an inexhaustible supply of pathway substrate and an unsaturable pool of products. To understand how to model source and sink metabolites it is instructive to consider how experimentalists tackle the problem. Setting up open systems experimentally can be problematic, involving methods such as injecting substrate and removing products, or keeping substrate products so high that they are effectively constant. Fortunately, the methods available to the simulator are rather more convenient. The concentrations of all pathway source substrates and product sinks are defined as constant. This process is termed '*clamping*' the external metabolites (Hofmeyr 1986). Clamped metabolites are denoted by X_i while variable metabolites are labelled by S_i.

2.3.5 Diagramatic Representation of Reactions

To define a model, Hofmeyr's method for representing metabolic reactions has been adopted. An example is shown in figure 2.03, where S and X are used to represent both the names and concentrations of the metabolites.

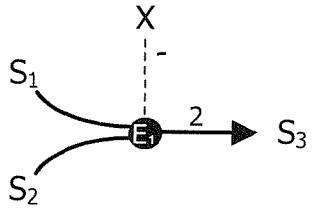

Figure 2.03: A representation of the enzymatic reaction $S_1 + S_2 \rightarrow 2S_3$.
Enzymes are circled, and chemical species are represented by a subscripted S (for variable metabolites) or X (for clamped metabolites – see text). Stoichiometric coefficients (when not unity) are associated with the line connecting a metabolite to an enzyme. Effectors are linked to the enzyme by broken lines and the type of effect indicated by + (activation) or – (inhibition) (Hofmeyr 1986).

2.3.6 Examples Structures

The examples that follow illustrate some of the consequences of putting the basic elements together and show how the balance equations and the stoichiometric matrices are constructed. This is rather trivial for some of these examples. However, the matrix method provides a systematic procedure that can be applied for more complex networks, so it is instructive to use it here.

The four networks to be examined are shown in figure 2.04, and include a linear chain, a branched chain, a network with multiple branches and loops and a network containing a simple cycle. For each case the stoichiometric matrix is constructed and then discussed.

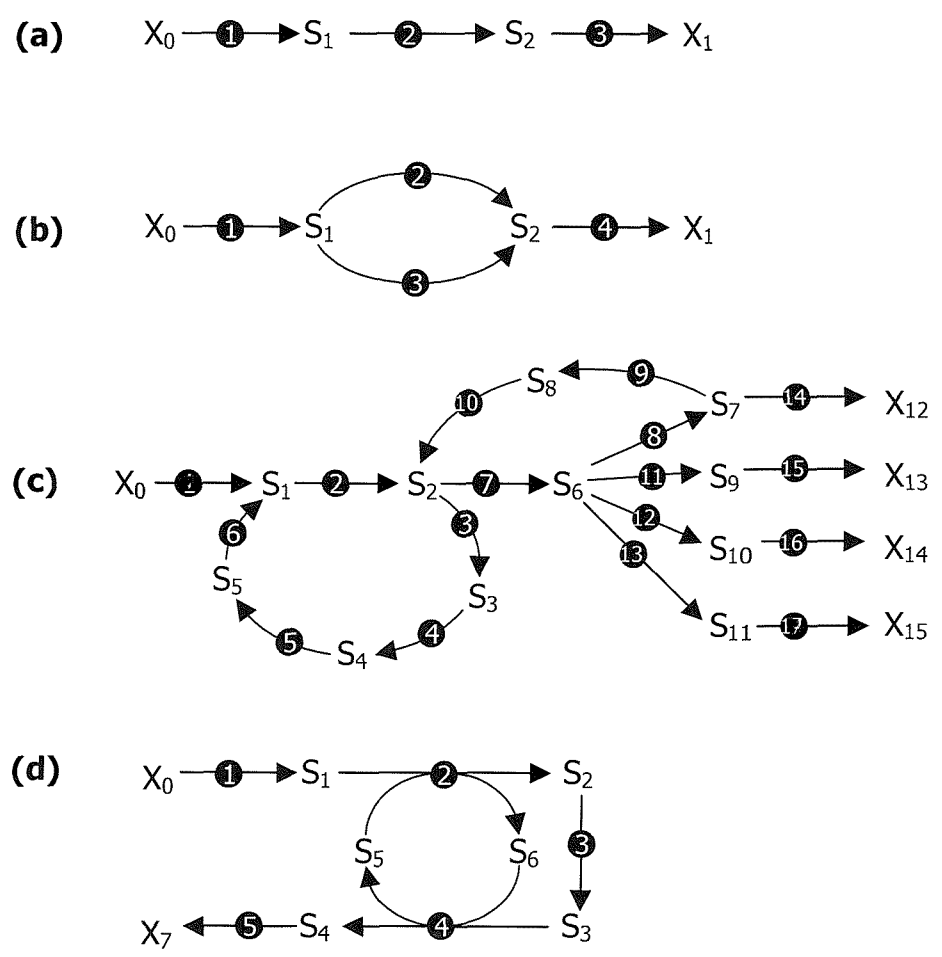

Figure 2.04: Four example networks categorised by the structures which they contain:
(a) Linear chain. **(b)** Branched chain. **(c)** Pathway with multiple branches and loops.
(d) Pathway containing a basic cycle.
The structures are chosen for illustrative purposes and do not represent real metabolic systems.

A. Linear chain

The network shown in figure 2.04 (a) is a simple linear chain. Inspection shows there is one flux through the network. The stoichiometric matrix is shown with the columns and rows labelled:

$$\begin{array}{c} \\ S_1 \\ S_2 \end{array} \begin{array}{c} \begin{array}{ccc} R1 & R2 & R3 \end{array} \\ \begin{pmatrix} 1 & -1 & 0 \\ 0 & 1 & -1 \end{pmatrix} \end{array}$$

The stoichiometric matrix contains the information from the two stoichiometric equations for S_1 and S_2. The first row describes that S_1 is the product of R1 and the substrate of R2. The second row contains the information that S_2 is produced by R2 and consumed by R3.

Extracting the stoichiometric equations, and equating each to zero, yields the balance equations. At steady state:

$$dS_1/dt = v_1 - v_2 = 0$$

$$dS_2/dt = v_2 - v_3 = 0$$

The two equations can be solved by inspection to give the result:

$$v_1 = v_2 = v_3$$

Clearly, if one flux is set, the others must be the same: the system has one *independent flux.* This is the easiest system to solve and has often served as the prototype of a metabolic pathway because the steady state may be solved analytically.

At the steady state, each reaction has the same flux since the metabolites have time-invariant concentrations only if their rates of production and consumption are balanced. In the next example, it is shown how simple branches give rise to a pathway with more than one steady state flux.

B. Branched chain

The network shown in figure 2.04 (b) is a branched pathway; specifically it is a parallel loop, with the conversion of S_1 to S_2 performed by two reactions. The stoichiometric matrix is:

$$\begin{array}{c} \\ S_1 \\ S_2 \end{array} \begin{array}{c} \begin{array}{cccc} R1 & R2 & R3 & R4 \end{array} \\ \begin{pmatrix} 1 & -1 & -1 & 0 \\ 0 & 1 & 1 & -1 \end{pmatrix} \end{array}$$

At steady state, the balance equations may be written:

$$dS_1/dt = 0 = v_1 - v_2 - v_3$$

$$dS_2/dt = 0 = v_2 + v_3 - v_4$$

The balance equations give the result:

$$v_1 = v_2 + v_3 = v_4$$

This is simply the formal statement that the sum of the branch fluxes equals both the entry and the exit fluxes. Note however that the stoichiometry of the network tells nothing about the relative flux through reactions 2 and 3. Here there are two independent fluxes. This means that, although there are different sets of fluxes from which the others may be found, the minimum number of fluxes that must be provided is two. Knowledge of any two independent fluxes allows the remainder to be found, as shown in figure 2.05. A suitable example set is v_1 and v_2 (v_3 is given by v_1 - v_2, v_4 from v_1). Note however, that v_1 and v_4 would not allow solution, since $v_1 = v_4$ these are not independent fluxes.

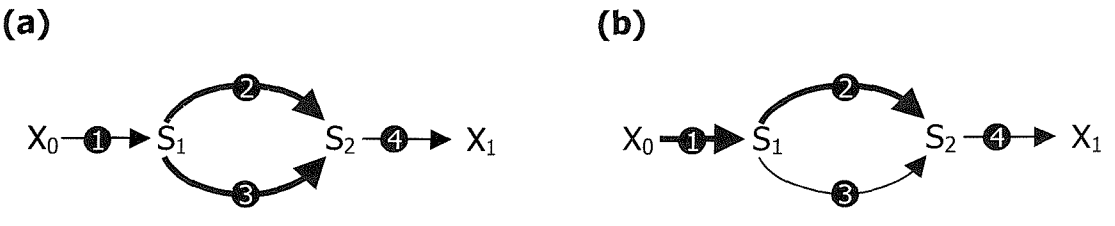

Figure 2.05: Independent fluxes.
Solution requires knowledge of one member of each independent flux group.
(a) Knowledge the two branch fluxes.
(b) Knowledge of one branch and the entry (or exit) flux.

C. Multiple branches and loops

The network shown in figure 2.04 (c) contains multiple branches and loops. With a structure of this complexity, it is appropriate to simplify the network before analysis. This can be achieved conveniently by treating each linear chain subunit as a single step. Using this method, the nodes represent only the branch point metabolites. The result of this simplification is shown in figure 2.06.

The number of independent fluxes (n_{inf}) was simple to find in the examples above. When the model is more complex, n_{inf} can be found using equation 2.08, where n_{enz} is the number of reactions and n_{var} the number of variable metabolites.

$$n_{inf} = n_{enz} - n_{var} \qquad \text{equation 2.08}$$

(Hofmeyr 1986)

The use of independent fluxes is illustrated by the following example. There are ten different steady state fluxes as shown in figure 2.06 (J_1 - J_{10}). Equation 2.08 reveals there are six independent fluxes (n_{enz} = 17, n_{var} = 11). There are different sets from which the others can be found, these require careful choice but the minimum number in each set is six. Two example sets are (J_1, J_3, J_4, J_6, J_8, J_9) and (J_3, J_5, J_6, J_8, J_9, J_{10}). The first set may be verified by inspection: knowledge of J_1 and J_3 sets J_2 (since it is the only unknown at the first branch point, node 1 in figure 2.06), similarly J_4 then sets J_7, J_8 then gives J_5, and finally J_6 and J_9 fix the value of J_{10}.

Again, the branched stoichiometry puts no constraints on the relative fluxes around the pathway. This information must be added to the network structure in order to solve for the fluxes. This will become clear in section 2.3.7, which details the methods by which the flux relationships are found.

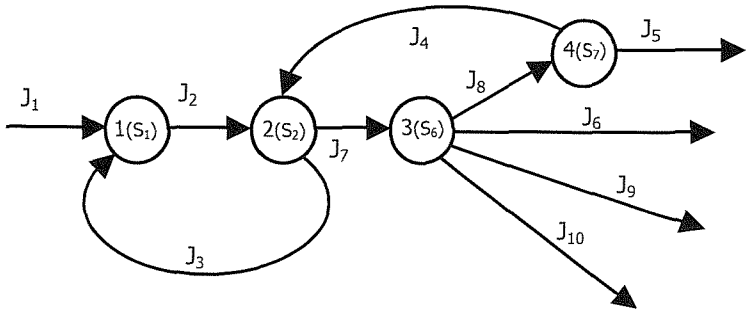

Figure 2.06: The Network from figure 2.04 (c) reduced to show only the branch points.
Branch point metabolites are shown as circles. The ten steady state fluxes (J_1-J_{10}) are also labelled.

D. Basic cycle: moiety conservation

The stoichiometric matrix for the pathway, containing a cycle, in figure 2.04 (d) is:

$$\begin{array}{c} \\ S_1 \\ S_2 \\ S_3 \\ S_4 \\ S_5 \\ S_6 \end{array} \begin{array}{c} \begin{array}{ccccc} R1 & R2 & R3 & R4 & R5 \end{array} \\ \begin{pmatrix} 1 & -1 & 0 & 0 & 0 \\ 0 & 1 & -1 & 0 & 0 \\ 0 & 0 & 1 & -1 & 0 \\ 0 & 0 & 0 & 1 & -1 \\ 0 & -1 & 0 & 1 & 0 \\ 0 & 1 & 0 & -1 & 0 \end{pmatrix} \end{array}$$

It can easily be seen that $v_1 = v_2 = v_3 = v_4 = v_5 = v_6$. There is only one (independent) flux since this is an unbranched structure; although it contains bimolecular reactions that create a cycle, it contains no true branches (each metabolite is created by one reaction and consumed by just one reaction). The type 2 linkages however, do cause other complications; careful inspection of the network structure reveals two conservation equations:

$S_5 + S_6 = c_1$

$S_2 + S_3 + S_5 = c_2$ where c_1 and c_2 are constants.

The features of the network that result in these conservation equations are shown clearly by the emphasis of the cycles in figure 2.07. If the balance equations (or rows of the matrix) for these species are summed the result is zero, since these rows are linear combinations of one another. This does not rely on the rows being set to zero, so these relationships therefore apply during transients as well as at steady state. Note that the stoichiometry of the network controls the maximum amount of $S_2 + S_3$ that can be present at any time; this control is due to the links that S_5 and S_6 form between reactions 2 and 4, as shown in figure 2.07.

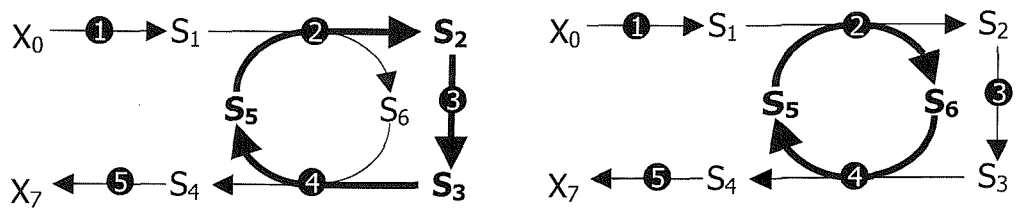

Figure 2.07: The pathway from figure 2.04 (d) with moiety conservation highlighted.

2.3.7 Solving for the Steady State Fluxes

To construct a simulation to reach a specific steady state it is necessary to find a set of parameters (reaction coefficients) that give this steady state.

A. Solving by inspection

Using simple mass action kinetics:

$$S_1 \rightarrow S_2$$
$$v_1 = k_1.S_1$$

It is simple to find k_1 from the flux, v_1. The problem therefore becomes one of finding the *flux distribution* through the pathway. For the linear chain pathway in figure 2.04 (a), inspection reveals that $v_1 = v_2 = v_3$ (as shown in section 2.36). For the parallel loop pathway in figure 2.04 (b), inspection shows $v_1 = v_2 + v_3 = v_4$. More information is required in order to find the flux distribution (the knowledge of two independent fluxes, this will be discussed in the examples later in this section).

B. Solving from the stoichiometric matrix

Solution by inspection becomes extremely difficult for large branched and/or looped pathways. For these complex models, it is most convenient to have a systematic procedure. The results found by inspection above may also be found by rearranging and combining the balance equations, as seen earlier. It follows that the result may also be obtained by 'solving' the stoichiometric matrix, which contains the same information. The key to finding the flux relationships from the stoichiometric matrix is the conversion of the matrix to its *row echelon form.*

The row-echelon and reduced row-echelon forms of a matrix

A matrix $A=[a_{ij}]$ is said to be in *row-echelon form (REF)* if $a_{ij} = 0$ for $i > j$. For a matrix in row-echelon form:

1. All zero rows are at the bottom.
2. The first non-zero entry from the left in each non-zero row is 1, the *leading 1* for that row.
3. Each leading 1 is to the right of the leading 1's in the rows above.

Examples: (a) $\begin{pmatrix} 1 & -2 & -2 & 3 \\ 0 & 1 & 3 & 17 \\ 0 & 0 & 1 & 5 \end{pmatrix}$ (b) $\begin{pmatrix} 1 & -2 & -2 \\ 0 & 1 & 3 \\ 0 & 0 & 1 \end{pmatrix}$

If a square matrix is in row-echelon form, as in (b), it is called *upper triangular*.

Why echelon form? Importantly all non-zero rows are linearly independent, i.e. not combinations of other rows. Suppose a matrix A can be carried to a matrix R in row-echelon form by a series of elementary row operations. The rank of A is equal to the number of non-zero rows of R; the significance of this will be shown in the solution of the examples that follows.

The *Reduced Row-Echelon Form* (RREF) is a matrix in row-echelon form with each leading 1 being the *only* non-zero entry in its column.

Examples: (c) $\begin{pmatrix} 1 & 0 \\ 0 & 1 \end{pmatrix}$ (d) $\begin{pmatrix} 1 & 0 & 0 \\ 0 & 1 & 0 \\ 0 & 0 & 1 \end{pmatrix} \begin{pmatrix} v_1 \\ v_2 \\ v_3 \end{pmatrix} = \begin{pmatrix} x \\ x \\ x \end{pmatrix}$

In the RREF form, as will be shown in the examples which follow, the matrix is solved. In example (d) above it is simple to find the values of v_1, v_2 and v_3 by rewriting the matrix as three equations: $v_1 = x$, $v_2 = x$ and $v_3 = x$.

Converting to the reduced row-echelon form

Conversion to the REF and RREF is achieved using the three *row operations:*

1. Multiply a row by a non-zero constant.
2. Replace a row by itself plus a multiple of another row.
3. Exchange Rows.

It is always possible, using these methods, to put a matrix into its REF. This will be illustrated by reducing the stoichiometric matrices for some examples.

C. Examples applied to simple metabolic pathways

The following details the reduction to the RREF of the stoichiometric matrices for the example networks in figure 2.04. Some are again trivial, but they illustrate the method and provide a systematic method when the model is complex.

Linear Chain

For the example in figure 2.04 (a) the stoichiometric matrix is:

$$\begin{array}{c} \\ S_1 \\ S_2 \end{array} \begin{array}{c} \begin{array}{ccc} R1 & R2 & R3 \end{array} \\ \begin{pmatrix} 1 & -1 & 0 \\ 0 & 1 & -1 \end{pmatrix} \end{array}$$

Note the stoichiometric matrix is already in row-echelon form (REF). In this form inspection shows:

$v_1 = v_2$ (from the balance for S_1)

$v_2 = v_3$ (from the balance for S_2)

$\therefore$ $v_1 = v_2 = v_3$

To explicitly solve the system it is necessary to provide at least one flux. If $v_3 = x$, where x is any value, clearly the solution will be $v_1 = v_2 = v_3 = x$. The balance equations (with $v_3 = x$ as an additional equation) may be written as a matrix, which may be more conveniently represented and manipulated as a *detached coefficient tableau* (Kemeny *et al.* 1966, p.257):

$$\begin{pmatrix} 1 & -1 & 0 \\ 0 & 1 & -1 \\ 0 & 0 & 1 \end{pmatrix} \begin{pmatrix} v_1 \\ v_2 \\ v_3 \end{pmatrix} = \begin{pmatrix} 0 \\ 0 \\ x \end{pmatrix} \quad \text{or} \quad \left(\begin{array}{ccc|c} 1 & -1 & 0 & 0 \\ 0 & 1 & -1 & 0 \\ 0 & 0 & 1 & x \end{array}\right)$$

detached coefficient tableau form

The first two rows are from the stoichiometric matrix, the third line sets $v_3 = x$. The matrix is in the REF already, converting to the RREF is performed as follows (the operations shown are performed on the previous tableau to give the new tableau, the arrow should be taken to mean 'is replaced with'):

operation	
	$\left(\begin{array}{ccc\|c} 1 & -1 & 0 & 0 \\ 0 & 1 & -1 & 0 \\ 0 & 0 & 1 & x \end{array}\right)$
row 2 → row 2 + row 3	$\left(\begin{array}{ccc\|c} 1 & -1 & 0 & 0 \\ 0 & 1 & 0 & x \\ 0 & 0 & 1 & x \end{array}\right)$

row 1 → row 1 + row 2

$$\left(\begin{array}{ccc|c} 1 & 0 & 0 & x \\ 0 & 1 & 0 & x \\ 0 & 0 & 1 & x \end{array}\right)$$

in matrix form

$$\begin{pmatrix} 1 & 0 & 0 \\ 0 & 1 & 0 \\ 0 & 0 & 1 \end{pmatrix} \begin{pmatrix} v_1 \\ v_2 \\ v_3 \end{pmatrix} = \begin{pmatrix} x \\ x \\ x \end{pmatrix}$$

This gives $v_1 = x$, $v_2 = x$, $v_3 = x$ or $v_1 = v_2 = v_3 = x$, the result given by inspection.

Branched Chain

For the example in figure 2.04 (b) the stoichiometric matrix is:

$$\begin{array}{c} \\ S_1 \\ S_2 \end{array} \begin{array}{c} \begin{array}{cccc} R1 & R2 & R3 & R4 \end{array} \\ \begin{pmatrix} 1 & -1 & -1 & 0 \\ 0 & 1 & 1 & -1 \end{pmatrix} \end{array}$$

Note the stoichiometric matrix is again in row-echelon form (REF). Inspection shows $v_1 = v_2 + v_3 = v_4$. If it is specified that $v_4 = x$, then the detached coefficient tableau may be written:

$$\left(\begin{array}{cccc|c} 1 & -1 & -1 & 0 & 0 \\ 0 & 1 & 1 & -1 & 0 \\ 0 & 0 & 0 & 1 & x \end{array}\right)$$

This matrix is in REF but it is not a square matrix and so cannot be converted to RREF to give a full solution. However, it can be manipulated to give a partial solution:

row 2 → row 2 + row 3

$$\left(\begin{array}{cccc|c} 1 & -1 & -1 & 0 & 0 \\ 0 & 1 & 1 & 0 & x \\ 0 & 0 & 0 & 1 & x \end{array}\right)$$

row 1 → row 1 + row 2

$$\left(\begin{array}{cccc|c} 1 & 0 & 0 & 0 & x \\ 0 & 1 & 1 & 0 & x \\ 0 & 0 & 0 & 1 & x \end{array}\right)$$

This partial solution again gives the result obtained from inspection. For a complete solution, either two independent fluxes (eg $v_4 = x$, $v_2 = y$), or the exit (or entry) flux and the ratio of v_2 and v_3 (the branch fluxes), must be provided. If $v_2 = \frac{1}{3}v_3$ is given, an extra row may be inserted into the matrix (which already contains $v_4 = x$) giving the square matrix:

$$\left(\begin{array}{cccc|c} 1 & 0 & 0 & 0 & x \\ 0 & 1 & 1 & 0 & x \\ 0 & 1 & -1/3 & 0 & 0 \\ 0 & 0 & 0 & 1 & x \end{array}\right)$$

row 3 → row 2 – row 3

$$\left(\begin{array}{cccc|c} 1 & 0 & 0 & 0 & x \\ 0 & 1 & 1 & 0 & x \\ 0 & 0 & 4/3 & 0 & x \\ 0 & 0 & 0 & 1 & x \end{array}\right)$$

row 3 → ¾(row 3)

$$\left(\begin{array}{cccc|c} 1 & 0 & 0 & 0 & x \\ 0 & 1 & 1 & 0 & x \\ 0 & 0 & 1 & 0 & \frac{3}{4}x \\ 0 & 0 & 0 & 1 & x \end{array}\right)$$

row 2 → row 2 – row 3

$$\left(\begin{array}{cccc|c} 1 & 0 & 0 & 0 & x \\ 0 & 1 & 0 & 0 & \frac{1}{4}x \\ 0 & 0 & 1 & 0 & \frac{3}{4}x \\ 0 & 0 & 0 & 1 & x \end{array}\right)$$

This solution satisfies $v_4 = x$, $v_2 = \frac{1}{3}v_3$ (set by the additions to the matrix) and $v_1 = v_2 + v_3 = v_4$ (set by the stoichiometry of the network). Note that due to the presence of two independent fluxes an additional equation was necessary.

Multiple Branches and Loops

The two previous examples have illustrated the information that must be provided to permit a solution. However, the solutions have been easy to find by inspection. Here the method is used to find a suitable set of fluxes for the multiple-branched pathway in figure 2.04 (c). Using the pathway simplified to show only the fluxes between the branch points, as in figure 2.06, reduces the size of the matrix from 17x17 to 10x10:

$$\left(\begin{array}{cccccccccc|c} 1 & -1 & 1 & 0 & 0 & 0 & 0 & 0 & 0 & 0 & 0 \\ 0 & 1 & -1 & 1 & 0 & 0 & -1 & 0 & 0 & 0 & 0 \\ 0 & 0 & 0 & 0 & 0 & -1 & 1 & -1 & -1 & -1 & 0 \\ 0 & 0 & 0 & -1 & -1 & 0 & 0 & 1 & 0 & 0 & 0 \\ 1 & 0 & 0 & 0 & 0 & 0 & 0 & 0 & 0 & 0 & 1 \\ 0 & 0 & 1 & 0 & 0 & 0 & -1 & 0 & 0 & 0 & 0 \\ 0 & 0 & 0 & 0 & 0 & -1 & 0 & 1 & 0 & 0 & 0 \\ 0 & 0 & 0 & 0 & 0 & 0 & 0 & 1 & -1 & 0 & 0 \\ 0 & 0 & 0 & 0 & 0 & 0 & 0 & 1 & 0 & -1 & 0 \\ 0 & 0 & 0 & 1 & -1 & 0 & 0 & 0 & 0 & 0 & 0 \end{array}\right)$$

1. SS Balance for branch point 1
2. SS Balance for branch point 2
3. SS Balance for branch point 3
4. SS Balance for branch point 4
5. Input flux (J_1) = 1
6. $J_3 = J_7$
7. $J_8 = J_6$
8. $J_8 = J_9$
9. $J_8 = J_{10}$
10. $J_4 = J_5$

The first four rows are the balance equations at branch points 1 - 4. The fifth row sets $J_1 = 1$. Rows six to ten set all exit fluxes from each branch equal e.g. for branch point 3 in figure 2.06, $J_8 = J_6 = J_9 = J_{10}$. The appended matrix can be converted to the RREF. With a matrix of this size, this is most easily achieved using a matrix solver:

$$\left(\begin{array}{cccccccccc|c} 1 & 0 & 0 & 0 & 0 & 0 & 0 & 0 & 0 & 0 & 1 \\ 0 & 1 & 0 & 0 & 0 & 0 & 0 & 0 & 0 & 0 & 2.1429 \\ 0 & 0 & 1 & 0 & 0 & 0 & 0 & 0 & 0 & 0 & 1.1429 \\ 0 & 0 & 0 & 1 & 0 & 0 & 0 & 0 & 0 & 0 & 0.1429 \\ 0 & 0 & 0 & 0 & 1 & 0 & 0 & 0 & 0 & 0 & 0.1429 \\ 0 & 0 & 0 & 0 & 0 & 1 & 0 & 0 & 0 & 0 & 0.2857 \\ 0 & 0 & 0 & 0 & 0 & 0 & 1 & 0 & 0 & 0 & 1.1429 \\ 0 & 0 & 0 & 0 & 0 & 0 & 0 & 1 & 0 & 0 & 0.2857 \\ 0 & 0 & 0 & 0 & 0 & 0 & 0 & 0 & 1 & 0 & 0.2857 \\ 0 & 0 & 0 & 0 & 0 & 0 & 0 & 0 & 0 & 1 & 0.2857 \end{array}\right)$$

$J_1 = 1$
$J_2 = 2.1429$
$J_3 = 1.1429$
$J_4 = 0.1429$
$J_5 = 0.1429$
$J_6 = 0.2857$
$J_7 = 1.1429$
$J_8 = 0.2857$
$J_9 = 0.2857$
$J_{10} = 0.2857$

The flux solution is shown in figure 2.08. Clearly, for this pathway balancing the fluxes by trial and error would be a lengthy process.

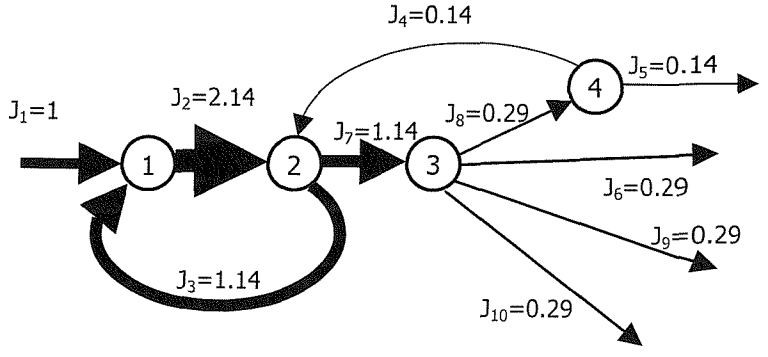

Figure 2.08: Flux in the model (network reduced to show only the branch points as figure 2.06). The weight of the arrows represents the relative flux at steady state.

Simple Cycle: moiety conservation

It is useful to compare the examples of the linear and branched chains. When the branch was added there was one extra reaction (a variable, and column of the matrix) but the same number of metabolites (each provides a balance equation, a row of the matrix). So in order to form a square matrix to allow reduction to RREF, an extra equation was required.

In contrast, when cycles are present, these are constructed with bimolecular reactions, and so there are extra species (extra rows in the matrix) but no extra reactions (columns in the matrix). There are more rows than columns. This results in rows that are not *linearly independent*; these rows are combinations of other rows and will therefore be eliminated when reducing to the RREF. Here the stoichiometric matrix is reduced for an example, to show the consequences of this.

Using the pathway in figure 2.04 (d), the stoichiometric matrix is:

$$\begin{array}{c} \\ S_1 \\ S_2 \\ S_3 \\ S_4 \\ S_5 \\ S_6 \end{array} \begin{array}{c} \begin{array}{ccccc} R1 & R2 & R3 & R4 & R5 \end{array} \\ \begin{pmatrix} 1 & -1 & 0 & 0 & 0 \\ 0 & 1 & -1 & 0 & 0 \\ 0 & 0 & 1 & -1 & 0 \\ 0 & 0 & 0 & 1 & -1 \\ 0 & -1 & 0 & 1 & 0 \\ 0 & 1 & 0 & -1 & 0 \end{pmatrix} \end{array}$$

Converting to the REF, rows 5 and 6 become zero rows since they are linear combinations of rows 2 and 3.

$$\begin{array}{c} \\ S_1 \\ S_2 \\ S_3 \\ S_4 \\ S_5 \\ S_6 \end{array} \begin{array}{c} \begin{array}{ccccc} R1 & R2 & R3 & R4 & R5 \end{array} \\ \begin{pmatrix} 1 & -1 & 0 & 0 & 0 \\ 0 & 1 & -1 & 0 & 0 \\ 0 & 0 & 1 & -1 & 0 \\ 0 & 0 & 0 & 1 & -1 \\ 0 & 0 & 0 & 0 & 0 \\ 0 & 0 & 0 & 0 & 0 \end{pmatrix} \end{array}$$

Setting $v_1 = x$ and solving:

$$\left(\begin{array}{ccccc|c} 1 & 0 & 0 & 0 & 0 & x \\ 1 & -1 & 0 & 0 & 0 & 0 \\ 0 & 1 & -1 & 0 & 0 & 0 \\ 0 & 0 & 1 & -1 & 0 & 0 \\ 0 & 0 & 0 & 1 & -1 & 0 \end{array}\right)$$

row 2 → row 1 – row 2

$$\left(\begin{array}{ccccc|c} 1 & 0 & 0 & 0 & 0 & x \\ 0 & 1 & 0 & 0 & 0 & x \\ 0 & 1 & -1 & 0 & 0 & 0 \\ 0 & 0 & 1 & -1 & 0 & 0 \\ 0 & 0 & 0 & 1 & -1 & 0 \end{array}\right)$$

Doing the same for rows 3 & 2, 4 & 3 and 5 & 4, the RREF is obtained:

$$\left(\begin{array}{ccccc|c} 1 & 0 & 0 & 0 & 0 & x \\ 0 & 1 & 0 & 0 & 0 & x \\ 0 & 0 & 1 & 0 & 0 & x \\ 0 & 0 & 0 & 1 & 0 & x \\ 0 & 0 & 0 & 0 & 1 & x \end{array}\right)$$

This shows $v_1 = v_2 = v_3 = v_4 = v_5 = v_6 = x$. So the moiety conserved cycle poses no problems for finding the flux relationship. However, when solving for the steady state by solving the roots of the balance equations directly (e.g. by Newton Raphson) there is insufficient information since there are less linearly independent rows than there are variable metabolites. The number of linearly independent rows is described by the rank of the matrix. In equation 2.09 n_{var} is the number of variable metabolites, r is the rank of the matrix and n_{cons} is the number of conserved sets of species.

$$n_{var} = r + n_{cons} \qquad \text{equation 2.09}$$

In the example in figure 2.04 (d), equation 2.09 gives $n_{cons} = 2$ ($n_{var} = 6$, $r = 4$), these were emphasised in figure 2.07. To solve the system, two of the balance equations must be replaced by the two conservation relations for the system. In most cases, this is performed by the simulation package used. Further details on the handling of moiety-conserved systems may be found in the literature (Cascante *et al.* 1996).

2.3.8 Robustness

In the simple structures examined, it has been noted how the stoichiometry of the network can limit metabolite concentrations and define the flux relationships. This section will discuss in more detail how the stoichiometry can influence the stability of the pathway. This has been termed *robustness*, but what is meant by this? In this work, robustness refers to the ability of a network to maintain a property within reasonable limits upon changes in the parameters of the system. For the specific model developed here, this is generally with respect to the stored elastic energy.

It has been argued that the key properties of biochemical networks should be robust in order to ensure their proper functioning (Barkai & Leibler 1997). In addition, the survival of living systems implies that the critical parameters are robust (Hartwell *et al.* 1999). This seems preferable to the alternative possibility that the rate constants and enzyme concentrations need to be precisely set, with any departure adversely affecting the networks functioning. However, it is important to note that robustness can be a characteristic of specific network properties and not the network as a whole. Some properties may be robust, whilst others remain sensitive to changes in the networks parameters (Barkai & Leibler 1997).

Here, some of the factors that may influence the robustness, through the construction of the network and the addition of integrative feedback, are outlined. This brief discussion will simply cover the basic features that help in the understanding of the work in this thesis. The first feature examined is the connectivity of a network and the difficulties associated in defining this property, particularly when considering metabolic networks*. Following this, factors that can provide stoichiometric control such as redundancy, leakage and plurifunctional cofactors are considered before looking at non-stoichiometric control.

---

* *The ideas on connectivity alone could form a project in their own right. More detail on robustness and connectivity may be found in the references given in this section. A more general and in-depth discussion may be found in 'Linked: The New Science of Networks'* (Barabasi 2002).

A. Connectivity of the stoichiometric network

One of the key problems in discussing connectivity is the difficulty in quantifying the property. Even in a simple system of nodes and vertices there is no single parameter that effectively describes all aspects of connectivity. Graph theory provides a number of parameters, the simplest being the average number of connections per vertex. The problem with using this as a measure of connectivity is shown in figure 2.09 (Morowitz *et al.* 1964). The two networks have the same average number of connections per vertex, but in (a) each node has one or two vertices, whereas in (b) one node has five vertices. The property that varies is the distribution of vertices. With large networks, the distribution of connections must be described statistically, using terms such as *exponential* or *scale-free*. The significance of the distribution of vertices is highlighted in studies looking at the connectivity properties of exponential and scale free networks which examine the resistance to attack and susceptibility to random failure (Albert *et al.* 2000).

Of course, further complications arise because metabolic pathways are not simple vertex and node systems. The vertices are replaced by reactions which all operate at different rates specific to the steady state. Clearly, this will affect the degree of connection. Furthermore, the nodes represent metabolites and the concentrations of these can vary. The reaction rates are a function of the kinetic constants and the metabolite concentrations, so clearly the connectivity will also be a function of these variables (Strogatz 2001). Interestingly, this may give a way of choosing the independent fluxes through a pathway. With investigation into how flux distribution influences connectivity, the relative fluxes at branch points could be chosen to maximise the connectivity. Steps with multiple substrates and products must also be considered. These allow cycles and loops, and can make a system more connected.

Figure 2.09: Effect of distribution of vertices on connectivity. Two networks with the same number of vertices per node but different connection properties (Morowitz *et al.*, 1964).

Even without a quantitative measure of connectivity, some general observations can be made (Morowitz *et al.* 1964). To illustrate this, a simple system with two inputs and two outputs connected by two intermediates can be considered. For this illustration, the simple node and vertex model will be used. If a system is defined with two inputs, two intermediates and two outputs then a range of connectivity can be added. Schematics are shown in figure 2.10 for a minimally connected network, a maximally connected network and a network with an intermediate level of connection:

In a *minimally connected* system, there are no lateral connections. One reaction sequence leads from each input to its corresponding output; there are no intermediates common to two or more pathways since there are no lateral connections. The network may be qualitatively described as *sparse.*

In an *intermediately connected* system, every substance can be produced from every other substance through a sequence of n reactions (n = 1,2,....) (this has been termed completely connected, but intermediate is preferable since it represents a range of connectivity between the minimally and maximally connected extremes).

In a *maximally connected* system, each substance can be produced from every other substance in a single reaction. The network may be qualitatively described as *saturated.*

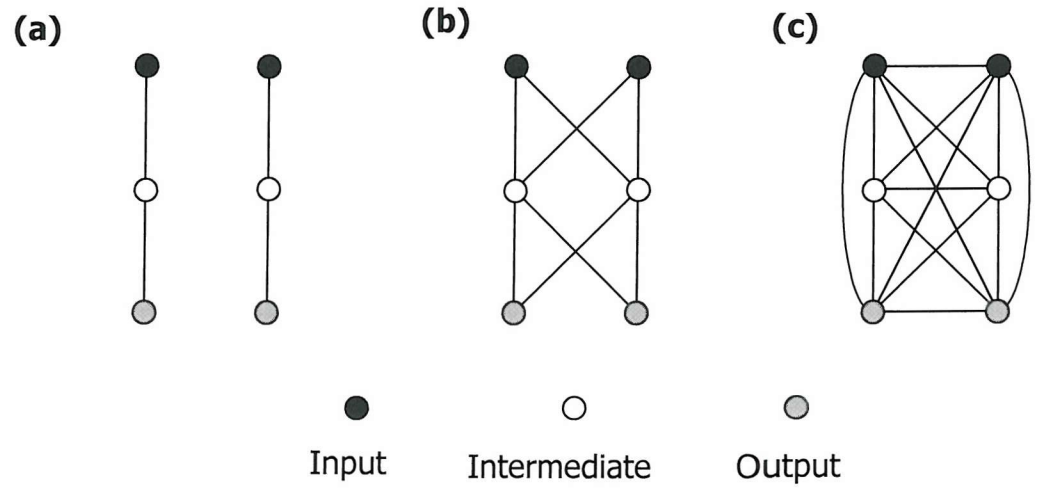

Figure 2.10: Schematics of three systems with different connectivities.
Each network has two inputs (black), two intermediates (white) and two outputs (grey).
(a) Minimally connected. **(b)** Intermediately connected. **(c)** Maximally connected.

B. A balance of robustness and connectivity

In the absence of a measure of connectivity, general statements can nevertheless be made about the effect of connectivity on robustness and efficiency. It is possible to consider the qualitative differences between minimally and maximally connected systems:

> A minimally connected system is *maximally efficient*, since it uses the minimum number of enzymes, but *minimally robust*; it is vulnerable since interruption of any step completely severs the pathway.
>
> A maximally connected system is *maximally robust*. Interruption of any step can be compensated for by flow through alternative steps. With many alternative pathways, the overall performance should be minimally altered. However, the system is *minimally efficient*; many enzymes are required and material will proceed through many metabolite pools between input and output.

Due to this competition between robustness and efficiency, a metabolic system would be expected to reside between these two extremes. High connectivity and communication is desirable. However, it would be unrealistic to have enzymes available to convert every species into every other species, the number of enzymes required would grow rapidly with the size of the system (in proportion to the square of the number of species); this would be inefficient with respect to the energetic costs and the less than complete reaction yields.

For a given system size, there should be an optimum level of connectivity which gives an ideal compromise between stability and robustness. It is difficult to be quantitative about this. The problems of measuring connectivity have already been mentioned. In addition, measures of robustness and efficiency would be required. These would vary from system to system and with the system properties under consideration as stated previously.

The remainder of this section looks at a number of features of metabolic pathways that can be important in designing, and analysing the structures and behaviour of, their stoichiometric networks.

C. Redundancy

Redundancy is a useful concept when considering the robustness and connectivity of a pathway. A section of a pathway has redundancy if there is more than one route for the conversion performed by that section.

Figure 2.11 illustrates the effect of different levels of redundancy. In figure 2.11(a), removal of a reaction (R5) causes the intermediate S_3 to grow in an uncontrolled manner. In figure 2.11 (b), an extra reaction (R7) is added to provide redundancy for the conversion of the intermediate to the end product of the pathway. This redundancy prevents the uncontrolled growth of S_3.

A consequence of lack of redundancy will be amplified sensitivity. In (a) R5 is essential to the pathways proper functioning, but in (b) it is not. The system in (a) will be more sensitive to the rate R5 than the system in (b). Examination of redundancy caused by the branching structure can therefore be of importance when looking at control of a pathway.

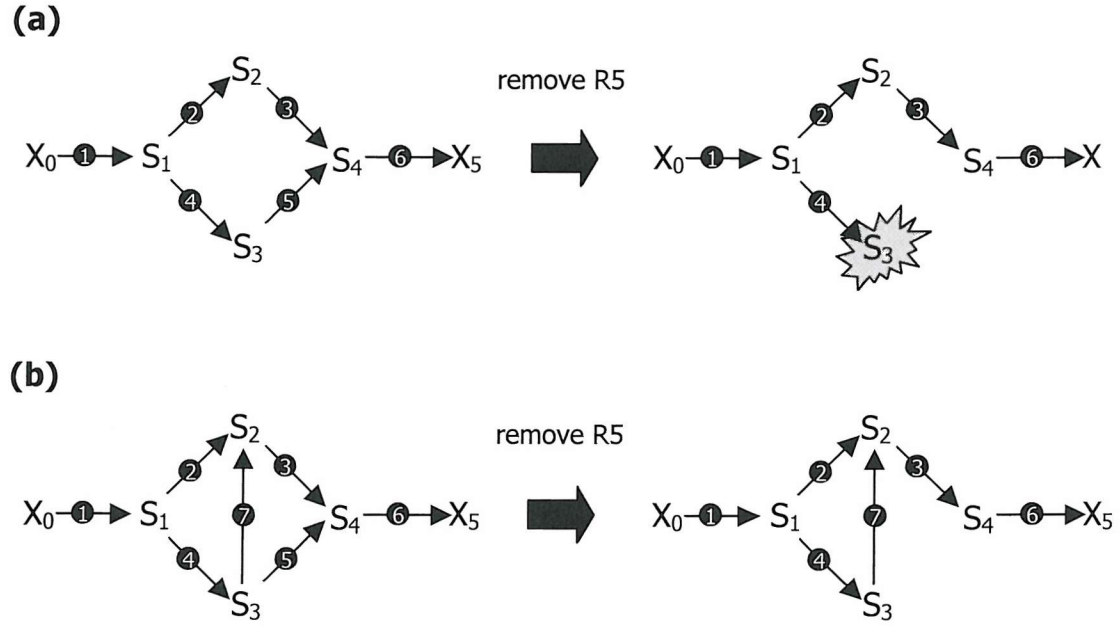

Figure 2.11: Benefits of redundancy.
Two similar systems with different levels of redundancy. **(a)** If R5 is removed the intermediate S_3 grows in an uncontrolled manner since there is no other step that consumes it. **(b)** If step R5 is removed the pathway is still viable due to the redundancy (R5 or R7 may be removed).

D. The importance of bimolecular reactions: concentration and flux limitation by plurifunctional cofactors

Bimolecular reactions allow the formation of moiety-conserved cycles, which can put stoichiometric limits on metabolite concentrations. Cofactors as well as being conserved may be plurifunctional; that is they may participate in multiple reactions. Such metabolites, e.g. ATP or CoA, can thus limit sums of fluxes. Many metabolic pathways involve one or more of these cofactors and often they are plurifunctional (Morowitz *et al.* 1964) within the pathway. For example, in the model of fermentation in figure 2.12 (Hofmeyr 1986) S_7 and S_8 link the fluxes of all the reactions and the metabolite concentrations providing stoichiometric control. Figure 2.13 shows the possible configurations of plurifunctional cofactors.

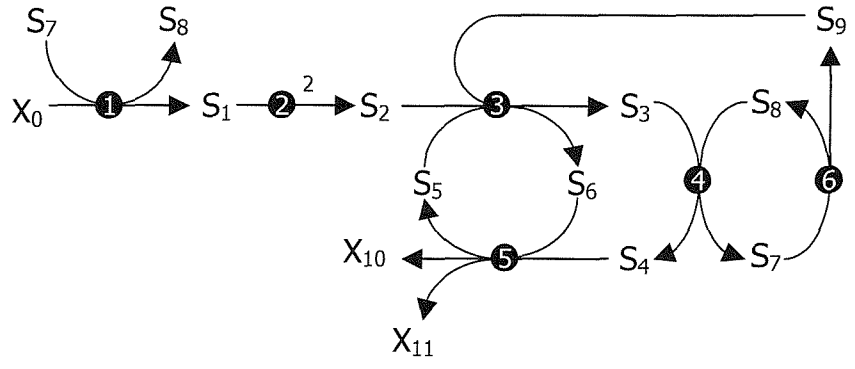

Figure 2.12: Network structure from a simple model of fermentation.
The network involves two sets of cofactors, one of which is plurifunctional (S_7 and S_8).

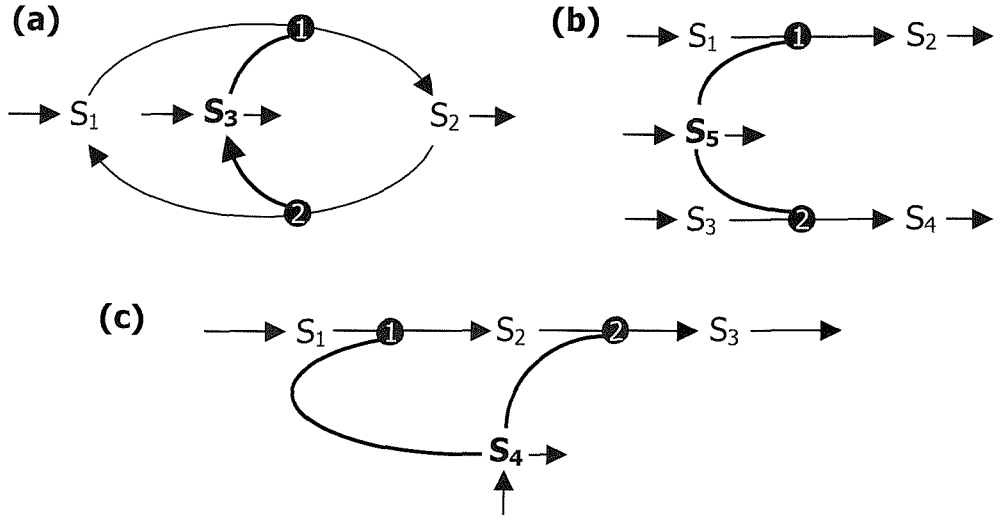

Figure 2.13: Structures for plurifunctional cofactors. **(a)** Opposed. **(b)** Parallel. **(c)** Consecutive. In complex networks, one metabolite can exhibit all three configurations.

E. Non-stoichiometric connectivity: elusive control

Previously it has been supposed that enzymes catalysing reactions that are far from equilibrium should exert most of the flux control. The reason for attributing control to irreversible reactions was that reactions near to equilibrium are highly responsive to changes in the substrate and product concentrations; an increase in activity would be countered by the subsequent decrease in substrate concentration and increase in product concentration. However, in biological systems, reactions that are far from equilibrium may be exquisitely sensitive to metabolite concentrations, for example via allosteric regulation. The metabolites act as feedback control for the enzyme thus removing control from the particular step. This can distribute control and increase the robustness of the pathway. This is summarised in figure 2.14 (Westerhoff *et al.* 1995).

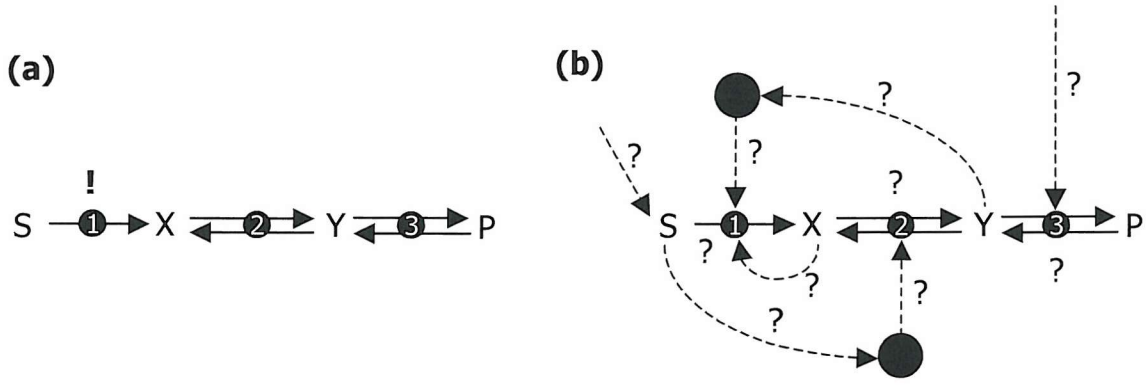

Figure 2.14: Elusive control.
(a) Control in a metabolic pathway is often attributed to the first enzyme catalysing an irreversible reaction. **(b)** Illustrates the complexity that may better reflect reality. Control may be distributed over the enzymes of the pathway, and control mechanisms that adjust the concentration or activity of the enzymes, or hide in hierarchical control mechanisms beyond the pathway.

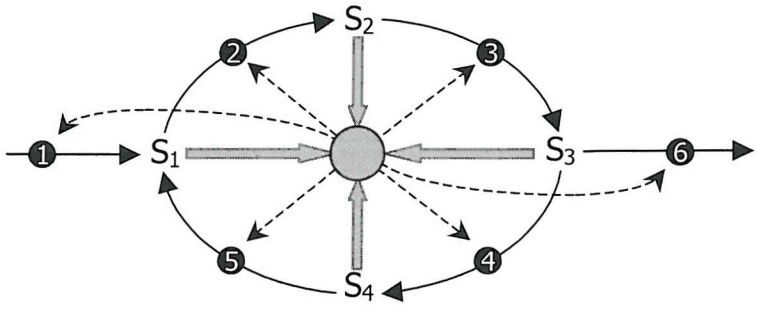

Figure 2.15: Non-specific effects can dramatically increase the connectivity of a pathway.
The physical factor (represented by the grey circle) is dependent on each of the metabolites present (grey arrows) and acts upon each of the enzymes, modulating the reactions (dotted arrows).

Simple enzyme behaviour can increase the connectivity of the pathway. When there is a non-specific mechanism acting on many enzymes, such as the membrane torque tension under study in this project, the extra connectivity may be very significant (see figure 2.15) and can allow a robust network with a small number of enzymes. This allows robustness a victory against the drive for maximum efficiency.

F. Saturation phenomena

With saturation of flux, the upper limit is imposed not by the substrate concentration but by the amount of enzyme present. This can be a stabilising factor, since a reaction cannot rapidly drain the system. However, it could also cause vulnerability of the system due to over flooded pools, since with saturation the rate cannot increase to counter the excess in a metabolite pool. These opposing effects again suggest a trade off, giving an intermediate, optimal amount of flux saturation in a pathway.

G. Leakage

Leakage is essentially a non-functional output with respect to the pathway's function. Leakage is however important as it can prevent concentrations from growing without limit until the system is destroyed. Absence of leakage in a system that is less than maximally connected can make the system vulnerable. This is shown in figure 2.16. However high leakage can cause inefficiency, preventing material from reaching the output, so it would be expected that there is again a trade off between robustness and efficiency leading to an optimum level of leakage.

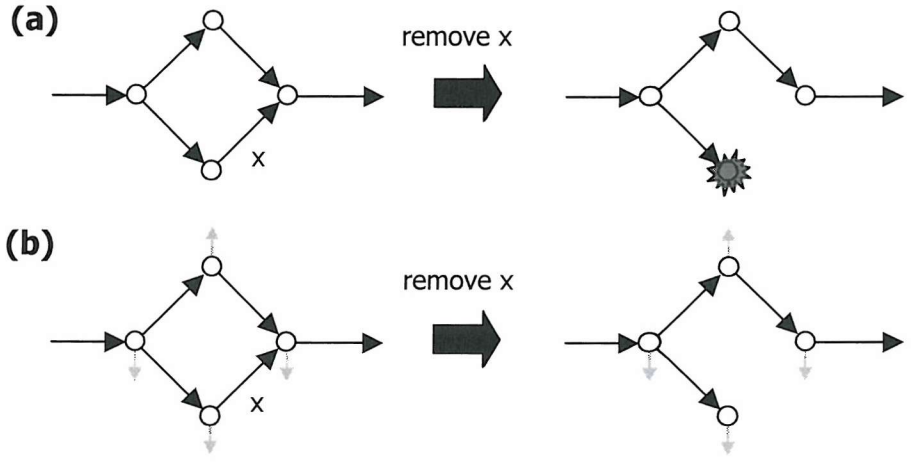

Figure 2.16: Benefits of leakage. The diagrams show leakage can save the system. In (a) removal of the step marked x causes the substrate to grow uncontrolled. Leakage from the network in (b) can prevent this. Leakage can therefore be valuable in the definition of a model.

2.4 Summary

The methods presented allow simulation of networks of reactions. Consideration of the example pathways has illustrated some of the problems faced when building such systems. In the next chapter, the specifics of the model developed in this work are explained.

2.5 References

Albert R, Jeong H & Barabasi A-L (2000)
Error and attack tolerance of complex networks.
Nature **406**: 378-382.

Atkins PW (1994) *Physical Chemistry*
Fifth edition. Oxford University Press.

Barabasi A-L (2002) *Linked: The new science of networks*
First edition. Perseus Books.

Barkai N & Leibler S (1997)
Robustness in Simple Biochemical Networks.
Nature **387**: 913-917.

Cascante M, Puigjaner J & Kholodenko B (1996)
Steady-State Characterization of Systems with Moiety-Conservations Made Easy: Matrix Equations of Metabolic Control Analysis and Biochemical System Theory.
J. theor. Biol **178**: 1-6.

Fell DA (1992)
Metabolic Control Analysis: a survey of its theoretical and experimental development.
Biochem. J. **286**: 313-330.

Garfinkel D (1981)
Computer modeling of metabolic pathways.
Trends. Biochem. Sci. **6**: 69-71.

Gear GW (1971) *Numerical Initial Value Problems in Ordinary Differential Equations*
New Jersey: Prentice-Hall.

Hartwell LH, Hopfield JJ, Leibler S & Murray AW (1999)
From molecular to modular cell biology.
Nature **402**: C47-C52.

Heinrich R, Rapoport SM & Rapaport TA (1977)
Metabolic Regulation and Mathematical Models.
Prog. Biophys. Molec. Biol. **32**: 1-82.

Hofmeyr JHS (1986)
Steady-state modelling of metabolic pathways: A guide for the prospective simulator.
Comput. Appl. Biosci. **2**: 5-11.

Hofmeyr JHS (1995)
Metabolic Regulation: A Control Analytic Perspective.
J. Bioenerg. Biomembr. **27**: 479-490.

Kemeny JG, Snell JL & Thomson GL (1966) *Introduction to Finite Mathematics*
Second edition. New Jersey: Prentice Hall International.

Morowitz HJ, Higinbotham WA, Matthysse SW & Quastler H (1964)
Passive Stability in a Metabolic Network.
J. Theor. Biol. **7**: 98-111.

Pilling MJ & Seakins PW (1996) *Reaction Kinetics*
First edition. Oxford University Press.

Stoer J & Bulirsh R (1980) *An introduction to numerical analysis*
Berlin: Springer Verlag.

Strogatz SH (2001)
Exploring Complex Networks.
Nature **410**: 268-276.

Westerhoff HV, Kholodenko BN, Cascante M & Dam KV (1995)
Elusive Control.
J. Bioenerg. Biomembr. **27**: 491-497.

Development of the Model

3

Contents

3.1 Introduction

In this chapter, the development of the model of the CDP-choline pathway for phosphatidylcholine synthesis will be detailed. First, the basic criteria used in the design of the model are outlined. This is followed by a summary of the conceptual starting point for the model and a discussion of how the model was developed from this.

To simplify the discussion, the development will be described in separate sections. There are three stages in the discussion of the construction of the model. The first stage is the construction of the stoichiometric network; this comprises the choice of the metabolites and the enzyme reactions that connect them. The second stage involves the flux distribution and the kinetics of the model. Finally, in the third stage, the feedback effect of the membrane torque tension is developed and included. These elements were evolved in parallel, rather than as separate stages, by working on and testing the model as a whole. However, the elements are covered here as separate stages for the purpose of clarity.

With the design of the model explained, the implementation of the model is detailed. This includes the methods by which the simulations are run, including the commercial computer software used and the custom routine written to verify the simulation data. Finally, the numerous approximations made in the development of the model are summarised.

3.1.1 Model Design Criteria

The aim of this work was to build a model to attempt to clarify the understanding of the regulation of the lipid biosynthetic pathways in terms of the modulation seen for the activity of CCT. A further aim was look for the correlation of the regulation with the homeostasis of membrane torque tension as described in the introduction (in section 1.5). For example, CCT has been demonstrated to be controlled by the membrane torque tension, but is this control consistent with homeostasis of the membrane torque tension? Another key aim was to help pinpoint areas for future experimentation.

The complexity of biological systems introduces many practical difficulties, some of which will be highlighted in this chapter. It would be extremely difficult, and ultimately not significantly more helpful in the understanding of homeostasis in biomembranes, to model the entire metabolic pathway of an organism. The aim is to keep the model simple enough that a useful interpretation and rationalisation of the results can be readily achieved.

Metabolism is divided into functional units but the answer to 'what constitutes a metabolic pathway?' depends on the aim of the study. In addition, groups of pathways are interconnected functionally, and by connecting metabolites, to form complex subsystems. A key challenge was therefore to isolate a subsystem (Barkai & Leibler 1997; Hartwell *et al.* 1999), appropriate to the problem, which could be investigated and analysed separately.

The phospholipid biosynthetic pathways were elucidated decades ago. However, there exists no full description of the phospholipid metabolic system. Indeed little is known of the rate laws or parameters of the system. For this reason the model developed in this work is being built as a preliminary step to a more detailed description. This approach has been termed the construction of an *idealized skeleton model* (Heinrich *et al.* 1977).

The model's aim is to represent, in the simplest manner, the essential dynamic features of the system. To fulfil this, the model must capture the fundamentals of the biochemistry, and the physics of the control mechanism under investigation: the homeostatic control of membrane curvature elastic stress. The model should allow us to answer such questions as 'how does the pathway react to an external signal?' and allow predictions such as 'which enzymes are important for the control of the flux of the metabolites and other key properties?'. The model must examine the effect of the enzymes on the membrane torque tension and the effect of control of the elastic energy stored in the biomembrane on lipid biosynthesis. The membrane torque tension is a property of the system, determined from all the lipid concentrations. For this reason, the approach is to examine system properties rather than the details of each reaction. The next section looks at the initial concept from which the model was developed.

3.1.2 Starting Point

The initial concept for the model is shown in figure 3.01. The diagram summarises the role of CCT in the synthesis of PC, and the role of PC in the modulation of CCT activity through its influence on the membrane torque tension. Also shown are some of the lipids for which PC is the precursor, and how these contribute to the MTT and the modulation of CCT. The challenge in building a model was to turn the schematic diagram in figure 3.01 into a more complete metabolic pathway, attempting to include as many reactions as possible. Details of the kinetics of the model and the MTT effects can be built upon the conceptual model shown in figure 3.01 to form a model of lipid synthesis and the effects of the membrane torque tension.

It is important to reiterate that there is little mechanistic information, which would be invaluable in model construction. There is no source for rate equations, kinetic constants or equilibrium constants for the biological pathway. Furthermore, it is impossible, due to the complexity of the system, to deduce the parameters using the model. The model must also include details of how the torque tension is determined and how the feedback acts. Much of the work in constructing a model is involved in developing methods to build a model without firm knowledge of these. The discussion of the construction of the model now begins by examining the challenges involved in defining the stoichiometric network.

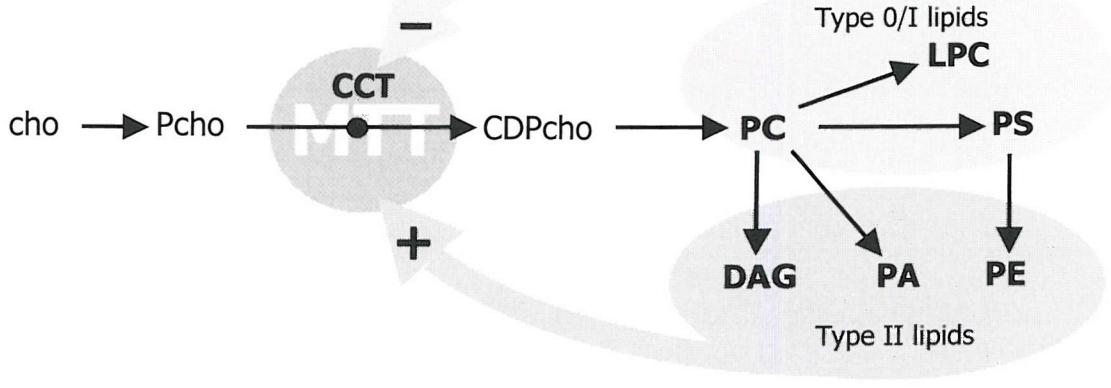

Figure 3.01: The starting point for the model. The scheme shows the CDP-choline pathway for the synthesis of phosphatidylcholine (PC). Also shown are the main phospholipids (for which PC is the precursor) and their influence, through the proposed integrative membrane torque tension (MTT) feedback mechanism, on the activity of CTP:phosphocholine cytidylyltransferase (CCT).

3.2 The Stoichiometric Network

The first step towards building a model, to investigate the hypothesised membrane torque tension control, was to build a stoichiometric network. Details of the phospholipid biosynthetic pathways are well established. However, defining the stoichiometric network in the model was one of the key challenges. The task was to select the key features to include and exclude to yield a simple but sufficiently inclusive model.

Here the process by which the stoichiometric network was built and developed is detailed. Three main networks will be discussed; these represent points where major refinements were made to the network. StN1 (Stoichiometric Network 1) is a basic model focusing on PC and CCT used to develop early ideas about the model. StN2 was a first attempt at a more complete representation of the lipid biosynthetic pathway. StN3 is the current model: a simplified version of StN2 which focuses on the major membrane lipid species and overcomes many of the problems encountered with earlier networks.

The models were used to develop and experiment with the kinetics and feedback functions (see section 3.3 and section 3.4 respectively). They also allowed the development of an understanding of the factors that affect the system's responses. However, results from early models will not be given. The stages are presented to show how the final model was arrived at, and to illustrate some of the problems encountered when constructing the model and how these were overcome. The features and failures of each network are examined before expansion and refinement of the network. This serves to illustrate how the methodology used was developed.

Prior to this work, a map of phospholipid biosynthesis was compiled from literature sources. This map, shown in figure 3.02 overleaf, is a generic (non tissue specific) representation of eukaryotic phospholipid biosynthesis pathways. The metabolic map was used as a basis from which a reduced model with shortened pathways could be set up. The initial aim was to focus on the 'central' part of the pathway. This central section involves PC, the most abundant phospholipid, the precursors of PC (shaded in figure 3.02) and several other key lipids including PS and PE.

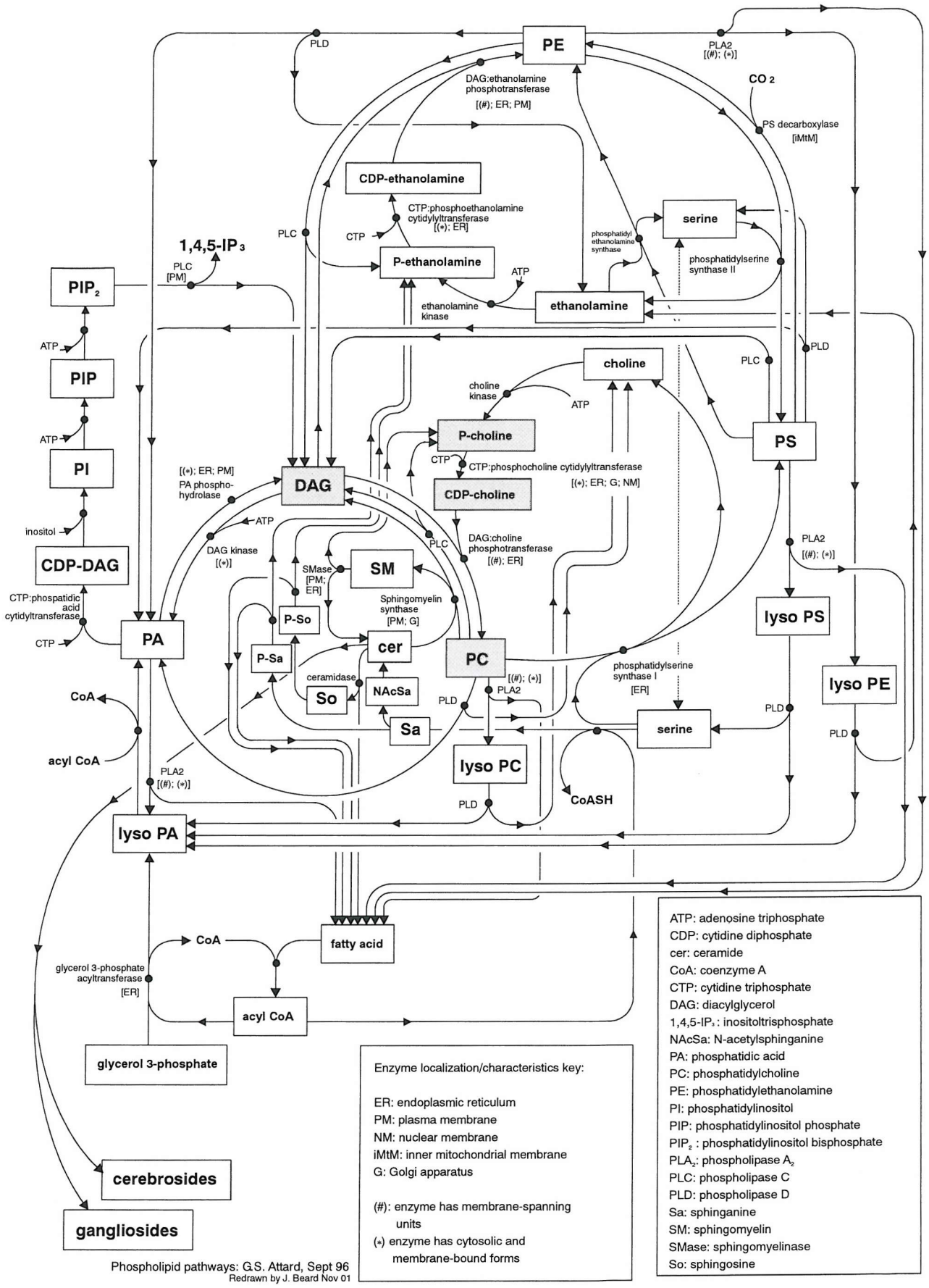

Figure 3.02: A generic map of eukaryotic phospholipid biosynthetic pathways.
The shading shows the location of CCT and PC in the pathway.
Reproduced with permission from a diagram by G.S. Attard.

3.2.1 StN1: A Basic Model

StN1 was the first stoichiometric network built. It was used as a basic network to gain experience in constructing models and to allow preliminary experimentation with the model. The network was used as a simple starting point to investigate how to build simulations and how to solve for the coefficients of the system, to learn about simulating branched systems and to test some initial ideas about the behaviour of the system.

Initially the focus of the investigation was on CCT and PC synthesis. For this reason, the first network developed reflected this; only later was the model developed and expanded to investigate further enzymes. Much of the work on the StN1 network was performed before the systematic techniques and formalisms detailed in chapter 2 had been developed. For example, prior to the application of the matrix solving techniques, the models parameters were solved by manual optimisation using crude sensitivity analysis. A minimal number of coefficients were found to be convenient in this respect.

StN1 is presented here because it is instructive to discuss the key reactions it is assembled from and how it was constructed. The discussion of these methods is facilitated by the relative simplicity of the network used in StN1, however the larger networks are constructed using the same methodology. The majority of the discussion will focus on the problems associated with simulating complex branched systems, the shortcomings of this initial stoichiometric network and the further development of the model.

A. The component reactions

The basic aim of this stoichiometric network was firstly to include PC synthesis, and secondly to incorporate the conversion of PC to the other main lipid species. This basic approach would allow the effect of CCT upon the lipid composition of the membrane to be investigated.

The first step included was the production of PC. PC is formed as the product of just one reaction, shown in figure 3.03 (a). CDPcho, a substrate for this reaction is produced by the reaction catalysed by CCT as shown in figure 3.03 (b). These

reactions are central to the stoichiometric network. However, further lipid species must be included since the model must allow investigation of the relationship between the lipid composition of the membrane and the activity of CCT. Of key importance is the effect of each lipid interconversion upon the membrane torque tension. The stoichiometric network therefore includes the other major lipid species and the main interconversions between them.

Based upon experimental data of typical lipid compositions of cell membranes the other major lipid species included in the StN1 model were PS and PE. PC acts as a precursor to these species through the reaction shown in figure 3.03 (c). PC can also be converted to PA as shown. Although PA is not present in high concentrations, it is significant. PA is a strongly type II lipid and (as will be seen in section 3.2.3 when sources and sinks are added to the model) it is a source of DAG from which PC is synthesised.

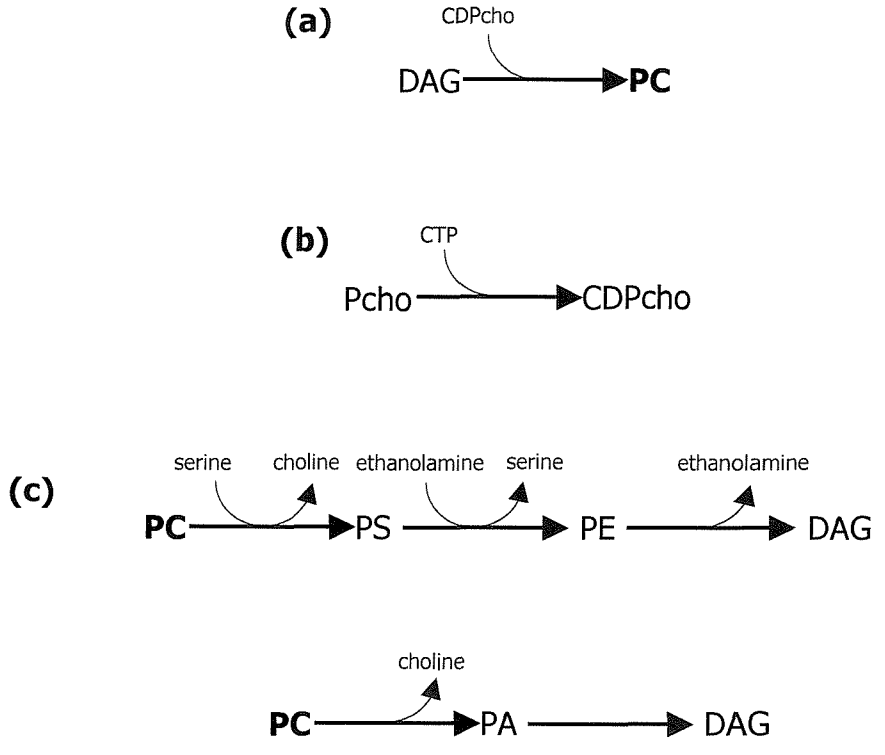

Figure 3.03: The components of StN1.
(a) The final step in PC production.
(b) The CCT reaction.
(c) The conversion of PC to the other major membrane phospholipids showing the cofactors involved.

B. Putting the reactions together: linking the components

The four reaction schemes in figure 3.03 incorporate the main phospholipid components of the membrane and the reactions of PC. To build these reactions into a stoichiometric network, which can be used for simulation, required careful manipulation, balancing and simplification. The first step was to join the main lipid species with their interconversions as shown in figure 3.04 (a).

The network in figure 3.04 (a) includes the main lipid interactions. However, the cofactors from figure 3.03 (c) (for example choline and serine) have been left out at this stage. Omission of the choline moiety cofactors has, it should be noted, not addressed the reaction of key interest: the reaction mediated by CCT.

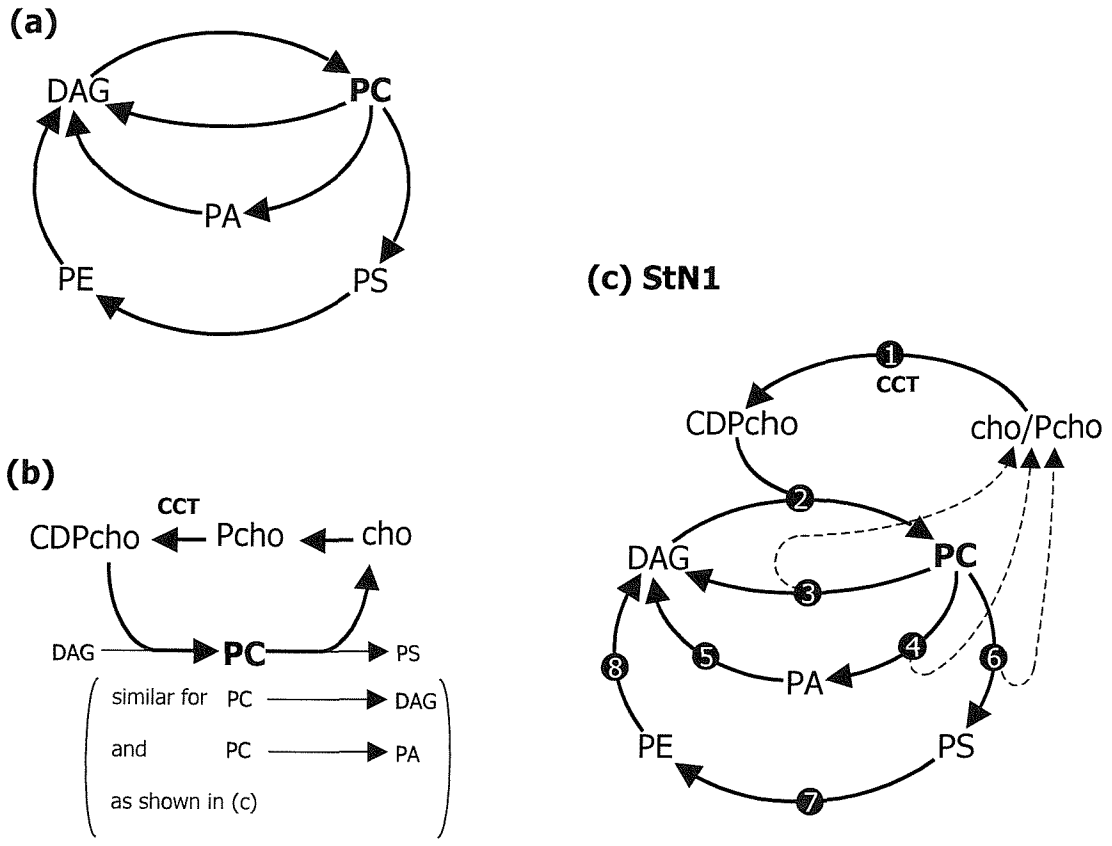

Figure 3.04: Constructing StN1.
(a) The major lipid interconversions.
(b) The choline cofactors involved in the synthesis and degradation of PC.
(c) The StN1 model combining (a) & (b).

The choline cofactors are central to the model to allow investigation of CCT. CCT catalyses the reaction which produces CDPcho; a substrate for the reaction which produces PC. A choline containing species (cho or Pcho) is released when PC is converted to a lipid species with a different head group. This was included by incorporating the choline containing cofactors as shown in figure 3.04 (b).

Combination of the elements in figure 3.04 (a) and (b) results in the network in figure 3.04 (c). It can be seen that inclusion of the choline containing moieties (and the bimolecular reactions which join them) significantly increases the complexity of the network. This is despite the fact that the other cofactors, the ethanolamine and serine containing moieties, have been neglected at this stage.

One of the challenges in dealing with bimolecular reactions and cycles is ensuring mass conservation by correctly balancing the stoichiometry of the network. For example, removal of any of the dotted lines in figure 3.04 (c) would result in loss of mass from the system, as the choline containing moieties would not be conserved. This situation is known as a 'short circuit' and is illustrated in figure 3.05 in a simple reaction network where the problem is more easily identified.

The nature of the complications introduced by the cofactors will now be examined in the discussion of StN1. Further development of the model will be preceded with an examination of the shortcomings of this simple model to illustrate some of the problems encountered.

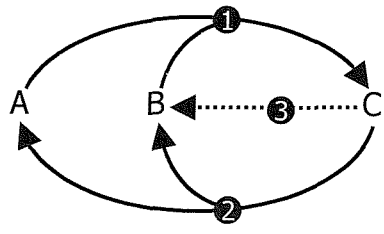

Figure 3.05: An example of a 'short circuit'. A simple pathway with the combination of A and B to give C (reaction 1) and the reverse reaction (reaction 2). The addition of reaction 3, shown dotted, would constitute a 'short circuit' in the pathway because it releases B, but not A. In this closed loop, A would be depleted by the short circuit. Here the problem is relatively easily seen, however in a model with complex branching careful balancing is required. Note alteration of the stoichiometry of reaction 1 or 2 could also cause a short circuit.

UNIVERSITY OF SOUTHAMPTON LIBRARY

C. Discussion

StN1 incorporated the basic features necessary to investigate the control of production of phosphatidylcholine and the basic effects of feedback. Included are the reactions that convert PC to the other major lipid species. Also included in the choline branch is the CCT step itself and the synthesis of PC from CDPcho. However, the model is far from ideal. The two main problems with the model are that the model is not open, and that the concentration distribution around the system is severely restricted.

The most obvious problem is that the model is not open, lacking any input and output. As mentioned previously, a feature of biological systems is that they are open. In fact, the StN1 model was only able to reach steady state due to the fact that it forms a closed 'futile' loop. This was physically unrealistic. In order to create an open system at least one source reaction and one sink reaction are necessary. The first problem in this respect is that provision of an appropriate source would require expansion of the model to include suitable source metabolites, the choice of these will be returned to later. The provision of a source was further complicated by the concentration restrictions encountered due to the stoichiometry of the model.

It has been shown how bimolecular reactions can complicate a network structure. Bimolecular reactions cause cycles and moiety conservation, which can limit the concentrations of selected metabolites. This can cause problems when simulating such pathways. StN1, an apparently simple model contains branches, with cycles on each branch of the pathway. In the layout in figure 3.04 (c), the cycles are not obvious. In figure 3.06 (a) one such cycle is shown separately, the PC-PA-DAG cycle. The species which enter and exit the cycle, CDPcho and choline, are themselves part of a cycle, the PC-Pcho-CDPcho cycle, see figure 3.06 (b). These cycles are not moiety-conserved cycles due to the presence of true branching at PC. However, to complicate matters further, the branch point at PC results in three branch structures each with two interlinked cycles analogous to those shown in figure 3.06 (these are the PC-DAG and the PC-PS-PE-DAG cycles).

As mentioned above, the cycles in figure 3.06 are not moiety conserved due to the presence of true branches. However, the presence of similar cycles on each branch

(i.e. a choline species is always released when PC undergoes head group exchange) results in two conservation rules for the network as a whole. The first rule is for the lipid species (the glycerol backbone), and the second is for the choline containing species. The conservation relations are given in equations 3.01 and 3.02

$$[PC] + [DAG] + [PS] + [PE] + [PA] = [\textit{lipid species}] = \text{Constant} \qquad \text{equation 3.01}$$

$$[Pcho] + [CDPcho] + [PC] = [\textit{choline species}] = \text{Constant} \qquad \text{equation 3.02}$$

These relationships always apply, and are not just valid at the steady state. They therefore put strict constraints on the concentration distribution in the system. This can be illustrated by considering various starting configurations. If the targets for the lipid concentrations give [*lipid species*] = 100, this can be distributed in various ways. If 100 units of PC are used as a starting point (with all other species at a concentration of zero), the system can redistribute the 'glycerol backbone' and 'choline headgroups' around the system. In this case, [*lipid species*] = 100 and [*choline species*] = 100, since PC is a member of both conservation relationships. If however, 100 units of PA are used as a starting point (with all other species at a concentration of zero), then [*lipid species*] = 100 but the [*choline species*] = 0 (since PA contains no choline moiety). The concentration of CDPcho must therefore be zero. Reaction 2 (DAG + CDPcho → PC) cannot proceed without CDPcho. Therefore, the system will therefore all end up as DAG.

It can be seen that a careful choice of initial concentrations is necessary in order for the system to function properly, not only must [*lipid species*] =100 but the [*choline*

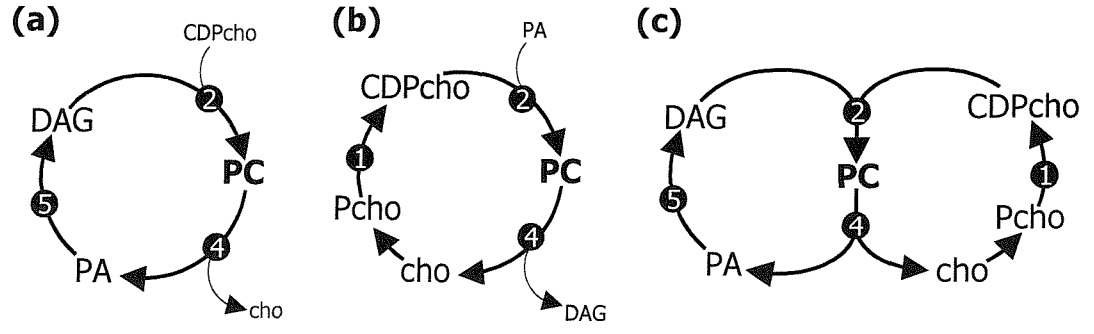

Figure 3.06: The interlinked cycles in StN1.
(a) The cycle of DAG, PC and PA is shown.
(b) The cofactors in (a) (CDPcho and Pcho) are also linked by a cycle.
(c) The two cycles together showing how PC forms the junction of each cycle in the StN1 model.

species] must be correct. In this instance, the simplest choice is to start with only PC (since PC is the branch point and common to all the cycles). However, if the analogous ethanolamine branch were included this would no longer be the case. There would be another conserved set of ethanolamine-containing moieties and more restrictions on the possible distribution of species. Furthermore, there would no longer be a species common to all the conservation equations.

How does this complicate the choice of sources? The concentration restriction problems, detailed above, are simple to deal with when selecting starting concentrations. It is simply a matter of ensuring that the starting concentrations fulfil the conservation equations in such a way that the desired steady state is achievable. Although this is a rather artificial process, it is nonetheless achievable. However, when the system is defined as open, material is supplied and removed and there is the possibility of growth. Even for the simple StN1 model, complications arise. PC is the only metabolite which would increase both [*lipid species*] and [*choline species*] and therefore maintain the correct balance. However, since the network is essentially a model of PC synthesis, PC is not a suitable choice for a source metabolite. It is therefore clear that there must be more than one source. If the [*lipid species*] grows then [*choline species*] must grow in order that the reaction of DAG with CDP-choline (to produce PC) can proceed. If [*choline species*] does not grow the system will all end up as DAG, as described previously. This idea can be more clearly illustrated with the simpler system in figure 3.07 where absence of a second source, a source for the metabolite labelled B, causes metabolite depletion. This type of

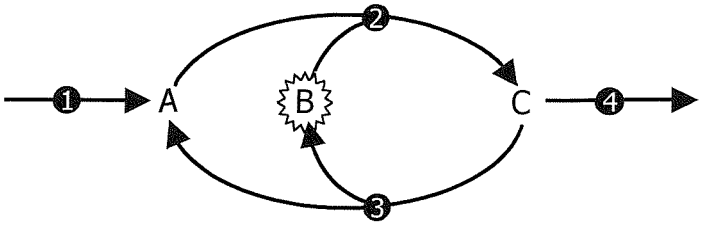

Figure 3.07: An incorrectly implemented source and sink.
The sink reaction that removes C is effectively indirectly removing A and B. The source reaction provides only A. The result is B will be depleted (by reaction with A to form C which can then leave the system). The lack of a source for B (and the indirect loss of B through the sink reaction acting on C) results in the depletion of B. It should be remembered that in a real model, the above problem could involve many reactions and branches and be significantly harder to find.

problem can be hard to spot by looking at a reaction network, but becomes very apparent when simulations are run. It is seen that the addition of sources will require careful analysis of the branch structure. In summary, it can be seen that although the implementation of source and sink reactions would remove the conservation relationships, the problems caused by the bimolecular reactions must be considered. Even in this simple model, more than one source is necessary. Development of the model calls for a careful choice of sources, one being required for each conserved set.

The models built from StN1 aided in the understanding of correctly putting the reactions together to form a network. However, as has been discussed there were problems with the network. Building StN1 therefore served to show how difficulties could arise with what initially appears to be a very simple stoichiometric network. In addition, StN1 did not incorporate several key features that were felt to be necessary, namely appropriate sources, sink reactions, the ethanolamine branch and the lysophospholipid species. These are detailed below.

Appropriate sources are necessary in an open system. Implementation of a source for the lipid species required examination of the reactions that lead to PA. Fatty acid (FA) is a dietary requirement and is involved in the reaction regarded as the first step in lipid biosynthesis: the conversion of water-soluble glycerol-3-phosphate (g3p) to the lipid product lysophosphatidic acid (LPA) by glycerol-3-phospate acyltransferase (Haldar & Vankura 1992; Yamashita & Numa 1972). FA is also important as it acts as a type II species in the presence of PC and is an important cofactor in the many acylation/de-acylation reactions. Sink reactions are necessary to allow the system to reach a steady state with source reactions implemented. The ethanolamine branch of the pathway is important in the production of PE, the second most abundant lipid in the cell membranes and the most abundant type II lipid species. This branch is essential in order to investigate the effect of ECT for comparison with CCT. Finally the lysophospholipids are of significance as they are strongly type I lipid species and act to relieve membrane torque tension, it is therefore reasonable to expect their production may be tightly controlled in order to maintain the stored elastic energy.

Expansion of the stoichiometric network was clearly necessary to incorporate these extra metabolites and reactions. Furthermore, the CCT step is not the only reaction in the pathway that is mediated by a membrane-associated enzyme, the activity of

which appears to be modulated by membrane curvature elastic stress. As discussed in the introduction, CCT was chosen as the first to be investigated since the reaction it mediates is considered as the rate-limiting step of the CDP-choline pathway for the synthesis of PC. The aim of this work was, in addition, to investigate the effect of membrane stress modulation functions (described in section 3.4.2) upon other steps, since control of additional steps may be important in increasing the robustness of the model.

The additions that were required are summarised in figure 3.08. The approach to expanding the network was to attempt to simulate the whole map as in figure 3.02. This obviously presented more of the linked-cycle problems. The task therefore became to use what was learnt from StN1 about branching structures to implement sources and sinks and to relax the concentration restrictions. The first task however, was to build an enlarged stoichiometric network, ensuring mass conservation.

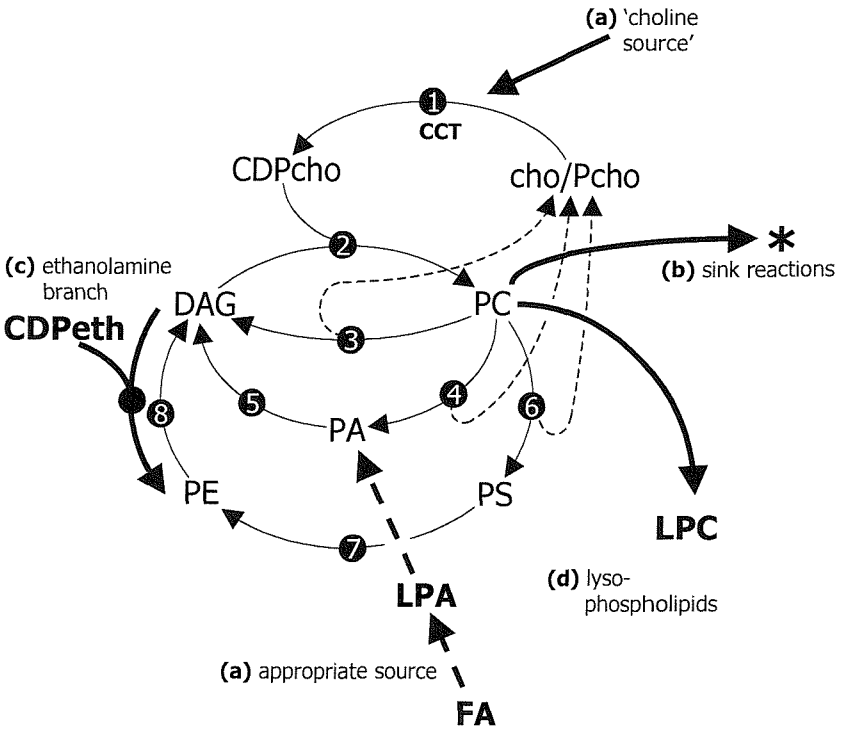

Figure 3.08: Additions required to StN1.
(a) Appropriate sources for each branch.
(b) Sink reactions.
(c) The ethanolamine branch, for comparison to the choline branch.
(d) Other key lipid species, including the lysophospholipids.

3.2.2 StN2: Expanding the Stoichiometric Network

The construction of StN2 primarily involved the construction of more of the lipid biosynthetic pathway. It was motivated by the need to incorporate the features, detailed previously, which were missing from StN1. This crucially included the route from FA through to PC, and also the lysophospholipids. To build a more complete model of phospholipid biosynthesis an attempt was made to model the entire reaction scheme shown earlier in figure 3.02.

StN2 was developed in order to check the structure of the entire pathway. The process of building a model facilitates checking the stoichiometry of the network and the discovery of short circuits. Short circuits arise when the stoichiometry is incorrectly defined, as shown previously in figure 3.05. The conservation of choline containing moieties, seen in StN1, is just one example where a 'chemical building block' can be traced around the network; following these building blocks is the key to balancing the network. This type of careful examination of the pathway, and testing using the model, was applied. Examples of corrections to the balancing of the stoichiometry include the breakdown of Psa and Pso (to balance the network this reaction must release serine, not Peth as shown in the generic representation) and the conversion of NacSa to ceramide (this reaction must consume FA for mass balance). The resulting balanced network, StN2 is represented in figure 3.09.

In its full version, StN2 was too complex to be used in any useful analysis. It was clear that significant simplification was needed. StN2 included the main features that were required including the significant lipid species and all the reactions of interest. However, the system was still a closed futile cycle. The branching of the pathway made implementation of an open system a significant challenge. Concentration restriction was also a larger problem. With StN1, it was shown how the concentrations had to satisfy the conservation rules. In StN2 there are 17 branch structures giving rise to five conservation equations. These will not be discussed here; the remainder of the discussion will focus on how this stoichiometric network was reduced. This will involve particular focus on how the implementation of source reactions removed the interlinked cycles, and produced a useable model of the conversions between the membrane lipid species.

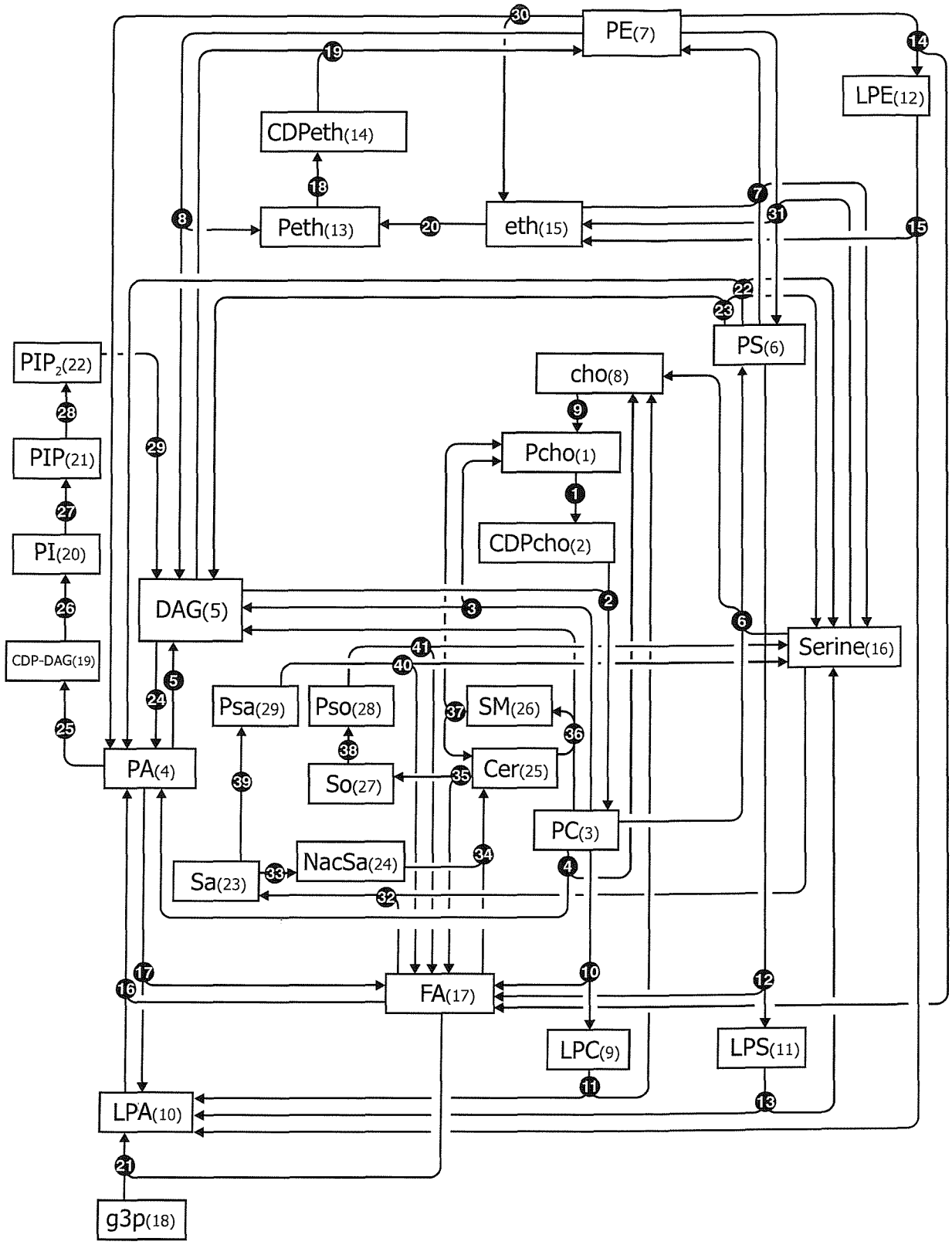

Figure 3.09: Stoichiometric Network 2 (StN2).
An expanded reaction network based upon the metabolic map shown in figure 3.02. The reaction network includes the lysophospholipid species and fatty acid. At this stage, the stoichiometric network is still closed, with no sources or sinks.

3.2.3 StN3: Development of a Simplified Open Network

The aim of the construction of StN3 was to create a network retaining most of the added lipid species and interconversions in StN2, but without the problems of the interlinked cycles. The other key aim was to introduce appropriate sources and sinks.

Initially, it was decided to reduce the number of lipid species in the model by limiting the model to the most abundant phospholipids. This process involved removing minor lipid species such as CDP-DAG, PI, sphingomyelin and ceramide. Some minor lipids, including DAG and PA, are retained. This is because these species are closely linked to the more abundant species and will be affected by the enzymes under investigation. For example, DAG and PA are immediate precursors to PC. As strongly type II species, DAG and PA are also extremely important in the determination of membrane torque tension.

The next aim was to modify the model to make it an open system. To achieve a *dynamic steady state* there must be a balance of the rate of formation and degradation of each species in the presence of a flow of material through the system. To achieve this 'there must be at least one substance (a source) that provides a reservoir of matter (or pool), and at least one other (a sink) into which the output of the pathway flows' (Fell 1992). Also for a pathway with bimolecular reactions there must be a source for each 'branch' of the supply chain as was shown in figure 3.07. A source of each of the 'component moieties' is required, one for each lipid chain, one for the glycerol backbone and one for the choline (or other) headgroup. To set up suitable sources, reference to the literature was made (Hjelmstadt & Bell 1991; Kent 1995; Longmuir 1993; Scherphof 1993; Tronchere *et al.* 1994; Vance 1996). An attempt to add a source of choline gave the first suggestion of how to simplify the model.

A. Clamping source metabolites

As was detailed in chapter 2, the process by which inexhaustible sources are added is known as 'clamping': in order to define a metabolite as a source, the concentration of that metabolite is held constant. It was found that this could have a simplifying effect on the model when a source for the choline moiety was chosen. Choline is a dietary requirement, and is rapidly converted to phosphocholine (Pcho) by the

cytosolic enzyme choline kinase (Vance 1996). Pcho is therefore present, in relatively high concentrations, in a cytosolic pool. This makes Pcho a suitable candidate for clamping. Pcho is therefore the choice for the source of the headgroup moiety for incorporation into PC.

The clamping of Pcho has a significant simplifying effect on the model, as shown in figure 3.10. The result of this treatment is that the model is not dependent on phosphocholine released from PC to regenerate CDPcho (for regeneration of PC). Clamping Pcho removes the interlinked choline cycles. The other effect is that the release of cho, a cytosolic species, is removed from the model. This branch is omitted in (b); the degradation reaction R4, is simplified from PC → PA + cho to PC → PA. The result is cho is effectively external to the model. Next, it is shown how this method may be extended to the clamping of the non-membrane species, in order to further simplify the network and to focus on the membrane lipids.

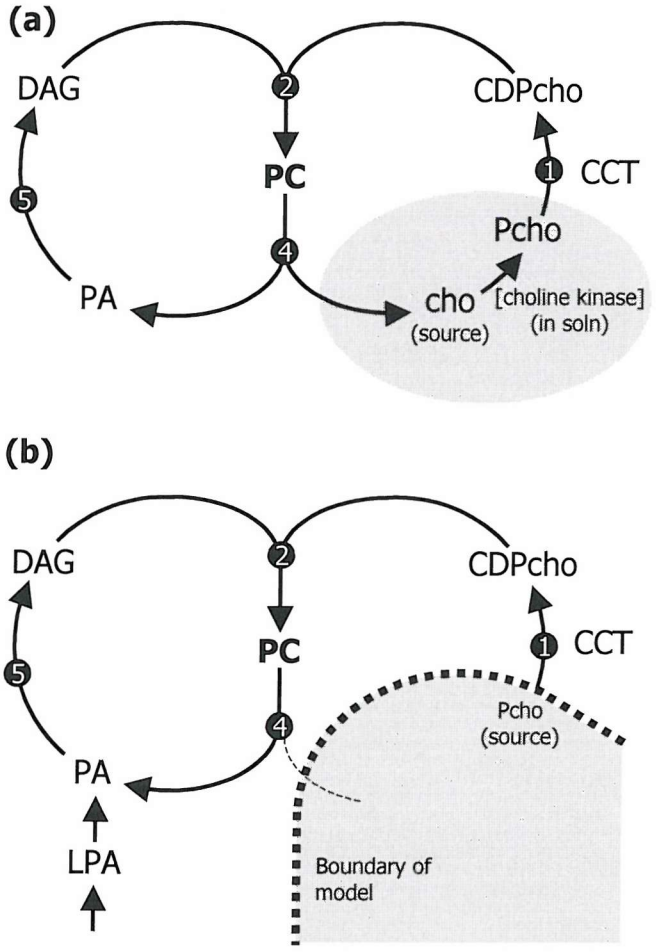

Choline (cho) is a dietary requirement. Phosphocholine (Pcho) is also cytosolic, is made by a soluble enzyme and is present in relatively high concentrations in the cytosol making it a good choice for clamping.

These metabolites are clamped to act as a source (shown by shading).

Treatment of Pcho as a clamped source metabolite sets the boundary of the model and consequently removes the interlinked cycles.

Note there must be sources for each of the substrates of the bimolecular reaction, R2 (these are the sources for the lipid chain and the headgroup moieties).

Figure 3.10: Simplification by location. (a) Treating phosphocholine as a clamped metabolite. **(b)** Clamping defines the boundaries of the model and effectively removes the interlinked cycles.

B. Clamping to focus on the membrane lipids

The simplification discussed, illustrated by treating Pcho as a source, leads to a method of differentiating between the metabolites by their location. The reactions modelled are not between species in a well-mixed solution; the lipid species are present within the fluid bilayer, however many of the species are located not in the membrane but in the cytosol. The metabolites in StN2 may therefore be classified as membrane or non-membrane (cytosolic) metabolites.

The method used to simplify the stoichiometric network was to focus on the major membrane lipid species, since the property of interest, the membrane torque tension, is dependent on the membrane lipid concentrations. In the procedure described above Pcho, as a source metabolite supplied from outside of the membrane, is clamped. This approach may also be adopted for the other cytosolic metabolites.

The procedure of clamping non-membrane species and the simplification it leads to can be illustrated by considering the headgroup exchange reactions. These usually involve one or more non-membrane metabolites. For example in reaction 6 in StN2 serine and choline are non-membrane species:

$$PC + \textit{serine} \rightarrow PS + \textit{choline}$$

The method was to clamp the non-membrane metabolites, in the example above serine and choline, effectively treating the pools of non-membrane metabolites in the cytosol as inexhaustible. Clamped metabolites form the boundaries of the model. This means that clamped species that are involved only in bimolecular reactions or as precursors to other clamped species are effectively external to the model (as was shown for cho in figure 3.10) and can be removed completely, both to simplify representations of the model and to reduce calculation times.

Using this procedure, the headgroup exchange reactions are simplified to straightforward single-substrate, single-product reactions. Reaction 6 is simplified by the removal of serine and choline to give:

$$PC \rightarrow PS$$

C. The resulting simplification

Bimolecular reactions and simple cycles were identified in the previous chapter as structures that can limit sums of fluxes in biological networks. It has been shown that in this model the interlinked cycles can be removed by considering the location of the metabolites. It is this distinction that suggests the cycles are unrealistic; the cytosolic 'pools' of non-membrane metabolites relax the restrictions.

Considered this way, the cycles are seen to artificially constrain the pathway by putting too many restrictions on the system. Removing them by addressing, in a simple way, the location of the metabolites greatly simplifies the model. In addition, this removal focuses the model on the conversions of the membrane lipids. Figure 3.11 summarises how the clamping procedure leads to a simplification of StN2, and which reactions are retained in StN3 (note that figure 3.11 is not a complete representation of StN3. A complete representation is shown in figure 3.15).

Figure 3.11 reveals that not all of the bimolecular reactions have been removed. The inclusion of fatty acid results in several bimolecular reactions, for example LPC + FA → PC. These reactions are not head group exchange but reactions in which an hydrocarbon chain is added or removed from a lipid species. Both the cleaved lipid and the fatty acid are membrane species and so are not clamped. Fatty Acid therefore acts as a plurifunctional cofactor (see chapter 2) and may be an important control metabolite. Fatty acid behaves as a type II lipid in the presence of PC and is involved in the lipid chain remodelling reactions; so tight control here would be expected.

Whilst this treatment addresses the inhomogeneity of the system in a very crude manner, it should be noted that the finer details of the inhomogeneity of the system are beyond the current scope of the model. These include the asymmetry of the membrane and the sub-cellular location of the enzymes; the enzymes that catalyse the reactions are varied in their spatial distribution in different regions of the cellular membrane and in the cytosol.

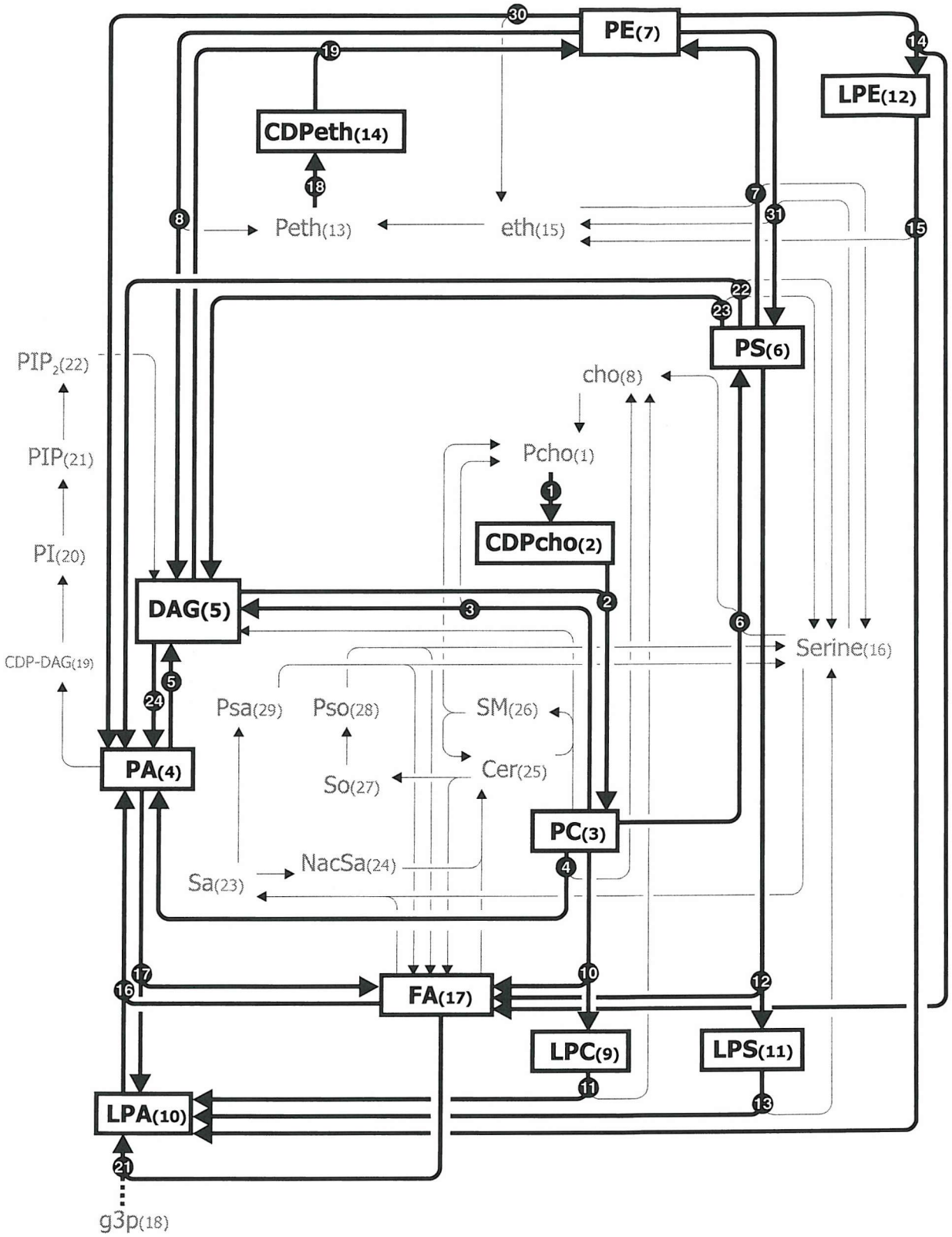

Figure 3.11: Stoichiometric Network 3 (StN3) as a reduction of StN2.
The diagram serves to show how elements of StN2 were retained and StN3 was constructed from these selected elements. However, note the network does not show StN3 in a complete form. For clarity, the sink reaction on each species and the acylation reactions of the lyso species (LPx + FA --> Px) added in StN3 are not shown. Also, the reaction and metabolite numbers are those from StN2. See figure 3.15 for a complete representation of StN3.

D. Exceptions to the clamping procedure

The clamping process detailed above results in some reactions being treated as external to the model. For example, the conversion of choline to Pcho is removed from the model due to the clamping of Pcho. Care must be exercised when removing reactions from the system. If all non-membrane metabolites were clamped then the CCT catalysed reaction would be made external to the model. For this reason, an important exception to the clamping process is CDPcho (and CDPeth). CDPcho is modelled with a variable concentration. This is justified by comparison with Pcho and consideration of the location of the enzymes that produce Pcho and CDPcho. Pcho is rapidly generated from choline, a dietary requirement, by a reaction mediated by choline kinase, a cytosolic enzyme (Vance 1996). Furthermore, Pcho is present in relatively high concentrations. CDPcho in contrast, is generated by the reaction mediated by CCT, which is only active when membrane bound. So, although CDPcho is soluble it is generated at the membrane. The concentration of CDPcho is 40 times smaller than that of Pcho (Vance 1996). In addition, the concentration of importance in the model is the concentration in the region of the membrane, since CDPcho must then combine with DAG in the membrane to be retained in the model. This process is shown in figure 3.12. The concentration of CDPcho at the membrane is therefore modelled as variable. In this way, the CCT-mediated reaction remains a valid reaction for inclusion in the stoichiometric network.

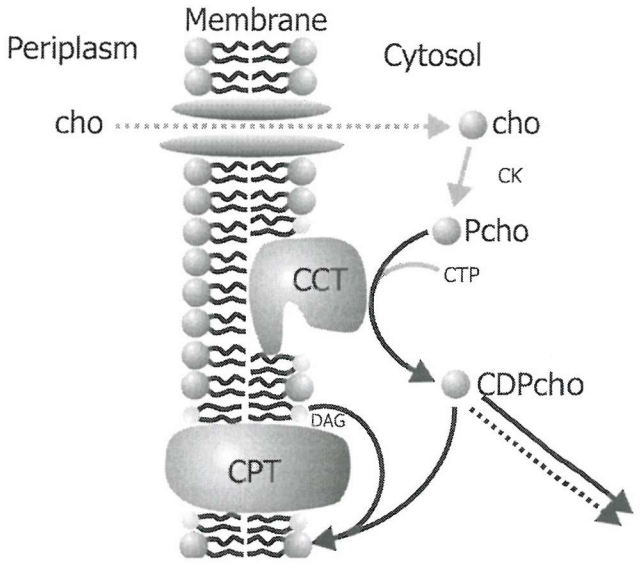

Figure 3.12: The modelling of CDPcho with CCT and CPT.
The diagram shows how CCT provides CDPcho at the membrane for reaction with DAG (reproduced with permission from a diagram by S. Jackowski).

E. Completing the sources

The clamping procedure yielded a simplified network and provided a source for the choline headgroup. It remained to complete the sources. As has been shown the model required a source for each branch of the pathway. With the pathway simplified, it was a simple matter to select sources for the remaining branches. The pathway for the glycerol backbone is shown in figure 3.13 (Scherphof 1993). The first reaction in this sequence is considered the first step in phospholipid biosynthesis (Snider & Kennedy 1977; and reviewed in Wilkison & Bell 1997). Glycerol-3-Phosphate (g3p), like Pcho, is soluble and present in high concentrations in the cytosol so is chosen as a source and boundary to the model.

The final source necessary was one for the lipid chains. Fatty Acid (FA) is the source of the lipid chains, the principal method of uptake in animal cells is dietary (Longmuir 1993). However, FA is a membrane component, and so must be modelled

Figure 3.13: Synthesis of the glycerol backbone.

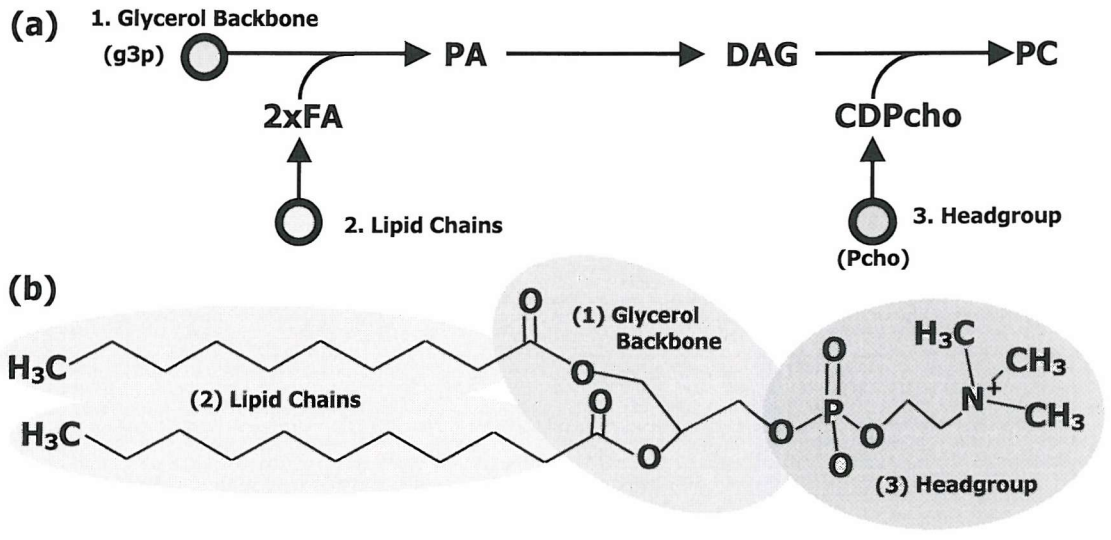

Figure 3.14: The choice of appropriate sources.
(a) a source for each branch. **(b)** How PC is made up from g3p (1), FA (2) and Pcho (3).

as a variable metabolite. A source of Fatty Acid was therefore added (see figure 3.14), resulting in a similar treatment to that for CDPcho and CDPeth. However, the source may be considered as a transport to the membrane, rather than a generation of FA, since the concentration of FA used in the model is the concentration of FA in the membrane. The sources added to the stoichiometric network are highlighted in figure 3.14 (a), which shows the pathway from source through to PC in a simplified way. Figure 3.14 (b) shows how the three sources provide the three 'building blocks' that make up the PC molecule: the lipid chains, the glycerol backbone and the headgroup. A fourth source, Peth (not shown), allows the conversion of DAG to PE (see the complete network in figure 3.15 on p.3.28).

F. Sinks – modelling loss

Clearly, a flow of mass into the model necessitates a route for removal of mass. This enables the attainment of a steady state in the presence of a flow of material. Metabolite mass could be lost due to transport away from the system, inefficiency of reaction steps (less than quantitative yields) and specific degradation steps which are not explicitly included (e.g. further phospholipase action to remove the lysophospholipid species). This overall loss was incorporated into the model by adding a sink (drain or leakage) reaction to each of the variable lipid metabolites. These simple drains represent the combination of the above losses.

Particularly important drain reactions in this model are those on metabolites that are substrates for two-substrate reactions. CDPcho is consumed by only one reaction, a two-substrate reaction in which CDPcho is combined with DAG to produce PC. This reaction can have its flux reduced by a lack of DAG. The supply from the source of phosphocholine could then cause the CDPcho concentration to grow in an uncontrolled manner (if the reaction which consumed CDPcho was a simple one-substrate reaction the rate would grow as the CDPcho concentration grows to restore the concentration). Of course, in reality, the CDPcho produced at the membrane would, in the absence of DAG to combine with, simply be lost by transport or degradation, reducing the concentration at the membrane. The drain for CDPcho in the stoichiometric network models this, and acts as a 'safety valve' on the CDPcho concentration. The drain was shown in figure 3.12, with the two lines (solid and dotted) representing the contributions of CDPcho degradation and diffusion from the

membrane. In the model, as for the other species, this is treated as a single drain step (with a larger flux than the other sink reactions).

3.2.4 Summary of the Features of StN3

In figure 3.15 overleaf, the final stoichiometric network, StN3, is represented. The layout has been changed from that used for StN2, for clarity. In addition, the involvement of FA in the acylation/deacylation reactions is indicated but not shown explicitly. The clamped sources are indicated by circles. The other clamped non-membrane species, which have been made external to the model, for example serine, have been removed. The drain reactions are shown as dotted lines. Furthermore, a list of the reaction steps and a numbering scheme is given in the legend.

In summary, the features of StN3 may be detailed. The stoichiometric network focuses on the precursors to PC (LPA, PA and DAG) and the other abundant lipid species PE and PS. The phospholipids are classified by their headgroup and number of chains only. In this way PC is differentiated from PE or LPC, however all PC variants are treated as one species. The network topology is based on the literature, and applies to mammalian eukaryotic cells, but not liver cells (since it does not include methylation of PE to provide PC). The stoichiometric network limits the model to the membrane, by clamping the soluble cofactors. In this way, the model treats the membrane as a well-mixed solution, ignoring the sub-cellular location of the enzymes, and any heterogeneity of the lipid species (primarily bilayer asymmetry). However, species from outside of the membrane are differentiated by their treatment as inexhaustible pools. The network is balanced so that it does not violate mass conservation. Sources are implemented and have been chosen based on the location and nature of the source metabolites. Finally, sink reactions are added for each metabolite to represent various loss processes.

With these features, StN3 represents a significant improvement over the previous attempts, StN1 and StN2, and forms the basis on which the rest of the model is built. The next stage in this construction is the modelling of the kinetics of the system. This starts with an outline of the process by which the flux distribution was determined.

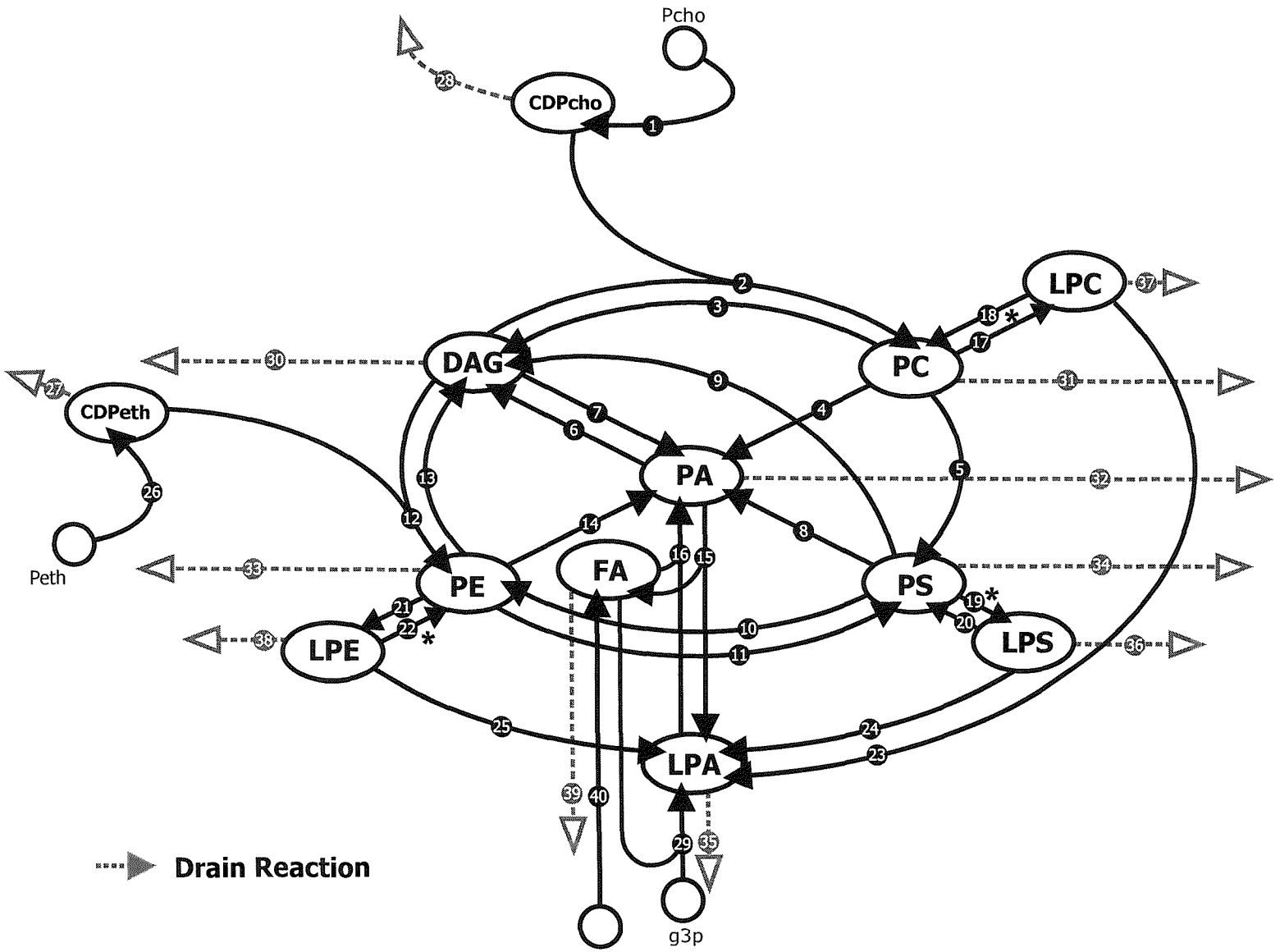

R1 Pcho -> CDPcho
R2 CDPcho + DAG -> PC
R3 PC -> DAG
R4 PC -> PA
R5 PC -> PS
R6 PA -> DAG
R7 DAG -> PA
R8 PS -> PA
R9 PS -> DAG
R10 PS -> PE
R11 PE -> PS
R12 CDPeth + DAG -> PE
R13 PE -> DAG
R14 PE -> PA
R15 PA -> LPA + FA
R16 LPA + FA -> PA
R17 PC -> LPC + FA
R18 LPC + FA -> PC
R19 PS -> LPS + FA
R20 LPS + FA -> PS
R21 PE -> LPE + FA
R22 LPE + FA -> PE
R23 LPC -> LPA
R24 LPS -> LPA
R25 LPE -> LPA
R26 PETH -> CDPeth
R27 CDPeth ->
R28 CDPcho ->
R29 GLYC + FA -> LPA
R30 DAG ->
R31 PC ->
R32 PA ->
R33 PE ->
R34 PS ->
R35 LPA ->
R36 LPS ->
R37 LPC ->
R38 LPE ->
R39 FA ->
R40 -> FA

Figure 3.15: Stoichiometric Network 3 (StN3). The clamped source metabolites are shown as circles, the drain reactions as dotted lines. The acylation/deacylation reactions (e.g reactions 17 and 18) do not show the involvement of FA for clarity (* indicates LPx to Px reactions involve FA in the same way as R15 and R16).

3.3 Steady State Fluxes and Reaction Kinetics

With the structure of the stoichiometric network defined, the next stage in the discussion addresses the kinetics of the model. With simple models of experimentally studied systems, this process would be based on mechanistic analysis and the model would use literature values for the rate coefficients. However, there is simply no mechanistic information on the reaction kinetics. In addition, the fact that the specific activities of many of the enzymes are known to vary by at least an order of magnitude, depending on the lipid composition, precluded an approach based on experimentally determined kinetic constants. Ironically, the feedback effect under investigation acts to hinder the parameterisation of the model.

Instead, a strategy was adopted in which a set of fluxes that satisfied the network topology was identified. Using a 'target steady state' composition for all of the lipid species in the network, the kinetic equations were then solved, by making assumptions about the rate laws for each step, to determine a set of rate constants consistent with this steady state. It is important to note that there are an infinite number of possible sets of rate constants, the set chosen is the result of a number of assumptions and these are detailed below.

3.3.1 Construction of the Stoichiometric Matrix

As detailed in chapter 2, at the steady state, the fluxes may be found by building a stoichiometric matrix to facilitate the solution of the steady state equations. The matrix contains the information from the balance equations, determined by the network structure. This matrix may be extended with additional equations in order to find the steady state fluxes. In this model, there are many branches, resulting in independent fluxes; so many extra equations are required. The process by which the stoichiometric matrix is constructed and supplemented is detailed below.

A. Steady state balance

A balance equation may be written for each variable metabolite in the model. For example, at the steady state for PC where v_i is the rate of reaction i.

$$d[PC]/dt = v_1 + v_{18} - v_3 - v_4 - v_5 - v_{17} - v_{31} = 0$$

In general, these equations may be written as shown in equation 2.07

$$\frac{dS_i}{dt} = \sum_{j=1}^{n_{enz}} c_{ij} v_j = 0 \quad \text{for } i = 1,2,\ldots.,n_{met} \qquad \text{as equation 2.07}$$

where c_{ij} is the stoichiometric coefficient. A matrix is constructed from the stoichiometric coefficients. The information from the balance equations gives the first twelve rows of the matrix in figure 3.17. Since the matrix has 40 columns, extra information is needed to build a 40-row matrix to permit a complete solution.

B. The independent fluxes problem

As was detailed in chapter 2, independent fluxes arise when a pathway contains branches. Since $n_{inf} = n_{enz} - n_{var}$, StN3 has 28 independent fluxes (there are 40 reactions and 12 variable metabolites) (see chapter 2 and Hofmeyr 1986). This reflects the complexity of the branching in the model and presents a significant problem in solving for the steady state.

In a model with just two independent fluxes, an example is shown in figure 3.16, there are an infinite number of solutions each with a different flux distribution between the two branches. The distribution in figure 3.16 may be fixed with the knowledge of the relative rates of the two reactions that consume S_1.

In StN3, the branching is rather more complex. Each metabolite is typically consumed by many reactions. PC for example is the substrate of reactions 3, 4, 5, 17 and 31. Examination of the stoichiometric network reveals that each metabolite is the substrate of many reactions: i.e. every metabolite is a branch point. There is no available data for the system, which would allow estimation of the ratios to fix the

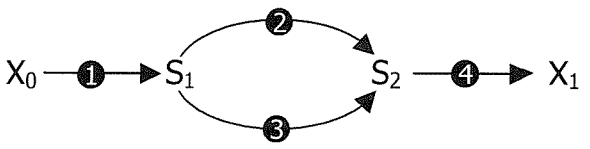

Figure 3.16: Independent fluxes in a simple branched pathway.
There are an infinite number of possible flux distributions. The distribution can be fixed by knowledge of the rates in the two branches, reaction 2 and reaction 3, which consume S_1.

independent fluxes. Instead, another method was found. The approach was simply to ensure that each of the competing reactions for each metabolite was 'significant'. To illustrate, if one reaction that consumes PC were to have a flux an order of magnitude smaller than other reactions that consume PC, that reaction would not be significant in terms of PC consumption. The aim was to avoid this, and ensure that each reaction in the model had a significant flux with respect to the branch structure of the network. To this end, it is assumed that the fluxes through reactions that have a common substrate are equal (the sink reactions are ignored in this procedure). This method will be referred to as the *equal branch-flux assumption*. The equal branch-flux assumption adds 15 rows to give a 27x40 matrix. Clearly, more rows are still required. The next stage is to set the sink reactions..

C. Setting the sink reactions

The sink reactions, also referred to as drains, are ignored when using the equal branch-flux assumption and are free to take any value. There is little information on how the drains should be handled. The approach adopted was to treat the drains as small and equal. The drain reactions for the non-membrane species are larger; these species are outside of the membrane and can be easily transported away.

There are 12 drain reactions, one for each species. The addition of 12 rows gives a 39x40 matrix. The addition of one further row, setting one flux, allows the matrix to be solved (by conversion to the reduced row-echelon form) for the fluxes. It should again be emphasised that the solution is unique only to the assumptions made. There are an infinite number of solutions that would satisfy the balance equations (these are the conditions for the steady state given in the first twelve rows of the matrix). In addition, only the relative values are important since the actual values are arbitrarily set by the entry in the final row of the matrix.

3.3.2 Resulting Stoichiometric and Flux Distribution Matrix

The resulting supplemented stoichiometric matrix is shown (as a detached coefficient tableau) in figure 3.17, including explanations of the origins of each row. Figure 3.18 shows the solution to the matrix found by conversion to reduced row echelon form and the resulting flux solution values.

		Reaction >>	1	2	3	4	5	6	7	8	9	10	11	12	13	14	15	16	17	18	19	20	21	22	23	24	25	26	27	28	29	30	31	32	33	34	35	36	37	38	39	40	
Steady State Conditions	**CDPcho**		1	-1	0	0	0	0	0	0	0	0	0	0	0	0	0	0	0	0	0	0	0	0	0	0	0	0	-1	0	0	0	0	0	0	0	0	0	0	0	0	0	0
	CDPeth		0	0	0	0	0	0	0	0	0	0	0	-1	0	0	0	0	0	0	0	0	0	0	0	0	0	1	-1	0	0	0	0	0	0	0	0	0	0	0	0	0	0
	PC		0	1	-1	-1	-1	0	0	0	0	0	0	0	0	0	0	0	-1	1	0	0	0	0	0	0	0	0	0	0	0	-1	0	0	0	0	0	0	0	0	0	0	0
	PS		0	0	0	0	1	0	0	-1	-1	-1	1	0	0	0	0	0	0	0	-1	1	0	0	0	0	0	0	0	0	0	0	0	0	-1	0	0	0	0	0	0	0	0
	PE		0	0	0	0	0	0	0	0	0	1	-1	1	-1	-1	0	0	0	0	0	0	-1	1	0	0	0	0	0	0	0	0	0	0	-1	0	0	0	0	0	0	0	0
	PA		0	0	0	1	0	-1	1	1	0	0	0	0	0	1	-1	1	0	0	0	0	0	0	0	0	0	0	0	0	0	0	-1	0	0	0	0	0	0	0	0	0	0
	DAG		0	-1	1	0	0	1	-1	0	1	0	0	-1	1	0	0	0	0	0	0	0	0	0	0	0	0	0	0	0	-1	0	0	0	0	0	0	0	0	0	0	0	0
	LPC		0	0	0	0	0	0	0	0	0	0	0	0	0	0	0	0	1	-1	0	0	0	0	-1	0	0	0	0	0	0	0	0	0	0	0	0	0	-1	0	0	0	0
	LPS		0	0	0	0	0	0	0	0	0	0	0	0	0	0	0	0	0	0	1	-1	0	0	0	-1	0	0	0	0	0	0	0	0	0	0	0	-1	0	0	0	0	0
	LPE		0	0	0	0	0	0	0	0	0	0	0	0	0	0	0	0	0	0	0	1	-1	0	0	0	-1	0	0	0	0	0	0	0	0	0	0	0	0	-1	0	0	0
	LPA		0	0	0	0	0	0	0	0	0	0	0	0	0	0	1	-1	0	0	0	0	0	0	1	1	1	0	0	0	1	0	0	0	0	0	-1	0	0	0	0	0	0
	FA		0	0	0	0	0	0	0	0	0	0	0	0	0	0	1	-1	1	-1	1	-1	1	-1	0	0	0	0	0	0	-1	0	0	0	0	0	0	0	0	0	-1	1	0
Equal Flux Assumption	**PC**		0	0	1	-1	0	0	0	0	0	0	0	0	0	0	0	0	0	0	0	0	0	0	0	0	0	0	0	0	0	0	0	0	0	0	0	0	0	0	0	0	0
	PC		0	0	1	0	-1	0	0	0	0	0	0	0	0	0	0	0	0	0	0	0	0	0	0	0	0	0	0	0	0	0	0	0	0	0	0	0	0	0	0	0	0
	PC		0	0	1	0	0	0	0	0	0	0	0	0	0	0	0	0	-1	0	0	0	0	0	0	0	0	0	0	0	0	0	0	0	0	0	0	0	0	0	0	0	0
	PS		0	0	0	0	0	0	0	1	-1	0	0	0	0	0	0	0	0	0	0	0	0	0	0	0	0	0	0	0	0	0	0	0	0	0	0	0	0	0	0	0	0
	PS		0	0	0	0	0	0	0	1	0	-1	0	0	0	0	0	0	0	0	0	0	0	0	0	0	0	0	0	0	0	0	0	0	0	0	0	0	0	0	0	0	0
	PS		0	0	0	0	0	0	0	1	0	0	0	0	0	0	0	0	0	0	-1	0	0	0	0	0	0	0	0	0	0	0	0	0	0	0	0	0	0	0	0	0	0
	PE		0	0	0	0	0	0	0	0	0	0	1	0	-1	0	0	0	0	0	0	0	0	0	0	0	0	0	0	0	0	0	0	0	0	0	0	0	0	0	0	0	0
	PE		0	0	0	0	0	0	0	0	0	0	1	0	0	-1	0	0	0	0	0	0	0	0	0	0	0	0	0	0	0	0	0	0	0	0	0	0	0	0	0	0	0
	PE		0	0	0	0	0	0	0	0	0	0	1	0	0	0	-1	0	0	0	0	0	0	0	0	0	0	0	0	0	0	0	0	0	0	0	0	0	0	0	0	0	0
	PA		0	0	0	0	0	1	0	0	0	0	0	0	0	0	0	-1	0	0	0	0	0	0	0	0	0	0	0	0	0	0	0	0	0	0	0	0	0	0	0	0	0
	DAG		0	1	0	0	0	0	-1	0	0	0	0	0	0	0	0	0	0	0	0	0	0	0	0	0	0	0	0	0	0	0	0	0	0	0	0	0	0	0	0	0	0
	DAG		0	1	0	0	0	0	0	0	0	0	0	-1	0	0	0	0	0	0	0	0	0	0	0	0	0	0	0	0	0	0	0	0	0	0	0	0	0	0	0	0	0
	LPC		0	0	0	0	0	0	0	0	0	0	0	0	0	0	0	0	0	1	0	0	0	0	-1	0	0	0	0	0	0	0	0	0	0	0	0	0	0	0	0	0	0
	LPS		0	0	0	0	0	0	0	0	0	0	0	0	0	0	0	0	0	0	1	0	0	0	0	-1	0	0	0	0	0	0	0	0	0	0	0	0	0	0	0	0	0
	LPE		0	0	0	0	0	0	0	0	0	0	0	0	0	0	0	0	0	0	0	1	0	0	0	0	-1	0	0	0	0	0	0	0	0	0	0	0	0	0	0	0	0
Sink Reactions	**DAG Drain**		0	0	0	0	0	0	0	0	0	0	0	0	0	0	0	0	0	0	0	0	0	0	0	0	0	0	0	0	0	1	0	0	0	0	0	0	0	0	0	0	0.01
	PC Drain		0	0	0	0	0	0	0	0	0	0	0	0	0	0	0	0	0	0	0	0	0	0	0	0	0	0	0	0	0	-1	1	0	0	0	0	0	0	0	0	0	0
	PA Drain		0	0	0	0	0	0	0	0	0	0	0	0	0	0	0	0	0	0	0	0	0	0	0	0	0	0	0	0	0	-1	0	1	0	0	0	0	0	0	0	0	0
	PE Drain		0	0	0	0	0	0	0	0	0	0	0	0	0	0	0	0	0	0	0	0	0	0	0	0	0	0	0	0	0	-1	0	0	1	0	0	0	0	0	0	0	0
	PS Drain		0	0	0	0	0	0	0	0	0	0	0	0	0	0	0	0	0	0	0	0	0	0	0	0	0	0	0	0	0	-1	0	0	0	1	0	0	0	0	0	0	0
	LPA Drain		0	0	0	0	0	0	0	0	0	0	0	0	0	0	0	0	0	0	0	0	0	0	0	0	0	0	0	0	0	-1	0	0	0	0	1	0	0	0	0	0	0
	LPS Drain		0	0	0	0	0	0	0	0	0	0	0	0	0	0	0	0	0	0	0	0	0	0	0	0	0	0	0	0	0	-1	0	0	0	0	0	1	0	0	0	0	0
	LPC Drain		0	0	0	0	0	0	0	0	0	0	0	0	0	0	0	0	0	0	0	0	0	0	0	0	0	0	0	0	0	-1	0	0	0	0	0	0	1	0	0	0	0
	LPE Drain		0	0	0	0	0	0	0	0	0	0	0	0	0	0	0	0	0	0	0	0	0	0	0	0	0	0	0	0	0	-1	0	0	0	0	0	0	0	1	0	0	0
	FA Drain		0	0	0	0	0	0	0	0	0	0	0	0	0	0	0	0	0	0	0	0	0	0	0	0	0	0	0	0	0	-1	0	0	0	0	0	0	0	0	1	0	0
	CDPcho Drain		0	0	0	0	0	0	0	0	0	0	0	0	0	0	0	0	0	0	0	0	0	0	0	0	0	0	1	0	0	0	0	0	0	0	0	0	0	0	0	0	8
	CDPeth Drain		0	0	0	0	0	0	0	0	0	0	0	0	0	0	0	0	0	0	0	0	0	0	0	0	0	0	0	1	0	0	0	0	0	0	0	0	0	0	0	0	8
	sets one flux		0	1	0	0	0	0	0	0	0	0	0	0	0	0	0	0	0	0	0	0	0	0	0	0	0	0	0	0	0	0	0	0	0	0	0	0	0	0	0	0	8

Figure 3.17: The matrix used to solve for the system fluxes. The matrix includes rows for each of the steady state conditions, rows for the equal flux assumption and rows to set the drain fluxes. Finally, the fixing of one flux in the final row is sufficient to solve for the remaining fluxes.

Reaction >>	1	2	3	4	5	6	7	8	9	10	11	12	13	14	15	16	17	18	19	20	21	22	23	24	25	26	27	28	29	30	31	32	33	34	35	36	37	38	39	40		
	1	0	0	0	0	0	0	0	0	0	0	0	0	0	0	0	0	0	0	0	0	0	0	0	0	0	0	0	0	0	0	0	0	0	0	0	0	0	0	0	**1.600E+01**	J_1
	0	1	0	0	0	0	0	0	0	0	0	0	0	0	0	0	0	0	0	0	0	0	0	0	0	0	0	0	0	0	0	0	0	0	0	0	0	0	0	0	**8.000E+00**	J_2
	0	0	1	0	0	0	0	0	0	0	0	0	0	0	0	0	0	0	0	0	0	0	0	0	0	0	0	0	0	0	0	0	0	0	0	0	0	0	0	0	**2.281E+00**	J_3
	0	0	0	1	0	0	0	0	0	0	0	0	0	0	0	0	0	0	0	0	0	0	0	0	0	0	0	0	0	0	0	0	0	0	0	0	0	0	0	0	**2.281E+00**	J_4
	0	0	0	0	1	0	0	0	0	0	0	0	0	0	0	0	0	0	0	0	0	0	0	0	0	0	0	0	0	0	0	0	0	0	0	0	0	0	0	0	**2.281E+00**	J_5
	0	0	0	0	0	1	0	0	0	0	0	0	0	0	0	0	0	0	0	0	0	0	0	0	0	0	0	0	0	0	0	0	0	0	0	0	0	0	0	0	**1.763E+01**	J_6
	0	0	0	0	0	0	1	0	0	0	0	0	0	0	0	0	0	0	0	0	0	0	0	0	0	0	0	0	0	0	0	0	0	0	0	0	0	0	0	0	**8.000E+00**	J_7
	0	0	0	0	0	0	0	1	0	0	0	0	0	0	0	0	0	0	0	0	0	0	0	0	0	0	0	0	0	0	0	0	0	0	0	0	0	0	0	0	**1.415E+00**	J_8
	0	0	0	0	0	0	0	0	1	0	0	0	0	0	0	0	0	0	0	0	0	0	0	0	0	0	0	0	0	0	0	0	0	0	0	0	0	0	0	0	**1.415E+00**	J_9
	0	0	0	0	0	0	0	0	0	1	0	0	0	0	0	0	0	0	0	0	0	0	0	0	0	0	0	0	0	0	0	0	0	0	0	0	0	0	0	0	**1.415E+00**	J_{10}
	0	0	0	0	0	0	0	0	0	0	1	0	0	0	0	0	0	0	0	0	0	0	0	0	0	0	0	0	0	0	0	0	0	0	0	0	0	0	0	0	**2.686E+00**	J_{11}
	0	0	0	0	0	0	0	0	0	0	0	1	0	0	0	0	0	0	0	0	0	0	0	0	0	0	0	0	0	0	0	0	0	0	0	0	0	0	0	0	**8.000E+00**	J_{12}
	0	0	0	0	0	0	0	0	0	0	0	0	1	0	0	0	0	0	0	0	0	0	0	0	0	0	0	0	0	0	0	0	0	0	0	0	0	0	0	0	**2.686E+00**	J_{13}
	0	0	0	0	0	0	0	0	0	0	0	0	0	1	0	0	0	0	0	0	0	0	0	0	0	0	0	0	0	0	0	0	0	0	0	0	0	0	0	0	**2.686E+00**	J_{14}
	0	0	0	0	0	0	0	0	0	0	0	0	0	0	1	0	0	0	0	0	0	0	0	0	0	0	0	0	0	0	0	0	0	0	0	0	0	0	0	0	**1.763E+01**	J_{15}
	0	0	0	0	0	0	0	0	0	0	0	0	0	0	0	1	0	0	0	0	0	0	0	0	0	0	0	0	0	0	0	0	0	0	0	0	0	0	0	0	**2.088E+01**	J_{16}
	0	0	0	0	0	0	0	0	0	0	0	0	0	0	0	0	1	0	0	0	0	0	0	0	0	0	0	0	0	0	0	0	0	0	0	0	0	0	0	0	**2.281E+00**	J_{17}
	0	0	0	0	0	0	0	0	0	0	0	0	0	0	0	0	0	1	0	0	0	0	0	0	0	0	0	0	0	0	0	0	0	0	0	0	0	0	0	0	**1.136E+00**	J_{18}
	0	0	0	0	0	0	0	0	0	0	0	0	0	0	0	0	0	0	1	0	0	0	0	0	0	0	0	0	0	0	0	0	0	0	0	0	0	0	0	0	**1.415E+00**	J_{19}
	0	0	0	0	0	0	0	0	0	0	0	0	0	0	0	0	0	0	0	1	0	0	0	0	0	0	0	0	0	0	0	0	0	0	0	0	0	0	0	0	**7.024E-01**	J_{20}
	0	0	0	0	0	0	0	0	0	0	0	0	0	0	0	0	0	0	0	0	1	0	0	0	0	0	0	0	0	0	0	0	0	0	0	0	0	0	0	0	**2.686E+00**	J_{21}
	0	0	0	0	0	0	0	0	0	0	0	0	0	0	0	0	0	0	0	0	0	1	0	0	0	0	0	0	0	0	0	0	0	0	0	0	0	0	0	0	**1.338E+00**	J_{22}
	0	0	0	0	0	0	0	0	0	0	0	0	0	0	0	0	0	0	0	0	0	0	1	0	0	0	0	0	0	0	0	0	0	0	0	0	0	0	0	0	**1.136E+00**	J_{23}
	0	0	0	0	0	0	0	0	0	0	0	0	0	0	0	0	0	0	0	0	0	0	0	1	0	0	0	0	0	0	0	0	0	0	0	0	0	0	0	0	**7.024E-01**	J_{24}
	0	0	0	0	0	0	0	0	0	0	0	0	0	0	0	0	0	0	0	0	0	0	0	0	1	0	0	0	0	0	0	0	0	0	0	0	0	0	0	0	**1.338E+00**	J_{25}
	0	0	0	0	0	0	0	0	0	0	0	0	0	0	0	0	0	0	0	0	0	0	0	0	0	1	0	0	0	0	0	0	0	0	0	0	0	0	0	0	**1.600E+01**	J_{26}
	0	0	0	0	0	0	0	0	0	0	0	0	0	0	0	0	0	0	0	0	0	0	0	0	0	0	1	0	0	0	0	0	0	0	0	0	0	0	0	0	**8.000E+00**	J_{27}
	0	0	0	0	0	0	0	0	0	0	0	0	0	0	0	0	0	0	0	0	0	0	0	0	0	0	0	1	0	0	0	0	0	0	0	0	0	0	0	0	**8.000E+00**	J_{28}
	0	0	0	0	0	0	0	0	0	0	0	0	0	0	0	0	0	0	0	0	0	0	0	0	0	0	0	0	1	0	0	0	0	0	0	0	0	0	0	0	**9.000E-02**	J_{29}
	0	0	0	0	0	0	0	0	0	0	0	0	0	0	0	0	0	0	0	0	0	0	0	0	0	0	0	0	0	1	0	0	0	0	0	0	0	0	0	0	**1.000E-02**	J_{30}
	0	0	0	0	0	0	0	0	0	0	0	0	0	0	0	0	0	0	0	0	0	0	0	0	0	0	0	0	0	0	1	0	0	0	0	0	0	0	0	0	**1.000E-02**	J_{31}
	0	0	0	0	0	0	0	0	0	0	0	0	0	0	0	0	0	0	0	0	0	0	0	0	0	0	0	0	0	0	0	1	0	0	0	0	0	0	0	0	**1.000E-02**	J_{32}
	0	0	0	0	0	0	0	0	0	0	0	0	0	0	0	0	0	0	0	0	0	0	0	0	0	0	0	0	0	0	0	0	1	0	0	0	0	0	0	0	**1.000E-02**	J_{33}
	0	0	0	0	0	0	0	0	0	0	0	0	0	0	0	0	0	0	0	0	0	0	0	0	0	0	0	0	0	0	0	0	0	1	0	0	0	0	0	0	**1.000E-02**	J_{34}
	0	0	0	0	0	0	0	0	0	0	0	0	0	0	0	0	0	0	0	0	0	0	0	0	0	0	0	0	0	0	0	0	0	0	1	0	0	0	0	0	**1.000E-02**	J_{35}
	0	0	0	0	0	0	0	0	0	0	0	0	0	0	0	0	0	0	0	0	0	0	0	0	0	0	0	0	0	0	0	0	0	0	0	1	0	0	0	0	**1.000E-02**	J_{36}
	0	0	0	0	0	0	0	0	0	0	0	0	0	0	0	0	0	0	0	0	0	0	0	0	0	0	0	0	0	0	0	0	0	0	0	0	1	0	0	0	**1.000E-02**	J_{37}
	0	0	0	0	0	0	0	0	0	0	0	0	0	0	0	0	0	0	0	0	0	0	0	0	0	0	0	0	0	0	0	0	0	0	0	0	0	1	0	0	**1.000E-02**	J_{38}
	0	0	0	0	0	0	0	0	0	0	0	0	0	0	0	0	0	0	0	0	0	0	0	0	0	0	0	0	0	0	0	0	0	0	0	0	0	0	1	0	**1.000E-02**	J_{39}
	0	0	0	0	0	0	0	0	0	0	0	0	0	0	0	0	0	0	0	0	0	0	0	0	0	0	0	0	0	0	0	0	0	0	0	0	0	0	0	1	**1.500E-01**	J_{40}

Figure 3.18: The solution found by reducing the matrix in figure 3.17 to its RREF as detailed in chapter 2. J_x indicates the flux through reaction x.

3.3.3 Target Steady State Concentrations

The fluxes, or the reaction velocities, are some function of the metabolite concentrations. In defining the kinetics, the task is to relate the lipid concentrations to the steady state fluxes. Of course, before this can be done, the steady state concentrations must be defined.

The lipid composition of biomembranes varies greatly. For the purposes of simulation a *'target steady state'* (TSS), which broadly conforms to what has been reported for the rough endoplasmic reticulum (RER), was identified. The concentrations of this TSS are given in table 3.01. This steady state is used in all simulations, unless otherwise stated.

Type I/0 Species	Relative Concentration	Type II Species	Relative Concentration
PC	50	PE	30
PS	12	PA	1
LPA	0.5	DAG	1
LPE	0.5	FA	0.5
LPC	0.5		
LPS	0.5		

Table 3.01: The Target Steady State (TSS).
The concentrations are typical of the rough endoplasmic reticulum in eukaryotic cells.

3.3.4 Kinetics

The kinetics of each reaction were modelled using 'mass action' rate equations. This is a straightforward kinetic type, which assumes that the rate law may be deduced directly from the stoichiometry of the reactions. For the single substrate reaction:

$$A \rightarrow \text{product(s)}$$

There is one substrate and so the rate in the model is first order with respect to the concentration of A. Therefore the reaction is modelled as first order overall. For the irreversible case, there is only one rate constant.

$$\text{Mass action rate} = k.[A]$$

The model also contains a step with two substrates:

$$A + B \rightarrow \text{product(s)}$$

the rate is then first order with respect to the concentrations of both A and B. The reaction is modelled as second order overall.

$$\text{Mass action rate} = k.[A].[B]$$

In general, the mass action rate equation is described in equation 3.03, where k is the rate constant and S_i is the concentration of substrate i.

$$v = k.\prod_i S_i \qquad \text{equation 3.03}$$

The advantage of the mass action rate equation is that the equation can be rearranged to find k as shown in equation 3.04.

$$k = \frac{v}{\prod_i S_i} \qquad \text{equation 3.04}$$

By using these mass action rate equations, each reaction is treated as a single step 'elementary reaction'. With this treatment, the reaction velocities are linear functions of the substrate concentrations and each rate equation may be deduced directly from the stoichiometry of the reaction. The model is therefore a *linear steady state treatment* (Heinrich & Rapoport 1974). Clearly, these enzyme-mediated reactions are not elementary reactions and there is no reason why the reaction kinetics should follow the simplified reaction stoichiometry used in the model. In many cases, they may not. For example, the reactions may operate at substrate saturation. In addition, the order of reaction can only be properly determined experimentally. However, there is no information available that would permit a more accurate modelling of the enzyme kinetics. Again, the challenge would be to disentangle saturation from effects like translocation. Using Hofmeyr's definition of metabolic regulation as *'the alteration of reaction properties to augment or counteract the mass-action trend in a network of reactions'* (Hofmeyr 1995), the addition of feedback to mass action controlled reactions allows the membrane torque tension effect to be seen in isolation.

With a method for determining a set of steady state fluxes and a target steady state defined, it is simple to find a suitable set of reaction coefficients. This is performed by dividing the flux by the product of the reaction's substrate concentrations, as described in equation 3.04. The kinetic constants for the flux solution and the target steady state are given in table 3.02.

	Reactions	Flux, J(Rx)	k(Rx)
R1	(Pcho) → CDPcho	16.000	16.000
R2	CDPcho + DAG → PC	8.000	0.400
R3	PC → DAG	2.281	0.046
R4	PC → PA	2.281	0.046
R5	PC → PS	2.281	0.046
R6	PA → DAG	17.628	17.628
R7	DAG → PA	8.000	8.000
R8	PS → PA	1.415	0.118
R9	PS → DAG	1.415	0.118
R10	PS → PE	1.415	0.118
R11	PE → PS	2.686	0.090
R12	CDPeth + DAG → PE	8.000	0.400
R13	PE → DAG	2.686	0.090
R14	PE → PA	2.686	0.090
R15	PA → LPA + FA	17.628	17.628
R16	LPA + FA → PA	20.884	83.536
R17	PC → LPC + FA	2.281	0.046
R18	LPC + FA → PC	1.136	4.543
R19	PS → LPS + FA	1.415	0.118
R20	LPS + FA → PS	0.702	2.810
R21	PE → LPE + FA	2.686	0.090
R22	LPE + FA → PE	1.338	5.351
R23	LPC → LPA	1.136	2.271
R24	LPS → LPA	0.702	1.405
R25	LPE → LPA	1.338	2.676
R26	(Peth) → CDPeth	16.000	16.000
R27	CDPeth →	8.000	0.400
R28	CDPeth →	8.000	0.400
R29	(g3p) + FA → LPA	0.090	0.180
R30	DAG →	0.010	0.010
R31	PC →	0.010	0.0002
R32	PA →	0.010	0.010
R33	PE →	0.010	0.000333
R34	PS →	0.010	0.000833
R35	LPA →	0.010	0.020
R36	LPS →	0.010	0.020
R37	LPC →	0.010	0.020
R38	LPE →	0.010	0.020
R39	FA →	0.010	0.020
R40	( ) → FA	0.150	0.150

Table 3.02: Calculated values for k(Rx).
k(Rx) values are calculated to give the steady state fluxes found from the solution of the stoichiometric matrix (see figure 3.17 and 3.18).

Just as there is no information on the rate laws for each step, there is little information on the equilibrium coefficients. Strictly, every reaction should follow the *principal of microscopic reversibility*. However, this is usefully applied only at equilibrium. It is known that biological systems operate far from equilibrium, with the product being removed.

Nearly all metabolic sequences are essentially 'unidirectional': this prevents 'futile cycles' or pseudocycles which would loop consuming ATP and wasting the cells energy (Atkinson 1977, p55). Separate enzymes, catalysing opposite directions, can be beneficial and must have evolved specifically because of the advantages of kinetic control of *direction* as well as control of rate (Atkinson 1977, p57). In addition, Hofmeyr has shown that the further a reaction is from equilibrium the greater the potential for regulation (Hofmeyr 1995). With limited knowledge of how reversible the reactions are in vivo, the reactions have been implemented in the direction reported and reverse reactions are included explicitly in the stoichiometric network only where they are reported.

It can be argued that the model contains little information about the details of each reaction. In general, Metabolic Control Analysis does not consider the details of enzyme reactions (Fell 1992), effectively treating the kinetic properties of the component enzymes as a 'black box'. Some have been critical of this level of abstraction, suggesting that investigating mechanisms is the only reason for studying kinetics. However, for understanding how entire pathways behave it has been found useful to decrease the emphasis on individual reaction mechanisms. This is essentially the approach adopted here. The next stage in the development of the model was the modelling of the stored elastic energy and its effects on the kinetics of the system.

3.4 Feedback Functions

The modelling of the stored elastic energy and the proposed feedback comprised two parts. The first stage involved the definition of a parameter to act as a proxy for the membrane torque tension and the provision of a method to calculate its value from the lipid composition. The second stage was to build an equation to model the modulation of the enzyme activity by the membrane torque tension. The following sections detail the way these parameters were calculated, and the reasons for the selections made.

3.4.1 The Torque Parameter

The first task was to create a parameter to act as a proxy for the torque tension. This proxy will be termed the *torque parameter*, λ. A proxy is used because calculation of the stored elastic energy in the membrane is not directly possible. This would require knowledge of the spontaneous curvature (c_0) and the elastic constant (κ_m) for each species in the complex mixed bilayer system.

A. Determining the torque parameter

The torque tension is determined by the relative amounts of type I/0 and type II amphiphiles. The torque parameter is therefore based as a first approximation on the proportions of type I/0 and type II lipids as shown in equation 3.05. Small values of λ would indicate low stress, whilst large values represent stressed bilayers.

$$\frac{\text{'TypeII lipids'}}{\text{'Type0 + TypeI lipids'}} \rightarrow \lambda \text{ which represents the MTT} \qquad \text{equation 3.05}$$

To evaluate the left hand side of equation 3.05, each lipid species is assigned a coefficient as shown in equation 3.06. The coefficient reflects the spontaneous curvature and the elastic constant of each lipid. For example, the relative sizes of a_1 and a_2 are assigned based on the relative shapes of PE and DAG. DAG, a more strongly type II lipid, will make a larger contribution to λ than will PE and should be given a larger coefficient.

$$\lambda = \frac{a_1[\text{PE}] + a_2[\text{DAG}] + a_3[\text{PA}] + a_4[\text{FA}]}{b_1[\text{PC}] + b_2[\text{PS}] + b_3[\text{LPA}] + b_4[\text{LPC}] + b_5[\text{LPE}] + b_6[\text{LPS}]} \qquad \text{equation 3.06}$$

B. Torque parameter coefficients

The choice of the magnitudes of the coefficients a_1 through a_4 and b_1 through b_7 were largely arbitrary. The relative values are of importance in the determination of the torque parameter, and these were chosen as the result of two conditions. The initial values were chosen as the reciprocal of the species' concentration at the TSS. Notionally, species that have a small effect on the membrane torque are present in high concentrations, whilst species that have a large effect on the torque are present only in small concentrations. Adjustment was then made to improve the coefficients; the relative magnitudes of the coefficients were based on a ranking of the species in the order of their spontaneous curvatures, and 'best guesses' of the combined effect of c_0 and κ_m. The order used is shown in table 3.03 and the coefficients used are summarised in table 3.04.

type I		type 0		type II
LPS > LPC > LPE > LPA	**>**	**PS ≈ PC**	**>**	**PA > PE > FA > DAG**
positive curvature	←	zero curvature	→	negative curvature

Table 3.03: Order of the spontaneous curvature.

Type I/0 species	Coefficient	Type II species	Coefficient
LPS	200	PA	10
LPC	150	PE	20
LPE	100	FA	100
LPA	50	DAG	300
PC, PS	1		

Table 3.04: The coefficients for the lipid species. The coefficients are based upon limited knowledge of the spontaneous curvature and the elastic constant.

$$\lambda = \frac{20[\mathrm{PE}] + 300[\mathrm{DAG}] + 10[\mathrm{PA}] + 100[\mathrm{FA}]}{[\mathrm{PC}] + [\mathrm{PS}] + 50[\mathrm{LPA}] + 150[\mathrm{LPC}] + 100[\mathrm{LPE}] + 200[\mathrm{LPS}]} \qquad \text{equation 3.07}$$

Using the coefficients in table 3.04, the equation for the torque parameter is given in equation 3.07. This allows monitoring of the changes in the torque tension. However, in order to implement feedback to investigate its effect, the next step is to develop a method to model the modulation of enzyme activity by the torque tension.

3.4.2 Modelling Enzyme Modulation by the Torque Tension

With a method to evaluate the torque by the calculation of the torque parameter λ, the next stage was to consider the modulation of enzyme activity. This is essential in order to implement explicit feedback. The first stage in this was the incorporation of a *modulation coefficient* in the rate equation.

A. The modulation coefficient σ

For a simple single substrate reaction obeying irreversible mass action kinetics the rate equation is:

$$v = -dS_i/dt = k.S_i$$

For an enzyme that is modulated, the rate coefficient k is the product of a constant k' and a variable σ, the modulation coefficient, as shown in equation 3.08. The variable σ represents the amount of enzyme bound, and models the change in activity. The rate v is then calculated as in equation 3.09.

$$k = k'.\sigma \qquad \text{equation 3.08}$$

$$v = k'.\sigma.\prod_i S_i \qquad \text{equation 3.09}$$

It is convenient if the value of σ at the target steady state, σ_{TSS}, is unity. In this way, the coefficient k used in the standard mass action equation to satisfy the steady state flux can remain conveniently unchanged when a feedback function is added.

$$k = k'.\sigma_{TSS} \quad \Rightarrow \quad k = k' \qquad \text{equation 3.10}$$

To ensure that $\sigma_{TSS} = 1$, a scaling constant c_1 is included to satisfy equation 3.11.

$$\sigma_{TSS} = c_1.\sigma'_{TSS} = 1 \qquad \text{equation 3.11}$$

in general, $$\sigma = c_1.\sigma' \qquad \text{equation 3.12}$$

σ' indicates the amount of enzyme that is active, and σ'_{TSS} the amount active at the target steady state. The equations used for σ', and the significance of σ'_{TSS} when considering feedback strength, are now examined.

B. Calculating the modulation coefficient from λ

The evaluation of σ´ in the model requires a function which determines a value for a given torque parameter λ. In order to find a suitable equation the behaviour of σ´ required as λ changes was considered. First 'normal' feedback will be considered. Normal feedback here describes feedback where an increase in stored elastic energy causes an increase in enzyme activity, as is exhibited by CCT. When λ is high, the stored elastic energy is high and CCT partitions to the membrane so σ'_{norm} should be high. Another important feature of the behaviour of σ'_{norm} is that when λ is very high σ'_{norm} must tend to unity: activity should reach a maximum value when all the enzyme is active. A simple function that behaves in this way is:

$$y = a.\exp[-(b.x)^{-1}]$$

The understanding of this function is important in the parameterisation of σ. This function is plotted in figure 3.19 for various values of *a* and *b*.

The proportionality relationship between σ'_{norm} and λ is given in equation 3.13. The remainder of this section details the way in which σ´ is parameterised.

$$\sigma'_{norm} \propto \exp(-1 / \lambda) \qquad \text{equation 3.13}$$

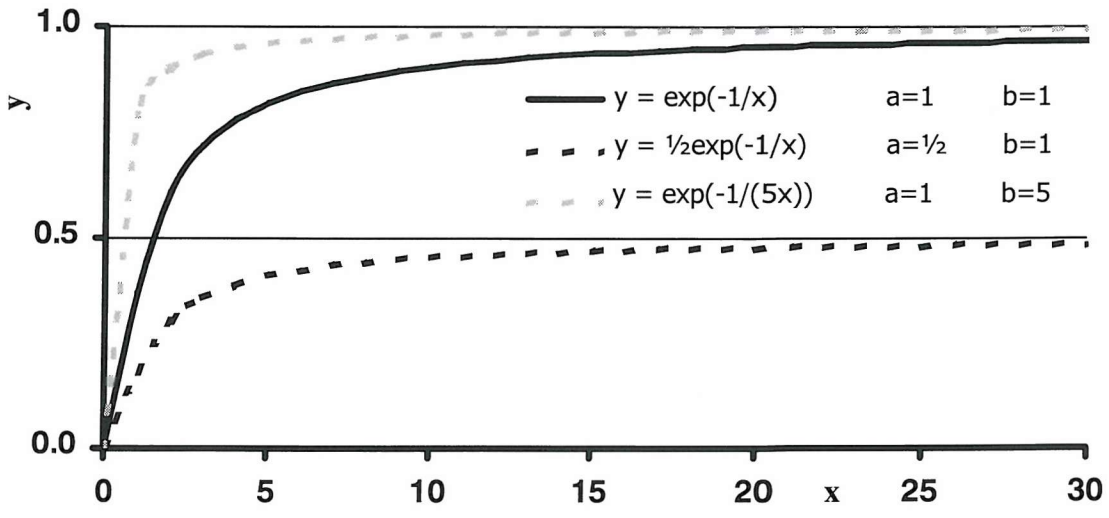

Figure 3.19: Plots of *y=a.exp(-1/(b.x))* to show the effect of the constants *a* and *b*.
The plot for *y=a*.exp(-1/(*bx*)) with *a*=1 and *b*=1 has an asymptote at 1. If *a*=½ the asymptote is ½. In general, the vertical scaling and therefore the asymptote, is determined by *a*. The constant *b* determines the horizontal scaling of the curve.

C. Parameterising the modulation coefficient: strength of feedback

If the relationship between σ and λ were a direct proportionality, the feedback strength would be determined by the gradient of the σ vs. λ plot. However, because of the exponential relationship defined, the gradient depends on the position on the curve and the definition of feedback strength is rather more complicated.

Figure 3.20 shows a plot of σ′ vs. λ. Two points (a) and (b) are marked. Position (a) corresponds to around half the maximum activity. If λ is increased, a large change in σ′ will occur to counter it. Position (b) corresponds to around 9/10 maximum activity. Here, if λ is increased the change in σ will be smaller. Position (a) therefore corresponds to a stronger feedback than position (b).

The relationship between σ′ and λ must be parameterised to allow the alteration of feedback strength by determining the amount bound, σ'_{TSS} at the target steady state torque parameter, λ_{TSS}. This is achieved by scaling the curves so either (a) or (b) correspond to λ_{TSS}. Horizontal scaling of $y = a.\exp(-(b.x)^{-1})$ is achieved by changing the value of b. A second coefficient, c_2 is now added to the equation for σ′ to allow the feedback strength to be set.

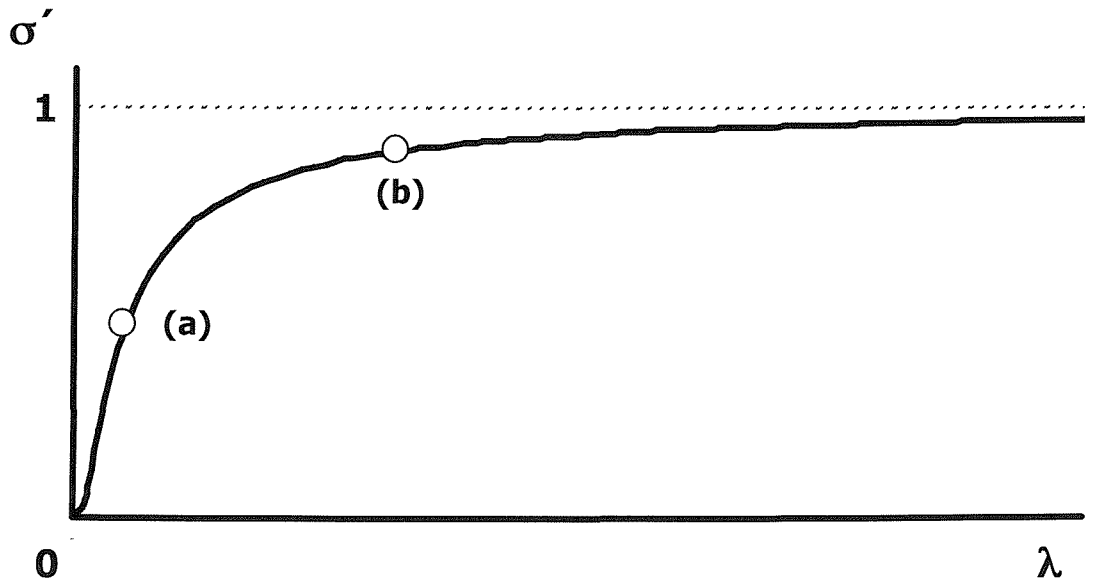

Figure 3.20: An example σ vs. λ plot to illustrate feedback strength.
The two marked points correspond to two possible values of σ at the TSS.
(a) Proportion of enzyme bound is small; value of σ is sensitive to the torque parameter, λ.
(b) Proportion of enzyme bound is large; value of σ is insensitive to the torque parameter, λ.

D. Setting σ'_{TSS}

A coefficient c_2 is added to the relationship between σ and λ, which is given in equation 3.14. The coefficient c_2 is used as a scaling factor, and determines the sensitivity to the lipid ratio by setting the value of σ'_{TSS}.

$$\sigma'_{norm} = \exp\left(-\frac{1}{c_2.\lambda}\right) \qquad \text{equation 3.14}$$

Figure 3.21 shows two possible plots of σ' against λ with two different values of c_2, giving two different values of σ'_{TSS}. The effect of increasing c_2 is to increase the proportion of the total enzyme bound at λ_{TSS}, this corresponds to weaker feedback as was shown in figure 3.20.

The next section examines plots of σ (rather than σ') against λ, this shows the result of the way σ is defined so that $\sigma_{TSS} = 1$.

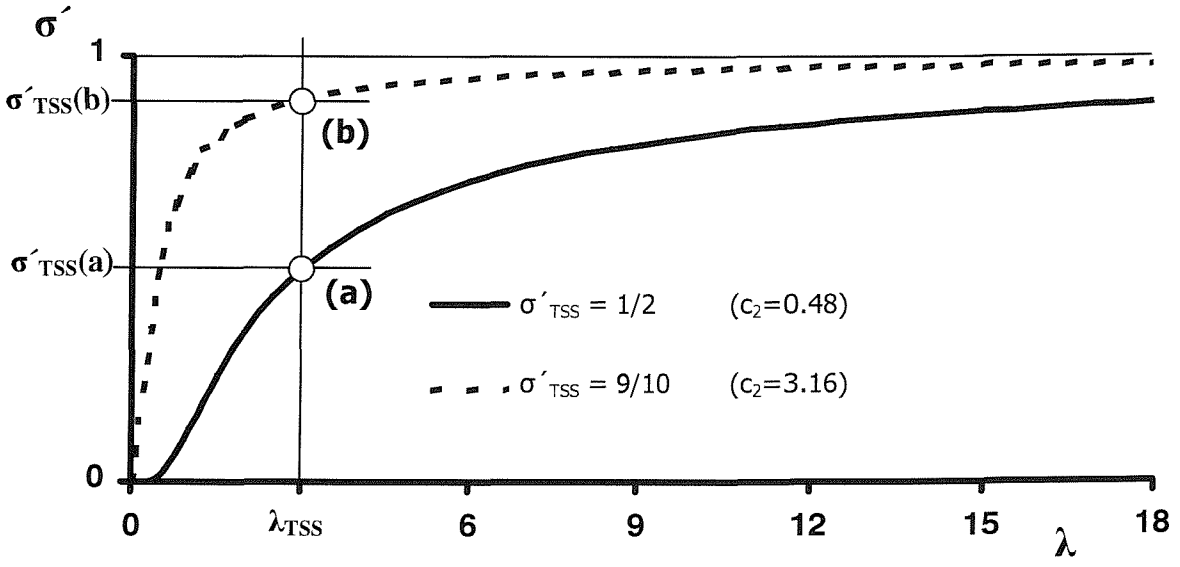

Figure 3.21: σ' vs. λ plot: the effect of the coefficient c_2.
c_2 is used to set the value of σ'_{TSS}. This sets the 'feedback strength'. σ'_{TSS} for (a) is ½, so at the target steady state ½ the enzyme is active. σ'_{TSS} for (b) is 9/10, the increase in σ' possible is smaller (the maximum value is 1) and σ' is insensitive to λ.

E. Plots of σ

Using equation 3.12 ($\sigma = c_1.\sigma'$), the equation for σ_{norm} is given in equation 3.15.

$$\sigma_{norm} = c_1.\exp\left(-\frac{1}{c_2.\lambda}\right) \qquad \text{equation 3.15}$$

When σ is plotted, rather than σ′, the curves are seen to cross at λ_{TSS} as shown in figure 3.22. This is because, in both cases, σ_{TSS} is unity (this is part of the definition of σ). The difference in the two plots is the value of σ'_{TSS}; in one case around half of the enzyme is active at the TSS ($\sigma'_{TSS} = ½$), in the other 9/10 is active ($\sigma'_{TSS} = 9/10$). It can be seen that in each case $\sigma_{TSS} = 1$, and σ varies between 0 and c_1.

The significance of c_1 and c_2 may now be examined. To set up a modulation expression for a step, c_1 and c_2 must be calculated. c_1 and c_2 may be calculated by substituting the values of σ'_{TSS} and λ_{TSS} into equation 3.14 and rearranging to give:

$$c_1 = 1/\sigma'_{TSS} \qquad c_2 = -1/(\lambda_{TSS} . \ln \sigma'_{TSS}) \qquad \text{equation 3.16}$$

This shows c_1 and c_2 are determined by the particular steady state composition and the fraction of lipid bound at this steady state. The equation also reveals the usefulness of c_1; since it is inversely proportional to σ'_{TSS}, c_1 is a measure of the feedback strength.

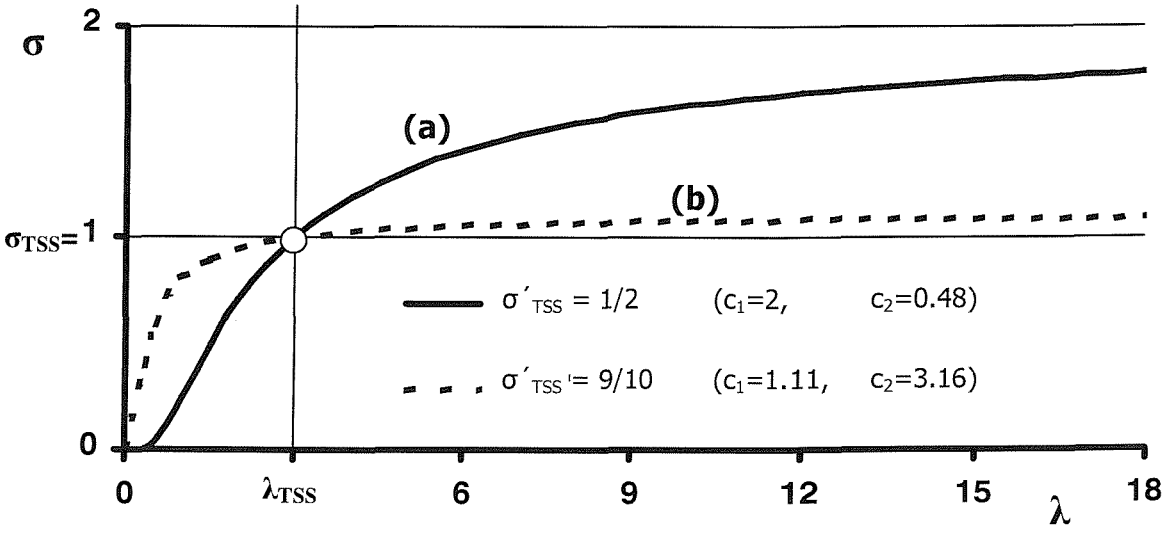

Figure 3.22: σ vs. λ plot: the effect of c_1 and c_2 upon σ'_{TSS}, the fraction of enzyme bound at the TSS. σ is scaled to unity in each case by c_1, it is the asymptote of sigma, which is set by c_1, that changes. c_1 shows how 'open' the reaction is at TSS, e.g. If c_1=2 the reaction is modulated to 1/2 = 0.5 = 50% at TSS. If c_1=1.11 the reaction is modulated to 1/1.11 = 0.9 = 90%.

F. 'Inverse' feedback

To recap, normal feedback models the feedback where an increase in MTT causes an increase in enzyme activity. Inverse feedback is defined where a decrease in membrane torque tension causes an increase in enzyme activity (the need for this type of feedback is revealed in the results presented in chapter 4).

To model inverse feedback, the expression for σ is modified to invert the relationship between σ and λ. It is important to note that σ'_{inv} still represents the proportion of enzyme that is active; the change is purely in the relationship between σ and λ. The different relationships are shown in equation 3.15 and equation 3.17. Two example plots of σ_{inv} against λ are shown in figure 3.23 (for comparison with figure 3.22 for normal feedback).

$$\sigma_{norm} = c_1.\exp\left(-\frac{1}{c_2.\lambda}\right) \qquad \text{equation 3.15}$$

$$\sigma_{inv} = c_1.\exp\left(-\frac{\lambda}{c_2.}\right) \qquad \text{equation 3.17}$$

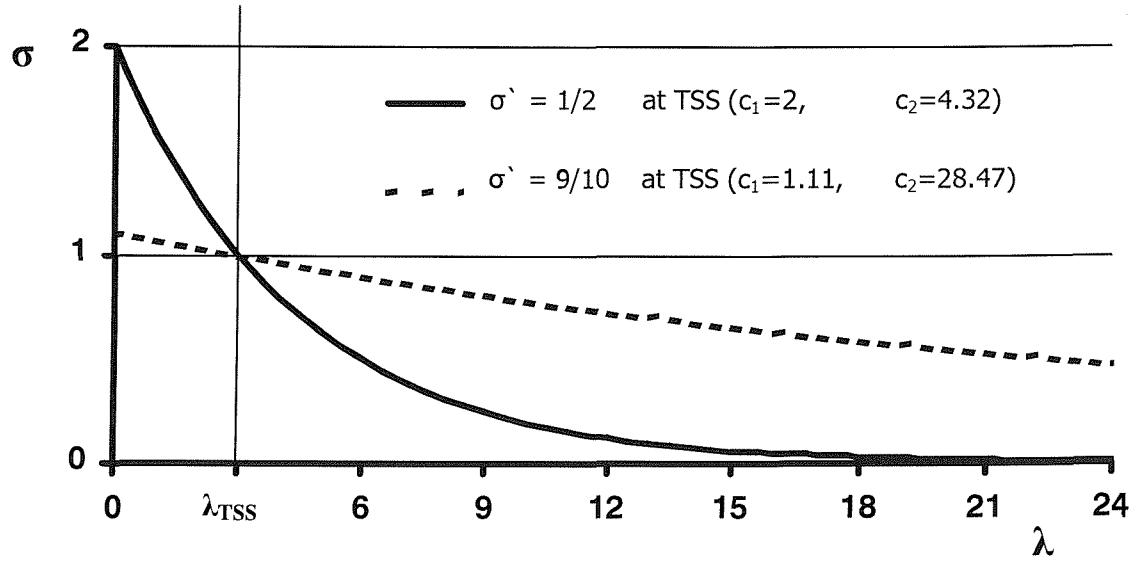

Figure 3.23: σ vs. λ plot: inverse feedback. σ against λ plots for a membrane with λ_{TSS} = 3 and σ'_{TSS} at 0.5 and 0.9. σ_{TSS} is scaled to unity in each case by c_1, the value of σ'_{TSS} and the intercept of σ varies. c_1 and c_2 are used to set the fraction of enzyme bound at the TSS.

3.4.3 Summary of the Modelling of Stored Elastic Energy Effects

In summary, there are two stages in the modelling of membrane torque tension effects. The first is the setting up of a proxy for the torque tension, the torque parameter λ. The calculation of λ from the lipid concentrations is given by equation 3.07.

$$\lambda = \frac{a_1[\mathrm{PE}] + a_2[\mathrm{DAG}] + a_3[\mathrm{PA}] + a_4[\mathrm{FA}]}{b_1[\mathrm{PC}] + b_2[\mathrm{PS}] + b_3[\mathrm{LPA}] + b_4[\mathrm{LPC}] + b_5[\mathrm{LPE}] + b_6[\mathrm{LPS}]} \qquad \text{equation 3.07}$$

The second stage is the modelling of the modulation of enzyme activity by the membrane torque tension. In order to explicitly implement feedback modulation, σ is used as a multiplier to modify the mass action rate equation as shown in equation 3.09.

$$v = k'.\sigma.\prod_i \mathrm{S}_i \qquad \text{equation 3.09}$$

σ_{norm} and σ_{inv} are calculated as in equation 3.15 and 3.17 for normal and inverse feedback respectively.

$$\sigma_{\mathrm{norm}} = c_1.\exp\left(-\frac{1}{c_2.\lambda}\right) \qquad \text{equation 3.15}$$

$$\sigma_{\mathrm{inv}} = c_1.\exp\left(-\frac{\lambda}{c_2.}\right) \qquad \text{equation 3.17}$$

Again, it is important to note that only the calculation of λ factors in the sensitivity analysis performed in this work; the final three equations are used only in the explicit implementation of feedback.

3.5 Software

With the model network finalised and the kinetics defined, the next requirement was for a method to implement and experiment with the model; the requirement was for numerical integration and steady state solving software. After experimenting with various engineering modelling software packages, a freeware biochemical reaction simulator called GEPASI was selected. Results from this were verified using a custom numerical routine (CNR). For each method there follows a description of its features, how it works and any limitations of the software.

3.5.1 Gepasi 3.21 (General Pathway Simulator)

'GEPASI is a software system for modelling chemical and biochemical reaction networks on computers running Microsoft Windows. For a system of up to 45 metabolites and 45 reactions, each with any user-defined or one of 35 pre-defined rate equations, one can produce trajectories of the metabolite concentrations and obtain a steady state (if it does exist).' (Mendes 1993).

Gepasi (copyright Mendes P 1989, 1992, 1993, 1996-1999) is a user-oriented program with a graphical user interface (GUI). Since it is a user-friendly biochemical simulation program, the system to be studied can be described by simply entering the balanced chemical reactions. The program generates the time course data, solves for the steady state and can analyse the steady state using Metabolic Control Analysis. Results can be viewed quickly and conveniently in graphical form by configuring the program to pass its data to GNUplot, a plotting program (copyright 1986 - 1993, 1998 Williams T, Kelley C). Gepasi is also capable of multi-compartment models and can perform *optimisation* and *fitting* to data (e.g. data from experiments). The time course and scan functions facilitate the altering of parameters. Crucially, it is possible to define custom kinetic types. Furthermore, user defined parameters, such as the calculation of λ, may be monitored by utilising the user-function features.

The algorithms used are more complex than the simple procedure outlined in chapter 2. For time course tracking, Gepasi integrates systems of differential equations with the *Livermore Solver of Ordinary Differential Equations* (LSODE) routine. This solver of ordinary differential equations (ODEs), is part of the

ODEPACK package of numerical methods for ODEs and was written by Petzold and Hindmarsh (Hindmarsh 1983). LSODE is a sophisticated algorithm that measures the stiffness of the equations and switches the integration method dynamically according to this measure of stiffness (Petzold 1983). The methods used are: for non-stiff regions, the Adams method with variable step size and variable order (up to 12th order) and for stiff regions, the Gear (or BDF) method with variable step size and order (up to 5th order).

The steady state is expressed by setting the differential equations that describe the time evolution of the metabolic system to zero. This forms a system of non-linear algebraic equations. To solve them, Gepasi uses a series of strategies utilising more than one numerical method. The user can choose among the following strategies. Firstly, use of the damped Newton method on the non-linear algebraic equations defining the steady state. The initial concentrations set by the user are taken as guesses for the solution. Secondly, the program can use the ODE solver to follow the time course, defined by the differential equations, until a steady state is reached. At 10^{10} units of time, if no steady state has been reached, the method halts with no solution. These methods may also be used in combination: the program can use the ODE method followed by the Newton method. Further details on GEPASI, its features and applications may be found in the literature (Mendes 1993; Mendes 1997; Mendes & Kell 1998).

The main limitation with any commercial software is that the program is a 'black box'. GEPASI does make it clear which algorithm it uses. However, the details of how the program works are not known. For example, GEPASI rounds rate constants entered (e.g. 0.0033333333 pasted from a spreadsheet became 3.33E-003 which caused disagreement with other results). It is of importance to verify the output from GEPASI to ensure that the model that is input is correctly implemented, this is particularly important when using custom kinetic functions, as used for the feedback. The functions for λ and σ are unique to the simulations in this work, so will not have been tested by other users. Therefore, it is vitally important to test that the entered functions are processed correctly. The other limitations are in the program's flexibility. Although in many ways the program is much more flexible than the code written for this work, it is not customisable in the same way.

3.5.2 Custom Numerical Routine (CNR1.0)

The routine written for this project uses a numerical integration algorithm (similar to that detailed in section 2.2.4 in chapter 2) to project the time evolution of the metabolite concentrations. The program is written in portable ANSI C language (ANSI 1990; Deitel & Deitel 1994; Kernighan & Ritchie 1988). The code is included in appendix 1. The principles of the routine are also depicted as a flow chart in figure 3.24 and the details of the simulation engine are explained in the following section.

The routine lacks some of the advanced methods and features of the commercial software. The program has no ability to detect the steady state or to use multiple strategies, as used in Gepasi, to solve for the steady state. The method is a simple 'brute force' numerical integration. For example, there is no algorithm to detect stiffness and adjust the method accordingly. A single time interval, set by the user, is used throughout the simulation. The simulations are thus perhaps not as efficient as they might be. In order to achieve accuracy to match Gepasi requires long runtimes (~20hours) simulating StN3. However, running at lower accuracy gives results with sufficient precision to see changes and trends prior to running a longer simulation.

Functions have been written to allow input in terms of the reactions producing and consuming each species. From this the program can determine the substrates and products of each reaction and from this the rate equations. The input however remains less convenient than that for Gepasi. For example, the parameters are entered by editing the code before compiling, rather than through a front-end GUI and file-system. User-friendly input and output is not a high priority, since the software was designed as a developable tool and is not intended for general use. The routine is therefore a useful simulation tool, but is best used in conjunction with other packages. The CNR is primarily used in this work to verify results from Gepasi. As mentioned previously, this is particularly important for testing the implementation of custom kinetic types, including the feedback effect, and user functions. The main advantages of using a custom routine are knowledge of how it works and control over the numerical integration algorithm used. Custom output is also an advantage (example output is shown in figure 3.25). This allows the introduction of new functionality and any desired output calculations, reducing the processing of data. For example, a calculation of the bilayer to non-bilayer ratio may be easily added.

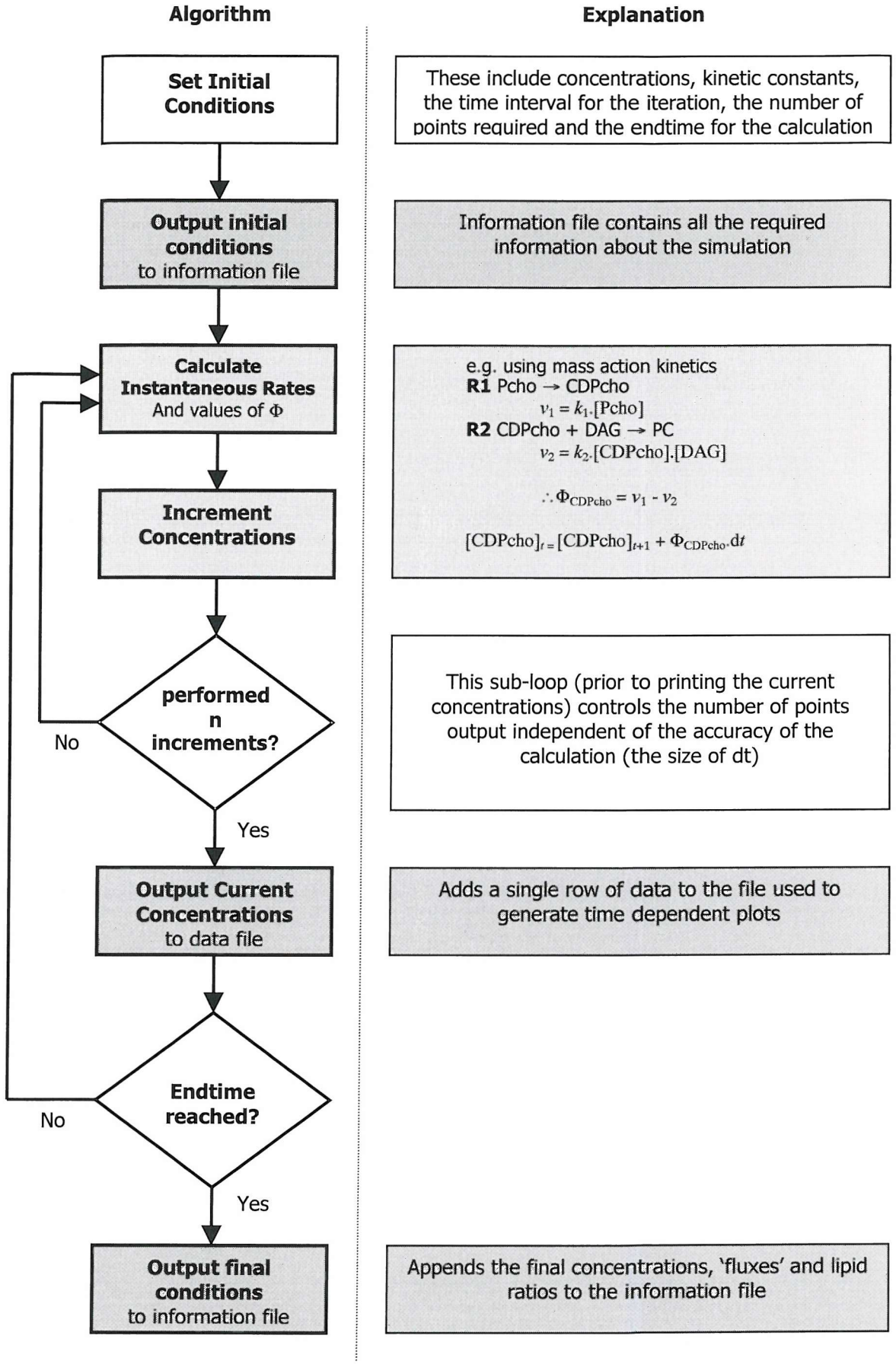

Figure 3.24: Flow chart showing the procedure used in the CNR.
The full code is listed in appendix 1.

```
Simulation Details
        ****insert important points here******
        ****insert important points here******
        ****insert important points here******

Date and Time      : Sat Aug 17 14:53:30 2002

Runtime Parameters
        Endtime             : 30000
        Time interval (dt): 0.000100
          (Iterations       : 300000000)

Connectivity Matrix
          spec      1  2  3  4  5  6  7  8  9 10 11 12 13 14 15 16 17 18 19 20 21 22 23 24 25 26 27 28 29
        r[ 1]      -1  1  0  0  0  0  0  0  0  0  0  0  0  0  0  0  0  0  0  0  0  0  0  0  0  0  0  0  0
        r[ 2]       0 -1  1  0 -1  0  0  0  0  0  0  0  0  0  0  0  0  0  0  0  0  0  0  0  0  0  0  0  0
        r[ 3]       1  0 -1  0  1  0  0  0  0  0  0  0  0  0  0  0  0  0  0  0  0  0  0  0  0  0  0  0  0
        ↓
        r[47]       0  0  0  0 -1  0  0  0  0  0  0  0  0  0  0  0  0  0  0  0  0  0  0  0  0  0  0  0  0

Flows from and to metabolites
        met: 1 (P-cho    )  in:    3    9   37       out:    1
        met: 2 (CDP-cho  )  in:    1                out:    2   42
        met: 3 (PC       )  in:    2                out:    3    4    6   10   36   44
        ↓
        met:29 (P-Sa     )  in:   39       out:   40

Reactions and Rates
        R(1)  k   :  0.75000 P-cho  -> CDP-cho
        R(2)  k   : 65.00000 CDP-cho  +   DAG  -> PC
        R(3)  k   :  0.00179 PC  -> P-cho  + DAG
        ↓
        R(47) k   :  0.00100   DAG  ->

Initial Concs
        0:          conc    : 0.0000000
        1:   P-cho conc     : 0.0100000
        2: CDP-cho conc     : 0.0100000
        ↓
        29:   P-Sa conc     : 0.0100000

Final Concs
        0:          conc    : 0.0000000
        1:   P-cho conc     : 0.0100000
        2: CDP-cho conc     : 0.0084527
        ↓
        29:   P-Sa conc     : 0.0033333

Species Fluxes
        P-cho      -0.001609925
        CDP-cho    -6.037293e-008
        PC          1.530598e-009
        ↓
        P-Sa       -3.74607e-014

Reaction Fluxes
        rate  1  0.0074999
        rate  2  0.0066547
        rate  3  0.0010425
        ↓
        rate 47  0.0000121
```

Figure 3.25: An example CNR information file. The file summarises the simulation. A data file is also output containing the time course data for each metabolite.

3.5.3 The CNR Simulation Engine

This section briefly explains the numerical integration algorithm used in the CNR. This is a Runge-Kutta method and is essentially an enhancement of the method described in section 2.2.4 in chapter 2.

Consider the elementary step A → B with *first order rate constant k*:

$$da/dt = -k.a \qquad \text{where } a = [A]_t$$

Integrating:

$$a = a_0.\exp(-k.t)$$

In the numerical technique used in the code the method is to evaluate the concentration of a at some time $a(t + dt)$ given the concentration at time t. Following the simple first order method detailed in chapter 2:

$$a(t + dt) = a(t) - k.a(t).dt$$

The method was shown to be equivalent to expanding the exponential as a series and neglecting terms in $(dt)^2$ and higher, making this a first order method. This method is fast, requiring only one evaluation per timestep. However, for complex systems, simply neglecting the higher terms may not be valid with reasonable timesteps. In this situation, more general approximations are required.

The Custom Numerical Routine has been programmed to perform a *fourth order Runge-Kutta* algorithm (Gear 1971; Pilling & Seakins 1996, p.201). To evaluate the concentration at $t + \delta t$ the method is:

$$a(t + \delta t) = a(t) + (\alpha_0 + 2\alpha_1 + 2\alpha_2 + \alpha_3)/6 \qquad \text{equation 3.18}$$

the second term is a weighted average of the following results

$$\alpha_0 = f(a(t)).\delta t \qquad \alpha_1 = f(a(t) + \alpha_0/2).\delta t$$

$$\alpha_2 = f(a(t) + \alpha_1/2).\delta t \qquad \alpha_3 = f(a(t) + \alpha_2).\delta t$$

where $da/dt=f(a)$, a function of a and, usually, other species.

The algorithm is more simply described graphically, as in figure 2.26. In the simple first order method α_0 was simply evaluated and added. The fourth-order Runge-Kutta algorithm is clearly more complex, requiring four evaluations of $f(a)$ for each timestep. However by evaluating $f(a)$ at values spread over the timestep, rather than simply for the conditions at the start of the time interval, the method predicts the forward behaviour of the system.

The Runge-Kutta method allows a much larger timestep giving the method greater reliability and efficiency. The method is however still susceptible to the problems associated with stiff coupled differential equations. This explains the long runtimes required in comparison with the more sophisticated approach adopted by the routines used in Gepasi.

In summary, the use of Gepasi and the CNR provides flexible high performance software and a custom routine able to verify the data produced. The final section of this chapter is a summary of the assumptions made in the development of the model.

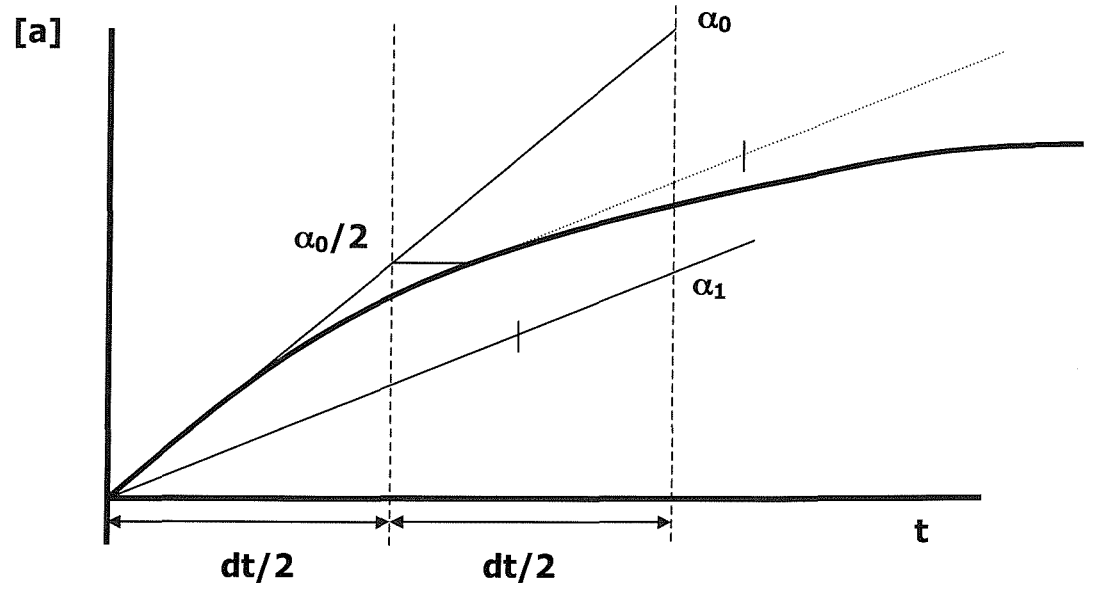

Figure 3.26: Graphical representation of the evaluation of α_0 and α_1 in the Runge-Kutta algorithm. α_1 reflects the gradient at t+dt/2. This shows how the algorithm predicts the forward behaviour of the system.

3.6 Summary of Model Assumptions

A significant number of assumptions are made in the construction of the model. These features of the model and the assumptions involved are summarised:

- The network topology is based on the literature and applies to a mammalian eukaryotic cell (but not a liver cell, as PEMT is not included).
- Lipids classified by headgroup and number of chains only, the effects of acylation/alkylation patterns are ignored.
- Stoichiometric network focuses on the central part of the pathway, including PC its precursors and the other abundant phospholipids, PS and PE.
- Model treats the membrane as a well-mixed solution, ignoring the sub-cellular location of the enzymes.
- Species external to the membrane treated as inexhaustible pools.
- Asymmetry of the bilayer is ignored.
- Arbitrary choice of steady state membrane lipid composition, the *target steady state,* that broadly conforms to that reported for the RER.
- Flux solution for the pathway found by using the *equal branch flux assumption.*
- Mass action kinetics with the order of reaction inferred directly from the stoichiometry of the reaction, since there is no mechanistic information available for the reactions.
- Irreversible kinetics, significant reverse steps included explicitly where reported.
- Kinetic constants found to satisfy the flux solution, not from any knowledge of the real parameters, this information is unknown.
- Membrane torque tension determined by a proxy, a ratio of lipid concentrations, termed the *torque parameter* λ.
- Enzymes are modelled as independent of other enzymes. The enzymes are also not included in the calculation of the torque parameter.
- Coefficients in λ are based on best guesses of behaviour in mixed bilayer
- Explicit feedback implemented using a simple saturating relationship between torque and the modulation of enzyme activity.

3.7 References

ANSI (1990) *American National Standard for Information Systems - Programming Language C (ANSI Document ANSI/ISO 9899: 1990)*
New York: American National Standards Institute.

Atkinson DE (1977) *Cellular Energy Metabolism and its Regulation*
New York: Academic Press.

Barkai N & Leibler S (1997)
Robustness in Simple Biochemical Networks.
Nature **387**: 913-917.

Deitel HM & Deitel PJ (1994) *C: How to Program*
Second edition. Prentice Hall International.

Fell DA (1992)
Metabolic Control Analysis: a survey of its theoretical and experimental development.
Biochem. J. **286**: 313-330.

Gear GW (1971) *Numerical Initial Value Problems in Ordinary Differential Equations*
New Jersey: Prentice-Hall.

Haldar D & Vankura A (1992)
Glycerophosphate Acyltransferase from Liver.
Method. Enzymol. **209**: 64-73.

Hartwell LH, Hopfield JJ, Leibler S & Murray AW (1999)
From molecular to modular cell biology.
Nature **402**: C47-C52.

Heinrich R, Rapoport SM & Rapaport TA (1977)
Metabolic Regulation and Mathematical Models.
Prog. Biophys. Molec. Biol. **32**: 1-82.

Heinrich R & Rapoport TA (1974)
A Linear Steady-State Treatment of Enzymatic Chains.
Eur. J. Biochem. **42**: 89-95.

Hindmarsh AC (1983) *ODEPACK, A Systematised Collection of ODE Solvers*, p.55-64.
In *Scientific Computing*
Edited by R S Stepleman et al. Amsterdam: North-Holland.

Hjelmstadt RH & Bell RM (1991)
Molecular Insights into Enzymes of Membrane Bilayer Assembly.
Biochemistry **30**: 1731-1739.

Hofmeyr JHS (1986)
Steady-state modelling of metabolic pathways: A guide for the prospective simulator.
Comput. Appl. Biosci. **2**: 5-11.

Hofmeyr JHS (1995)
Metabolic Regulation: A Control Analytic Perspective.
J. Bioenerg. Biomembr. **27**: 479-490.

Kent C (1995)
Eukaryotic Phospholipid Biosynthesis.
Annu. Rev. Biochem. **64**: 315-343.

Kernighan BW & Ritchie DM (1988) *The C Programming Language*
2nd edition. New Jersey: Prentice Hall.

Longmuir KJ (1993) *Phospholipid Biosynthesis*, p.65-95.
In *Phospholipids Handbook*
Edited by G. Cevc. New York: Marcel Dekker.

Mendes P (1993)
GEPASI: A software package for modelling the dynamics, steady states and control of biochemical and other systems.
Comput. Applic. Biosi. **9**: 563-571.

Mendes P (1997)
Biochemistry by numbers: simulation of biochemical pathways with Gepasi 3.
Trends Biochem. Sci. **22**: 361-363.

Mendes P & Kell DB (1998)
Non-linear optimization of biochemical pathways: applications to metabolic engineering and parameter estimation.
Bioinformatics **14**: 869-883.

Petzold LR (1983)
Automatic Selection of Methods for Solving Stiff and Nonstiff Systems of Ordinary Differential Equations.
SIAM J. Sci. Stat. Comput. **4**: 36-148.

Pilling MJ & Seakins PW (1996) *Reaction Kinetics*
First edition. Oxford University Press.

Scherphof GL (1993) *Phospholipid Metabolism in Animal Cells*, p.777-800.
In *Phospholipids Handbook*
Edited by G. Cevc. New York: Marcel Dekker.

Snider MD & Kennedy EP (1977)
Partial Purification of Glycerophosphate Acyltransferase from Escherichia coli.
J. Bacteriol. **130**: 1072-1083.

Tronchere H, Record M, Terce F & Chap H (1994)
Phosphatidylcholine Cycle and regulation of phosphatidylcholine biosynthesis by enzyme translocation.

Biochim. Biophys. Acta **1212**: 137-151.

Vance DE (1996) *Glycerolipid Biosynthesis in Eukaryotes*, p.153-181.
In *Biochemistry of Lipids, Lipoproteins and Membranes*
Edited by D. E. Vance & J. E. Vance. Elsevier Science.

Wilkison WO & Bell RM (1997)
sn-Glycerol-3-phosphate acyltransferase from Escherichia coli.
Biochim. Biophys. Acta **1348**: 3-9.

Yamashita S & Numa S (1972)
Partial Purification and Properties of Glycerophosphate Acyltransferase from Rat Liver.
Eur. J. Biochem. **31**: 565-573.

Application of the Model

4

Contents

4.1 Introduction

In this chapter, the focus moves from looking at the construction of the model, to detailing the way the model is used to investigate the system, its responses and the effect of feedback. The results begin with the basic behaviour of the model. This involves examining the nature of the steady state achieved and how the model's parameters, primarily the individual rate coefficients, may be altered to investigate how the model responds. A method for systematically altering the system and methods for examining and presenting these changes graphically are then detailed. Next, the effect of implementation of feedback, and the nature of the homeostasis brought about, is investigated by looking at the impact of feedback on the torque parameter and the lipid concentrations. Furthermore, examination of feedback strength and the number of feedback points is performed. Using this, an argument for multiple integrative feedback points, providing distributed control, is presented.

The usefulness of sensitivity analysis to select feedback points is demonstrated. The system is examined by looking at the effect of the individual reaction steps and then groups of reactions that belong to '*enzyme classes*'. These results provide a method to predict which reactions could act to provide homeostasis of membrane torque tension; these will be the reactions that have the largest effect on the torque parameter. The enzymes that mediate these reactions would be expected to have activities that are sensitive to the stored elastic energy, a property manifested as sensitivity to the proportion of type II and type I/0 lipids in a membrane system. The predictions of the model may therefore be validated against the available experimental evidence from the literature. This provides a method to test the output of the model and also importantly, the hypothesis that the membrane torque tension is the homeostatically controlled parameter in biomembranes (see section 1.5 and specifically section 1.5.5 in chapter 1).

Finally, in a key result, the model is used to help explain the importance of feedback control of CCT activity, by investigation of the role of CCT in the pathway. The model is also used to examine the interesting differences in behaviour between CCT and ECT. These results are explained by using the torque tension hypothesis, and analysing the effect of CCT and ECT on the torque parameter using arguments about control of the reaction network revealed by results from the model.

4.2 Basic Behaviour and Analysis of the Model

In this section, the basic behaviour of the model will be examined. This behaviour is examined by simulating the 'uncontrolled' network: the system of reactions obeying mass action kinetics with no feedback control implemented. The initial conditions for a stable steady state are shown, and the stability of the steady state is demonstrated; this behaviour shows that the model is properly constructed and suitable for the analysis of perturbations in its steady state.

The key methods of manipulating the model are then explained. The results presented show that the steady state, although stable with respect to time, is sensitive to the values of the rate coefficients of the system. The type of plot adopted to analyse the behaviour of the model and present the results is detailed. Finally, sensitivity analysis is introduced. It is then established how this can be used to test the hypothesis that the purpose of the modulation of CCT activity (by the stored elastic energy) is to ensure the homeostasis of the membrane torque tension.

It is important to note that many of the results in this section are presented for illustrative purposes, primarily to explain the methods used for the sensitivity analysis performed later. For this reason the results shown are not intended to form a comprehensive examination of the system.

4.2.1 Initial Targets for the Model

There were two initial targets for the model. Firstly, the simulation had to attain and maintain a stable steady state. Secondly, the steady state was required to have the lipid concentrations in the correct ratios as defined by the *target steady state* (TSS). Achievement of these goals was dependent on a correctly constructed model. The maintenance of a steady state indicated that the inputs and drains were correctly implemented and that the model was conserving mass, with balanced reaction stoichiometry. Any violations here would cause the concentrations to rise or fall and prevent steady state behaviour. In addition, attainment of the correct steady state indicated that the flux solution was valid and that the kinetic constants were calculated correctly from the flux values and implemented appropriately. With the final model, this may seem a trivial result, however it is a simple and valuable check

that the model is correctly parameterised (including any feedback points added as the model is developed).

A. Maintenance of steady state

The maintenance of the TSS was verified. This was done by setting the model parameters to values appropriate to the TSS. A simulation was then run, starting from the TSS. The results are shown in figure 4.01. Both the time course data and the steady state solution may be used to verify that the TSS is maintained.

B. Stability of steady state

The next step was to verify that the steady state is *dynamically stable*. A metabolic system is said to be dynamically stable if a slight perturbation in the amount of a metabolite results in the system returning to its original state (Fell 1992). If the system is unstable, even a small perturbation can make the system diverge from its original state.

The stability of the steady state is important in the analysis of the system performed in this work. This involves altering the reaction coefficients and examining the changes after the system has settled to a new steady state. Divergent behaviour would hinder the analysis of changes in the steady state.

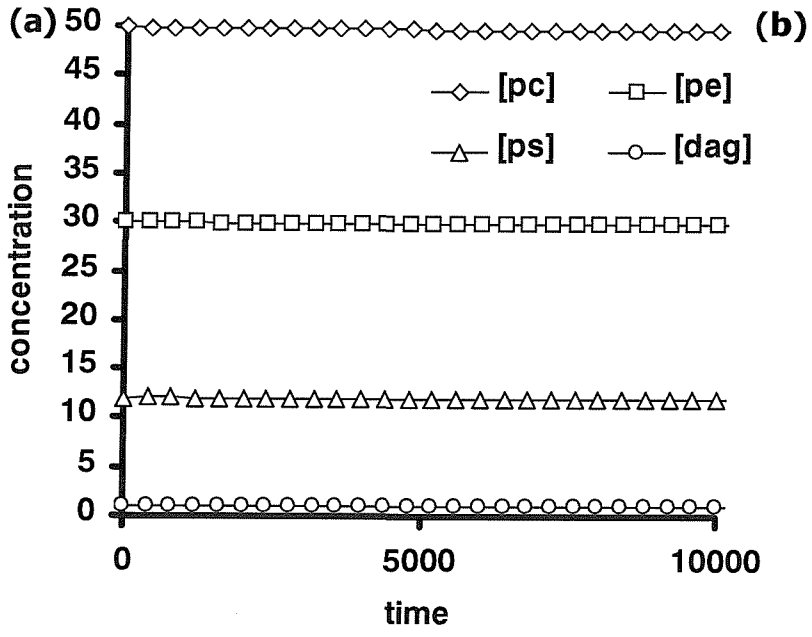

Steady State Solution	concentration
PC	49.69
PE	29.90
PS	12.01
DAG	1.00
PA	1.00
LPA	0.50
LPC	0.50
LPS	0.50
LPE	0.50
FA	0.50
λ_{TSS}	3.1

Figure 4.01: Maintenance of the Steady State. The time course data (a) and steady state solution (b) demonstrate that the model maintains a steady state with appropriate concentrations.

To demonstrate that the steady state is dynamically stable it must be stable in the presence of small changes in metabolite concentrations. This dynamic stability is made possible by the flow of material through the system. Early versions of the model, including StN1 and StN2 as detailed in chapter 3, were not suitably constructed as open systems. These networks lacked an inexhaustible source and appropriate drain reactions. Consequently, upon any perturbations, the system was unable to return to the same steady state; material could not enter or leave the system in order to restore the steady state. The best that could be achieved was a state near to that of the original, with similar relative concentrations. Further complications were caused by the conservation relationships imposed by the construction of these networks (see the discussion of StN1 in section 3.2.1). To recap, these conservation rules inhibited the distribution of material around the system; the relative amounts of the conserved moieties could be unbalanced by any changes in individual metabolite concentrations. The source and sink reactions and model boundaries used in the final model, which allow material to enter and leave the system, also break down the conservation relations, enabling the system to return to the same steady state. In this way, the dynamic stability of the steady state can be seen as another indicator of a suitably constructed network stoichiometry.

To test the stability of StN3, the steady state was perturbed by changing the concentration of a metabolite and observing the return to the steady state. This may be repeated for each species. A sample plot is shown in figure 4.02 (a), which shows the effect on the system concentration for a step decrease in the concentration of PC. Furthermore, the stability may be shown by starting simulations from widely varying starting positions. The convergence to a stable steady state is demonstrated in figure 4.02 (b) indicating that this is the uniquely stable state within this concentration regime. If this applies to all concentrations this would be termed *globally asymptotically stable* (Heinrich *et al.* 1977), however this is difficult to test rigorously. The plots in figure 4.02 are evidence that the network is dynamically stable simply via the mass action response of the network. As mentioned previously, the stability of the network is important for further investigation of the systems behaviour. The results show that alterations may be made to model parameters without the concentrations diverging from steady state behaviour, allowing the changes between steady states to be monitored.

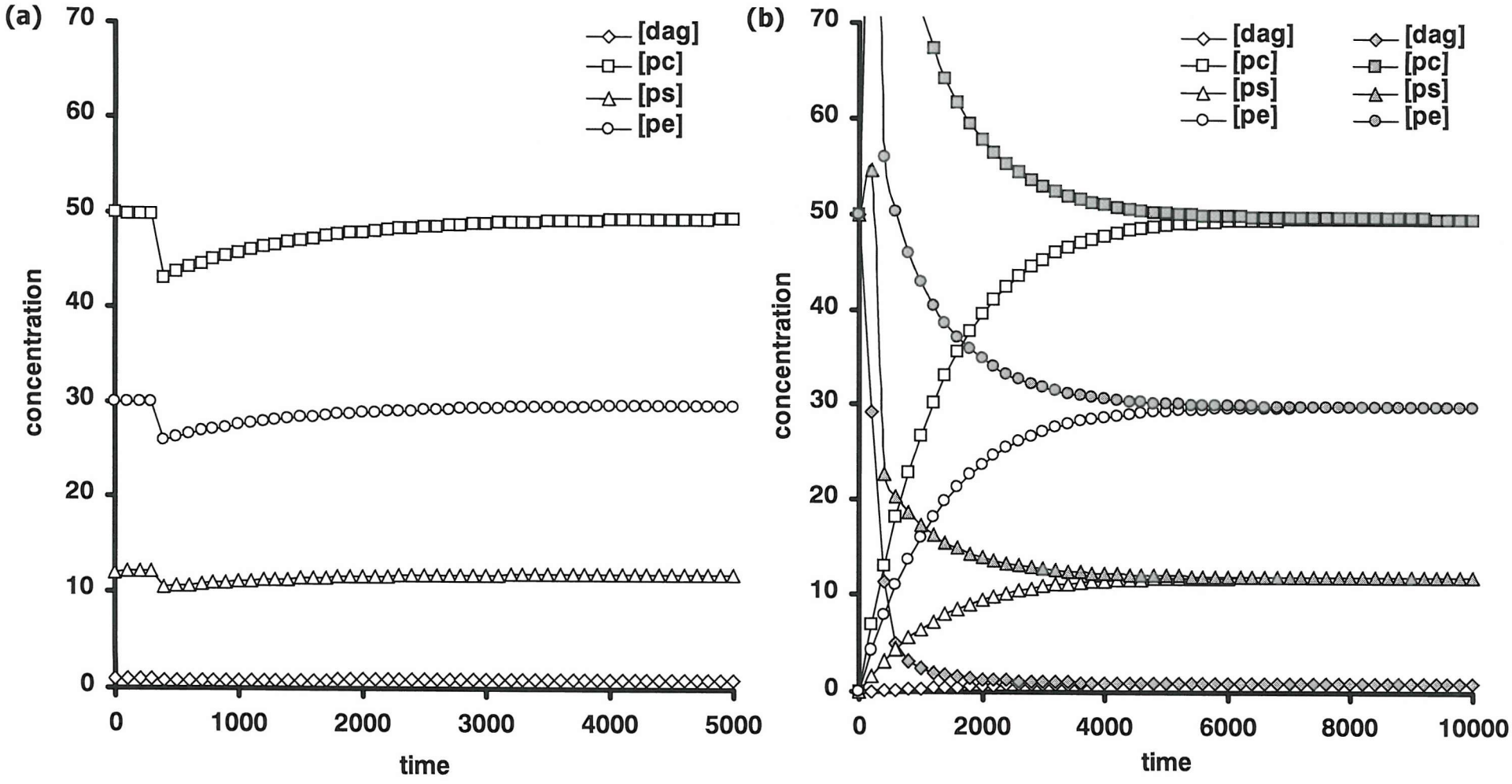

Figure 4.02: Stability of the steady state.
(a) The steady state is dynamically stable as shown by the return to the same steady state after a perturbation in the concentration of PC.
(b) The steady state is uniquely stable with the same steady state found from widely varying starting points.

4.2.2 Alteration of Reaction Coefficients

The aim of this research is to investigate how the enzymes involved in phospholipid biosynthesis may act as part of a feedback loop to confer stability on the membrane torque tension. The first step in investigating this was to experiment with how the activity of the enzymes impacts upon the steady state concentrations of the lipids. In the model, alteration of the enzyme activity is modelled by changing the rate coefficient for the appropriate reaction(s). The initial, and most simple, experiment involved taking a system at the TSS and altering a rate coefficient to simulate a change in enzyme activity. The final concentrations are noted to show the new steady state into which the system settles. An example plot is shown in figure 4.03, which shows the change in concentration of PC upon alteration of the rate coefficient for reaction 1, k(R1). This is the reaction mediated by CCT. A full list of reactions and their numbers may be found in chapter 3, or in table 4.02 (p.4.44). Figure 4.03 shows that when k(R1) is doubled the concentration of PC is increased. Note that the transient behaviour is not of significance here since the abrupt change in the enzyme activity is not intended to represent a real time event. The important result is the final concentration; the new steady state value.

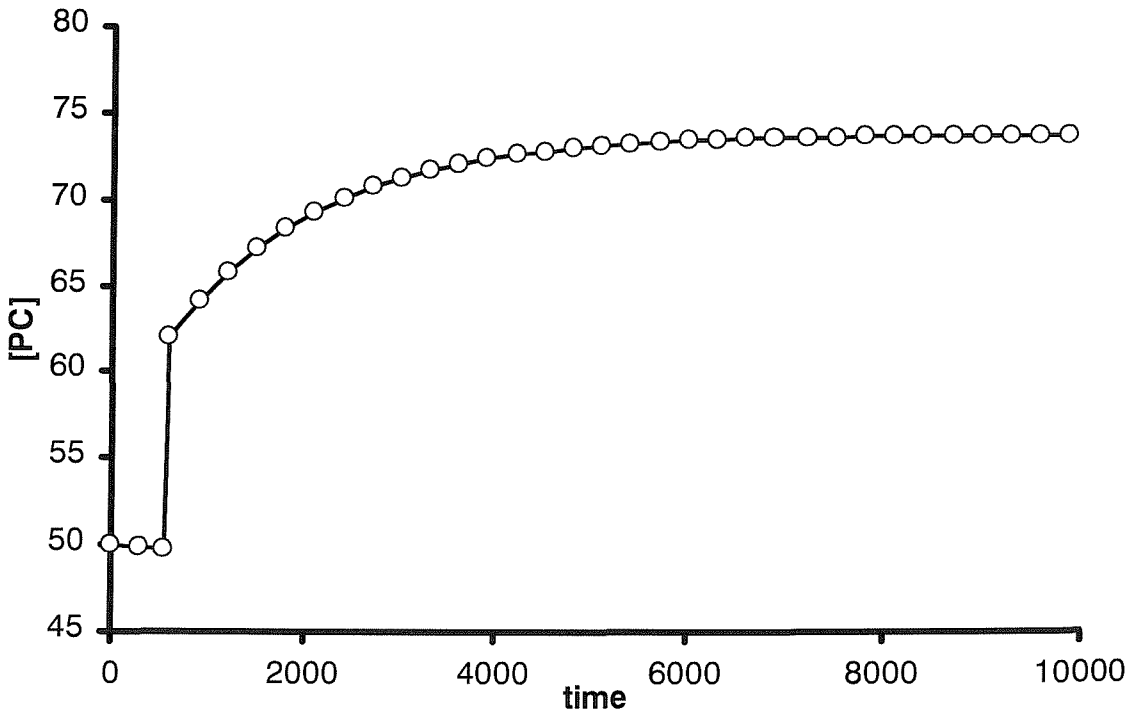

Figure 4.03: The change in concentration of PC upon a change in k(R1). At t=75, k(R1) is altered from 16 to 32 to simulate an increase in activity of CCT, the enzyme which mediates R1.

4.2.3 Concentration vs *k* Plots

Given that the new steady state value is the parameter of interest rather than the transient behaviour, the reaction coefficient may be set to various values and the new steady state value noted in each case. The results may then be combined and plotted as *concentration vs. k plots* to show how the steady state concentrations vary as the reaction coefficient is changed. The use of this type of graph is developed later in this chapter and is used extensively to look at the behaviour of the system*.

Figure 4.04 shows how concentration vs. k plots are built up from simple coefficient alteration results. Figure 4.04 (a) and (b) show the changes in concentration of DAG and PC for changes of k(R1) to (a) 32 and (b) 0.016 ($k(\mathrm{R1})_{\mathrm{TSS}} = 16$). By repeating this for a series of intermediate values of k(R1), a set of new steady state concentrations may be plotted against the corresponding values of k(R1). The steady state concentrations of PC and DAG in the two experiments in (a) and (b) form two points on the concentration vs. k. plots in (c) which show how the steady state concentrations of PC and DAG change as k(R1) is varied.

---

* *These types of variations were initially performed to investigate the stability of the model during its development. Early implementations of StN1 were too simple to withstand significant alteration of the reaction coefficients. With a small number of reactions in the network, small changes in the constants caused large changes in concentration. Generally, low 'connectivity' results in high sensitivity to individual rate coefficients. Therefore, the network used in StN3, with more reactions implemented, source and sinks reactions and suitably defined model boundaries, is more robust. The extra connectivity and selective clamping of species provides many pathways through the model and prevents the accumulation of species. However, the system remains dynamic in the sense that the concentrations remain responsive to the rate coefficients. For example, as the rate of reaction 1 is changed the concentrations of PC and DAG are seen to vary in figure 4.04. The model finds a new steady state as the rate of reaction 1 is changed and the concentration vs. k plots facilitate the presentation of this.*

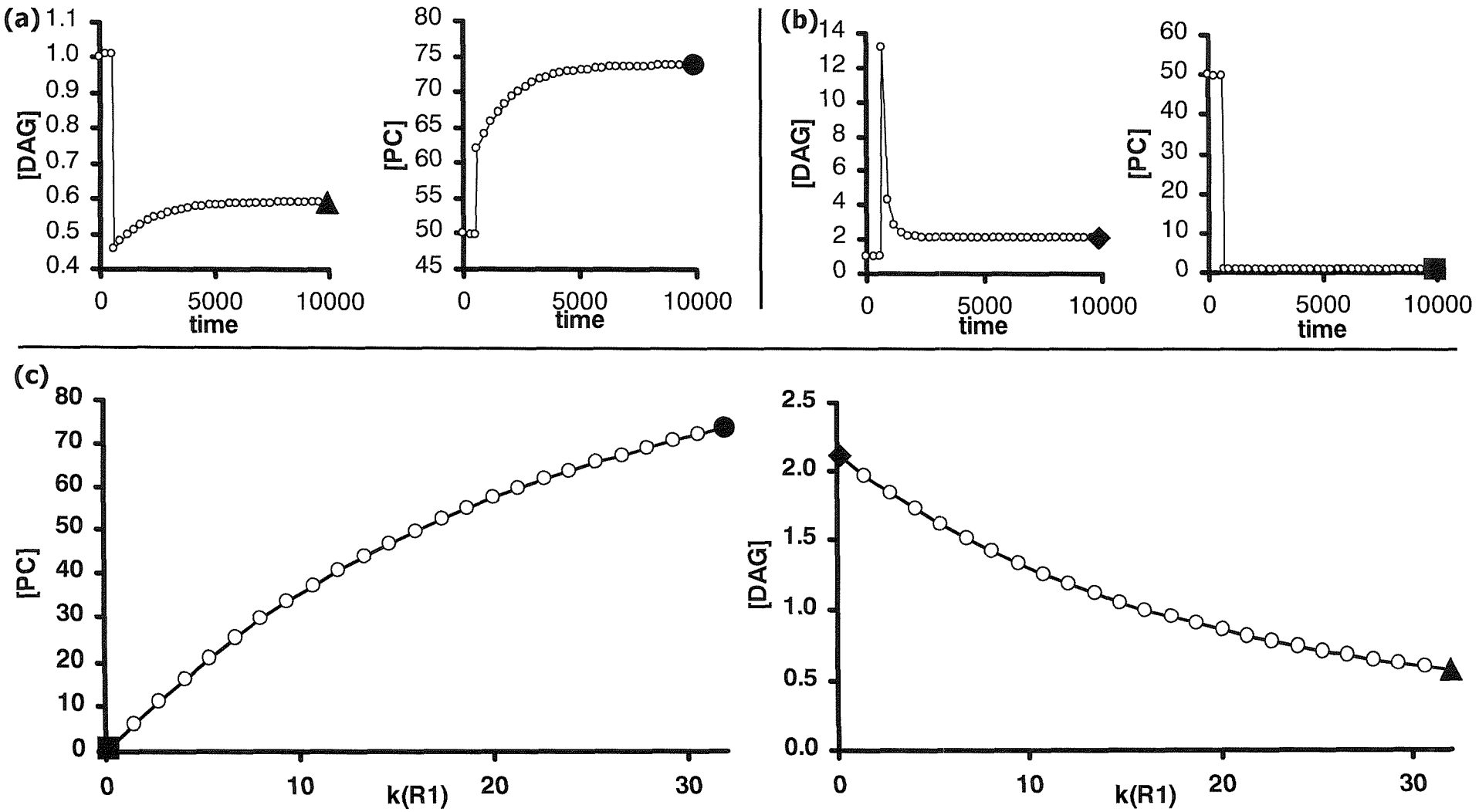

Figure 4.04: The construction of concentration vs. k plots.
(a) changes in concentrations of PC and DAG upon a doubling of k(R1) **(b)** changes in concentrations of PC and DAG when k(R1) is cut to $1/100^{th}$ of its TSS value.
(c) how the steady state concentrations of DAG and PC vary as k(R1) is changed. Note that the marked points in each curve in (c) correspond to the final concentrations in (a) and (b), these are the modified steady state values of DAG and PC.

4.2.4 Sensitivity Analysis: development of concentration vs. k plots

Here the development of the concentration vs. *k* plots, used in the analysis of the system, is presented. Sensitivity analysis is the main method used in this work to investigate the models behaviour. As described in chapter 2, sensitivity analysis is a method that is commonly used both by experimentalists, to investigate reaction mechanisms, and by modellers to investigate the behaviour of networks of reactions.

The modeller, interested in the rate of production of an end product, can vary each of the individual rate coefficients noting the effect on this species. The reactions that cause the largest changes in concentration, the reactions towards which the concentrations are most sensitive, will be of primary interest. Results of sensitivity analysis can provide pointers to the dominant mechanisms occurring in a reaction system and reactions worthy of further analysis, model refinement and/or experimental investigation. The reasons for using this method in this work are revealed in section 4.4 with a more comprehensive look at how the reaction rates impact on the system. Here, some of the possibilities of concentration vs. *k* plots are presented to introduce their use in the technique of sensitivity analysis.

A. Examination of the effect on multiple metabolites

It has been shown that using concentration vs. *k* plots, the reaction rates may be varied to show how the concentration of an individual metabolite changes. It is possible to combine graphs of how the concentrations of two species (e.g. PC and DAG) change, as a single rate coefficient is changed*. This reveals the sensitivity of each metabolite to the rate of a given reaction. An example plot is shown in figure 4.05 (a).

---

* *Plots of the type shown in figure 4.05 (a) were used to find the rate coefficients for the TSS in early work. If the concentration of PC was too low, a reaction that resulted in the production of PC could be increased. Later in the work, with a larger model and the higher associated number of reactions and species, this method proved inconvenient and, ultimately, unnecessary with the development of the matrix solution and branching assumptions. However, this type of concentration vs. k plot can give clues to how each reaction impacts on the system (as shown in the analysis of CCT and ECT presented in section 4.8).*

Further information can be gained from looking at other parameters such as the flux through reactions, or sums of concentrations, for example the total concentration of lipid species. Each of these provides information on how a reaction influences the system and are used later, in some detail, to examine the effect of the reaction mediated by CCT (see section 4.8).

B. Examining the effect of multiple reactions

In addition to examining the changes in a selection of concentrations as a single rate coefficient is changed, it is convenient to examine the change in the concentration of a single species as each member of a set of coefficients are separately altered. For example, graphs of the effect of R1 (CCT) and R26 (ECT) on the concentration of PC may be examined to compare how each reaction influences the amount of PC. This type of plot shows the relative sensitivity of a metabolite concentration towards each rate coefficient. Experiments of this type form the basis of the sensitivity analysis of the system performed in this work (in section 4.4).

C. Scaling of concentration vs. *k* plots

Sensitivity analysis is concerned with relative changes in the parameters. To facilitate the combination of plots for different rate coefficients, which in the model vary over several orders of magnitude, and to make it clear the ranges over which the coefficients are being changed, the k values on the x-axis need to be scaled.

The x-axis is simply scaled by dividing the altered value of k for reaction x ($k(\mathrm{R}x)'$) by that for the TSS ($k(\mathrm{R}x)_{\mathrm{TSS}}$). The value used on the x-axis is then $k(\mathrm{R}x)'/k(\mathrm{R}x)_{\mathrm{TSS}}$. In this way, unity on the x axis corresponds to the TSS, with values lower than one representing a decrease in $k(\mathrm{R}x)$ and higher than one an increase in $k(\mathrm{R}x)$. Graphs are presented in this way throughout the rest of this chapter. Consistent ranges have been used for clarity: each parameter sweep is done for $k(\mathrm{R}x)'/k(\mathrm{R}x)_{\mathrm{TSS}}$ values between 0 and 2.

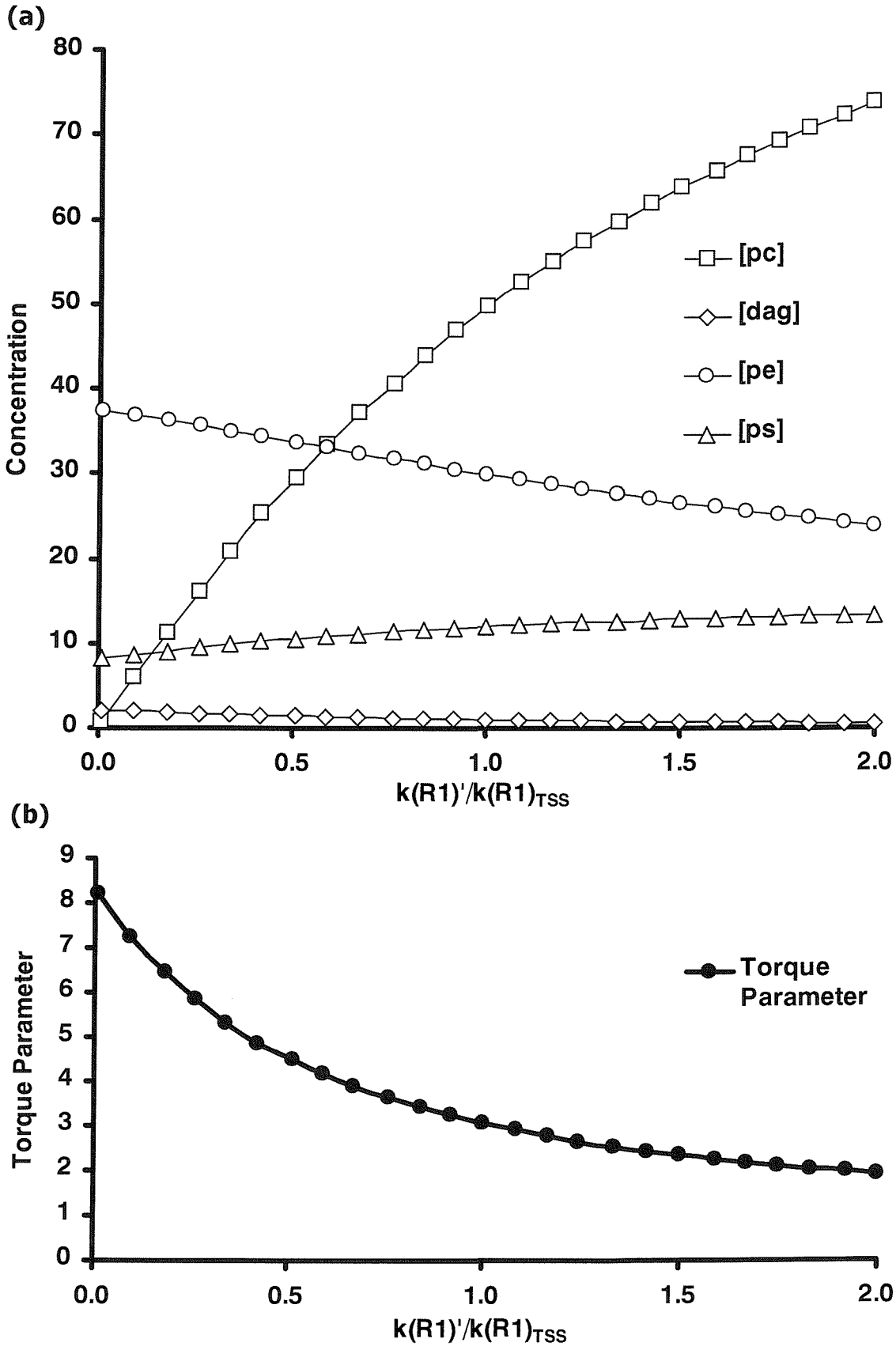

Figure 4.05: Monitoring the steady state concentrations and the torque parameter.
(a) Plot to show the variation of the steady state concentrations as k(R1) is changed.
(b) Plot to show the variation of the torque parameter calculated from the steady state concentrations.

D. Monitoring changes in the torque parameter

Sensitivity analysis is often used to identify a rate-determining step or how control is distributed. As discussed previously, this is normally with respect to a 'final product'. In this work, the quantity of interest is the torque parameter λ, which is a proxy for and gives a measure of the stored elastic energy in the membrane.

The central hypothesis under test in this work is the proposal that the membrane torque tension is the homeostatically controlled parameter in biomembranes. This postulate is made based on evidence that a key lipid biosynthetic enzyme, CCT is driven to its active membrane bound state by the elastic energy stored in the membranes with which it associates. If the reason for this modulation is to maintain the torque tension it follows that CCT must have a significant effect of relieving the elastic energy stored in the bilayer. If this were not the case, control of CCT activity would not be effective in the control of, and therefore the homeostasis of, the torque tension. One of the aims of the model is therefore to test if CCT is significant in the control of stored elastic energy. This is achieved by examining the effect a change in the rate of R1 has on the torque parameter.

λ may be calculated, from the steady state for each value of k, and plotted against $k(\mathrm{R}x)'/k(\mathrm{R}x)_{\mathrm{TSS}}$. This type of graph is a *'λ vs. k plot'*, an example is shown in figure 4.05 (b). λ vs. k plots are used extensively throughout this chapter to monitor the behaviour of this important property of the system.

4.2.5 Control of CCT Activity is Consistent with Control of λ

Figure 4.05 (b) shows the effect of k(R1) on the torque parameter, λ. The increase in PC and PS, and the decrease in DAG and PE (and other lipid species concentration changes, not shown), upon an increase in k(R1) shown in figure 4.05 (a) result in a decrease in the torque parameter. This basic result suggests that an increase in CCT activity will cause a decrease in the stored elastic energy in the membrane. To form an effective feedback loop to control the value of λ, CCT must therefore be stabilised (in the model) by 'normal' type feedback (the use of λ vs. k plots to select the type of feedback is returned to later, and justified, when the effect of implementation of feedback is examined in section 4.3).

Normal type feedback corresponds to activation by type II lipids (high stored elastic energy), providing a tentative first agreement of output of the model with the experimentally shown lipid dependence. The criterion for the model's prediction that CCT is a candidate for feedback is that it could be used to maintain the torque tension, due to the sensitivity of λ towards the activity of CCT. This result is therefore consistent with the postulate that the purpose of the membrane torque tension modulation of enzymes is to maintain the torque tension homeostatically.

Examination of the effect of CCT is performed in more depth towards the end of this chapter (section 4.7). The type of analysis described above for CCT may also be extended to other steps in the pathway. For each reaction, examining the effect on λ, predicting key candidates for torque tension modulation and finally, looking for correlations with reported lipid dependence, if any. This is addressed in section 4.4 and section 4.5. However, before using this type of analysis, the effects of implementation of feedback in the model were investigated. Section 4.3 serves to examine, and attempt to understand the nature of the stabilisation provided, and the implications of this type of feedback.

4.3 Fundamental Effects of Implementation of Feedback

This section shows the result of adding feedback to various reactions in the network. This serves to demonstrate the effect of feedback on the system and shows the nature of the stabilisation seen. Initially feedback modulation was tested on the activity of CCT, since CCT has been shown to be sensitive to the stored elastic energy in a membrane and the reaction mediated by CCT is widely regarded as the rate-determining step in the synthesis of PC. It is therefore proposed that CCT is central to homeostatic control of membrane torque tension. The sensitivity of λ towards k(R1) is shown in models with various strengths of feedback acting on the activity of CCT. Examination of the effect on the torque tension and the metabolite concentrations is shown. Clearly, λ is the primary parameter of interest, but in some instances, examination of the individual lipid concentrations provides further insight into what is happening to the system. The limitations of feedback at a single point and some of the benefits of feedback at multiple points are then demonstrated; a result that necessitates the identification of a set of feedback points. Finally, the nature of the stabilisation produced by the torque parameter feedback is summarised.

4.3.1 Comparison of Controlled and Uncontrolled Networks

In order to look at the effects of membrane torque tension (MTT) modulated feedback, λ / concentration vs. k sensitivity sweeps were performed (as described in the section 4.2) on the network without feedback: this will be referred to as the 'uncontrolled network' or as 'solely under mass action control' due to the absence of feedback. These results are then compared to the results for models with feedback applied to one or more reaction steps. Changes in the behaviour of λ and the metabolite concentrations, shown by the λ / concentration vs. k plots, are used to analyse the effect of feedback upon the model. Shading of the plots is used to clarify the stabilisation, as shown in figure 4.06. The shaded regions essentially represent destabilisation. A curve representing stabilisation of torque will pass through the unshaded region shown in figure 4.06, between the curve for the uncontrolled network and the horizontal line at λ_{TSS}*.

* *Strictly, the test for stabilisation is a reduction in the area under the curve. For example, the theoretical curve a in figure 4.07 would represent greater stability than*

the plot for the uncontrolled network. However due to the way torque is stabilised, the resulting curves are seen to have reduced gradients, as for the curve marked (b), rather than gradients of opposite sign as for (a). Since stabilising feedback doesn't change the sign of the gradient, or change the shape in a dramatic way, any curve that represents stabilisation will pass through the unshaded region. The shading is a useful visual cue, providing an immediate recognition of stabilisation that would not be provided by measurement of the area under the curve. (As will be seen, for the concentrations, results like those in figure 4.07 (a) can be produced; the sign of the gradient can change and therefore, for the concentrations, shading is not used).

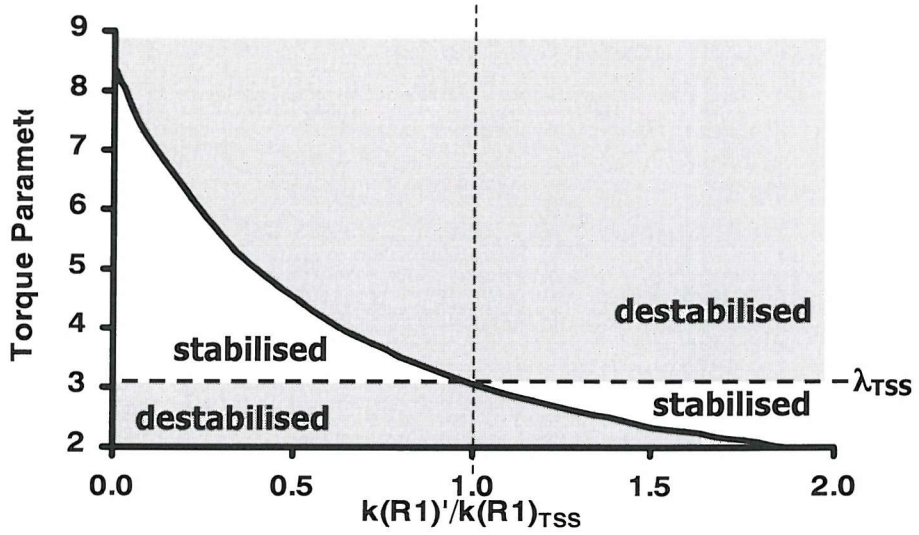

Figure 4.06: Sample plot to show the use of shading to highlight stabilisation.
Curves that represent stabilisation of λ will pass through the unshaded region between the curve for the uncontrolled network and the horizontal line at λ_{TSS}.

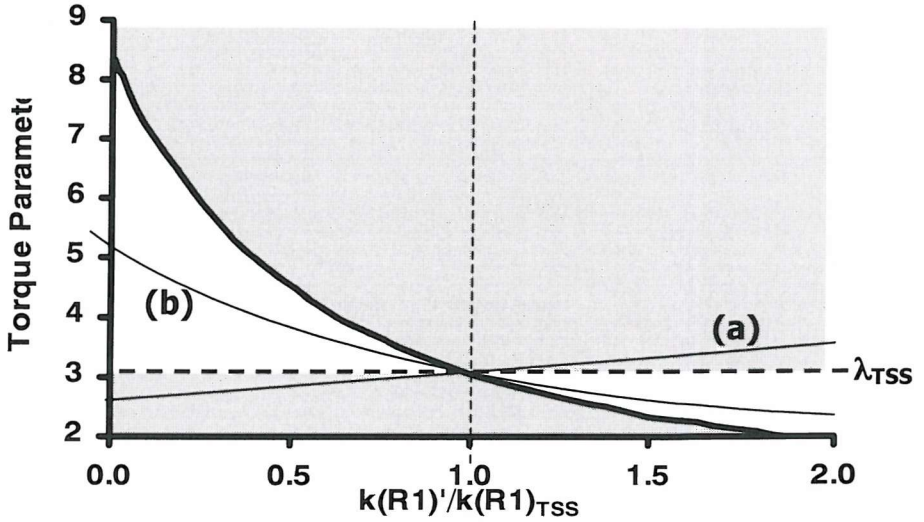

Figure 4.07: Theoretical plots to show the limitations of shading to highlight stabilisation.
Strictly, the measure of stabilisation is given by the area between the curve and the horizontal line at λ_{TSS}. Using this definition (a) would represent a more stable plot than (b). However in practice feedback will lead to a flattening of the original curve, so only plots of the type in (b) are observed making the shading a useful device to visualise the stabilisation.

4.3.2 Describing the Feedback Applied to the Model

Feedback points applied to the model can be described by using *N* to denote normal feedback, for example R1(*N*). This is particularly convenient when there are multiple feedback points to describe, e.g. R1(*N*), R29(*N*) to indicate normal feedback at R1 and R29. Inverse feedback, also described in this section, is labelled *I*, for example R3(*I*).

The feedback strength can also be included, for example R1(N;c_1=100) The value of c_1 describes the feedback strength, as described in chapter 3. The effect of feedback strength is investigated later, in section 4.3.7.

4.3.3 Effects of Feedback at a Single Reaction in the Network

The first stage in investigating feedback within the network, and the extent of stabilisation, was to look at how the network behaved with a feedback control point applied at one reaction within the system. The results presented look at three reactions to examine the different effects on the system. This section examines how feedback applied to R1 (CCT), R29 and R3 impact upon the system, by examining how the sensitivity of λ, and the metabolite concentrations, to each rate coefficient is changed by feedback.

A. Single point feedback at CCT: R1(*N*)

The plots in figure 4.08 show how alteration of k(R1) influences the torque parameter in two models; the first the uncontrolled network and the second the model with normal feedback at R1, R1(N;c_1=100). The plots show that the value of λ changes less, as k(R1) is altered, due to the action of the feedback; λ is stabilised with respect to k(R1) by the feedback modulation acting upon the rate of R1.

The concentrations of the metabolites are also stabilised, the plots for four of the lipids are shown in figure 4.08. The lipid plots shown are for PC, DAG, LPA and FA. PC and DAG are shown because R1 (CCT) has been shown to control production of PC, and DAG is the substrate for the final step in PC production. LPA and FA are shown as metabolites which are 'further away' in the network, to represent species upon which CCT activity would be expected to have less effect.

PC and DAG show the strongest effect, they are significantly stabilised when feedback control at R1 is applied. This is expected; PC and DAG are closely coupled to R1 since they are involved in a reaction with CDPcho, the product of R1. The stabilisation of the concentration of PC suggests that control of CCT will exert control on the production of PC as has been shown experimentally, this point will be returned to in more detail in section 4.7. Changes in the concentrations of FA and LPA caused by the change in k(R1) are, as predicted, smaller than for PC and DAG but these changes are again reduced in the presence of feedback control at R1.

For a more rigorous analysis of stability, examination of the behaviour upon a change in each rate coefficient, k(R1) - k(R29), is necessary. This analysis will be done later, but here the sweep of k(R1) is shown alone for illustration. The choice to look at the effect of altering k(R1) with feedback acting on R1 is actually a special case; the parameter change and the feedback act at the same point; the feedback control can be described as *coincident* with the change in reaction coefficient. In this situation, the feedback acts to directly reduce the changes induced by the change of k(R1). As k(R1) is increased the torque parameter is decreased. The feedback modulation acts to reduce the rate of R1, directly opposing the change caused by the increase of k(R1).

If the feedback and the imposed change are at different points, for example feedback at R1 stabilising a change in k(R2), the control and the coefficient change can be described as *non-coincident*. A non-coincident reaction coefficient change will be examined in the next example, which examines the effect of feedback control at a different reaction.

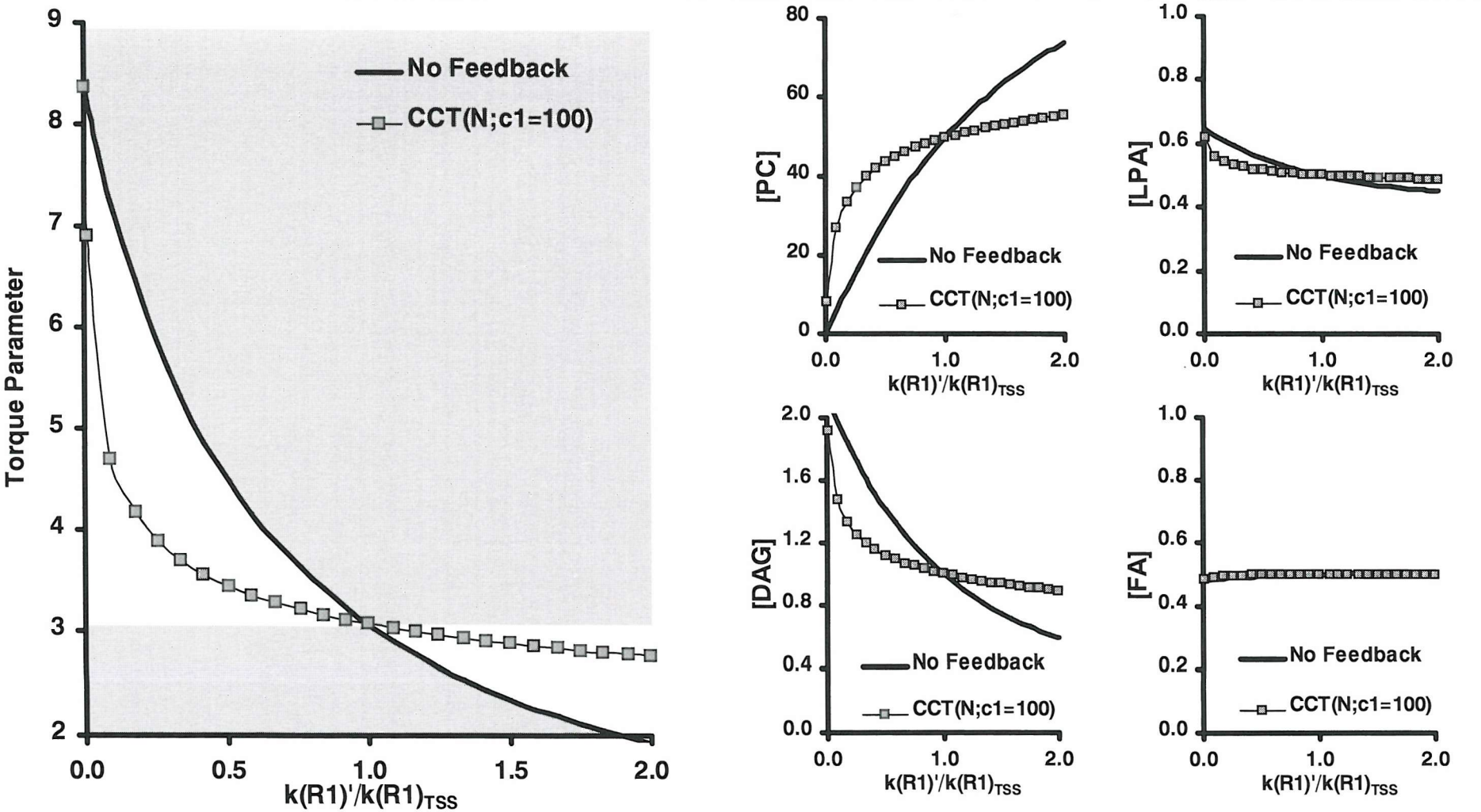

Figure 4.08: The effect of feedback at R1 (CCT).
The plots show the effect of alteration of k(R1) on λ and the concentrations of PC, DAG, LPA and FA for models defined with no feedback, and feedback at CCT(*N*;c1=100).

B. Single point feedback at R29: R29(*N*)

R29 (g3p + FA → LPA) was selected as an alternative point to experiment with feedback control. R29 converts FA, a species which exhibits type II behaviour in membranes, to LPA, a type I lipid. It would be expected, by examination of its substrate and product, to be activated by type II lipids. The network should therefore be stabilised by normal feedback at R29. In the previous section, the effect of feedback at R1 was examined by altering k(R1); the feedback and the coefficient alteration were coincident. Here, feedback at R29 is first investigated by altering k(R29), this is also a coincident change (to allow comparison with the previous observations for feedback at R1). The effect of altering k(R1) with feedback at R29 is then shown as an example of a non-coincident change.

The results for the coincident change, the alteration of k(R29) with feedback at R29, are presented in figure 4.09. As with feedback at R1, stabilisation of λ is seen. Examining the lipid concentrations, the stabilisation is particularly significant for FA and LPA, the substrate and product of R29, rather than PC and DAG as seen with feedback at R1. This would be expected since, upon a change in rate of a reaction, the largest impact in a mass action controlled network is on the species directly involved in the altered reaction, the reaction's substrate(s) and product(s).

Another notable feature is that the concentrations of PC and DAG drop significantly at small values of k(R29), this is also expected since R29 is the crucial first step in lipid biosynthesis. Again even PC and DAG, as 'distant metabolites', are stabilised by the feedback. This is because the feedback is coincident to the parameter change and is therefore acting directly against the imposed change in rate of R29.

In summary, the behaviour of the model upon alteration of k(R29) with feedback at R29 is very similar to that for alteration of k(R1) with feedback at R1. The feedback acts directly to minimise the change in flux through R29, stabilising λ, and the concentrations of the substrate and product of the controlled reaction and other metabolites. The next result presented is the alteration of k(R1) with feedback at R29. Analysis of this single-point feedback and non-coincident parameter alteration reveals a different response.

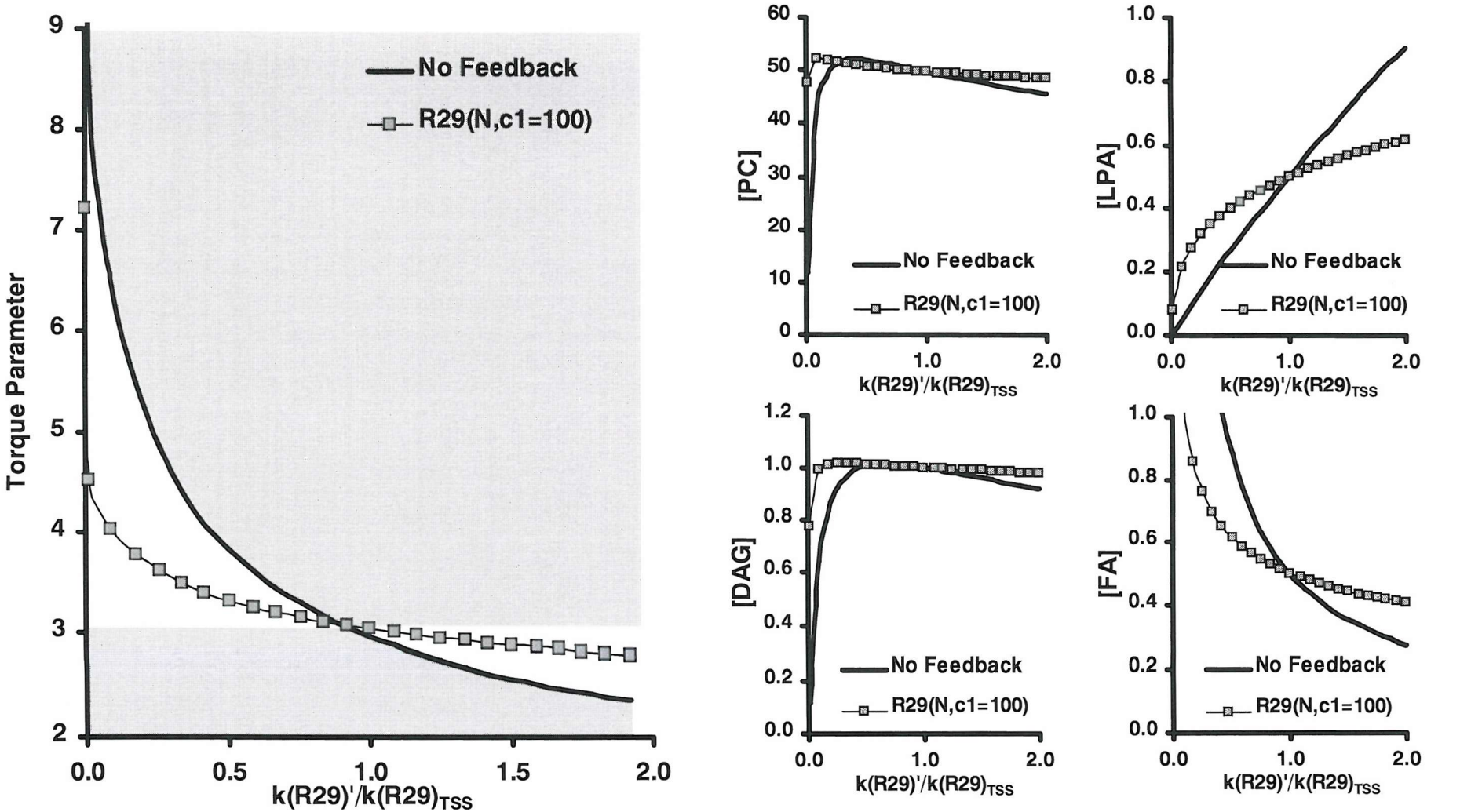

Figure 4.09: The effect of feedback at R29, changing k(R29).
The plots show the effect of alteration of k(R29) on λ and the concentrations of PC, DAG, LPA and FA for models defined with no feedback, and feedback at R29(*N*;c1=100) Since the feedback acts at R29, the change in k(R29) is a 'coincident' change, see text for definition.

In figure 4.10 the effect of scanning k(R1) with feedback at R29 is seen. Again, λ is stabilised. The plots of λ for the alteration of k(R1) and k(R29), in figures 4.08 and 4.09, are similar; stabilisation across the range. The intercept is smaller in figure 4.09 (the reasons for this are revealed when feedback strength is examined in section 4.3.7). The important result however, is that stabilisation of λ is again observed.

To look at the differences between the previous coincident changes and this non-coincident coefficient change, the concentration plots must be examined. The most important feature to note is that when k(R1) is altered, the concentration changes for the substrate and product of R29 (FA and LPA) with feedback at R29 are larger than the changes in the uncontrolled network; the concentrations of FA and LPA are destabilised by the feedback. This is a different type of response to that seen when the coefficient change and feedback point are coincident. This observed destabilisation of the lipid concentrations might initially appear surprising.

The destabilisation of the concentrations can be explained by considering the effect on the torque parameter. The feedback cannot directly prevent the change that is occurring in the concentrations of PC and DAG due to the change in rate of R1 (although stabilisation of PC and DAG by the feedback is seen, this effect is moderate due to the separation in the network). However, the change induced in R29 by the feedback, acts to restore the torque tension, despite the destabilisation of some concentrations. Stabilisation of λ, the primary target of the feedback function, is again seen; the crucial difference is in the method by which stabilisation occurs.

In summary, the effect on the torque for a non-coincident change is the same as for a coincident change. However, the concentrations are affected in a different way. Stabilisation is achieved through a feedback-driven response to a non-coincident change, rather than the direct action seen to prevent the coincident change. It might be supposed that harnessing of both types of response, acting to inhibit any change and responding to compensate for the change, may lead to greater stabilisation. This could be provided by feedback at more than one reaction. These effects therefore provide one reason to argue for feedback at multiple points. The benefits of feedback at multiple points and the nature of the homeostasis generated will be returned to and examined in more detail in section 4.3.8 and section 4.3.9.

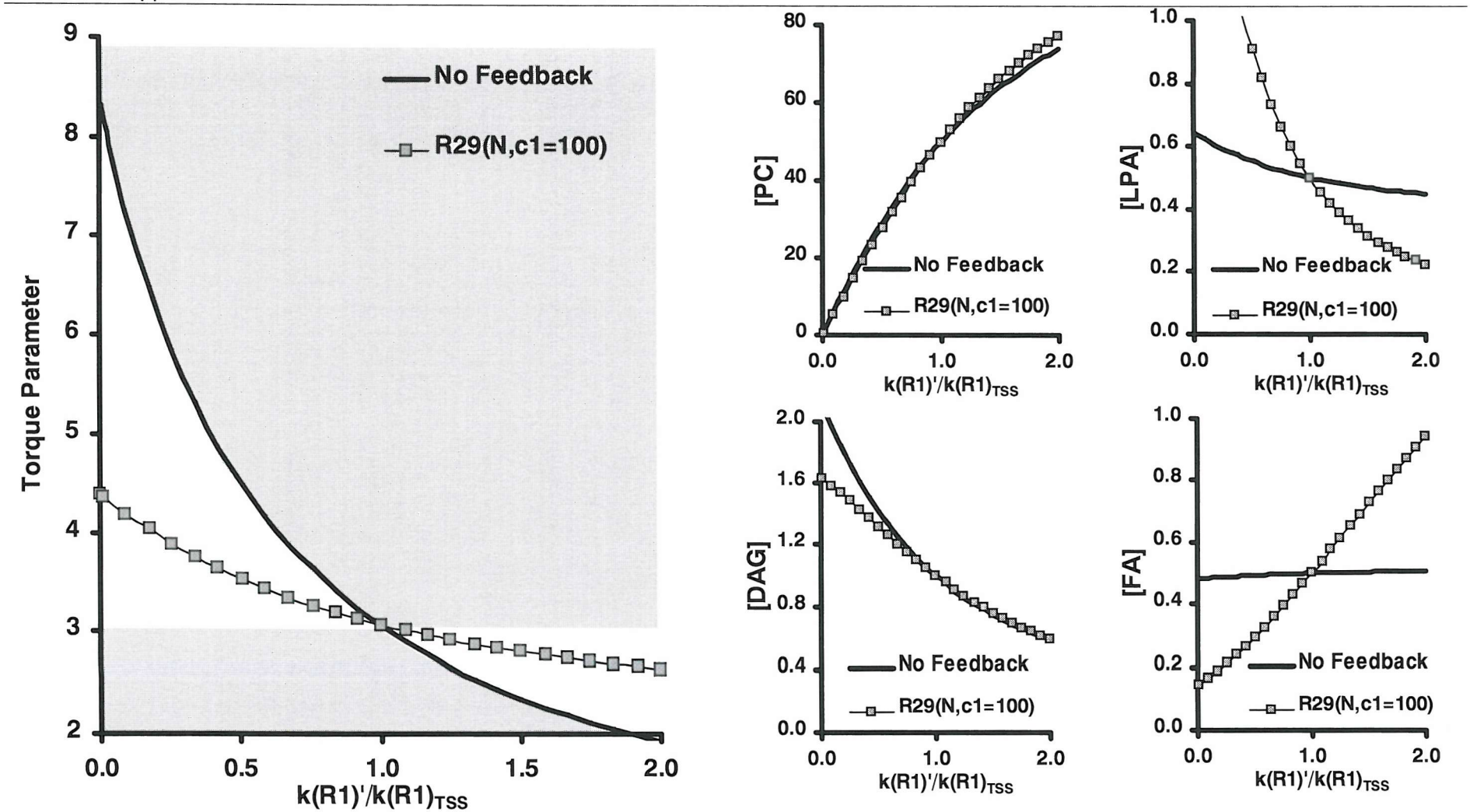

Figure 4.10: The effect of feedback at R29, changing k(R1).
The plots show the effect of alteration of k(R1) on λ and the concentrations of PC, DAG, LPA and FA for models defined with no feedback, and feedback at R29(*N*;c1=100) Since the feedback acts at R29, the change in k(R1) is a 'non-coincident' change, see text for definition.

C. Single point feedback at R3: R3(*N*) and R3 (*I*)

In figure 4.11 (a), the effect of feedback at R3 (PC → DAG) is shown. It is clear that normal feedback destabilises the torque. The change in λ for the controlled network is greater, than for the uncontrolled network, for all values of *k*(R1). The dotted section of the plot represents a regime where the system does not find a steady state at all, but oscillates between states.

The simplest method to predict whether a reaction would be activated or deactivated by type II lipids (normal or inverse behaviour respectively) is to examine its substrate and product. The substrate and product analysis is a crude way to guess at how the action of the conversion will affect the torque in the membrane, although it often works. An analysis of the substrate and product show that this reaction converts PC, a type 0 lipid, to DAG, a type II lipid. Normal feedback equates to activation by type II lipids. Application of normal feedback would cause the product of the reaction to activate the reaction. It should be expected that this *positive feedback* by the product would be destabilising.

Next, the effect of feedback where type II lipids deactivate the reaction is examined. This necessitated the building of an *inverse feedback* function. As described in the previous chapter, inverse feedback results in a decrease in reaction rate upon an increase in torque. Figure 4.11 (b) shows the effect of inverse feedback at R3, the result is stabilisation of the torque.

These results demonstrate the need for a method to predict which type of feedback is appropriate. The stabilisation associated with feedback at R3 is smaller than that seen for feedback at R1 or R29. The difference in the observed degree of stabilisation highlights the need to pick the points that will have the largest stabilising effect. In the next section, the use of multiple λ vs. *k* plots to select candidates for feedback control is introduced. In contrast to simple substrate and product analysis, it is shown how the model allows examination of the whole system rather than isolated reactions. Therefore it is demonstrated how the analysis of substrate and product can be extended to consider the overall effect on the metabolites.

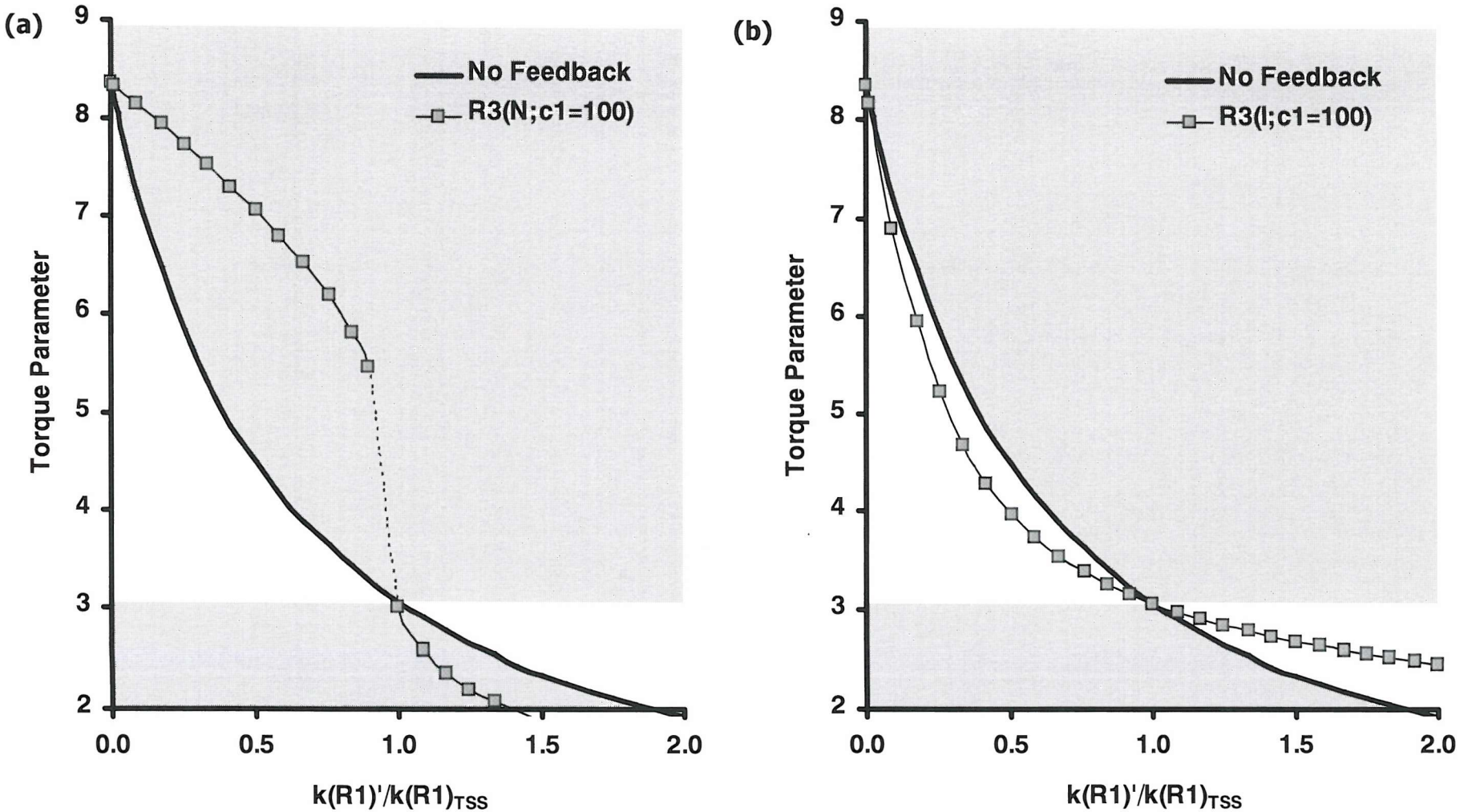

Figure 4.11: The effect of feedback at R3, changing k(R1).
(a) Normal feedback, R3(*N*;c_1=100), causes destabilisation of the torque parameter (λ is made more sensitive to the k(R1) by the feedback).
(b) Inverse feedback, R3(*I*;c_1=100), causes stabilisation of the torque parameter (λ is made less sensitive to the k(R1) by the feedback).

4.3.4 Identification of Feedback Type Using λ vs. k Plots

It was discussed briefly, in section 4.2.5, that the effect of CCT activity on the torque parameter could be used to make a prediction of feedback type necessary to stabilise λ, and that this was consistent with the type of feedback seen experimentally. Examination of the effect upon λ of alteration of *k*(R1), *k*(R29) and *k*(R3), with λ vs. *k* plots as shown in figure 4.12, reveals why the type of feedback that provides stabilisation in the model differs for R3. R1 and R29 act to decrease λ (an increase in the rate of R1 or R29 leads to a decrease in λ). Therefore, a feedback loop with high torque activating CCT provides stabilisation of the torque parameter. From the positive gradient of the λ vs. *k* plot for *k*(R3), it is seen that R3 has the opposite effect on λ; R3 acts to increase λ, so deactivation by type II lipids (high torque), modelled by inverse feedback, will lead to stabilisation of λ. R3 has a smaller gradient, and smaller stabilisation with feedback at R3 was seen. In section 4.4, this method is applied to all the reactions to examine which exert control over λ and thus to choose the key candidates for feedback control.

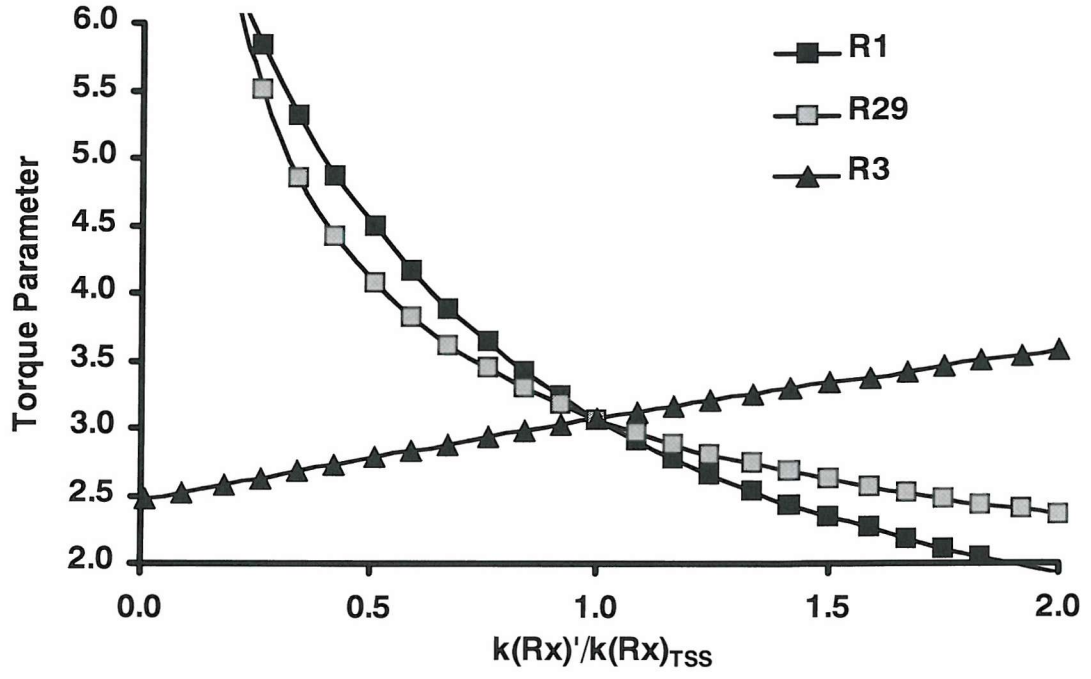

Figure 4.12: λ vs k. sensitivity plots for R1, R29 and R3.
The sign of the gradient identifies if the reaction increases or decreases the torque. A reaction that acts to decrease the torque (here, R1 and R29) will be stabilised by normal feedback, whilst one that increases the torque (here R3) requires inverse feedback for stabilisation as shown in section 4.3.3.

4.3.5 Describing the Effect of a Reaction on the Torque Parameter

A shorthand method to describe the effect of the action of an enzyme on the torque tension is convenient. To illustrate, the effect of R1 on the torque may be denoted R1(λ-). The notation indicates that R1 acts to decrease torque (an increase in activity will lead to a decrease in torque) and therefore this reaction would be predicted to be stabilised by normal type feedback (as shown in section 4.3.3).

The behaviour of the three reactions shown in figure 4.12 may be summarised as R1(λ-), R29(λ-) and R3(λ+). The argument used for R1 above, leads to a prediction of the feedback regimes required at these three points in order to stabilise the system: R1(*N*), R29(*N*) and R3(*I*)*.

* *It is important to note here that* Rx(λ+/-) *describes the effect of the reaction on the torque parameter.* Rx(*N*/*I*)*, in contrast, is used to specify the feedback applied in a simulation, and does not provide information on the effect of the reaction or indicate whether this type of feedback will provide stabilisation.*

4.3.6 Substrate and Product Analysis vs. λ Sensitivity Analysis

The sensitivity analysis method, which will be used to predict the lipid dependence of the enzymes, is more sophisticated than looking at the lipid types of the substrate and product of the reaction (Cornell & Arnold 1996). The substrate and product analysis considers just one reaction and two or three metabolites. For example, for R3 (PC → DAG) the transformation is from a type 0 substrate to a type II product. The substrate and product analysis therefore leads to the prediction that the reaction will be inhibited by type II lipids. In this case, this is in agreement with experiments with the model (the result in figure 4.12). However, the substrate and product analysis ignores how one reaction affects the others in the system and how the concentration ratios, rather than individual concentrations, determine the torque. For this reason it can oversimplify the analysis[†].

[†] *The weakness of the substrate and product analysis, and the necessity of looking at changes in the overall system, will be seen later in an examination of the prediction of the effect on the torque caused by the actions of CCT and ECT, enzymes which mediate reactions with non-membrane substrates and products.*

4.3.7 Effect of Feedback Strength

Alteration of the parameters of the feedback function, allow changes in the strength of feedback. The rate equation for a controlled step and the relationship between σ and λ is given in equations 3.09, 3.15 and 3.17 (these were detailed in chapter 3).

$$v = k'.\sigma.\prod_i S_i \qquad \text{equation 3.09}$$

$$\sigma_{norm} = c_1.\exp\left(-\frac{1}{c_2.\lambda}\right) \qquad \sigma_{inv} = c_1.\exp\left(-\frac{\lambda}{c_2.}\right) \qquad \text{equation 3.15, 3.17}$$

A. Setting the feedback strength

In equations 3.15 and 3.17, the coefficient c_1 is a scaling factor that ensures $\sigma_{TSS} = 1$. For example, if c_1=10 then 10% of the enzyme is bound at the TSS (σ´=0.1) whilst for c_1=100, 1% is bound (σ´=0.01). As described in chapter 3 and shown in figure 4.13, this value reflects the relative size of the reservoir of inactive enzyme compared to the amount bound. The smaller the fraction of enzyme that is bound at the TSS, the more is available upon an increase in torque. The feedback strength is a measure of the sensitivity of the enzyme to the bilayer stress. The nature of the feedback function gives rise to a greater change in activity for a given change in λ when there is a smaller fraction bound and so this corresponds to higher feedback strength.

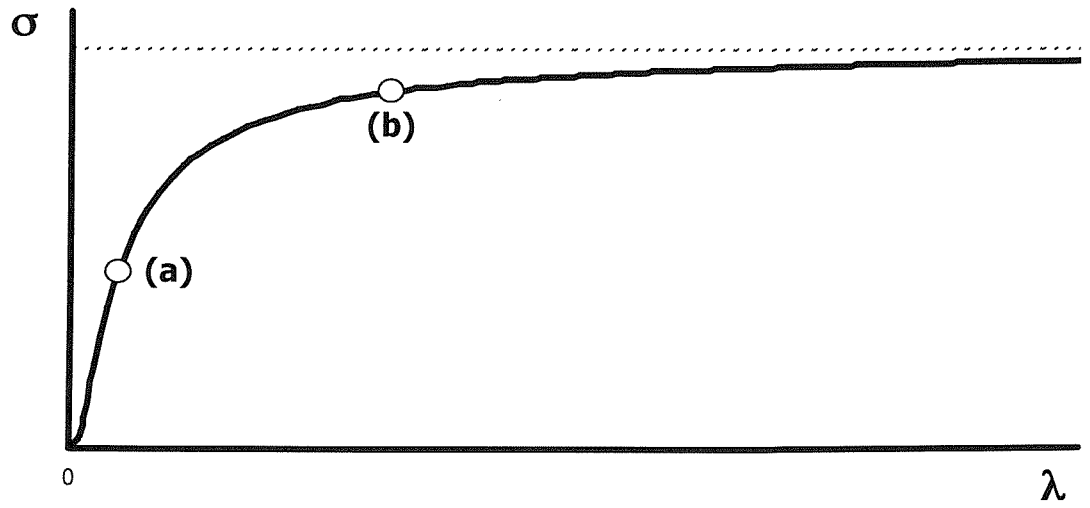

Figure 4.13: An example σ vs. λ plot to illustrate feedback strength.
The two marked points correspond to two possible values of σ at the TSS.
(a) Proportion of enzyme bound is small; the value of σ is sensitive to the torque parameter, λ.
(b) Proportion of enzyme bound is large; the value of σ is insensitive to the torque parameter, λ.

B. Feedback strength experiments

Feedback control at CCT with three strengths were run. The coefficient c_1 was set to three values (10, 100 and 10000000). For each value of c_1, c_2 is calculated to maintain $\sigma_{TSS} = 1$ (see chapter 3). The values used are given in table 4.01.

		c_1	c_2
weak feedback	CCT(N;c_1=10)	10	0.141242938
	CCT(N;c_1=100)	100	0.070621469
strong feedback	CCT(N;c_1=10000000)	10000000	0.020177563

Table 4.01: Values of c_1 and c_2 used to modify feedback strength.

The effect on the λ vs. k plot for the three strengths of feedback is given in figure 4.14 (a). The results show the stronger the feedback, the larger the changes in rate necessary for a given change in torque and therefore greater the stabilisation.

An interesting result was revealed by this experiment. For any coincident change (where the reaction at which the feedback acts is altered) no matter the feedback strength, the intercept on the y-axis remains the same. The value of λ for $k(R1)'/k(R1)_{TSS} = 0$ is around 8.5 in each case. The common intercept highlights a shortcoming of single point feedback. Feedback control upon an enzyme is of no use if the enzyme is completely deactivated. This means feedback modulation of an enzyme's activity cannot stabilise effectively in the event of significant depletion of that enzyme.

One plot where a different intercept was seen was figure 4.10 with feedback at R29 and alteration of k(R1), a non-coincident alteration. Experiments on non-coincident alterations showed that stabilisation towards k(Rx) can be caused by feedback at other points. Importantly stabilisation can be provided at $k(R1)'/k(R1)_{TSS} = 0$. This result is shown in figure 4.14 (b) with feedback at R29. As the strength of the feedback is changed, so is the intercept. This shows stabilisation at low $k(R1)'/k(R1)_{TSS}$ could be provided by feedback at a point other than R1. This is a second reason to argue for feedback at multiple points. Recognising that there are reasons for feedback at more than one point, and the limitations of having feedback at only one point, the next section examines the effect of feedback at multiple points.

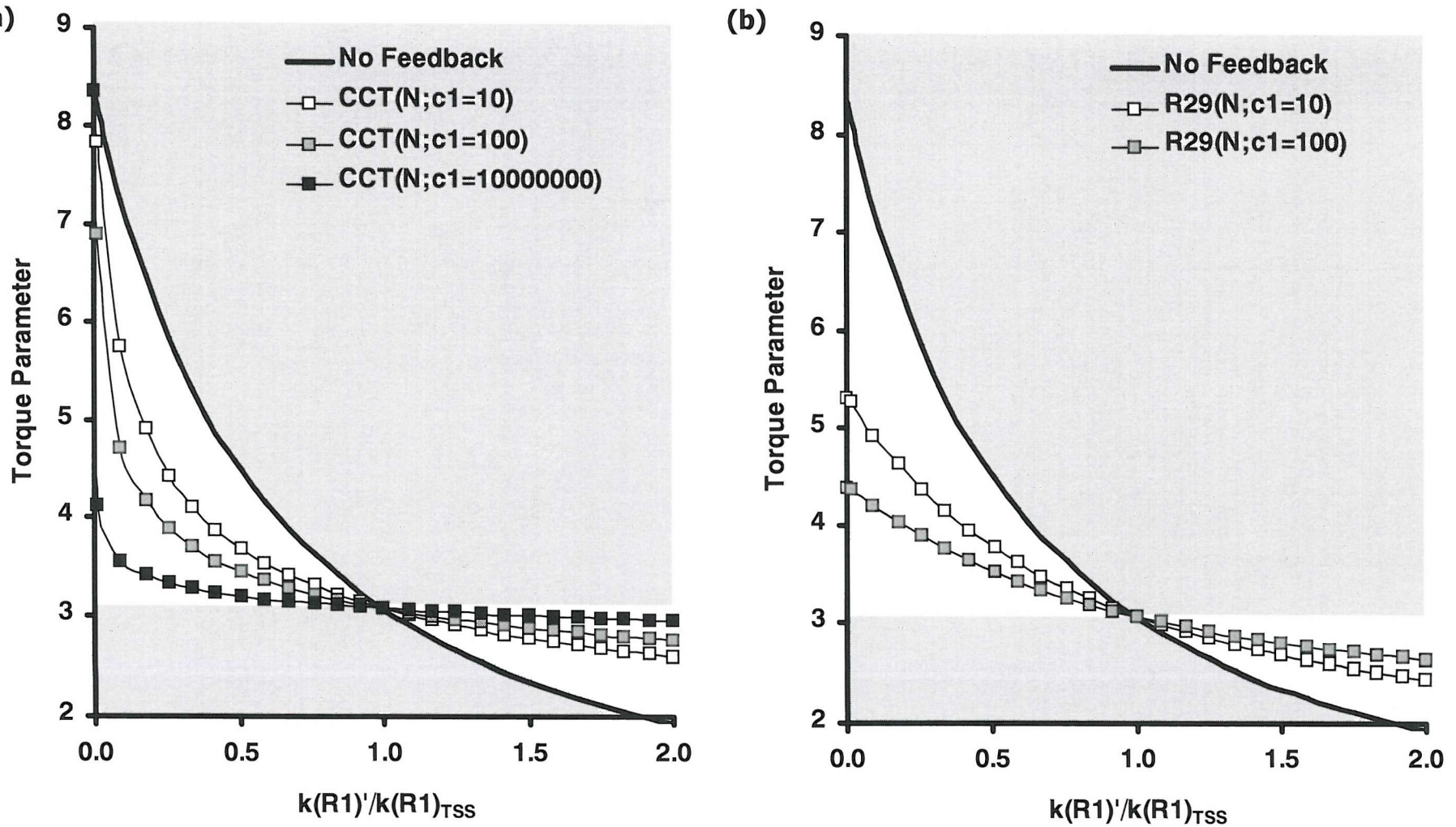

Figure 4.14: The effect of strength of feedback.
(a) Feedback at CCT (R1) with alteration of k(R1): a coincident change, note the common intercept on the y-axis: feedback at R1 cannot provide stabilisation at $k(R1)'/k(R1)_{TSS}=0$. **(b)** Feedback at R29 with alteration of k(R29): a non-coincident change, feedback at R29 can provide stabilisation at $k(R1)'/k(R1)_{TSS}=0$.

4.3.8 Effect of Feedback at Multiple Points

The result presented in figure 4.14 shows that control at low CCT activity (as $k(\mathrm{R1})'/k(\mathrm{R1})_{\mathrm{TSS}} \rightarrow 0$) can be increased by feedback at another point in the pathway and this is further illustrated in figure 4.15. Figure 4.15 (a) shows the effect of adding various strengths of feedback at R1 to feedback at R29. The result demonstrates that the intercept is determined by the non-coincident feedback control (R29 since the change made is in k(R1)). The change in the feedback strength at R1 has little effect on the intercept. The main feature to note is that the weak second feedback point at R29 has a dramatic effect when present in combination with feedback at R1.

The extra stabilisation is shown clearly in figure 4.15 (b). Here Feedback at CCT alone (c_1=100) is compared to weaker feedback at CCT and R29 (c_1=10 for each). The plot for weak feedback at CCT and 29 (c_1=10 for each) shows nearly the same amount of stabilisation as stronger feedback at CCT alone (c_1=100) and the intercept is smaller for the combination. This extra stabilisation shows that there is a robustness increase with multiple points of feedback.

In summary, the model suggests a benefit, in terms of robustness, to multiple control points. In addition, there is experimental evidence for lipid activation of enzymes other than CCT in the pathway as discussed in the introduction. A method is therefore required to predict from the model which enzymes would be expected to show strong lipid activation by MTT arguments. This is where the sensitivity analysis is used later (section 4.4). The discussion however now continues by looking at another possible reason for multiple point feedback: an illustration that stabilisation of the torque does not equate to homeostasis of concentrations, by examination of the effects of two-point feedback in more detail.

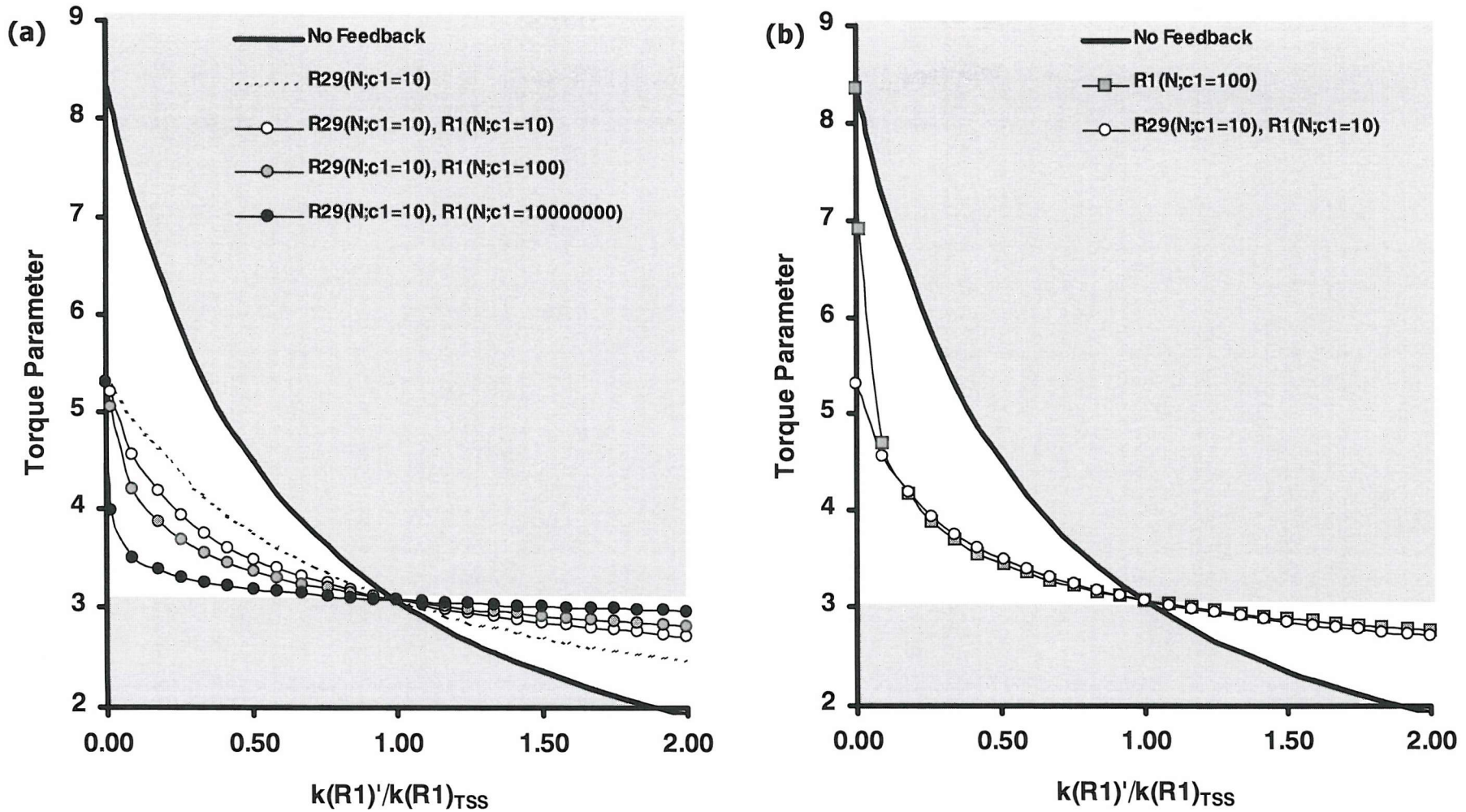

Figure 4.15: Effect of multiple point feedback.
(a) Feedback at R29 combined with varying strength of feedback at R1. The intercept at $k(R1)'/k(R1)_{TSS}=0$ is determined by the control of R29 (dotted line).
(b) Comparison of weak feedback at R29 and R1 (circles), with stronger feedback at R1 only (squares).

A. Two point feedback experiments

In this section, the effect of feedback on the torque and the concentrations is used to explain the nature of the homeostasis of torque that emerges as a result of the integrative feedback. The analysis also serves to examine how multiple point feedback changes the response of the system. In many of the experiments involving comparison of controlled and uncontrolled networks, a stabilisation of concentrations is seen. It may initially be assumed that λ is maintained by homeostatically controlling the concentration of each metabolite. With this control, there would be a fixed ratio of species. However, this is not the case. The destabilisation of metabolite concentrations for a non-coincident change was the first time this was observed (figure 4.10). To look at this in more detail, the effect on the torque and the concentrations in a model with two feedback points implemented is analysed.

In the model used in this experiment feedback control points operate at R1 (CCT) and R29 (both with c_1=100). The results are presented to show how the system responds upon alteration of the two associated rate constants, k(R1) and k(R29). With two feedback points, the concept of coincident and non-coincident coefficient changes is less useful. The analysis is also more complex because the combined effect of the action of the two feedback points must be considered.

Experiments were run by independently sweeping the rate coefficients. The results for k(R1) and k(R29) are presented in figure 4.16a-c (p.4.39-p.4.41). Figure 4.16a shows the effect on λ for each sweep. In each case, stabilisation of λ is seen. In addition, the multiple feedback points provide extra stabilisation and reduce the intercept for the feedback curves for each rate coefficient. The two plots in figure 4.16a are very similar. To examine the difference in behaviour between the changes in k(R1) and k(R29), the concentrations must be studied by reference to the concentration vs. k plots shown in figure 4.16b and 4.16c.

Figure 4.16b shows the concentration changes upon changes in k(R1). The species shown are DAG and PC, the lipid species nearest R1 in the network, and FA and LPA, the substrate and product of R29. Comparing the controlled and uncontrolled curves, a difference in the effect on these pairs of concentrations is seen. PC and DAG are stabilised with respect to the uncontrolled network. However, the changes

seen for FA and LPA are larger than for the uncontrolled network. It is apparent that the concentrations are not being uniformly stabilised.

Figure 4.16c shows the concentration changes upon alteration of k(R29). Here stabilisation of the concentrations of FA and LPA are seen. However, the concentrations of PC is destabilised with respect to the uncontrolled network. The change in the behaviour of DAG with feedback is different again. The concentration of DAG increases as k(R29) is increased, but in the uncontrolled network it decreases.

B. Analysis of the two point feedback results

To explain the results shown in figure 4.16a-c, a suitable subsystem model can be described, to focus on the changes occurring. The subsystem considers only the two reactions, shown in figure 4.17. The alteration in rate constants will, of course, cause changes throughout the network. However, the major changes are seen at the two reactions that are altered. Moreover, without feedback control, a change in one reaction will not significantly affect the other reaction due to the separation between them in the model. With the system solely under mass action control, if k(R1) is altered the concentrations of PC and DAG will change but the concentrations of FA and LPA change to a much smaller degree, as seen in the plots for 'no feedback' in figure 4.16b. Therefore, in the subsystem model the two reactions can be considered as isolated for the purposes of interpreting the full model output.

To understand why the concentrations are not homeostatically controlled by the application of feedback, it is necessary to understand how the two feedback control points will modify the mass action controlled behaviour. The effect of the feedback is shown schematically in figure 4.18. First, consider how the feedback controlled

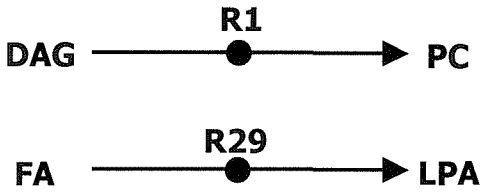

Figure 4.17: Subsystem model to rationalise the effect of two-point feedback at R1 and R29. To examine the difference in behaviour of the controlled and uncontrolled network, the reactions may be considered as isolated due to the separation in the pathway.

network behaves when k(R1) is decreased. As a direct result of the decrease in k(R1), the concentration of DAG increases whilst PC decreases. These changes cause an increase in λ. The increase in torque will activate R1, since it is controlled by normal feedback. This acts against the alteration in k(R1); DAG, PC and λ are stabilised with respect to the change which occurs in the uncontrolled network. However, λ is still increased and this will act to increase the rate of R29, since this reaction is also controlled by normal feedback. The effect of the increase of the rate of R29 is that FA decreases and LPA increases. This change also helps stabilise λ. However, the changes in the concentrations of FA and LPA are greater than would occur in the uncontrolled network, where FA and LPA would not change significantly. These changes were shown in figure 4.16b. Note the concentrations of DAG and PC are stabilised but FA and LPA are destabilised; the concentration of LPA is increased more, and the concentration of FA is decreased more than in the uncontrolled network. What is important to note is that both changes act to stabilise λ; the changes in concentration occur because they are necessary to maintain λ.

Moving to look at the effect of altering k(R29) shown in figure 4.16c, it is seen that the concentrations of FA and LPA are stabilised, but the concentrations of DAG and PC are destabilised. This may be rationalised by following the same process detailed above for k(R1). The result shows that the concentration of a lipid may be either stabilised or destabilised and which occurs depends on where the alteration in rate takes place. This demonstrates that the model predicts homeostatic control of λ but not individual concentrations.

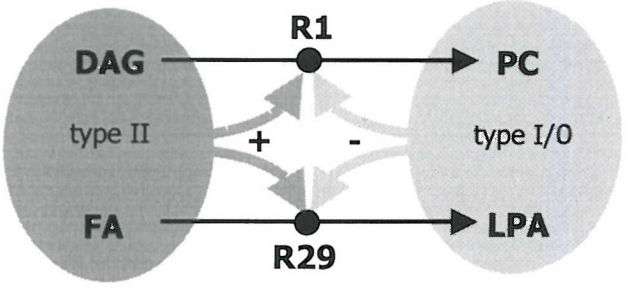

Figure 4.18: Increased connectivity, due to feedback control points, results in homeostatic control of torque but not concentrations. If k(R1) is decreased the torque will increase, the feedback control at R1 and R29 increases the flux through R1 and R29 to maintain the torque. The net change in the flux through R1 is then less than without feedback. However, the net change in the flux through R29 is more than without feedback. The result being that the concentrations of DAG and PC are stabilised but the concentrations of FA and LPA are destabilised (with respect to changes seen in the absence of feedback).

4.3.9 Homeostatic Control of MTT not Concentrations

Crucially, the results discussed in section 4.3.8 show that λ is not stabilised by maintaining each of the lipid concentrations in fixed ratios. What is seen is a combination of the stabilisation of some concentrations and the opposing response, both of which stabilise λ. There is no 'cost' to changing the concentration of a lipid species, the determinant is whether it provides the benefit of maintaining the torque. This is consistent with the argument that homeostasis of torque tension does not require a fixed ratio of lipids, but a fixed ratio of type II, to type I/0 lipids. This behaviour emerges naturally as a consequence of basing the feedback on the torque tension using λ, the torque parameter.

Maintaining the torque tension is a significantly more relaxed condition than controlling the lipid concentrations homeostatically. Maintaining each of the lipid species, in a single defined steady state with fixed ratios of lipid concentrations, would require a high degree of control of enzyme activities and a method to coordinate this control. Also, there would exist only one target state for this control to maintain. In contrast, there are many combinations of lipid concentrations that provide the same balance of type II, to type I/0 lipids and therefore the same torque tension. The system will be free to explore these combinations. This may help explain the diversity of lipid compositions seen in biological systems. The simplicity of the control required also makes the maintenance of torque tension a much more viable proposition.

Another important point to reiterate is that the multiple point feedback, shown in figure 4.18, increases the connectivity without the addition of further reactions. This highlights how the integrative feedback may overcome the cost of chemical reactions, allowing high efficiency (Morowitz *et al.* 1964) (due to the minimal number of reactions, see section 2.3.8 in chapter 2) and high robustness (due to the extra non-stoichiometric connectivity) to be achieved in the same pathway. This would confer significant advantage. The feedback also shortens the 'distance' between metabolites and enzymes in this less than maximally connected pathway as shown in figure 4.18. The next section of this chapter looks at how the model can be used to identify the enzymes that exert the greatest control on the membrane torque tension. This leads to the prediction of control reactions.

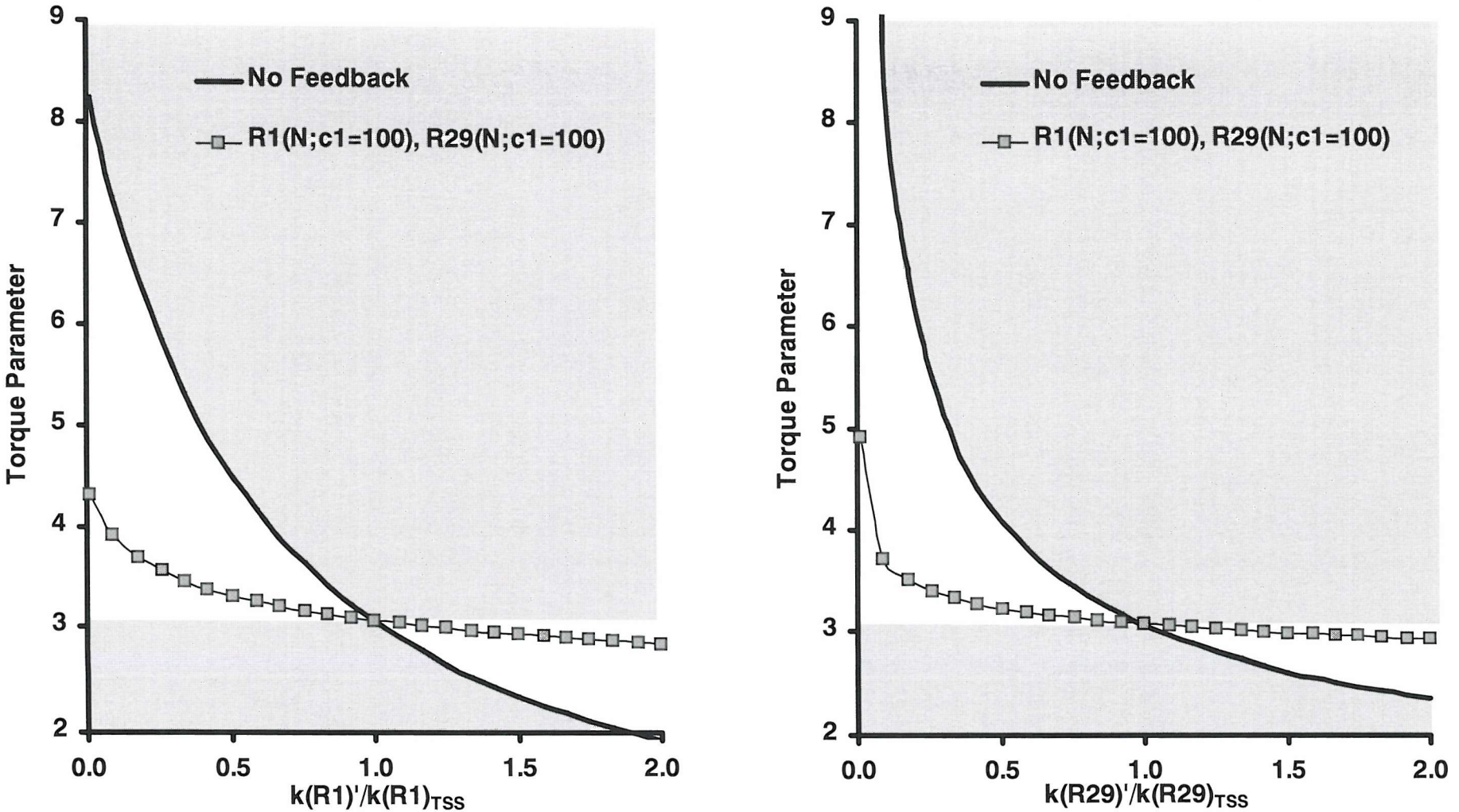

Figure 4.16a: Effect of two-point feedback at CCT and R29 on the torque parameter sensitivity to k(R1) and k(R29).
The action of feedback at two points provides similar stabilisation of the torque towards k(R1) and k(R29).

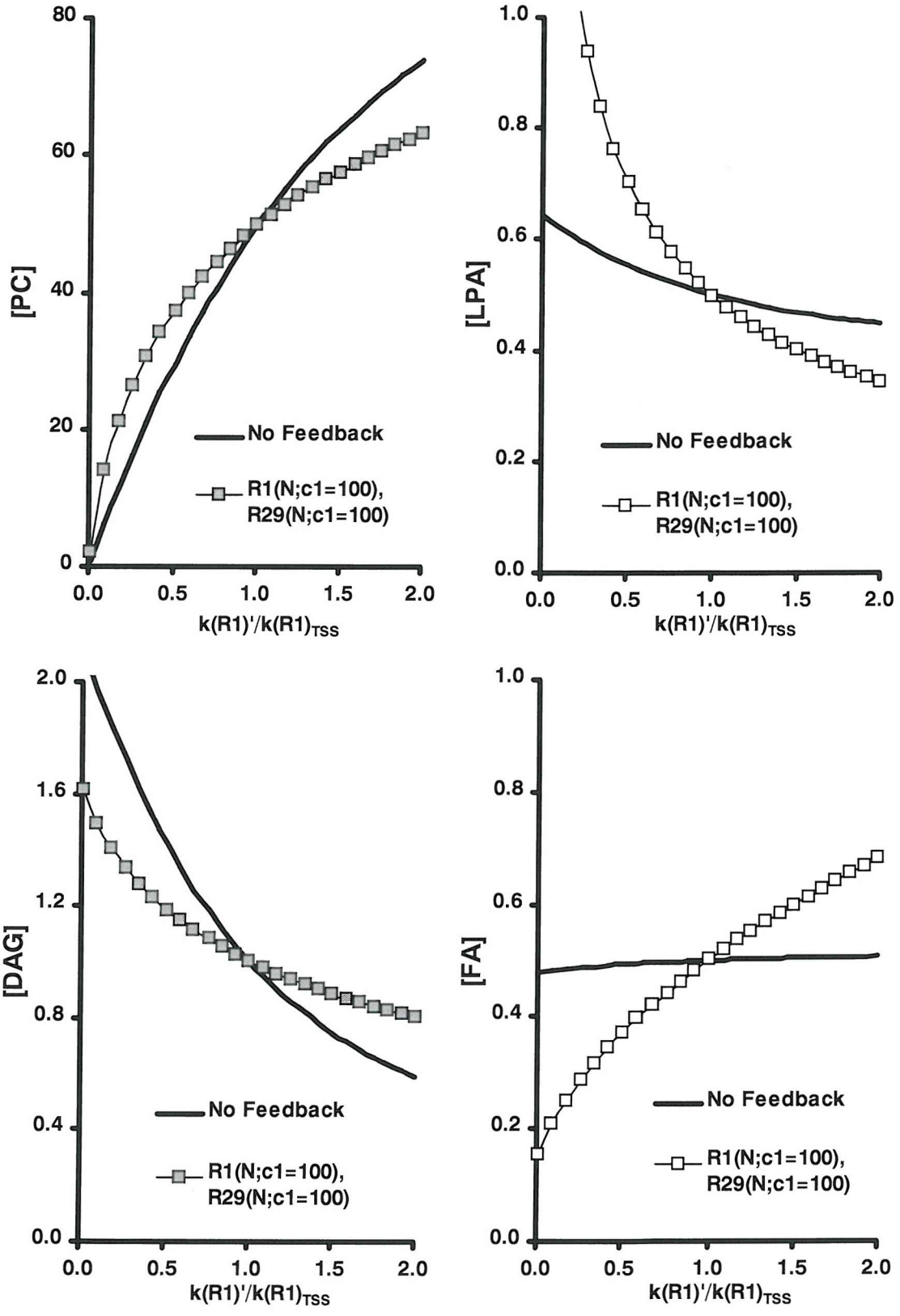

Figure 4.16b: Effect of two-point feedback at CCT and R29 on the sensitivity of the concentration to k(R1). The behaviour of the concentrations may be understood by comparing this figure to figure 4.08 for the change of k(R1) with feedback at CCT only. The concentration plots, in figure 4.08, show that with feedback at CCT only, stabilisation of λ is provided by the stabilisation of the concentrations of PC and DAG. In the plots in this figure, the torque is also stabilised because LPA and FA are changed by the feedback at R29. The conclusion is that the torque is stabilised, but the lipid concentrations are not. In fact, they can be significantly destabilised, as seen here for LPA and FA.

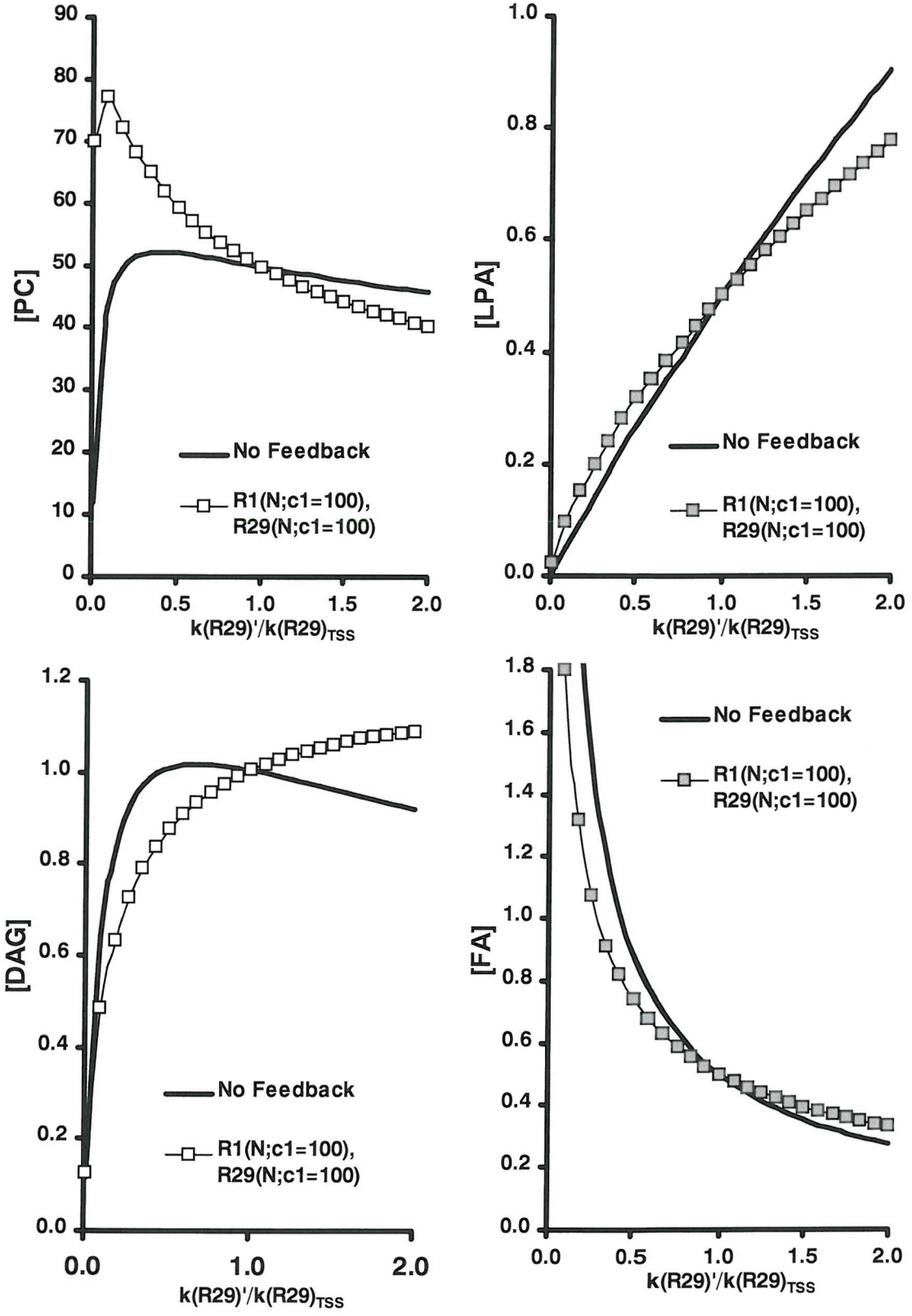

Figure 4.16c: Effect of two-point feedback at CCT and R29 on the sensitivity of the concentration to k(R29). When k(R29) is changed, the concentration behaviour is different to that seen when k(R1) was altered. Here the concentration of FA and LPA are stabilised (to a small degree). However, the concentrations of PC and DAG are destabilised by the feedback control at R1. It is seen that the concentrations which are stabilised or destabilised depends on which reaction coefficient is changed; the determining factor is that the changes lead to a stabilisation of the torque parameter as seen in figure 4.16a.

4.4 Prediction of Control Reactions

In this section, the system is analysed to allow the prediction of a set of control reactions. The previous section, which examined implementation of feedback, provided an understanding of how the feedback affects the system. The experiments with feedback suggested there are benefits of multiple feedback points. To build on the understanding gained in the previous experiments it was necessary to perform a more in depth analysis of the system. This was achieved primarily by extending the sensitivity analysis to examine all of the reactions.

Having observed that there may be benefits, in terms of robustness, to feedback at more than one reaction, the next step was to use the model to identify/predict the reactions that would provide enhanced robustness. The criterion for robustness here is stabilisation of the torque parameter. The task is therefore to identify the reactions that control the torque tension. If the role of the feedback is to ensure homeostatic control of the torque tension, these reactions are where this type of feedback would be expected to act in the lipid biosynthetic network to provide such control.

The first stage in the identification of control points is a *'global sensitivity analysis'* of the effect of the reactions on the torque parameter. The purpose of using sensitivity analysis was to examine which reactions exert significant control on the torque parameter. Since the feedback simply controls torque, not the individual metabolite concentrations, an effective feedback combination would need to control the reactions that have a significant effect on the torque. A reaction that gives a very small gradient on a λ vs. k plot will not impact significantly upon the torque and would be unable to form part of an effective torque dependent feedback loop; control of the reaction's rate would not contribute significantly to the control of the torque.

Also important, is the sign of the gradient of the λ vs. k plots. The sign of the gradient indicates if the action of the enzyme will lead to an increase or decrease in the stored elastic energy. Earlier, it was seen that application of normal feedback upon the rate of some reactions destabilised the system (figure 4.11). This is consistent with reports that some of the enzymes appear to be deactivated by type II lipids (Rao & Sundaram 1993). These two pieces of evidence combined, lead to the prediction of two responses to torque, one in which the enzymes are activated by

high torque and one where enzymes are deactivated by high torque. Two types of feedback have been proposed, and termed normal, for activation by high torque (e.g. CCT), and inverse, for deactivation by high torque (e.g. R3). Therefore, in addition to identifying strong candidates for feedback control, there is a need to identify candidates for each type of feedback.

Previously it was seen how the λ vs. k plot for CCT provided a feedback prediction that was consistent with experimental evidence of activation by increased stored elastic energy. Further, it was shown for R1, R29 and R3 how the λ vs. k curves could be used to identify the expected effect on the torque, and therefore the feedback type, which would lead to stabilisation (section 4.3.4). Similar λ vs. k curves are used in this section to predict both feedback type and strong candidates for each type. These results allow predictions about the lipid sensitivity that would be expected if the control were acting to maintain the stored elastic energy. By reference to the literature, these results can be validated by looking for a correlation with lipid dependence studies for the enzymes involved.

4.4.1 Experimental

It has already been shown how λ vs. k sensitivity plots can be used to identify the feedback type which, applied to a reaction, will stabilise the system (section 4.3.4). The reactions that have the greatest effect on the torque will be the best candidates for controlling the torque, as discussed above. Examination of the effect of reactions on the torque parameter is here expanded to include all of the reactions in the model.

In order that the results may be compared, and plotted together, each rate coefficient is changed over the same relative range. As described previously, the range is such that for each of the 27 rate coefficients* k(Rx) is varied over the range between $0.01 < k(\mathrm{Rx})'/k(\mathrm{Rx})_{\mathrm{TSS}} < 2$. The $k(\mathrm{Rx})_{\mathrm{lower}}$ and $k(\mathrm{Rx})_{\mathrm{upper}}$ values are given in table 4.02. The λ vs. k plots are generated by running 25 simulations between $k(\mathrm{Rx})_{\mathrm{lower}}$ and $k(\mathrm{Rx})_{\mathrm{upper}}$ for each rate coefficient. The results are then processed from the data from the 675 (25x27) simulations.

** The drain reactions were not altered. The drains simply model loss to outside of the boundaries of the model and do not represent defined enzyme mediated reactions.*

		flux	$k(Rx)_{TSS}$	$k(Rx)_{lower}$	$k(Rx)_{upper}$
R1	(Pcho) → CDPcho	16.000	16.000	0.16	32
R2	CDPcho + DAG → PC	8.000	0.400	0.004	0.8
R3	PC → DAG	2.281	0.046	0.00046	0.092
R4	PC → PA	2.281	0.046	0.00046	0.092
R5	PC → PS	2.281	0.046	0.00046	0.092
R6	PA → DAG	17.628	17.628	0.17628	35.256
R7	DAG → PA	8.000	8.000	0.08	16
R8	PS → PA	1.415	0.118	0.00118	0.236
R9	PS → DAG	1.415	0.118	0.00118	0.236
R10	PS → PE	1.415	0.118	0.00118	0.236
R11	PE → PS	2.686	0.090	0.0009	0.18
R12	CDPeth + DAG → PE	8.000	0.400	0.004	0.8
R13	PE → DAG	2.686	0.090	0.0009	0.18
R14	PE → PA	2.686	0.090	0.0009	0.18
R15	PA → LPA + FA	17.628	17.628	0.17628	35.256
R16	LPA + FA → PA	20.884	83.536	0.83536	167.072
R17	PC → LPC + FA	2.281	0.046	0.00046	0.092
R18	LPC + FA → PC	1.136	4.543	0.04543	9.086
R19	PS → LPS + FA	1.415	0.118	0.00118	0.236
R20	LPS + FA → PS	0.702	2.810	0.0281	5.62
R21	PE → LPE + FA	2.686	0.090	0.0009	0.18
R22	LPE + FA → PE	1.338	5.351	0.05351	10.702
R23	LPC → LPA	1.136	2.271	0.02271	4.542
R24	LPS → LPA	0.702	1.405	0.01405	2.81
R25	LPE → LPA	1.338	2.676	0.02676	5.352
R26	(Peth) → CDPeth	16.000	16.000	0.16	32
R27	CDPeth →	8.000	0.400	*	*
R28	CDPeth →	8.000	0.400	*	*
R29	(g3p) + FA → LPA	0.090	0.180	0.0018	0.36
R30	DAG →	0.010	0.010	*	*
R31	PC →	0.010	0.000	*	*
R32	PA →	0.010	0.010	*	*
R33	PE →	0.010	0.000333	*	*
R34	PS →	0.010	0.000833	*	*
R35	LPA →	0.010	0.020	*	*
R36	LPS →	0.010	0.020	*	*
R37	LPC →	0.010	0.020	*	*
R38	LPE →	0.010	0.020	*	*
R39	FA →	0.010	0.020	*	*
R40	( ) → FA	0.150	0.150	*	*

Table 4.02: The limits for the global sensitivity analysis scans.
Each kinetic constant k is varied so that $0.01 < k(Rx)'/k(Rx)_{TSS} < 2$. *Drain reactions not altered

4.4.2 Graphical Analysis of Results

For each simulation, the final steady state concentrations allow calculation of λ. Plotting λ against $k(Rx)'/k(Rx)_{TSS}$ yields the sensitivity plots presented which provide a graphical comparison of the effect on λ of each reaction. Graphical analysis was found to be the most convenient way to analyse and compare the results. The wide variation in reaction coefficient, a factor of 200, means that important information on the role of a reaction can be garnered by looking at features such as the shape of the curve or the behaviour at very low $k(Rx)$. This information would not be shown by a simple measurement of the gradient at the TSS, the basis of Metabolic Control Analysis. Metabolic Control Analysis was not, therefore used in this work but may prove valuable in the future for more quantitative work. The graphical method importantly facilitates comparison of different sensitivities and identification of the reactions with the largest effects on λ over the ranges used.

The torque parameter sensitivity analysis performed here is a crude tool to facilitate the selection of a set of control points. In section 4.4.8, for example, the possibility of variability of the effect on λ of the reactions will be investigated. However, the sensitivity analysis is a significant improvement over previous methods that have been used to predict lipid dependence, which relied largely on substrate/product analysis of lipid types. Nevertheless, the method has limitations. It should be noted that the ranges used for the variation of the kinetic constants are deliberately large; there is little information on what values of k_{lower} and k_{upper} would be physiologically relevant. Over these ranges, the lipid concentrations may have changed to values that would cause the system to become non-viable. The lipid concentrations are not monitored for this type of behaviour. As has been shown previously the concentrations are not stabilised in a consistent manner so a global analysis of concentration behaviour would be difficult to interpret*.

---

* *Information on the changes occurring to the lipid concentrations can be useful in understanding the effect on λ when analysing specific individual reactions. Examination of the changes in individual concentrations will be returned to in section 4.8 in a more detailed analysis for a specific result concerning the interesting differences in regulation observed for CCT and ECT.*

Despite its limitations, as a first step, the sensitivity analysis allows identification of a set of likely feedback control points. Crucially, since the feedback will be manifested as a sensitivity to type I/0 and type II lipids, these simulations provide output that may be compared with experimental studies of lipid dependence to test the model.

4.4.3 Sensitivity Analysis Results – Individual Reactions

The results of the sensitivity analysis are shown in figure 4.19. The plot shows the effect on the torque of each individual step. Only selected curves are marked with points, the rest are shown as unmarked lines. This has been done for the purpose of visual clarity; it is difficult to clearly label all the individual plots. However, it is important to show all of the plots on one chart in order to put the high gradient curves in context. The results from which the graphs are plotted are given in full, in tabular form, in the appendix to this thesis (table A1). From the plots of these results, the steps with the greatest effect on the torque may be identified.

Prediction of candidates for stabilisation by normal feedback, which will provide maximum robustness, is straightforward. The curves with the largest negative gradients are clearly seen. R1 (CCT) is easily identified as having a strong effect on the torque. R1 (Pcho → CDPcho), R29 (g3p + FA → LPA) and R2 (DAG + CDPcho → PC) are the three strongest normal plots, in that order. R19 (PS → LPS + FA) and R11 (PE → PS) also have a significant impact on the torque such that normal feedback would lead to stabilisation.

For candidates for inverse feedback, those with plots with positive gradients, the interpretation of the results is rather more complicated. R3 and R4 are potential candidates, as the curves with the largest positive gradients. Other potential candidates include R6 and R16, due to the effect on λ if the rates of these reactions are set to small values, despite the smaller gradient at $k(\mathrm{R}x)_{\mathrm{TSS}}$. Which are regarded as the most significant candidates would depend on whether the overall curve or simply the gradient at the TSS is looked at. It should be noted that the type of response seen for R6 and R16 would be missed by simply examining the gradient at $k(\mathrm{R}x)_{\mathrm{TSS}}$, the method used to find simple sensitivity coefficients.

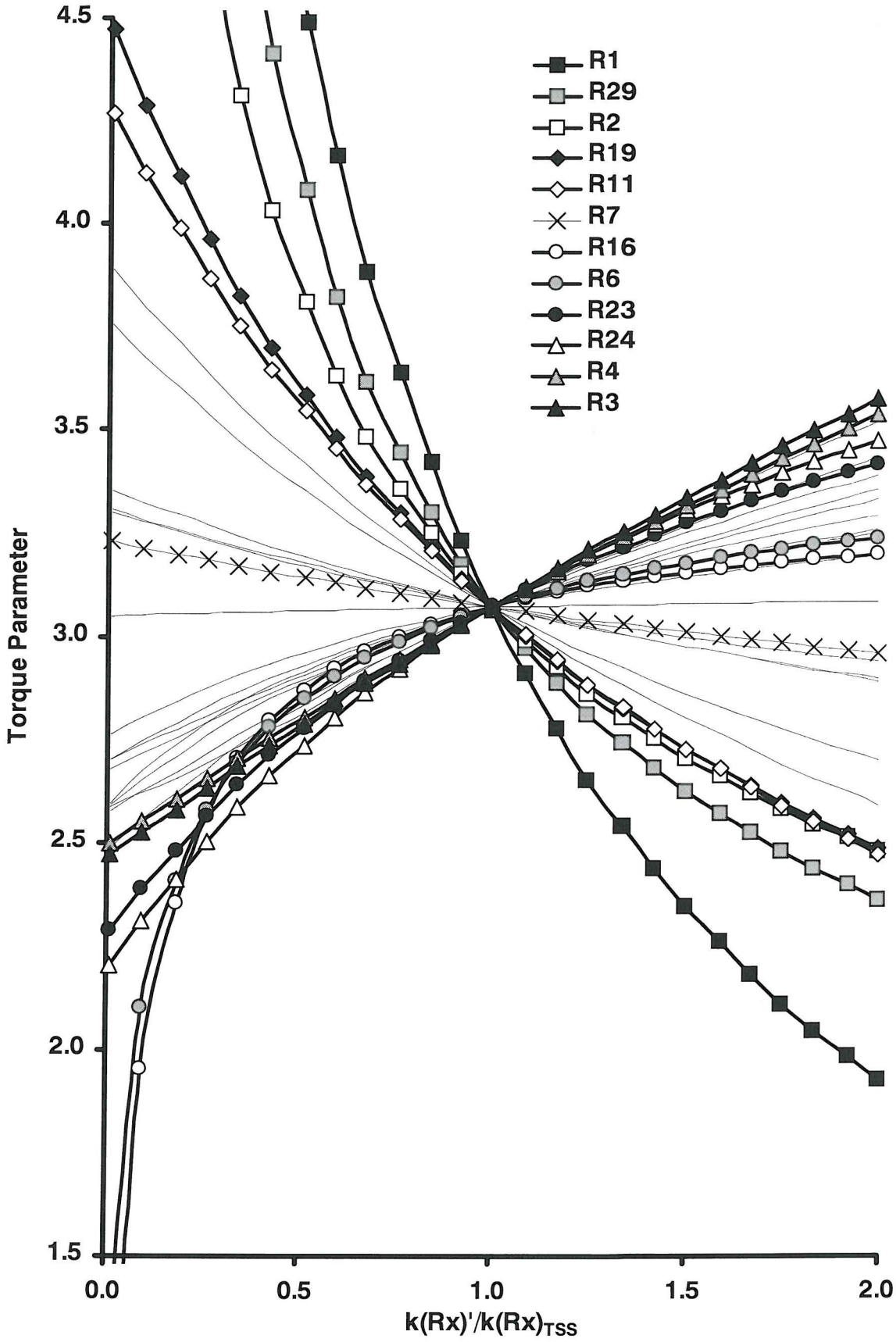

Figure 4.19: Global sensitivity analysis of the torque parameter to the reaction rates. The chart is a λ vs. k plot for each reaction step. The purpose of these plots is to identify the reactions with the greatest effect on the torque.

4.4.4 Reaction Classification by Enzyme

The reaction network used in the model contains 40 steps. In an effort to look at how the plots may be grouped, the idea was formed of considering the enzyme "class" with which the transformation is associated. Consideration of the enzymes that mediate the reactions leads to a simplification of the sensitivity plots. More importantly, this approach also facilitates correlation with literature data, which is performed in the next section.

Consider for example R3 (PC → DAG). A phospholipase C (PLC) enzyme mediates this reaction. PLCs are lipid-hydrolysing enzymes that are responsible for three of the reactions within the model (PC → DAG, PS → DAG and PE → DAG). Although species specific PLCs are known, for example PC-specific PLC, the activities may be grouped as a first approximation. This process is shown schematically in figure 4.20.

To model this grouping, a simple modification of the way in which the rate coefficients are changed is made. Instead of changing each rate coefficient independently, groups of coefficients corresponding to the given enzyme class may be changed together. For example, to achieve a sensitivity plot for the general activity of PLCs, rather than for the individual reactions that they mediate, the activities of the three reactions may be changed together in step. This will follow the effect of a change in activity of the PLC enzymes; if the activity of PLCs were doubled, the rate of each of the three reactions following mass action kinetics may be assumed to double. This assumption, of course, ignores isoforms, which are known to exist and in some cases could exhibit different activity profiles.

Accepting the assumption about substrate specificity and activity, this approach allows the generation of λ vs. k plots for each enzyme class. An example is shown in figure 4.21. A single curve for PLC replaces the sensitivity plots for the three individual reactions and shows the effect of PLC action on the torque parameter. This type of plot is a particularly useful result for comparison to an experimental study of PLC. The process outlined for PLC may be extended for all the reactions in the model.

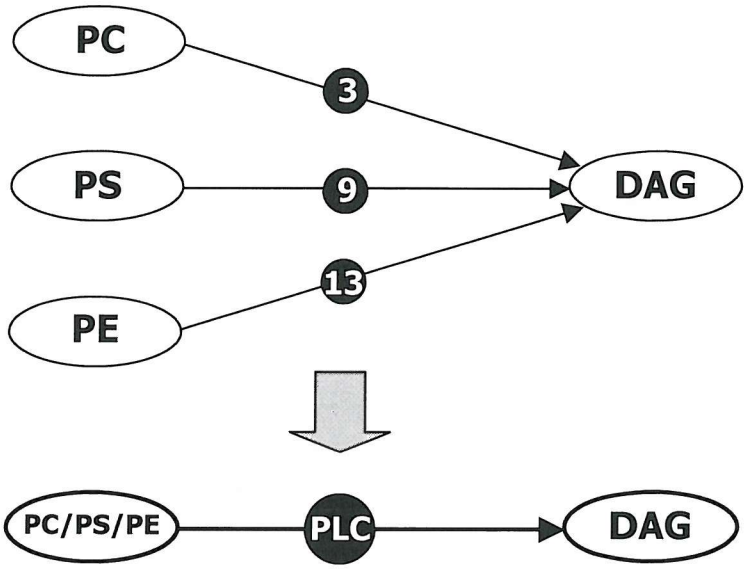

Figure 4.20: The three reactions in the model mediated by Phospholipase C (PLC).
These reactions may be grouped as an 'enzyme class' activity.

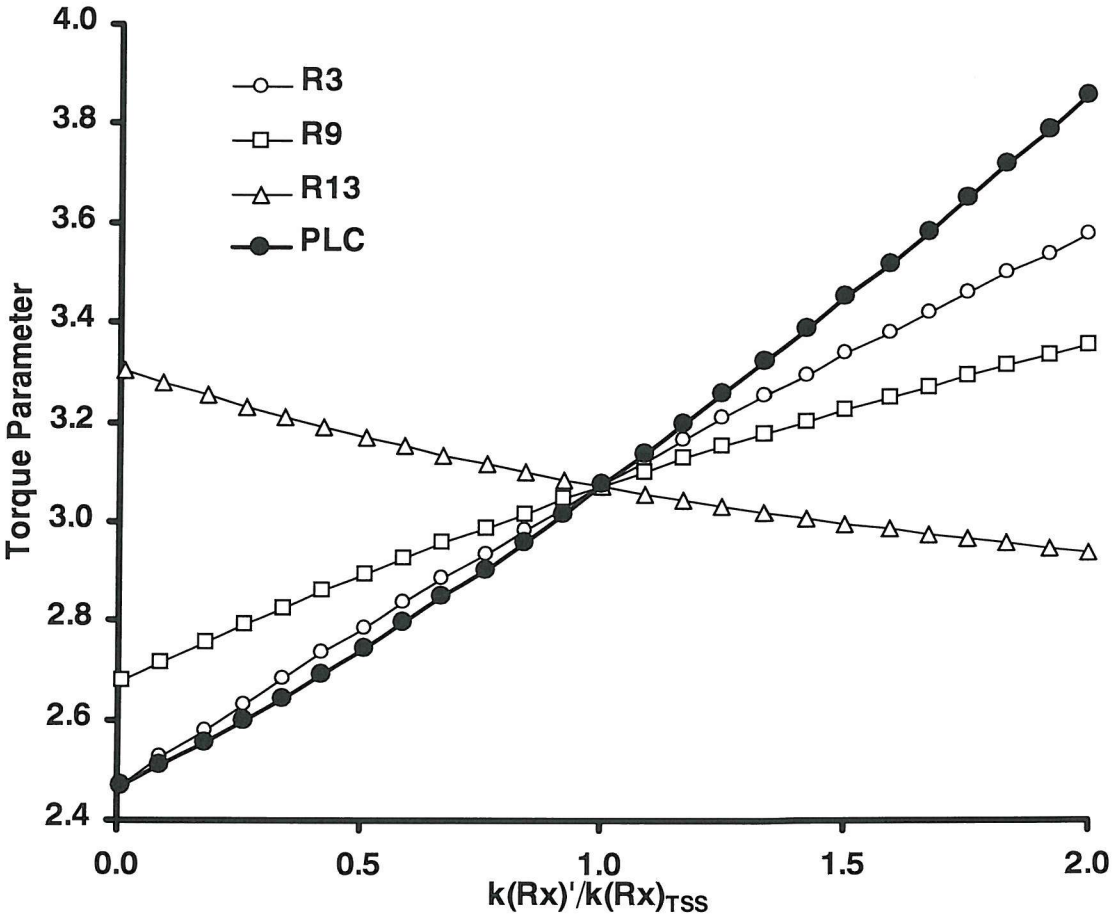

Figure 4.21: The λ vs. k plots for R3, R9 and R13 and the plot for Phospholipase C (PLC).
The plot for PLC is the result of altering the individual reaction coefficients for R3, R9 and R13 simultaneously.

The grouping process is repeated for each enzyme class. Table 4.03 summarises the enzyme classes and the reactions that are members of each class. The grouping criterion generally ignores specificity or preference for a particular substrate. However, for enzymes where there are definite separate activities, for example for choline and ethanolamine cytidylyltransferase (CCT and ECT), the sensitivities are presented as separate plots. This is particularly important, as one of the interesting results of the study is an examination of the different effects of these enzymes on the stored elastic energy. The model, with enzymes labelled, is shown in figure 4.22.

Label	Enzyme "Class"	Reactions
ACT	**Acyltransferase**	R16,R18,R20,R22
PLA_2	**Phospholipase A_2**	R15,R17,R19,R21
PLC	**Phospholipase C**	R3,R9,R13
PLD	**Phospholipase D**	R4,R8,R14,R23,R24,R25
CCT	CTP:phosphocholine cytidylyltransferase	R1
CPT	Choline phosphotransferase	R2
ECT	CTP:ethanolamine cytidylyltransferase	R26
EPT	Ethanolamine phosphotransferase	R12
g3pACT	Glycerol-3-phosphate acyltransferase	R29
DGK	Diacylglyerol kinase	R7
PAP	PA phosphohydrolase	R6
PSD	Phospatidylserine decarboxylase	R10
PSSI	Phosphatidylserine synthase I	R5
PSSII	Phosphatidylserine synthase II	R11

Table 4.03 "Enzyme classes", their labels and the individual reactions in each class

The choice of how to select the members of an enzyme class is interesting. For many of the enzymes the response of the torque tension is similar, giving one criterion in support of grouping them. The presence of one enzyme activity controlling multiple reactions could be another way the system maximises the connectivity of the

pathway in order to confer robustness. The torque tension is on the whole more sensitive to a change in enzyme class activity compared with changes of activity of the individual steps. Feedback control of a group of reactions, through the control of an enzyme class, would therefore lead to greater robustness. In this way, instead of control of a large number of individual reactions, the same stability could be established by control of a few enzyme classes. This leads to the prediction that if control acts on a class of enzyme this should be reflected in common motifs and regulation of the enzymes in this class. This has not yet been investigated in detail, but is an interesting possibility nonetheless.

It is however also possible to conceive the disadvantages of control of enzyme classes. Control of enzyme classes would reduce the potential for fine-tuning, through the independent alteration of reaction rates. There may also be advantages to substrate specificity within the enzyme classes, since a change in substrate can cause a difference in the effect of the reaction on the torque tension. For example, in the plot for PLC, in figure 4.21, it can be seen that one of the three steps acts to decrease the torque whilst the others act to increase it. The differing plot is for the cleaving of PE, a type-II lipid, whilst the two that increase the torque parameter have type 0 substrates (PC and PS). This may provide a criterion for independent control. For simplicity however, PLC activity is currently modelled as one class. One important enzyme where a distinction is made is glycerol-3-phosphate acyltransferase (g3pACT). This is kept separate from the general acyltransferase class (ACT), which includes conversions of the type LP*x* + FA → P*x*. g3pACT mediates one of the entry reactions in the model. The two processes (g3p → LPA and LPA → PA) are catalysed by distinct enzymes (Yamashita & Numa 1981). In addition, g3pACT acts to generate type I lipids while the ACT class consume type I lysophospholipids and make two chain lipids, so their effects on λ are very different.

In summary, it is seen that there are arguments for and against grouping the reactions by type, by using the concept of enzyme classes. The general conclusion drawn is that the control behaviour would lie somewhere between the control of each reaction independently and the control of the enzyme classes detailed here. In this respect, it is useful to look at the sensitivity of the torque to the enzyme class activities, in addition to the previous sensitivity analysis for the individual reaction steps.

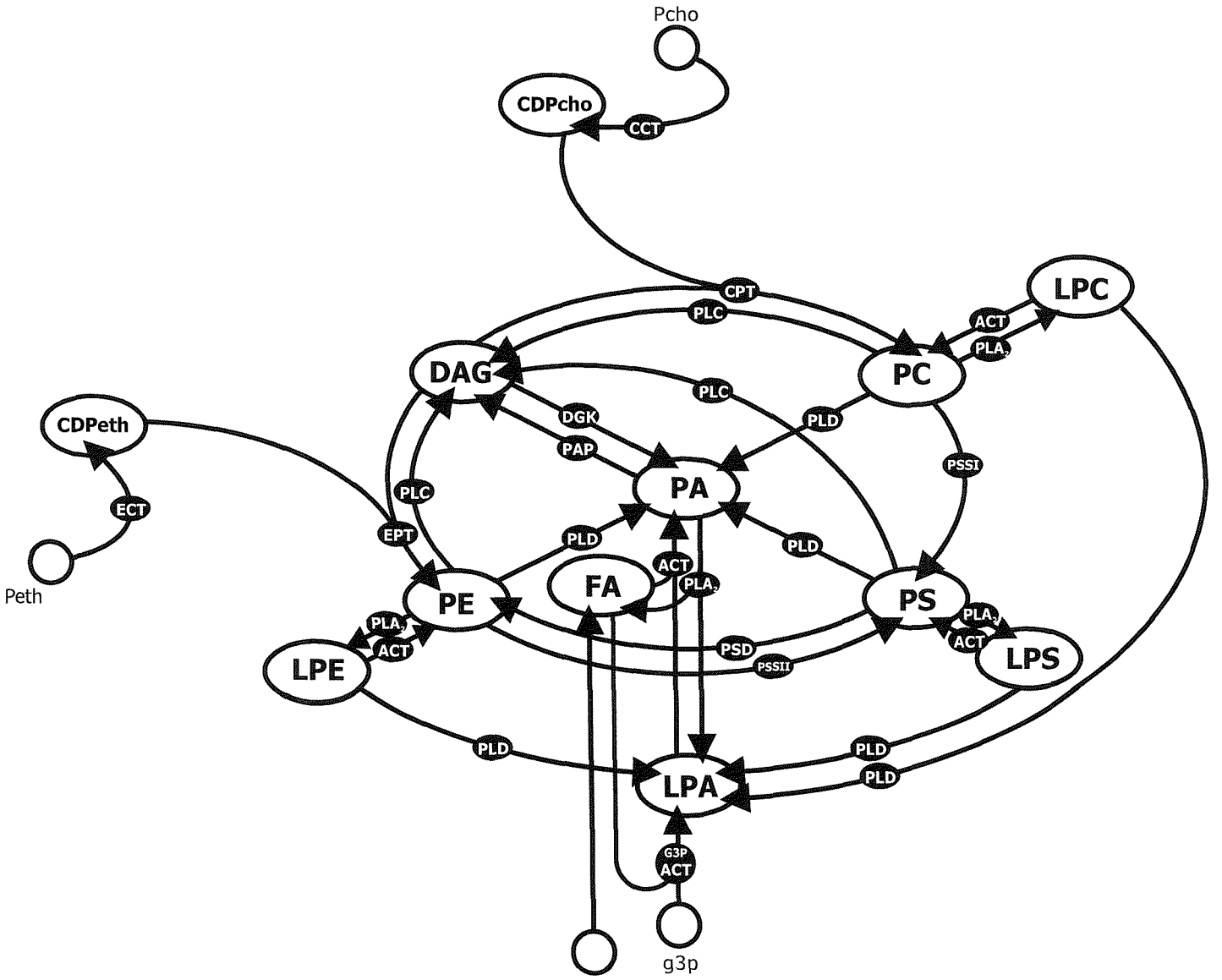

Label	Enzyme Class
ACT	Acytransferase
PLA_2	Phospholipase A_2
PLC	Phospholipase C
PLD	Phospholipase D
CCT	CTP:phosphocholine cytidylyltransferase
CPT	Choline phosphotransferase
ECT	CTP:ethanolamine cytidylyltransferase
EPT	Ethanolamine phosphotransferase
g3pACT	Glycerol-3-phosphate acyltransferase
DGK	Diacylglycerol kinase
PAP	PA phosphohydrolase
PSD	Phospatidylserine decarboxylase
PSS I	Phosphatidylserine synthase I
PSS II	Phospahtidylserine synthase II

Figure 4.22: Stoichiometric Network 3 (StN3) with enzyme class labels.
(The drain reactions and the involvement of FA in all LPx to Px reactions (as for LPA to PA) have been omitted in the diagram).

4.4.5 Sensitivity Analysis Results – Enzyme Classes

The results are shown in figure 4.23. The plot shows the effect on the torque of the rate for each enzyme class as defined in table 4.03. From these results, the steps with the greatest effect on the torque may be identified. The results from which the graphs are plotted are again given in full in tabular form in the appendix to this thesis (table A2).

Prediction of candidates for stabilisation by normal feedback, which will provide maximum robustness, is straightforward. The curves with the largest negative gradients are clearly seen. R1 (CCT) is again easily identified as having a strong effect on the torque. PLA_2 (P*x* → LP*x* + FA), CCT, g3pACT (R29, g3p + FA → LPA) and choline phosphotransferase (CPT) (R2, DAG + CDPcho → PC) are the four strongest normal plots, in that order. Phosphatidylserine synthase II (PSSII) (R11, PE → PS) and diacylglycerol kinase (DGK) (R7, DAG → PA) also have an effect on the torque such that normal feedback would lead to stabilisation. It is notable that the torque is most sensitive to PLA_2, a change in the rate of four individual steps. However, it is significant that CCT, which controls an individual reaction, has almost as large an effect on its own.

For candidates for inverse feedback (positive gradients) the interpretation is clearer than for the single step sensitivity analysis. The phospholipases PLC and PLD show large positive gradients as does the plot for ACT (LP*x* + FA → P*x*). Positive gradients are also seen for phosphatidylserine decarboxylase (PSD), PA phosphohydrolase (PAP) and also ethanolamine cytidylyltransferase (ECT) and ethanolamine phosphotransferase (EPT).

The next step is to use the sensitivity results presented to select a set of control points. These will then be validated, in section 4.5, through reference to literature reports of lipid dependence. Furthermore, the effect of implementing feedback at these points on the behaviour of the system is then investigated, in section 4.6, by examining the effect on the torque parameter, the lipid concentrations and lipid accumulation.

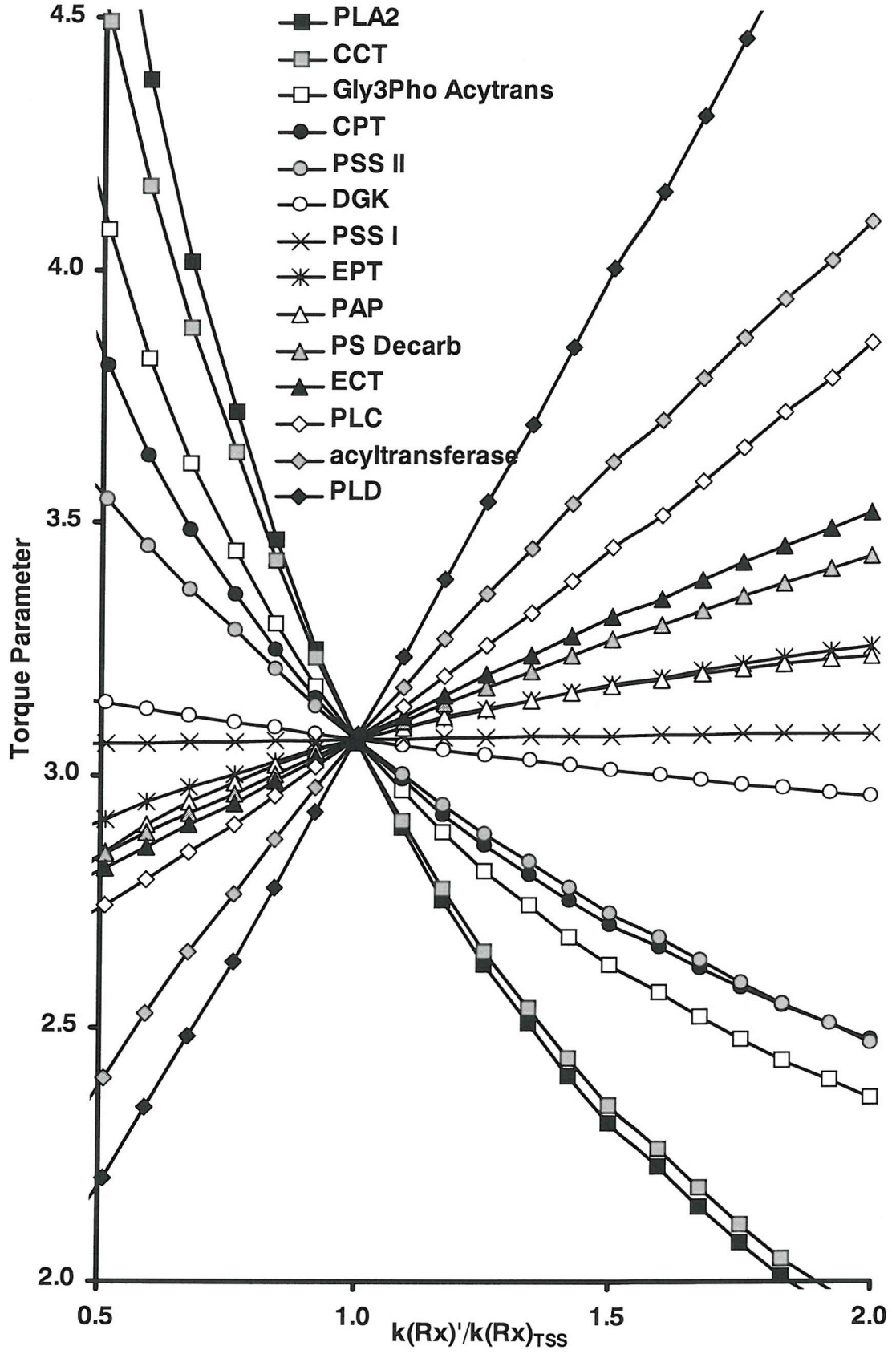

Figure 4.23: Global sensitivity analysis of the torque parameter to 'enzyme class' activities
The chart is a λ vs. k plot for each enzyme class. The purpose of these plots is to identify the generic enzyme activities with the greatest effect on the torque.

4.4.6 Likely Control Points

As discussed at the beginning of section 4.4, if the target of control of lipid biosynthesis is to maintain the stored elastic energy within an allowed range, then controlling the enzymes to which the torque tension is most sensitive is the key. A change in the rate of these enzymes will have the maximum effect on the torque tension, resulting in an efficient feedback mechanism.

It is clear from the sensitivity analysis results that there is no single 'rate determining step' that exerts sole control over the torque tension. Rather, the control of torque tension is distributed around the pathway. Another important point is that the sensitivity analysis only identifies points where feedback is likely or not likely to be found, how many points are required for stability is not revealed. To determine this, feedback must be explicitly implemented and its effect examined (this is performed in section 4.6).

A. Key reactions (from sensitivity of λ to individual reactions)

The likely candidates for feedback control, predicted from the torque sensitivity scans of the individual rate coefficients in section 4.4.3, are given in table 4.04. These are the reactions with high gradients commented on previously.

Decrease Torque (λ-) (λ stabilised by normal type feedback)		**Increase Torque (λ+)** (λ stabilised by inverse type feedback)	
R1	(Pcho → CDPcho)	**R16**	(LPA + FA → PA)
R29	(g3p + FA → LPA)	**R6**	(PA → DAG)
R2	(DAG + CDPcho → PC)	**R3**	(PC → DAG)
		R4	(PC → PA)

Table 4.04 Key candidates for feedback control from the curves for the individual steps.

The three strongest candidates for normal control points are: R2, which converts the strongly type II lipid DAG into the major membrane component PC. Also R1, which provides CDPcho, one of the substrates of R2. Finally R29, which is the first step in glycerolipid synthesis.

Of the four candidates for inverse control, two, R3 and R4, are responsible for the conversion of PC into the type II lipids DAG and PA. The other two, R16 and R6,

are reactions that link the important reactions R29 and R2. These last two reactions have small gradients at the TSS but the effect of λ at low *k*(R6) or *k*(R16) is dramatic. The maintenance of the activity of these reactions is clearly important, and could be ensured by activation of a non-active reservoir of enzyme.

B. Key enzymes (from sensitivity of λ towards enzyme classes)

When the sensitivity is looked at by enzyme type, the results are somewhat different. The enzyme classes selected as strong candidates for feedback control, in section 4.4.5, are shown in table 4.05. Grouping by enzyme class, CCT is no longer the strongest control point, but it is the strongest single reaction step. The identification of these enzymes, as potentially important in the control of stored elastic energy, facilitated the literature search performed for validation of the model in section 4.5.

Decrease Torque (λ-) (λ stabilised by normal type feedback)	**Increase Torque (λ+)** (λ stabilised by inverse type feedback)
PLA_2	PLD
CCT	ACT
g3pACT	PLC
CPT	ECT
PSSII	

Table 4.05 Key candidates for feedback control from the curves for the enzyme classes.

4.4.7 Visualisation of Strong Candidates

Analysis of the candidates for feedback control may be performed by marking them on the stoichiometric network. For this visualisation, a simplified three-dimensional arrangement of the stoichiometric network is convenient. Figure 4.24 shows the candidates picked from the individual reaction results. The feedback control points act on the reactions that form the sole route for PC synthesis. Figure 4.25 shows the candidates resulting from the classification into enzyme classes. Here a different arrangement is seen. Despite the differences, it is significant that control remains at g3pACT and R1 which are the starting points for the two branches of PC synthesis*.

* *The importance of source reactions is returned to later in a closer look at the role of CCT in the network (section 4.7).*

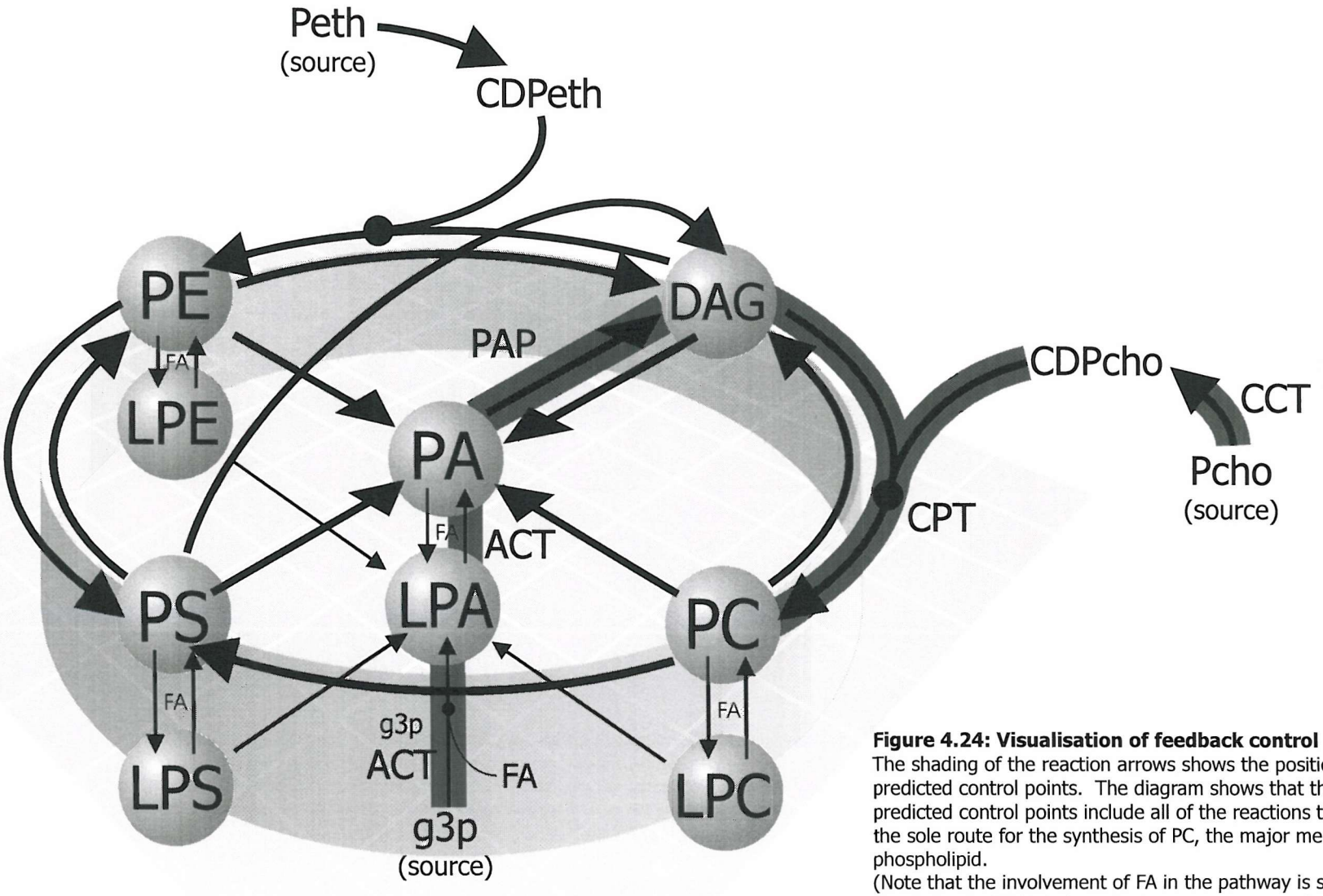

Figure 4.24: Visualisation of feedback control points.
The shading of the reaction arrows shows the positions of the predicted control points. The diagram shows that the predicted control points include all of the reactions that form the sole route for the synthesis of PC, the major membrane phospholipid.
(Note that the involvement of FA in the pathway is shown simply by the 'FA' labels at the LPx to Px reactions).

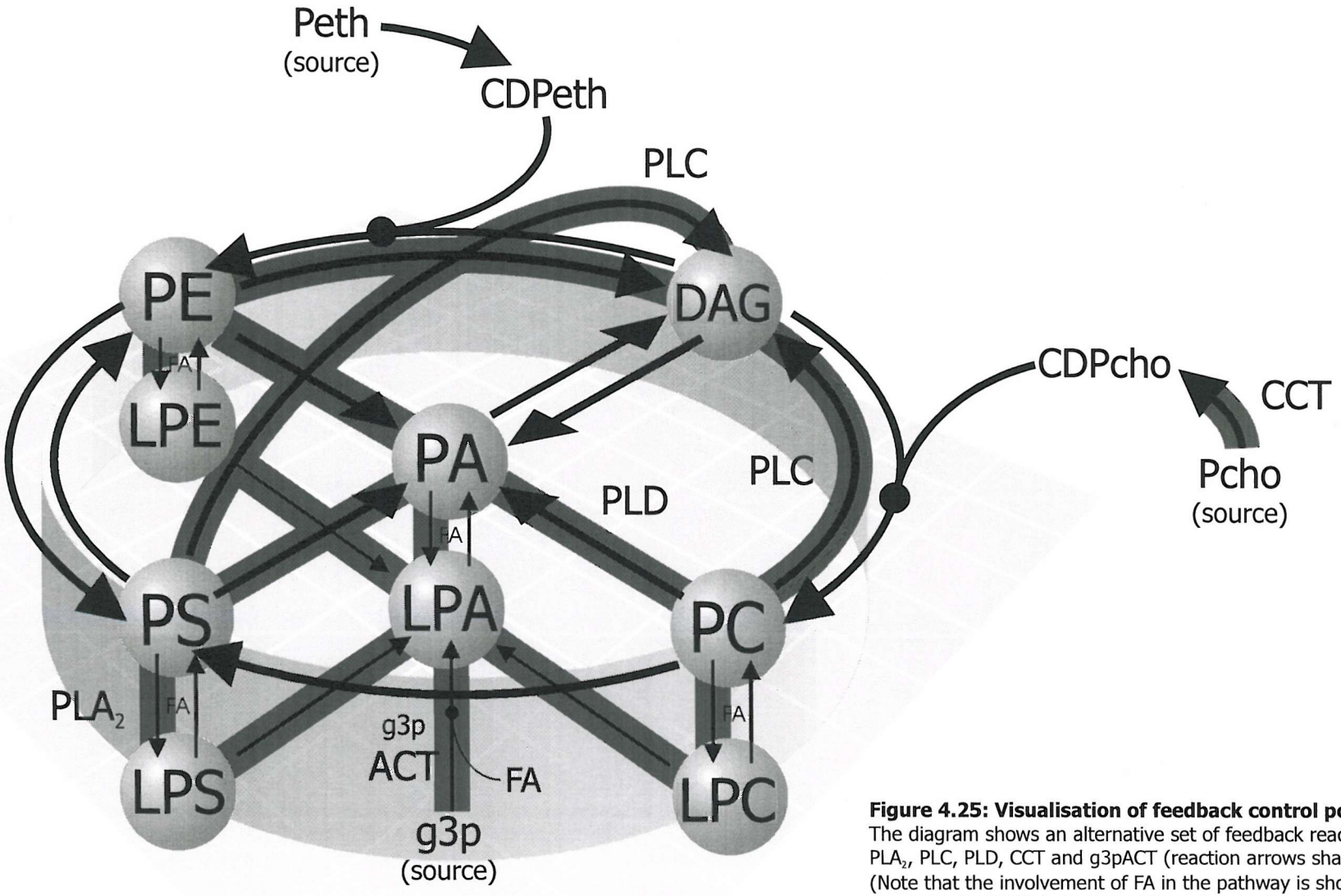

Figure 4.25: Visualisation of feedback control points. The diagram shows an alternative set of feedback reactions at PLA_2, PLC, PLD, CCT and g3pACT (reaction arrows shaded). (Note that the involvement of FA in the pathway is shown simply by the 'FA' labels at the LPx to Px reactions).

4.4.8 Variation of Conditions

In figure 4.11, the effect of adding normal feedback to R3, a step that acts to increase the torque parameter, was seen. The effect was dramatic destabilisation of the system. It is imperative therefore that, if feedback is to act at a step, not only must the effect on the torque tension be significant it must also always be of the same sign (i.e. the behaviour must not change from R$x(\lambda+)$ to R$x(\lambda-)$). This will ensure that the feedback is always stabilising. In order to test this, consideration must be given to how the conditions may vary.

It must be remembered that, although the model exhibits steady state behaviour, the system is still dynamic. Alteration of rate constants or other perturbations will change the concentrations (which are not homeostatically controlled by the torque tension feedback) and it is important that such changes do not cause the feedback to become destabilising. For this reason the effect on the torque tension must not change with the concentrations, or other conditions. It is suggested that the effect of each reaction on the torque must be non-varying if feedback is to act.

In setting up a simulation, a number of conditions are set arbitrarily. The target steady state itself is one, and through this, the steady state membrane torque parameter is set. Since the composition of membranes varies it was desired to investigate if any changes are seen at different compositions. Variations of the model were defined for different concentration balances and for different values of λ. Another assumption made in order to solve the model was the 'equal branch flux assumption'. This was a step, in solving for the flux distribution, in which it was assumed that all reactions that consume a common species would have equal fluxes, essentially ensuring each branch has a significant role in the pathway. This rule can be changed in order obtain a different flux distribution. This is important because the fluxes around the system will vary as enzyme activity is changed, and so this variation could potentially cause a stabilising feedback to become destabilising.

The variations were chosen to represent different balances of the major lipids and different torque tensions. They were not designed to be realistic compositions, being used simply to look at the influence of the changes. The variations were set up to check that the predictions of the sensitivity analysis were not dependent on the

choice of TSS or the rate constants used, which had been set largely arbitrarily, but were purely a result of the network structure and the distribution of lipid types.

Five variations upon the standard model were set up. In the first four, the reactions coefficients are recalculated from the fluxes to give new target steady states. These are chosen for the different balances of metabolite concentrations or different values of λ. In the fifth variation, the flux distribution is recalculated for a different branching rule. In this way, the three main assumptions of TSS concentration, TSS torque and flux branching are all varied. The variations are summarised in table 4.06, which gives the details of the steady state concentrations, the associated value of λ and, in one case, the altered flux branching rule.

	Standard$_{TSS}$	**Variation 1**	**Variation 2**	**Variation 3**	**Variation 4**	**Variation 5**
		same λ	high λ	low λ	unity	alt branch
PC	50	**20**	**20**	50	**1**	50
PS	12	**42**	12	12	**1**	12
PE	30	**40**	**40**	30	**1**	30
DAG	1	**0.33**	1	1	**1**	1
PA	1	1	1	1	**1**	1
LPA	0.5	0.5	0.5	0.5	**1**	0.5
LPC	0.5	0.5	0.5	**2.5**	**1**	0.5
LPE	0.5	0.5	0.5	0.5	**1**	0.5
LPS	0.5	0.5	0.5	0.5	**1**	0.5
FA	0.5	0.5	0.5	0.5	**1**	0.5
λ	**3**	**3**	**4**	**1.5**	**1**	**3**

Table 4.06: A summary of the variation of conditions. The table show the concentrations for each TSS (those altered are shown in bold) and the associated torque parameter. **Standard$_{TSS}$** is the original condition chosen to be representative of the RER. **Variation 1** has the same λ as Standard$_{TSS}$ but different concentrations, with higher concentrations of PE and PS as the major lipid species. **Variation 2** corresponds to higher torque, importantly with PE, rather than PC as the major lipid species. **Variation 3** has a smaller value for λ, featuring broadly the same lipid concentrations but with more LPC. **Variation 4** has all lipid concentrations equal at unity; an extreme concentration distribution to investigate whether the concentration distribution is a factor. **Variation 5** shares the same TSS as the standard model, but has an altered flux distribution as the 'equal flux branching rules' are modified (DAG branch fluxes R2:R12:R7 2:1:3, PC branch R3:R4:R5:R17 2:1:3:1).

For each of the first four variations, the reaction coefficients are recalculated using the target steady state values in table 4.06. With the coefficients calculated the new k_{lower} and k_{upper} can be determined and the sensitivity analysis repeated. Details of the coefficients are given in the appendix to this thesis in table A5-A9. For variation 5, the process is more involved. The new branching rules must be inserted into the stoichiometric matrix, which is then solved for the new flux distribution. With the new flux solution, the process of finding the reaction coefficients and the scan limits is as for the other variations.

It is important to note that the network structure and the lipid types (the coefficients used in the calculation of the torque parameter) remain unchanged. These are fixed properties, determined by the simplification of the stoichiometric network and best guesses for the torque parameter coefficients. The distinction is that these properties will not change, as the concentrations and fluxes do, when the activities of enzymes are altered. For this reason, these factors (for example that DAG is modelled as a strongly type II lipid) should be distinguished from concentrations and fluxes, which are variables of the system.

The results in figure 4.26 show λ vs. k plots for the variations for the key enzyme classes picked out previously. For CCT, and the other results in figure 4.26, it is seen that the effect on the torque is both strong and consistent. The results show that only small differences in the plots for the key predicted points are seen. There are no differences significant enough to change the predictions. These results suggest that the sensitivity of the torque to each enzyme is determined largely by the structure of the reaction network and the distribution of lipid types in the system*.

The next section of this chapter examines the experimental evidence that may be used to validate the predictions from the model presented here. This begins with a look at the type of experiment necessary to provide information on the effect of membrane torque tension on enzyme activity.

---

* *In section 4.8, a reaction with a variable effect will be identified and examined, to explain how variable behaviour can occur.*

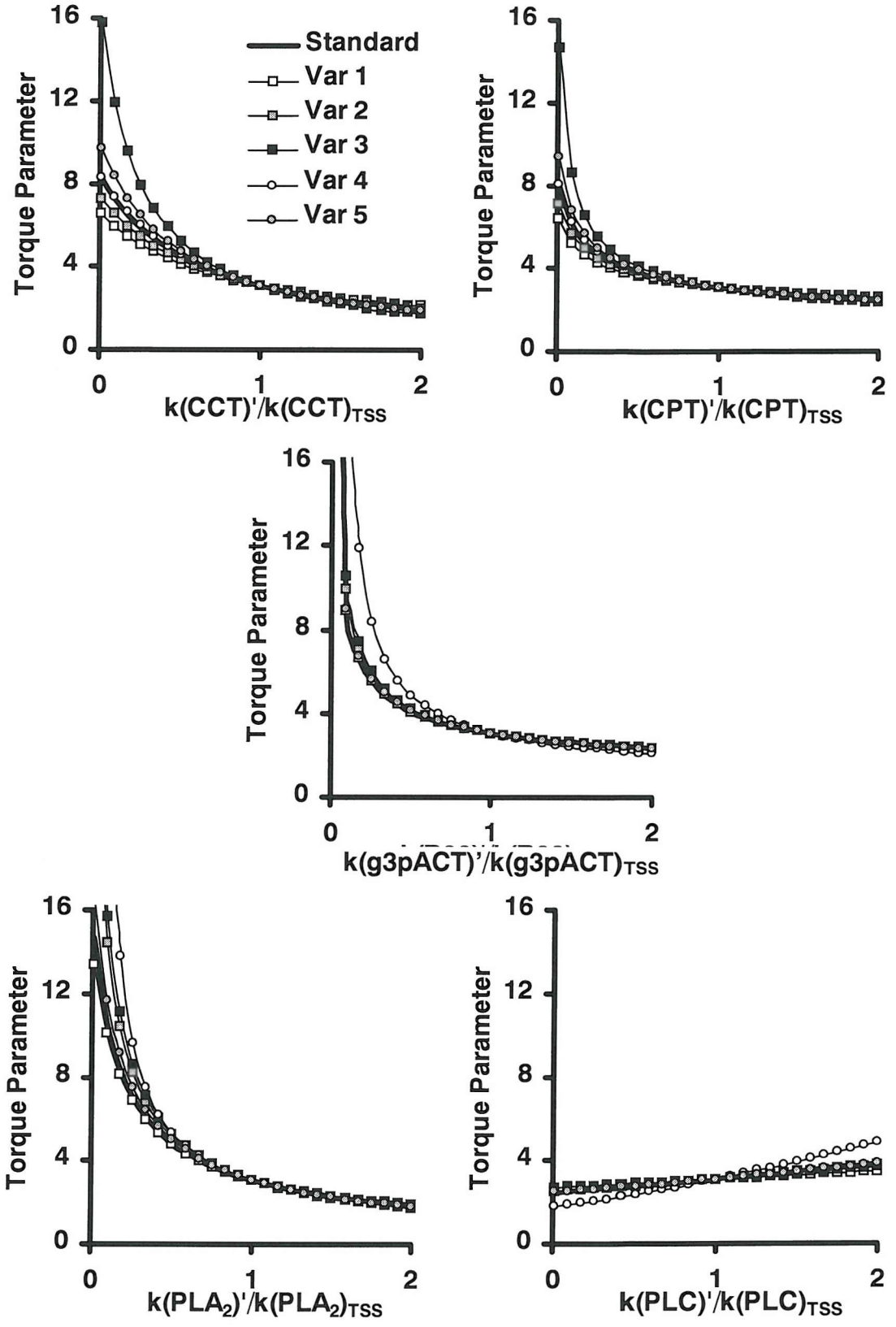

Figure 4.26: Scaled λ vs. k plots to examine changes in the sensitivity of the torque parameter to predicted key enzyme classes, upon variation of the model. The plots are scaled for variation 2, 3 and 4 such that λ_{TSS} is as for the standard TSS. The changes seen are small. There are no changes in the sign of the gradient, and changes in the magnitude are such that they do not change the predictions of these activities as candidates for feedback (Table A15-A18 appendix 2).

4.5 Model Validation

If the postulate that torque tension is the homeostatically controlled parameter in membranes is valid, then it would be expected that the reactions identified by sensitivity analysis to have the largest effect on λ will be those that should be subject to control. This control manifests itself as activation or inhibition by type II or type I/0 lipids. Therefore, the results from the sensitivity analysis of the model may be tested, at least qualitatively, by comparing the findings with experimental studies from the literature.

The literature was searched for studies of lipid biosynthetic enzymes that included information on lipid dependence and data on activity. These studies were examined for correlation between the data on enzyme activity, the associated information on patterns of lipid activation and the predictions from the sensitivity plots from the model. This validation represents the best way to test the useful output of the model, where suitable experiments can be found.

4.5.1 Criteria for Assessing Relevance of Literature Observations

Caution must be used when using literature observations. This caution is necessary to ensure that the experiments can provide information on how membrane torque tension modulates the activity of the enzyme studied. Finding such suitable experimental evidence is difficult for a number of reasons. Firstly, the enzyme must have been purified and be free of intrinsic lipids. Some of the enzymes are membrane bound (intrinsic membrane enzymes) whilst others, including CCT, are soluble enzymes which associate with membranes (extrinsic membrane enzymes). Purification can be a particular challenge for intrinsic membrane proteins. Also, most of the enzymes will alter the composition of the membrane through their action. Note that this is not the case for CCT, which acts at the membrane but produces lipid precursors. This complicates the methods for measuring activity and must be accounted for.

It is also of vital importance that the correct type of experiment is performed. The enzyme must be reconstituted with lipid in a specific way. Reconstitution into micelles is not suitable. Micelles have no bilayer structure and so are inappropriate model systems for the study of the effect of stored elastic energy. These simple,

unphysiological experiments cannot therefore be used to understand the behaviour of the enzymes upon changes in bilayer stress in the cell membrane. Unfortunately, prior to the suggestion that enzymes may be modulated by bilayer stress, reconstitution experiments commonly used micellar reconstitutions for convenience.

Vesicles are suitable model systems. However, there are further criteria. Vesicles should ideally be unilamellar to reflect the single bilayer that comprises the cell membrane. Multilamellar vesicles can lead to artifacts which may be associated with surface accessibility (Sen *et al.* 1991). Furthermore, the size of the vesicles is important. Experiments with small unilamellar vesicles (SUV) are less than ideal. The high curvature of SUVs results in the complication of geometric stress. Any reconstitution and activity study experiments must therefore preferably be performed with large unilamellar vesicles (LUVs) with a diameter of the order of 1 μm. Additionally, preparations that contain type I amphiphiles are not ideal because of their dramatic effect on the stored elastic energy (Attard *et al.* 2000). For this reason care must be taken with results using preparations involving the use of non-ionic detergents. Finally, even the experiments which use vesicles generally use them, not specifically to adjust the torque tension, but because, as bilayer structures, they are physiological. Investigation of torque tension effects requires carefully designed experiments with the use of suitably chosen purified lipids (both in terms of headgroup and alkyl chain identity). The selection of non-charged species is also preferable. Where charged lipids are used it can be difficult to disentangle the different effects caused by charge and curvature.

Often the experiments found are not specifically designed to vary the stored elastic energy in isolation. However, since the type of control is manifested as sensitivity to type II and type I/0 lipids, this behaviour can be looked for. In most cases the results are simple changes in activity for different lipid constitutions. At least qualitative comparison is possible since the validation involves simply the identification of a modulation by membrane stress and the direction of change. Identification that type II lipids consistently activate/deactivate in synthetic vesicles provides indication of torque tension driven activation and this may be correlated with the model data. Significant correlation would reinforce the hypothesis upon which the model is based, that enzyme modulation acts to maintain the stored elastic energy.

4.5.2 Relevant Supporting/Contradictory Biochemical Data

The criteria used significantly limits the number of reports used to test the model. However, suitable studies were found with experimental procedures which broadly follow the requirements detailed previously. These results can be interpreted in terms of the response of the enzymes to lipid types, which provides evidence of modulation by membrane torque tension. Correlation with the model provides evidence that the modulation is such that it would lead to homeostasis of the stored elastic energy. Evidence was searched for in the literature for the reaction steps which showed a strong influence on the torque parameter in the model. These were summarised in section 4.4.6 and include CCT, phospholipase A_2, choline phosphotransferase and glycerol-3-phosphate acyltransferase. The findings are summarised, starting with a look at the preparation used for CCT.

A. CTP:Phosphocholine Cytidylyltransferase (CCT)

(R1, Pcho → CDPcho, EC 2.7.7.15)
model predicts normal feedback (activation by type II lipids)

As noted earlier, Attard, Smith, Templer, Hunt and Jackowski examined the activity of CCT upon isothermal variation of torque through the systematic variation of the lipid composition of large unilamellar vesicles of the uncharged lipids, DOPC and DOPE (Attard *et al.* 2000). Large vesicles (ca. 2 μm) ensure principal curvatures are much smaller than the spontaneous curvature and that binding of CCT has a small effect on the vesicle, eliminating effects of membrane compression. CCT was isolated in a delipidated form, free of phospholipid and detergent. The solubility of the substrate and the product is also helpful; the composition of the vesicles is unchanged and the product is released into solution. The results include correlation of experimental data with calculated values based on relief of torque tension.

There is a wealth of further literature reports on the activity of CCT and the influence of lipid preparations (Arnold & Cornell 1996; Bladergroen *et al.* 1998; Boggs *et al.* 1995; Choy & Vance 1978; Clement & Kent 1999; Cornell 1991a; Cornell 1991b; Cornell & Arnold 1996; Jackowski 1994; Jackowski 1996; Jamil *et al.* 1993; Jamil *et al.* 1990; Kent 1997; Lykidis & Jackowski 2001; Northwood *et al.* 1999; Tronchere *et al.* 1994; Vance 1996). Whilst not all look specifically at curvature effects, the data is broadly consistent. The remainder of this section focuses on studies of the other enzymes identified in the sensitivity analysis.

B. *sn*-Glycerol-3-phosphate acyltransferase (g3pACT)

(R29, g3p + FA → LPA, EC 2.3.1.15)
model predicts normal feedback (activation by type II lipids)

The enzymatic activity of *sn*-Glycerol-3-phosphate acyltransferase is firmly membrane associated, as the enzyme is an intrinsic membrane protein. Green and Bell performed asymmetric reconstitution of homogeneous Escherichia coli sn-Glycerol-3-phosphate acyltransferase into phospholipid vesicles (Green & Bell 1984). The enzyme was purified using Triton X-100 detergent (Green *et al.* 1981). The reconstitution experiment uses 90nm single walled phospholipid vesicles, these fall into the range of SUVs and so are less than ideal. The enzyme is incorporated from mixed micelles containing detergent but the final detergent concentration in the vesicles is low (less than 2% Triton X-100 and 5% β-octyl glucoside). The removal or reduction of detergent is stated as a major goal in order to demonstrate that the enzyme was reconstituted by physical association with single-walled phospholipid vesicles. Although the effect of geometric curvature and non-ionic detergents as type I amphiphiles on enzyme activity can be dramatic (Attard *et al.* 2000), the effects here will be consistent allowing at least qualitative comparison of the results.

The paper is focussed primarily on the asymmetric reconstitution into vesicles, although it does usefully contain limited activity data for the enzyme incorporated in vesicles with different lipid constitutions. The paper reports that when PC is present in the lipid mixture the glycerol-P acyltransferase activity was lowered. A 1:1 mixture of PC and PE:PG:CL, 6:1:1, was only 50% as active as vesicles with the latter mixture alone. Furthermore, enzyme reconstituted into PC alone was only 15% as active as enzyme reconstituted using the standard procedure (PE:PG:CL, 6:1:1). This may be more clearly summarised:

$$\text{Activity}_{\text{Standard}} > \text{Activity}_{\text{PC + Standard (1:1)}} > \text{Activity}_{\text{PC}}.$$

(where Standard is PE:PG:CL, 6:1:1. A strongly type II mixture)

The addition of PC to the standard mixture leads to a reduction in the membrane torque tension and a decrease in the activity of glycerol-P acyltransferase. This is consistent with the predictions of the model.

Other studies were rejected because of high concentrations of detergent (Scheideler & Bell 1992; Yamashita & Numa 1972), the use of unsized vesicles (Kito *et al.* 1978; Snider &

Kennedy 1977), or reconstitution to micelles (Scheideler & Bell 1989). Also, the use of anionic species (Coleman 1988; Kessels *et al.* 1984) made the contribution of charge and stored elastic energy hard to interpret.

C. Phospholipase A_2 (PLA_2)

(R18, Px → LPx + FA, EC 3.1.1.52)
model predicts normal feedback (activation by type II lipids)

There are several PLA_2s. Secreted PLA_2s function in digestion and toxicity, the cell associated PLA_2s function in phospholipid turnover. Secretory PLA_2s have been most thoroughly studied. The enzymes are soluble, but activity is enhanced by a lipid bilayer (Cornell & Arnold 1996).

Sen Isac and Hui investigated the susceptibility to phospholipase A_2 of mixed dilinoleoylphoshatidylethanolamine and palmitoyloleoylphosphatidylcholine vesicles (Sen *et al.* 1991). This work examined the rate of phospholipid hydrolysis of pancreatic PLA_2 as a function of the mol% DlinPE in POPC MLVs and LUVs (with and without cholesterol). The changes in activity are correlated with the onset of non-lamellar phases. The activity is seen to fall upon transformation to the H_{II} phase. The largest enhancement is observed just prior to the L_α to H_{II} phase transition, in agreement with the prediction of the model. Rate enhancements are compared to the calculated curvature stress stored in the LUVs. It is interesting that the authors note that PE appears to be more susceptible than PC to PLA_2. This fits with the model of activation presented in this thesis since the cleaving of the S_N2 bond in PE will lead to a greater relief of stress than would be the case with PC.

Zidovetski, Laptalo and Crawford examined the effect of diacylglycerols on the activity of cobra and bee venom and pig pancreatic phospholipase A_2 (Zidovetski *et al.* 1992). This paper examined the response of various secretory PLA_2s to packing stress in PC MLVs by various DAGs. The results show that negative curvature stress caused by DAG in PC membranes stimulates activity. In addition, diolein activated PLA_2 at temperatures below that required for H_{II} formation, suggesting activity is modulated by bilayer torque tension rather than non-lamellar phases. There are also reports that PLA_1 (Lin *et al.* 2000) (not currently in the model) showed an increase in activity when diacylglycerol and cholesterol were included in SUVs.

D. Diacylglycerol Kinase (DGK)

(R7, DAG → PA, EC 2.7.1.107)
model predicts normal feedback (activation by type II lipids)

DGK is an extrinsic membrane protein, which has been observed to shuttle between the cytosol and the membrane (Topham & Prescott 1999) as with CCT. This raises the interesting possibility of altering the activity of the enzyme by translocation to areas where DAG has accumulated (Thomas & Glomset 1999a). Thomas and Glomset investigated the factors that influence the binding of a soluble Ca^{2+}-independent diacylglycerol kinase to unilamellar vesicles (Thomas & Glomset 1999b). The experiments study the interactions of DGKs with well-characterised 100nm unilamellar lipid vesicles and analyse the effect of membrane lipids on the interactions. The paper also gives details of the lipid chain lengths and unsaturation.

The model predicts normal feedback for DGK. The experiments performed by Thomas and Glomset suggest that the enzyme exhibits increased activity in highly stressed membranes. The authors working hypothesis involves electrostatic interactions between DGK and the negatively charged surface of PS containing vesicles, with the phosphocholine headgroup of PC inhibiting this interaction. The problem with this explanation is that it requires the assumption that PE headgroups do not have the same effect. In addition, the strong effect of DAG is explained by an alteration of the vesicles surface and interaction with the enzyme substrate-binding site. This working hypothesis therefore uses at least two modulating factors.

The results presented in the paper may be more satisfactorily interpreted by considering membrane torque tension; the membrane torque tension hypothesis is able to explain all of the observations using a single property. However, whilst the results are consistent with this, they must be reinterpreted. The authors discount the possibility that PE and cholesterol may be positive effectors of DGK activity since their molecular structures have so little in common. Considering the effects on the stored elastic energy, it becomes apparent what PE and cholesterol have in common; they are both type II lipids. The argument that PE cannot be a positive effector, since >75 mol % PE substitution in PS vesicles caused a 'precipitous decrease' in enzyme activity, is also likely to be erroneous; at such high PE concentrations it is highly likely that the bilayer has broken down to a H_{II} structure. To further support stimulation by stressed membranes, vesicle binding is increased with DAG. In

addition DAG has a greater effect than PE or cholesterol, as would be expected when considering MTT. It is stated that without substituting for PC, PE and cholesterol have no effect; it would appear that the PC is capable of maintaining the membrane stress at sufficiently low levels to prevent activation of DGK, although this is not certain. DGK is responsible for removing DAG, an extremely type II lipid, so it would be expected to only be active under conditions of high membrane stress.

E. Phospholipase C (PLC)

(R3, PC/PS/PE → DAG, EC 3.1.4.3)
model predicts inverse feedback (deactivation by type II lipids)

PLC is an extrinsic membrane protein with a hydrophobic surface near its active site, which it is thought may function in binding to the lipid membrane (Cornell & Arnold 1996). PLCs from bacterial, rather than eukaryotic, sources have been most widely studied due to ready access to the enzyme. Rao and Sundaram investigated the response of PLC from Bacillus cereus to lipid packing in vesicles (Rao & Sundaram 1993). Both the phase behaviour and enzyme activities are monitored using SUVs and MLVs containing DOPC, DOPE, cholesterol, lysoPC and gramicidin. DOPE, cholesterol and gramicidin (all favour H_{II} phases) are correlated with decreases in enzyme activity. Furthermore, LPC is shown to increase enzyme activity. The size of the SUVs is not given but results with MLVs suggest that the activity of PLC is independent of the geometric curvature and morphological differences between the MLVs and SUVs. The interpretation suggests that negative curvature may interfere with PLC access to the substrate phosphoester bond. In addition, the discussion highlights the difference in behaviour of PLC and PLA_2 (Sen *et al.* 1991) a difference predicted by the sensitivity analysis of the model presented here.

The significance of these results is that deactivation of PLC seen for type II lipids is consistent with the inverse feedback used in the model. This modulation will clearly be different to that presented in the model of the modulation of CCT activity by membrane torque tension (section 1.4.2): this involved the proposed ability of CCT to stabilise the bilayer structure. Here binding may deactivate the protein or the enzyme may destabilise the bilayer structure, this has been proposed for intrinsic membrane proteins through studies of gramicidin (Killian & deKruijff 1986), although for an extrinsic protein this is harder to reconcile. A reasonable model for this behaviour in terms the stored elastic energy has not been published. The model

therefore suggests that this type of modulation would lead to homeostasis of the torque tension, but the process by which this could be achieved remains unclear.

F. CTP:Phosphoethanolamine Cytidylyltransferase (ECT)

(R26, Peth → CDPeth, EC 2.7.7.14)
model predicts inverse feedback (deactivation by type II lipids)

ECT has, due to its relationship to CCT, been quite extensively studied for the effects of lipids on its activity. It is widely accepted that the activity of ECT is not affected by phospholipid (Bladergroen & Van Golde 1997; Vermuelen *et al.* 1993). This result initially appears contrary to the results of the model. If ECT followed the behaviour of CCT, as might be expected, 'normal' type feedback would be predicted. In contrast, the sensitivity analysis of the model predicts inverse feedback. The interesting case of the similarities of CCT and ECT and the contrasting regulatory behaviour is returned to in detail in section 4.8. The review now examines several of the enzymes for which suitable experimental reports were not found, looking at the reasons for this.

G. Phospholipase D (PLD)

(R4, PC/PS/PE → PA), EC 3.1.4.4)
model predicts inverse feedback (deactivation by type II lipids)

There is some evidence that the activity of PLD behaves in a similar way to PLC (and in the opposite way to PLA_2) in membranes in the presence of membrane-active peptides such as gramicidin which affect lipid packing in the membrane (Rao & Sundaram 1993). However, no detailed studies of PLD in bilayer systems monitored for stored elastic energy were found.

H. CDP-Choline:1,2-diacylglycerol Phosphotransferase (CPT)

(R2, DAG + CDPcho → PC, EC 2.7.8.2)
model predicts normal feedback (activation by type II lipids)

Choline phosphotransferase is a tightly bound intrinsic membrane bound protein and attempts to solubilize it with a variety of detergents failed (O & Choy 1990). As recently as 1997, CPT had not been purified from any source and mammalian cholinephosphotransferase cDNA had not been isolated (McMaster & Bell 1997). However, human cDNA that codes for a cholinephosphotransferase specific enzyme has now been cloned (Henneberry *et al.* 2000). Interestingly, a cloned choline / ethanolaminephosphotransferase cDNA that codes for a dual specificity C/EPT has been identified (Henneberry & McMaster 1999). This dual specificity may help explain

why regulation is essential at the cytidylyltransferase step to allow independent control of PC and PE biosynthesis (the differences between CCT and ECT, their specificity and separate regulation are returned to in section 4.8).

The only activity experiments performed to date have been mixed micellar analyses to examine the substrate specificity of CEPT1 (Wright & McMaster 2002). These experiments unfortunately tell little of the effect stored elastic energy may have on CPT. The role of CPT in the regulation of PC biosynthesis remains poorly understood (Lykidis & Jackowski 2001).

I. Phosphatidylserine synthase II (PSS II)

(R11, PE → PS, EC 2.7.8.8)
model predicts normal feedback (activation by type II lipids)

The activity of the base-exchange enzyme PSS II is recovered largely in ER fractions (Jelsema & Morre 1978). The protein is firmly embedded in the membrane, its solubilization requires detergents and it has proved unstable after this (Kanfer 1980). These properties have hindered purification, as for CPT. Due to this little is currently known about the regulation of PSS II activity (Kuge & Nishijima 1997).

J. Phosphatidate Phosphatase (PAP)

(R6, PA → DAG, EC 3.1.3.4)
model predicts inverse feedback (deactivation by type II lipids)

It is reported that 'although there have been studies suggesting that PAP enzymes can be modulated by non-bilayer forming lipids... none paid attention to the effects of the various lipids on the physical properties of the lipid preparations' (Cornell & Arnold 1996). The use of mixed micelle dispersions mean the effects of the non-bilayer lipids cannot be attributed to bilayer stress effects.

It has been argued that PAP does not involve structural components of the membrane (Cornell & Arnold 1996). However, this is also true for CCT. Yet CCT has been shown to control the production of PC, which is an important structural component. Since the CPT reaction is known to be controlled by substrate supply (Bladergroen & Van Golde 1997; Vance 1996), the synthesis of DAG by PAP may also be important in the production of PC. In addition, although DAG is not a major lipid or a structural component by virtue of its concentration, it must be considered so when its potency as a type II lipid is considered.

4.5.3 Summary of Literature Results

The result of reference to the literature is good correlation for a number of enzymes, as summarised in table 4.07. Crucially there were no suitable literature reports found that were in opposition with the predictions from the model. Therefore, although the number of reports that broadly fit the criteria is small, this is excellent agreement.

Enzyme	Model predicts	Literature reports
CCT	Normal	Activated by type II lipids
g3pACT	Normal	Activated by type II lipids
PLA_2	Normal	Activated by type II lipids
DGK	Normal	Activated by type II lipids
PLC	Inverse	Inhibited by type II lipids
PLD	Inverse	Inhibited by type II species – limited data
CPT	Normal	None available
PSS II	Normal	None available
PAP	Inverse	None available
ECT	Inverse	No lipid activation*

Table 4.07: Correlation of the sensitivity analysis results with literature reports.

It should be remembered that the sensitivity analysis can only identify strong candidates and the type of feedback necessary, it is not a suitable test to eliminate an enzyme since all the plots show a gradient and could control the torque to some degree. Furthermore, an idea of how many feedback points are required can only be gained from explicit implementation of feedback. Therefore, the effects of implementation of feedback, at some of the predicted points, are investigated in the next section.

* *The result for ECT is somewhat of a special case, in that there are reports that it is not activated by lipids due to the contrasting behaviour of CCT. No other reports of a negative (i.e. no effect of lipid) were found. To address this, the sensitivity analysis method was supplemented by use of the model to examine the effect of CCT and to contrast the effects of the CCT and ECT reactions in more detail. This helps to explain the behaviour of CCT, and why this is different for ECT. These results are presented in section 4.8.*

4.6 Implementation of Predicted Feedback Combinations

Having investigated possible feedback sites, a first test of integrative feedback at the predicted points is performed here. The aim is to test the network and the choice of feedback points for their ability to maintain λ within acceptable limits.

4.6.1 Effect of Feedback on λ vs k Plots: Homeostasis of Torque

The sensitivity analysis performed previously was repeated for the reaction network with feedback implemented at multiple points. The feedback combination used was R1(N,c_1=100), R2(N,c_1=100), R29(N,c_1=100), R16(I,c_1=100), R6(I,c_1=100). The sensitivity plot is shown in figure 4.27 (b) (with selected curves shown for clarity) and can be compared to the sensitivity analysis for the uncontrolled network reproduced to the same scale in (a). The increase in robustness in terms of the maintenance of λ is seen graphically*. The stabilisation is significant. In addition, it can be clearly seen that all of the curves are stabilised in similar way. These results show the dramatic effect of only a few feedback control points and suggest that only a few feedback points are necessary to produce a high degree of robustness.

The observation of stabilisation of the torque parameter is somewhat obvious, because the feedback implemented is physically driven by the torque parameter. This type of comparative sensitivity analysis is repeated in sections 4.6.4 and 4.6.5 to look at the effect of feedback on the lipid concentrations and the total concentration of lipid species. Next, the effect of different feedback combinations on λ is detailed.

---

* *In principal, the visual comparison in figure 4.27 could be extended to give a numerical value for the relative stabilisation of torque, the criterion for robustness. This could be achieved by summing the area between the curve and the horizontal line at* λ_{TSS} *for every reaction, between the limits* k_{lower} *to* k_{upper}*, and repeating this for each feedback combination. This would clearly be a time-consuming task. More importantly, there would also be the problem of selecting the value of the limits to use, as it is not known which are physiologically relevant. Moreover, at this stage in investigating the responses of the network, graphical analysis often reveals more about the system than a number could. For these reasons, such quantitative methods will not be developed here.*

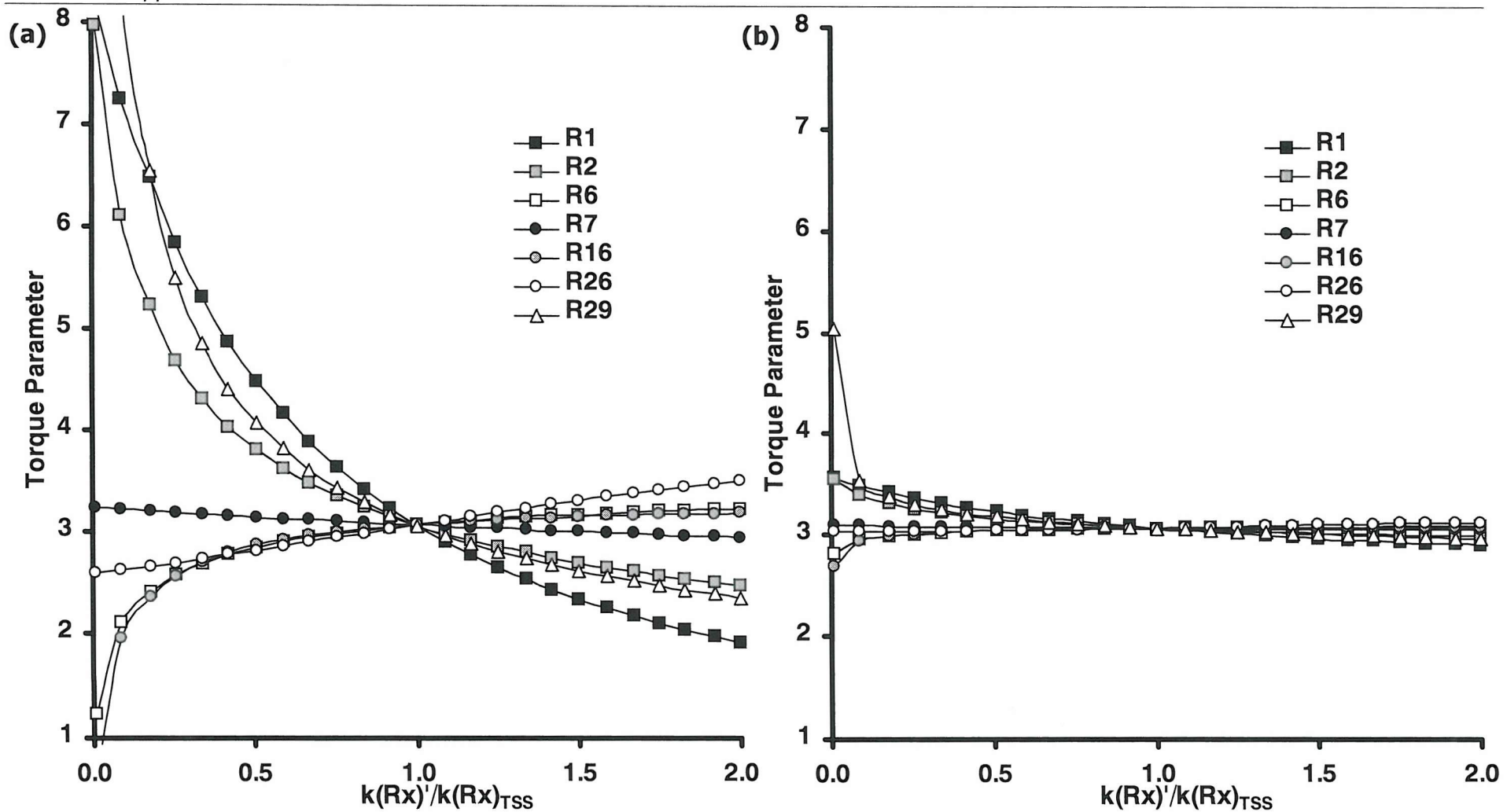

Figure 4.27: Stabilisation of torque parameter by feedback.
(a) Network without feedback. **(b)** Feedback at R1(N,c_1=100), R2(N,c_1=100), R29(N,c_1=100), R16(I,c_1=100), R6(I,c_1=100).
(Only selected lines are shown for clarity).

4.6.2 Progressive Stabilisation of λ

In section 4.3, the effects of two-point feedback were seen and it was shown that this could be very effective. Here, this is extended to look at the effects of feedback at the multiple points predicted. Figure 4.28 shows the effect on the sensitivity of the torque parameter to *k*(R1) for three feedback combinations. It was seen in figure 4.27 that each plot was affected in a similar way by feedback; here only one curve is shown to facilitate comparison of the different feedback combinations. The points chosen are those predicted from the enzyme class sensitivity analysis, details are given in the figure legend. The torque parameter is progressively stabilised by the addition of extra feedback points. The system is seen to become highly robust with only a few control points.

To further understand the effects multiple point feedback can have on the model, and how the system can still respond when it is perturbed, there is a need to look at the concentrations as it has been seen that these are not uniformly stabilised. For these reasons the effect of the feedback points on the concentrations, starting with the total concentration of lipid species, will now be explored.

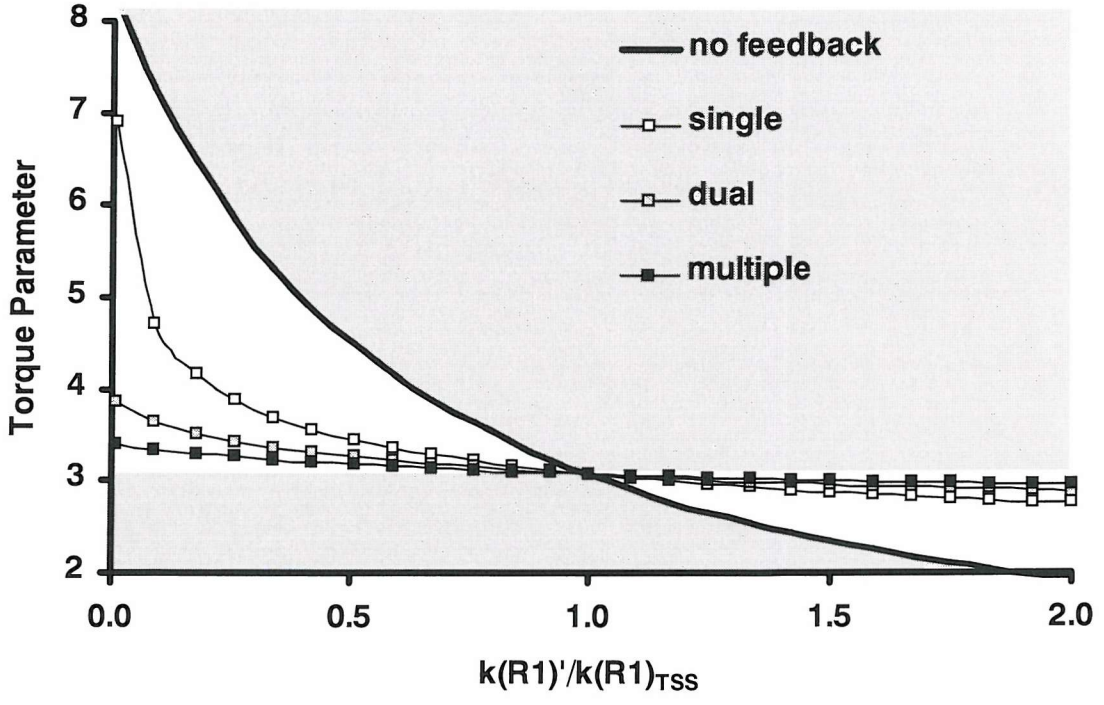

Figure 4.28: How different feedback configurations affect the sensitivity of the torque parameter: single CCT(N;c_1=100), **dual** CCT(N;c_1=100), PLA_2(N;c_1=100), **multiple** CCT(N;c_1=100), PLA_2(N;c_1=100), g3pACT(N;c_1=100), PLC(I;c_1=100), ACT(I;c_1=100). The plots show that addition of feedback at multiple points progressively stabilises the torque parameter.

4.6.3 Total Lipid Sensitivity Analysis

In this section, a sensitivity analysis for the total concentration of lipid species is performed. The total concentration of lipid species will be referred to as the *total lipid* for brevity. The response of the total lipid to each rate constant will identify the steps that control lipid accumulation in the same way that control of the torque parameter was identified. The total lipid is not the property proposed to be under homeostatic control, and is not a factor in the proposed integrative feedback mechanism. For this reason the results are not used to select candidates for feedback. However, examination of control of total lipid is important because there may be effects on lipid accumulation caused by the feedback mechanism proposed. This may be illustrated by considering the effect control of CCT activity may have. CCT has been identified as controlling PC production. Correlations between CCT activity and phospholipid accumulation have also been observed (Lykidis & Jackowski 2001). If CCT activity is controlled by feedback, will the sensitivity of the total lipid to CCT be reduced, as the sensitivity of λ to CCT is? This is important since production of phospholipid prior to cell division is essential to provide adequate membrane to contain the resulting daughter cells. In general, the question is, does the proposed integrative feedback reduce the ability of the network to accumulate lipid? In the next section, the effect of implemented feedback on lipid accumulation will be investigated. First, the sensitivity analysis is used to identify the steps that control the total lipid concentration.

A. Experimental – individual step sensitivity analysis

The sensitivity analysis is performed as for the torque parameter global sensitivity analysis in section 4.4. The total lipid is calculated from the steady state by summing the new steady state lipid concentrations as shown in equation 4.01.

$$Total\ Lipid = PC + DAG + PE + PS + PA + LPA + LPE + LPC + LPS + FA \qquad \text{equation 4.01}$$

B. Results

The results are shown in figure 4.29. R1 has a strong effect on the total lipid, as does R2. R6 and R16 also have a positive impact on the total lipid. Each of these reactions form part of the main route by which PC is formed. Reactions that have a

negative effect are R3, R4, R5 and R17; each of these consumes PC. This can be rationalised due to the contribution PC makes to the total lipid concentration. As the major lipid species it accounts for around half of the lipid mass. In fact, as expected all the reactions that form the main route of synthesis of PC (g3p → LPA → PA → DAG → PC) have a positive effect on the total lipid, with one exception: R29.

The curve for R29 is unique as the only plot that does not show a consistent effect on the total lipid; the sign of the gradient changes over the range used. This result can be understood by examining its unique location in the network. As the first step in the pathway, reaction 29 has two lipid-precursors as its substrates, FA and g3p, and forms the lipid LPA. Since the reaction is the first step in the synthesis of new lipid an increase in its rate would be expected to cause a net increase in total lipid. This is the case for low $k(\mathrm{R29})'/k(\mathrm{R29})_{\mathrm{TSS}}$. However at $k(\mathrm{R29})'/k(\mathrm{R29})_{\mathrm{TSS}} > 0.5$, the amount of lipid is decreased as $k(\mathrm{R29})'$ is increased. This counter intuitive effect is caused by the involvement of FA in the network. FA is involved in many reactions, significantly all of the further acylation reactions. An increase in the rate of R29 decreases the amount of FA via increased consumption. This impacts on the rate of the other acylation reactions, those that convert the lysophospholipids into two chain phospholipids (LP*x* + FA → P*x*). These include the step which follows R29, R16 (LPA + FA→PA). R16 is a key step in the biosynthesis of PC, and appears to act as a bottleneck due to depletion of FA when R29 is increased. FA appears to act to stabilise the system, by flux limitation, through the connectivity it creates as a plurifunctional cofactor involved in consecutive reactions. These results are not investigated here in detail*. A significant result however, is that the involvement of FA in the first step of lipid synthesis appears to leave CCT, which controls the supply of the choline moiety, as the primary control of lipid accumulation. This is consistent with experiments that have noted the correlation of CCT activity and phospholipid accumulation (Jackowski 1994).

---

* *Detailed modelling of FA would require refinement of the model, mainly in the area of FA supply, which is crudely handled at present. However the methods which will be used to analyse CCT and ECT (in section 4.8) could be applied here and used to look at the role of FA in more detail, which reactions control the concentration of FA and how FA influences the system.*

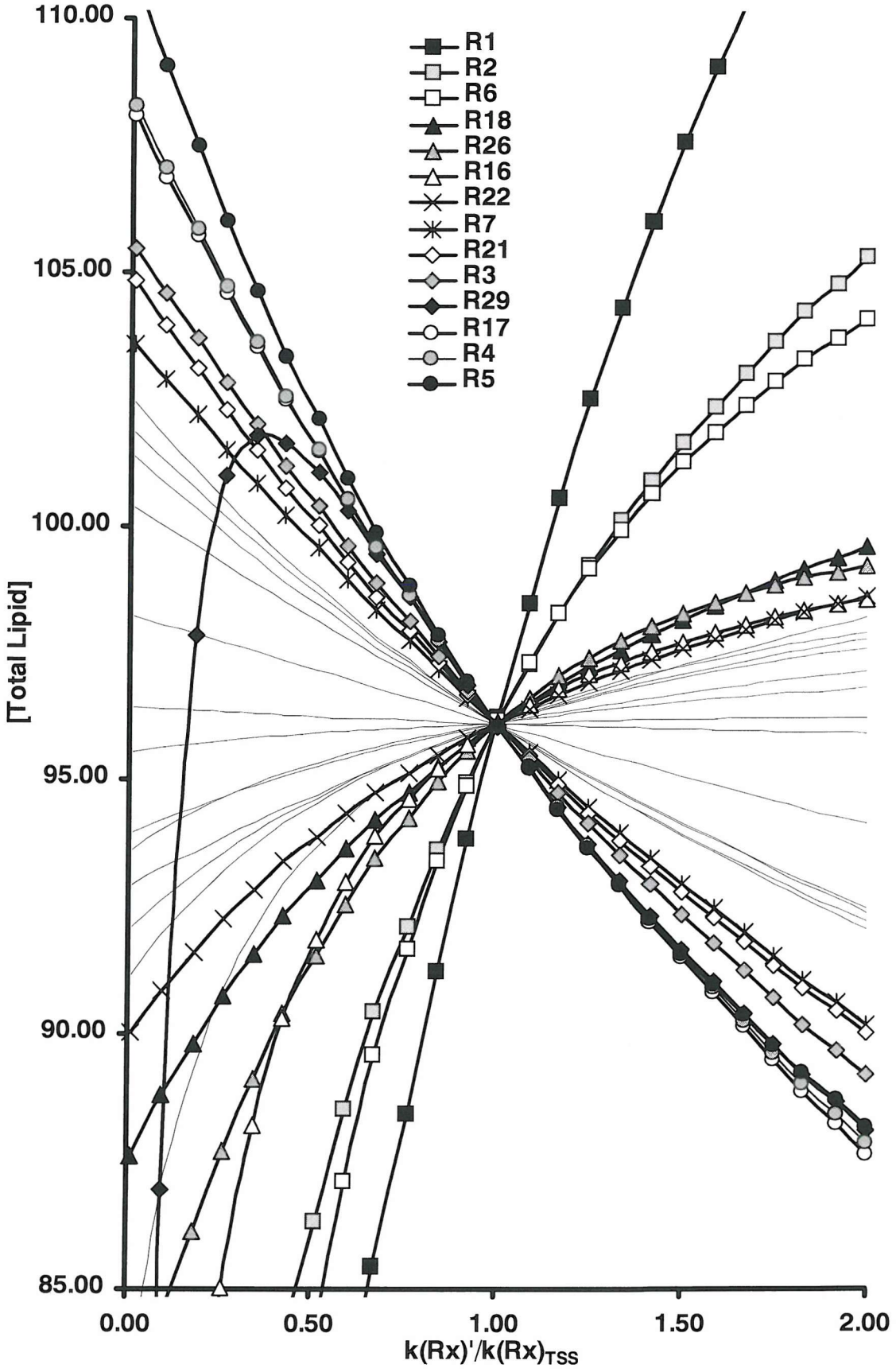

Figure 4.29: Global sensitivity analysis of the total lipid to reaction rates.
The chart is a total lipid vs. k plot for each reaction step. The purpose of these plots is to identify the reactions with the greatest effect on phospholipid accumulation. See table A3 in appendix.

C. Experimental – enzyme class sensitivity analysis

The total lipid sensitivity analysis was performed with respect to the enzyme classes defined in table 4.03. The results are shown in figure 4.30 and given as a table in table A4 in the appendix.

D. Results

CCT again displays the largest positive gradient with PLA_2 exhibiting the largest negative gradient. This is consistent with a recent review of regulation of cell membrane biosynthesis (Lykidis & Jackowski 2001) which argues that 'the molecular control points for phospholipid homeostasis reside with CCT to supply an abundance of PC molecules for increasing the membrane, and with a phospholipase for the controlled degradation that limits the number of PC molecules'.

E. Denoting total lipid behaviour

The notation described previously to summarise the effect of the rate of a step/enzyme activity on the torque parameter may be extended to indicate the effect on the total lipid (TL).

e.g. R1(λ-;TL+) to indicate R1 increases the total lipid.

The effect on the concentration of an individual metabolite may also be added.

e.g. R1(λ-;TL+;PC+) to indicate R1 acts to increase the PC concentration.

This notation is useful to summarise each feedback point when assessing multiple feedback combinations.

Analysis of the total lipid remains a side issue in this work. In contrast to the torque parameter analysis, there is little opportunity to test the results against experimental data. The investigation of total lipid is therefore limited to an examination of how the control of membrane torque tension under investigation affects the total lipid and the ability of the network to accumulate lipid. In the next section, the focus moves to look at how different feedback combinations impact on the total lipid. The usefulness of these results will be seen when looking at the implementation of multiple feedback points, and how distributed control could allow lipid accumulation to occur whilst maintaining the torque.

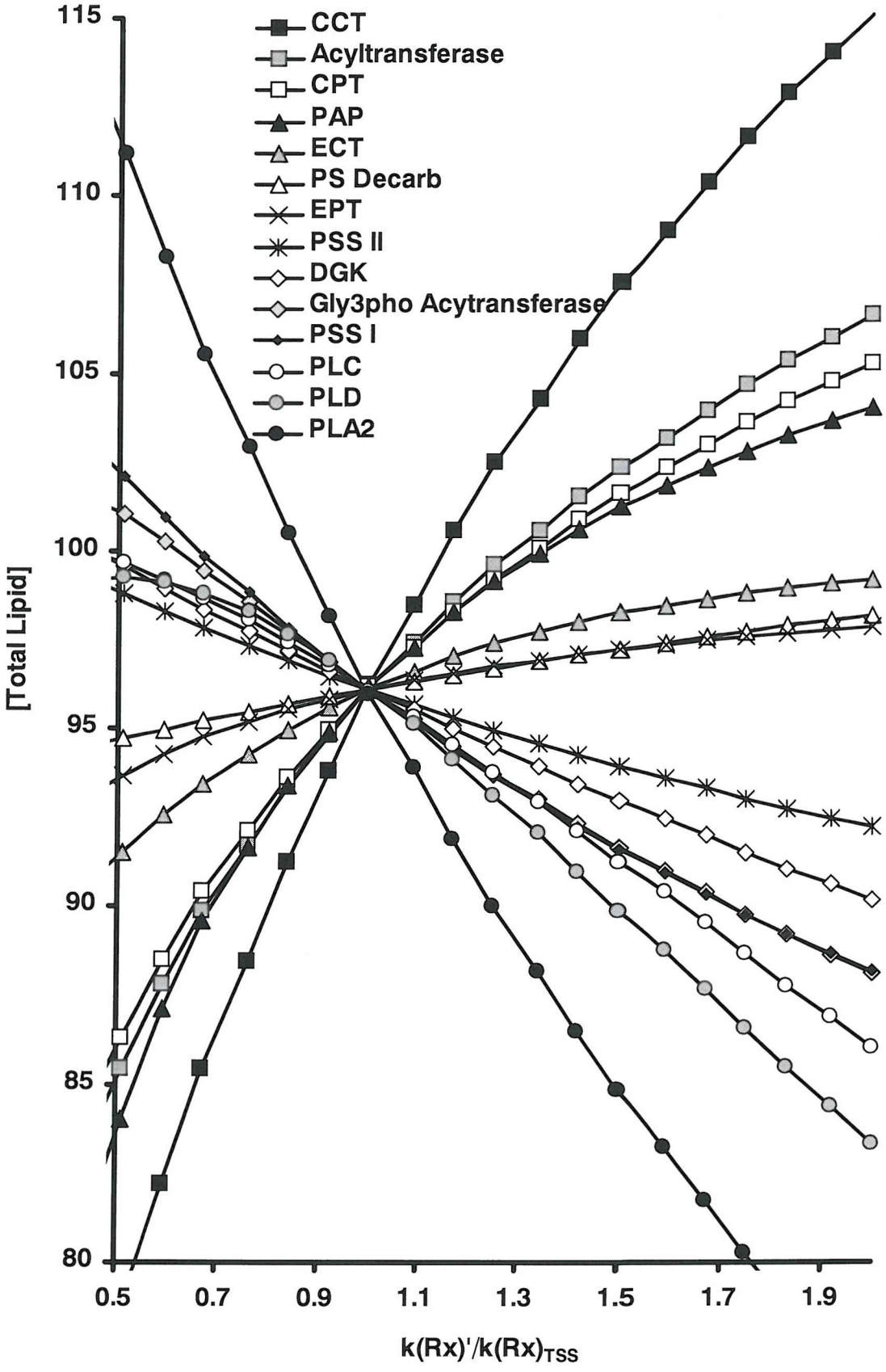

Figure 4.30: Global sensitivity analysis of total lipid to enzyme class activities
The chart is a total lipid vs. k plot for each enzyme class. The purpose of these plots is to identify the generic enzyme activities with the greatest effect on the total concentration of lipid species.

4.6.4 Effect of Feedback on Total Lipid

The question was raised in section 4.6.3 that if the reactions rates are controlled in order to maintain the stored elastic energy, is the lipid accumulation inhibited? This would be an undesirable side effect of the proposed feedback action due to the importance of lipid accumulation. As for the torque parameter, there is a need to investigate the effect on the total lipid of the implementation of feedback control points and how single and multiple point feedback affect the total lipid response.

A. Single point feedback

It has been seen that the lipid concentrations are not homeostatically controlled by the feedback. Here, the effect of feedback on the total lipid is examined. In figure 4.31 it is seen that lipid accumulation is inhibited by feedback at R1. As k(R1) is increased the feedback acts to slow the reaction. This acts to control the torque but prevents CCT being used to accumulate lipid. Any increase in the reaction coefficient is countered by a decrease in σ, controlling the flux through the reaction.

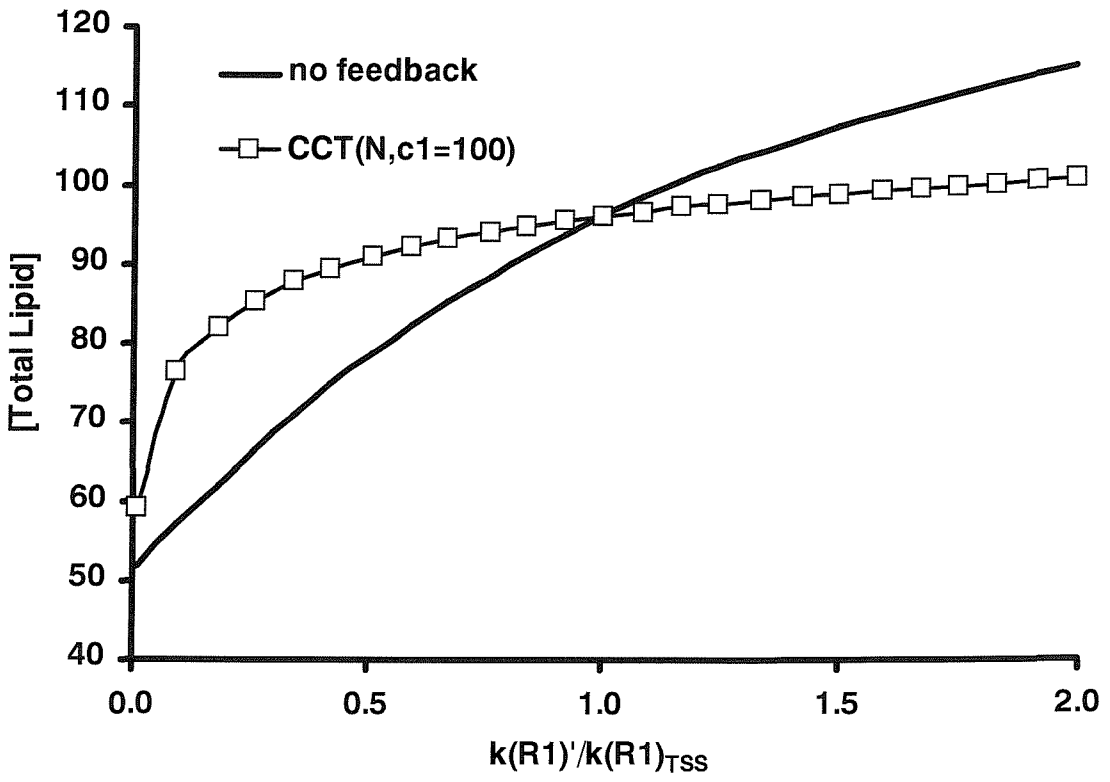

Figure 4.31: Total lipid vs. k plot to show the effect of single point feedback at CCT on the sensitivity of total lipid to k(R1). The plot shows that single-point membrane torque driven feedback at R1, acts to reduce the sensitivity of total lipid to the activity of CCT.

This may be disadvantageous since the system needs to able to accumulate lipid. One way to overcome this would be not controlling the reactions that control the total lipid. However, this would mean CCT, PLA_2 or g3pACT, should not be controlled. Reference to the literature used in the validation of the model in section 4.5 reveals that this is clearly not the case (Attard *et al.* 2000; Green & Bell 1984; Sen *et al.* 1991; Zidovetski *et al.* 1992). Another possibility is the use of multiple point feedback. Arguments for multiple feedback points providing increased robustness of the torque parameter were presented in section 4.3. Therefore, the next step is to look at the effect of multiple point feedback on the accumulation of phospholipid.

B. Multiple point feedback

The plots in figure 4.32 for a model with multiple feedback points reveal that inhibition of total lipid does not occur. If more rates are being controlled it may be expected that the ability of the system to accumulate lipid would be further suppressed. The results however, show this is not the case. Figure 4.32 compares the total lipid sensitivity for the uncontrolled network to a network with multiple feedback points. The feedback combination used in figure 4.32 (b) is the same as that used in figure 4.27: R1(N,c_1=100), R2(N,c_1=100), R29(N,c_1=100), R16(I,c_1=100), R6(I,c_1=100). In figure 4.27, a dramatic increase in the robustness of the torque parameter was seen. The model with multiple point feedback implemented in figure 4.32 (b) has total lipid sensitivity very similar to that for the network without feedback control, shown in figure 4.32 (a). Following the results for single point feedback seen in figure 4.31, where the sensitivity of the total lipid to the activity of CCT was decreased in the controlled network, this may seem rather surprising.

This prompts the question, why do multiple feedback points, whilst providing tight control of the membrane torque, allow accumulation of lipid in contrast to the results seen for single point feedback? To answer this, and to understand what is occurring, it is necessary to look in more detail at this implication of multiple point feedback. This is performed in the next section, by examining the effects of various feedback combinations on the torque parameter and the lipid concentrations, in a development of the experiment detailed in section 4.6.2.

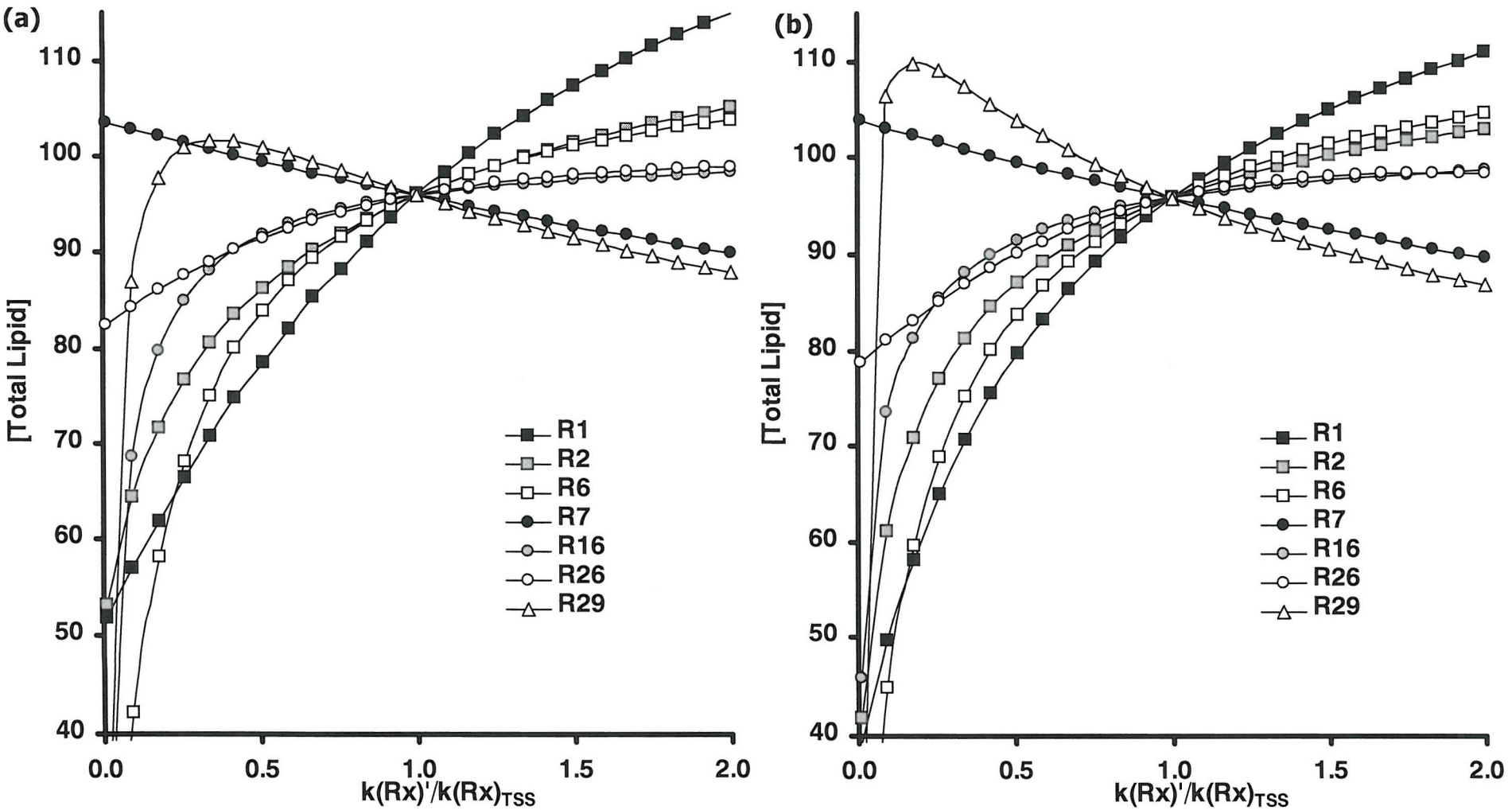

Figure 4.32: Effect of multiple point feedback on lipid accumulation.
(a) Network without feedback. **(b)** Feedback at R1(N,c_1=100), R2(N,c_1=100), R29(N,c_1=100), R16(I,c_1=100), R6(I,c_1=100) (only selected lines are shown for clarity). It is seen that the sensitivity of total lipid to the rate of the reactions is not decreased. This result contrasts with that seen for single point feedback in figure 4.31.

4.6.5 Comparison of Various Feedback Combinations

The graphs in figure 4.33 show the sensitivity of the torque parameter and the total lipid to k(R1). The results are an extension of the data presented in section 4.6.2 that looked at the torque parameter only. Here, the results include the effect on the total lipid and individual lipid concentrations to examine the contrasting effect of multiple point feedback on these properties of the system.

Figure 4.33 shows that whilst extra feedback increases robustness of λ, it decreases the stabilisation of PC (again the results simply show the sensitivity towards k(R1) to facilitate comparison). The torque parameter curves are as detailed in section 4.6.2. The addition of more feedback points leads to further stabilisation. However in contrast, examination of the individual concentrations (PC and PE shown here for illustration) reveals that these do not follow such a pattern. The additional feedback (the dual and multiple plots) can, for PC, allow a change as large as for the uncontrolled network. This is also seen for the total lipid. This result shows that multiple feedback points can allow changes in enzyme activity to cause a change in total lipid but maintain torque within a narrow range. The key to understanding this is to look at how each feedback controlled reaction responds to changes in torque and how these changes impact upon the total lipid.

With a single feedback point in the model, an example was shown in figure 4.31, it was seen that the lipid accumulation could be inhibited. Feedback at CCT prevents an increase in CCT activity from being used to increase the total lipid as the feedback acts against the increase in activity. The effect is that the increase in total lipid is inhibited. Multiple point feedback can overcome this problem. With multiple feedback points, providing distributed control, there is the possibility of more finely tuned control. Consider if feedback acts at CCT and PLA_2. These results are given by the plots labelled 'dual' in figure 4.33, the feedback combination may be described as CCT(N), PLA2(N). It is shown that this dual feedback maintains the ability of CCT to control the total lipid. This can be explained by examining the effect of the two control points on the torque and the total lipid. The effect of these enzymes may be summarised as CCT(λ-;TL+) and PLA_2(λ-;TL-). If the activity of CCT is increased, feedback will act to reduce the flux through R1, inhibiting the accumulation of lipid. However, the feedback control point at PLA_2 will reduce the

activity of PLA_2 decreasing the degradation of PC through this route. This enhances the ability of the network to accumulate lipid. The opposing effects on the total lipid help maintain the ability of the network to accumulate phospholipid.

To achieve this result a dual point feedback must be a 'suitable' combination, a suitable correlation of the effect on the torque and the total lipid. There are two possibilities. Firstly, two normal feedback points where one increases and one decreases the total lipid, as discussed for CCT and PLA_2. Alternatively, the same type of control may be provided by one normal feedback point and one inverse feedback point, where both increase the total lipid. For example CCT(λ-;*TL*+) and ACT(λ+;*TL*+).

With a larger number of control points, this correlation scenario is more likely; when the feedback acts to stabilise torque, some of the control points will act to decrease the total lipid whilst others act to increase it. For example, the feedback combination labelled 'multiple' in figure 4.33 may be described as CCT(λ-;*TL*+), PLA_2(λ-;*TL*-), g3pACT(λ-;*TL*-), PLC(λ+;*TL*-), ACT(λ+;*TL*+). This gives a good balance of opposing effects as described above and leads to a response like that for the uncontrolled network. A similar result was seen in figure 4.32 for the multiple point feedback combination used there: R1(λ-;*TL*+), R2(λ-;*TL*+), R6(λ+;*TL*+), R16(λ+;*TL*+), R29(λ-;*TL*-).

It can also be argued that feedback would positively facilitate lipid accumulation. During accumulation, the feedback control maintains the torque, which ensures the maintenance of the integrity of the bilayer. The total lipid is then easily altered, an increase in one of a number of reactions can generate extra lipid. The key difference the feedback provides is that whilst the accumulation occurs, the membrane torque and therefore the integrity will be maintained. Without feedback this sort of change in total lipid, whilst maintaining the stored elastic energy, would require a careful coordinated change in a set of rate coefficients. The integrative feedback provides this coordination of the changes in the enzyme activities. The results in figure 4.33 therefore provide another argument for distributed control, as this ability to maintain the stored elastic energy and accumulate lipid cannot be achieved without multiple feedback points. The results also show a common motif of regulation, the robustness of certain parameters but not all properties of the system (Barkai & Leibler 1997).

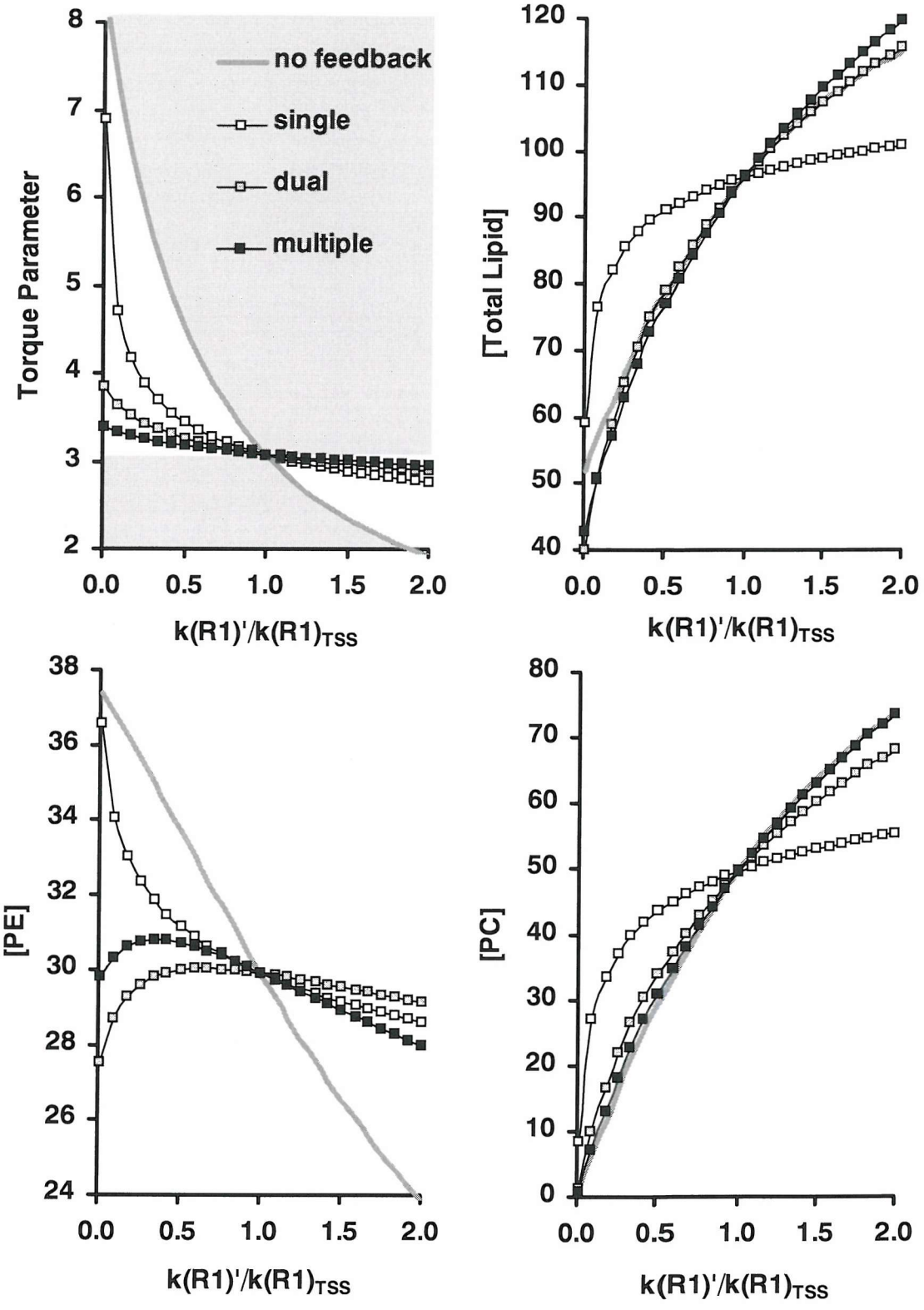

Figure 4.33: How feedback affects the torque parameter, the total lipid and the individual concentrations for different feedback configurations:
single CCT(N;c_1=100), **dual** CCT(N;c_1=100), PLA_2(N;c_1=100),
multiple CCT(N;c_1=100), PLA_2(N;c_1=100), g3pACT(N;c_1=100), PLC(I;c_1=100), ACT(I;c_1=100).
Addition of feedback at multiple points progressively stabilises the torque parameter.
No such pattern is seen for the concentration plots. A key result is that the 'multiple point' plots show a similar sensitivity of concentrations (both individual and total) to those seen for the uncontrolled network.

4.6.6 Simulating the Addition of Anti Tumour Lipid

Implementation of feedback allowed preliminary experiments with the modelling of ATLs. The expression for λ is modified to include a coefficient for the ATL:

$$\lambda = \frac{a_1[\mathrm{PE}] + a_2[\mathrm{DAG}] + a_3[\mathrm{PA}] + a_4[\mathrm{FA}]}{b_1[\mathrm{PC}] + b_2[\mathrm{PS}] + b_3[\mathrm{LPA}] + b_4[\mathrm{LPC}] + b_5[\mathrm{LPE}] + b_6[\mathrm{LPS}] + b_7[\mathbf{ATL}]}$$

In the plot in figure 4.34, it is seen that upon addition of ATL (at t = 2) the torque parameter drops and the feedback control causes PC to decrease. In addition, PE increases as reported experimentally (Zhou & Arthur 1995). These changes help restore the torque parameter, as shown in the plot.

Addition of ATLs was not investigated further. It was an area of initial interest because of links to synthetic work on ether lipids. However, the results of sensitivity analysis proved the more successful, particularly for the validation of the model. In the future, the model may be used to explain what happens in more detail on addition of ATLs etc, including total lipid changes. This could include addressing the difference between small and large doses (the model doesn't explain this yet). This will require more carefully chosen and fully optimised set of feedback loops (i.e. the relationship between σ and λ. For example, a different treatment of the relationship between σ and λ for translocating and trans-membrane proteins since they represent very different physical processes of activation).

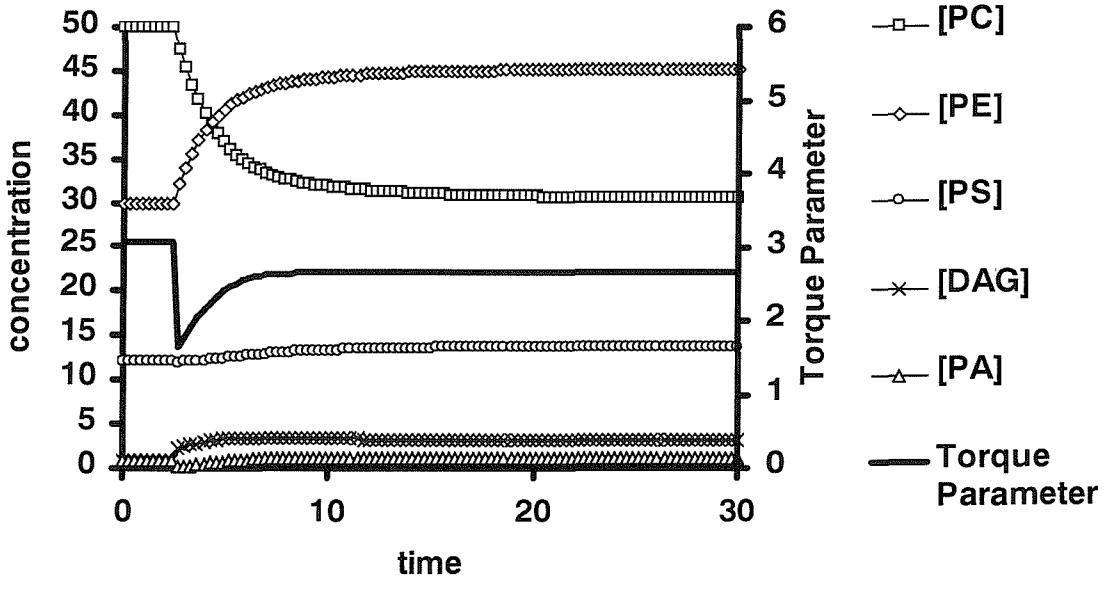

Figure 4.34: The effect of the addition of ATL. ATL concentration of 2, coefficient in λ, b_7 = 250. Feedback at R1(N,c_1=100), R2(N,c_1=100), R29(N,c_1=100), R16(I,c_1=100), R6(I,c_1=100).

4.6.7 Rationalisation of Candidates for Feedback Control

Can the feedback points be predicted by inspection of the stoichiometric network? Several possibilities were considered. Does a reaction inter-convert lipid types? This is the simple analysis of substrate and product and so ignores the position in the pathway. It is important to reiterate that it cannot account for the behaviour of CCT, which has a non-membrane substrate and product. However, it can still be useful to mark the lipid types on the model to help identify the position of the key reactions and the lipid boundaries. This analysis is shown in figure 4.35, showing 'lipid type boundaries'. R6 does not cross a lipid boundary but is essential for the synthesis of PC; this is also shown in figure 4.35. This raises the concept of essential reactions: a reaction that is part of a critical chain that, for example, synthesises PC, or supplies a key metabolite. This is a consideration of the role of a reaction within the pathway. In a similar vein, the flux through reaction and the supply of substrate and product may be important. A reaction could be less important if it has a small flux as a link in one of many branches, so this relates to the concept of essential reactions.

None of the criteria detailed above provide the whole answer. Initially attempts were made to explain predicted feedback candidates using the 'lipid type boundaries'. There is general correlation. However, R6 and crucially R1 do not convert lipid types. Results have shown the situation can be less straightforward than the simple substrate and product analysis. The results seen from the model are a combination of all of the above effects. It is possible to comment on a reaction being a source reaction or a crucial step towards the synthesis of PC etc. These factors can be used to construct and discuss subsystem models (e.g. figure 4.17), however it is necessary to use results from the full simulation since the torque is a system property. Local arguments do not always work. Therefore, there is a need to understand the system. For example, a small concentration change in a highly type II lipid may effect the MTT more than the local change at the reaction being altered. The model facilitates sensitivity analysis of system properties but this has its limitations. For example, it has been shown that the concentrations are not necessarily stabilised by the feedback. To fully understand the effect of the reactions on the torque, it is necessary to investigate the changes occurring in the concentrations. This analysis is used now to look at CCT and ECT, enzymes for which there are extensive experimental studies on lipid dependence, showing an interesting and marked difference in behaviour.

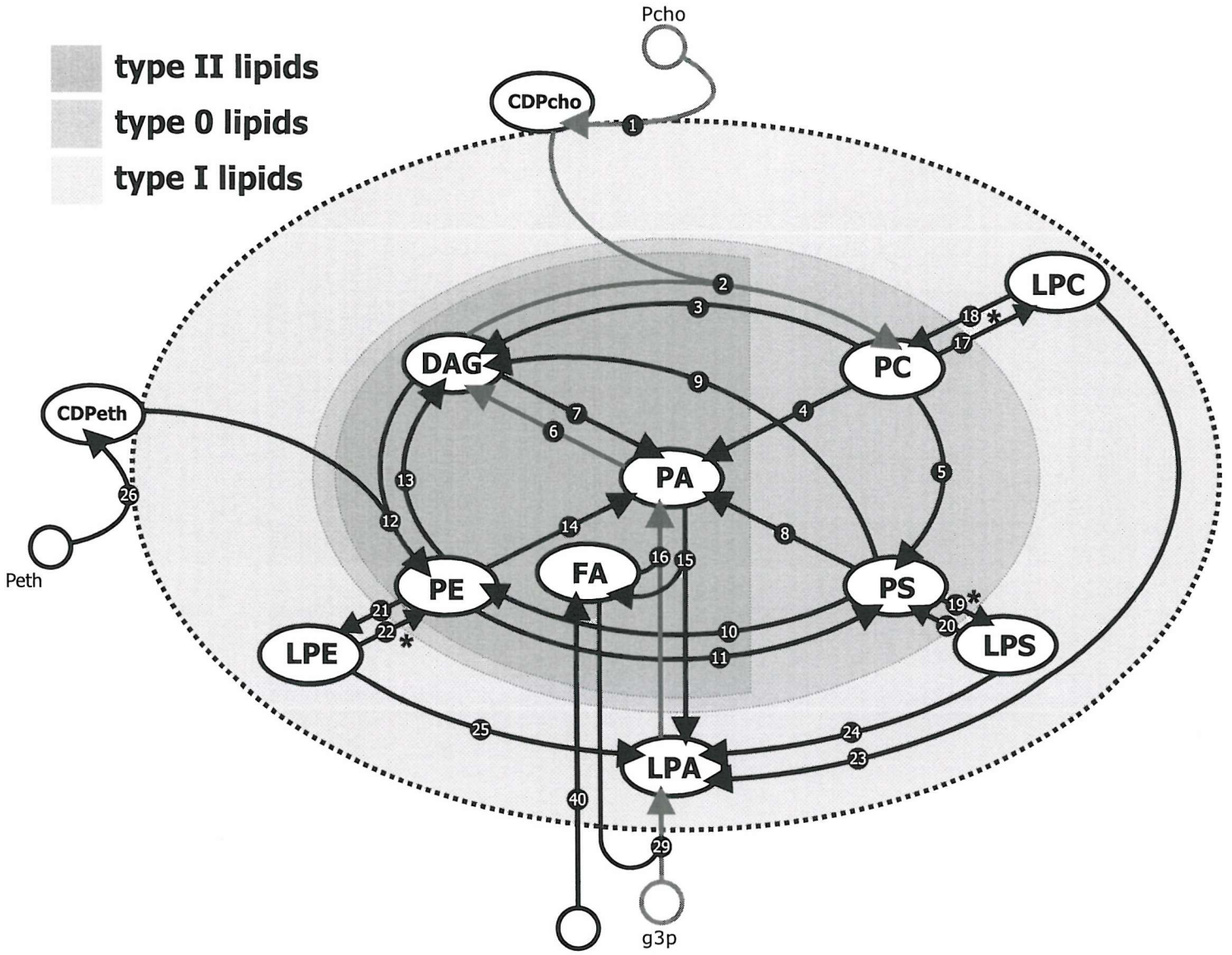

R1 Pcho -> CDPcho
R2 CDPcho + DAG -> PC
R3 PC -> DAG
R4 PC -> PA
R5 PC -> PS
R6 PA -> DAG
R7 DAG -> PA
R8 PS -> PA
R9 PS -> DAG
R10 PS -> PE
R11 PE -> PS
R12 CDPeth + DAG -> PE
R13 PE -> DAG
R14 PE -> PA
R15 PA -> LPA + FA
R16 LPA + FA -> PA
R17 PC -> LPC + FA
R18 LPC + FA -> PC
R19 PS -> LPS + FA
R20 LPS + FA -> PS
R21 PE -> LPE + FA
R22 LPE + FA -> PE
R23 LPC -> LPA
R24 LPS -> LPA
R25 LPE -> LPA
R26 PETH -> CDPeth
R27 CDPeth ->
R28 CDPcho ->
R29 GLYC + FA -> LPA
R30 DAG ->
R31 PC ->
R32 PA ->
R33 PE ->
R34 PS ->
R35 LPA ->
R36 LPS ->
R37 LPC ->
R38 LPE ->
R39 FA ->
R40 -> FA

Figure 4.35: Stoichiometric Network 3 (StN3) with shading of 'lipid boundaries'.
The shading emphasizes the reactions that perform a conversion between lipids which favour different spontaneous curvature.

4.7 Key Result 1: CCT is a Key Control Point

The discussion now moves from the global analysis of the reactions of the network to focus in more detail on CCT. Identification that CCT activity correlates with the membrane torque tension (Attard *et al.* 2000) was the result that prompted the construction of the model to investigate the implications of the homeostasis of torque tension. Furthermore, the global sensitivity analysis from the model has identified CCT as an enzyme that has significant control over both the torque parameter and the total concentration of lipid species. The analysis in this section will look at this in more detail in order to explain these results.

As shown in sections 4.3.4 and 4.4.3, the torque parameter sensitivity analysis reveals the effect of the enzymes in the pathway on the torque tension and provides a method for predicting the feedback type that would stabilise the MTT. For example, CCT is shown to have a strong effect on λ and is identified as a strong candidate for normal feedback. This result however, does not show *why* CCT has a strong effect on the torque tension. To investigate this requires a further analysis of the function of CCT, and its effect on the pathway to provide an understanding of how the reaction affects the system, its fluxes and concentrations. In this section, the role of CCT in the network will be looked at in detail. This process will identify why CCT has control over the concentration of PC, the total lipid and the torque parameter.

4.7.1 The 'CCT-CPT Pair' as a Subsystem Model

To look at the effect of CCT on the reaction network, it is instructive to concentrate on the local changes, rather than the whole network, as a first step. An important point to note about the reaction mediated by CCT is that its substrates and products are all are non-membrane species. The effect of CCT activity on the stored elastic energy cannot therefore be rationalised, using the basic substrate and product analysis, by considering the reaction in isolation. This further illustrates the point, made in section 4.6.7, concerning how a reaction must be examined in terms of its function within the network, in addition to its local properties. To assist in this, a suitable subsystem model can be described. This is done to focus on and test which changes are important for the effect being examined; here this is the control CCT exerts on the torque tension and the concentration of PC.

Choline phosphotransferase (CPT) is the enzyme that mediates R2, the reaction of DAG with CDPcho to form PC. This involves the conversion of the strongly type II lipid DAG to the major component of cell membranes, type 0 PC. This conversion would therefore be expected to act to significantly reduce the stored elastic energy, as shown in the sensitivity analysis plots in section 4.4. Another key point is that the other substrate of R2 is CDPcho, the product of the reaction mediated by CCT. CDPcho therefore forms a direct link between the CPT and the CCT reactions.

As has been stated, neither the product nor the substrate of the CCT reaction is a membrane species. Therefore, considered in isolation, the reaction has no impact on the torque tension. The smallest section of the model that may be used to explain the changes occurring is therefore a two-reaction combination. To examine how CCT controls the production of PC, the reactions catalysed by CCT and CPT must be examined together using a sub-system model. The CPT reaction is chosen because it is directly coupled to the reaction mediated by CCT, and the CPT reaction itself exerts a large effect on the torque. This subsystem model will be referred to as the *'CCT-CPT pair'**. The reactions are shown together in figure 4.36.

* *It is important to note here that using a subsystem model may overlook significant changes occurring elsewhere in the network (this point will be returned to in the examination of a different subsystem model in section 4.8). For this reason, the CCT-CPT pair subsystem model is used here simply to explain the results presented, which are generated from the full model. In this way, the validity of the subsystem model can be assessed (The subsystem model is considered valid, for a particular result, if it can be used to successfully explain that result).*

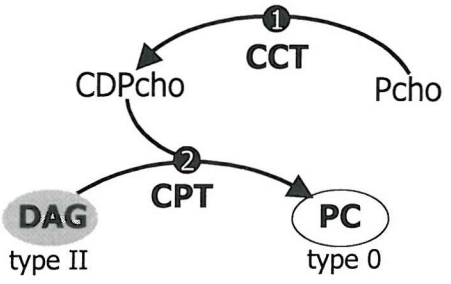

Figure 4.36: The 'CCT-CPT pair', a subsystem model to examine the action of CCT.
The two reactions must be considered together since CCT isolated would have no effect on the lipid concentrations, and therefore would not impact on the torque tension.

4.7.2 Analysis of the Effect of the Activity of CCT and CPT

The sensitivity analysis of the system showed that CPT has a large effect on λ. This can be rationalised by examining its substrate and product. Understanding the effect of CCT on the torque becomes a problem of explaining why it has a larger effect than CPT. The answer lies in understanding that CCT exerts control over (acts as the 'rate-determining step' for) the change mediated by CPT.

In order to investigate the behaviour of CCT and CPT, sensitivity analysis experiments were run in which the rate coefficient for the CCT and CPT reactions were swept whilst the flux, J(Rx), and the product for each reaction were monitored. Following these parameters, rather than simply the torque parameter provides more information on the changes that occur in the system. The sensitivity of J(R2) to the values of k(R1) and k(R2) are followed to show the effect of the activities of CCT and CPT on the rate of conversion of DAG to PC. Examination of the concentrations reveals the relative effects of CCT and CPT on the concentrations of DAG and PC. The results of the experiments to look at the fluxes and concentrations are shown in figure 4.38 and figure 4.39 (p.4.94-p.4.95).

Before discussing the plots, it is necessary to consider what determines the flux through a reaction. The flux through Rx is a product of the reaction coefficient k(Rx) and the concentration of each substrate, as described in equation 4.02 where J(Rx) is the flux through Rx, k(Rx) is the rate coefficient and S_i is the concentration of substrate i.

$$J(Rx) = k(Rx).\prod_i S_i \qquad \text{equation 4.02}$$

The plots for the change in k(R2) (activity of CPT) are shown in figure 4.38. As k(R2) is increased, it is seen that J(R2) increases and the concentration of PC rises. However whilst k(R2) is doubled, J(R2) rises by only around 25%. The flux through R2 is limited by the depletion of CDPcho (and DAG the other substrate of R2, not shown).

The plots for the change in k(R1) (activity of CCT) are shown in figure 4.39. The plots for k(R2) are also repeated for comparison. Here it should be noted that the flux through R1, J(R1) rises proportionally to k(R1). This occurs because the

concentration of the substrate of R1, Pcho, is fixed. The increased flux increases the concentration of CDPcho. This in turn increases the flux through R2, the reaction mediated by CPT, and results in increased PC (and decreased DAG, not shown). The plots show that J(R2) and the concentration of PC are indeed more sensitive to k(R1) than k(R2). This shows that control of the reaction mediated by CPT lies to a large degree with the activity of CCT and reveals why CCT has a large effect on the torque parameter.

4.7.3 The Role of Source Reactions

The key to control lying with CCT is the fixed concentration of Pcho. As described in the development of the model, Pcho is present in relatively high concentrations in a pool external to the membrane. The clamping in the model therefore reflects the real system. CCT exerts control on the torque because it is an entry reaction and is closely coupled to, and controls, a reaction that has a significant effect on λ. Both the CCT and CPT reactions are also high flux reactions that act to increase the total lipid.

The CCT reaction is not the only entry point in the model. The source reactions are highlighted in figure 4.37, which shows the position of R1 and also R29. R29, the reaction mediated by g3pACT, was also shown, in section 4.4, to have a strong effect on the torque. To some extent, this response will be reduced, since R29 has one fixed concentration substrate and one lipid substrate FA that is modelled as a variable metabolite. Earlier it was discussed how FA exerts flux control as a 'plurifunctional cofactor' (see chapter 2 and 3 and Morowitz *et al.* 1964).

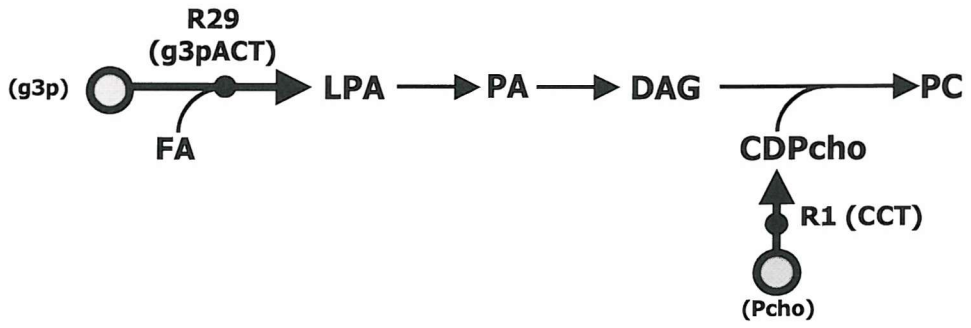

Figure 4.37: The importance of source reactions: location of two of the important control reactions. Both g3pACT and CCT mediate entry reactions to the model and use substrates with fixed concentrations.

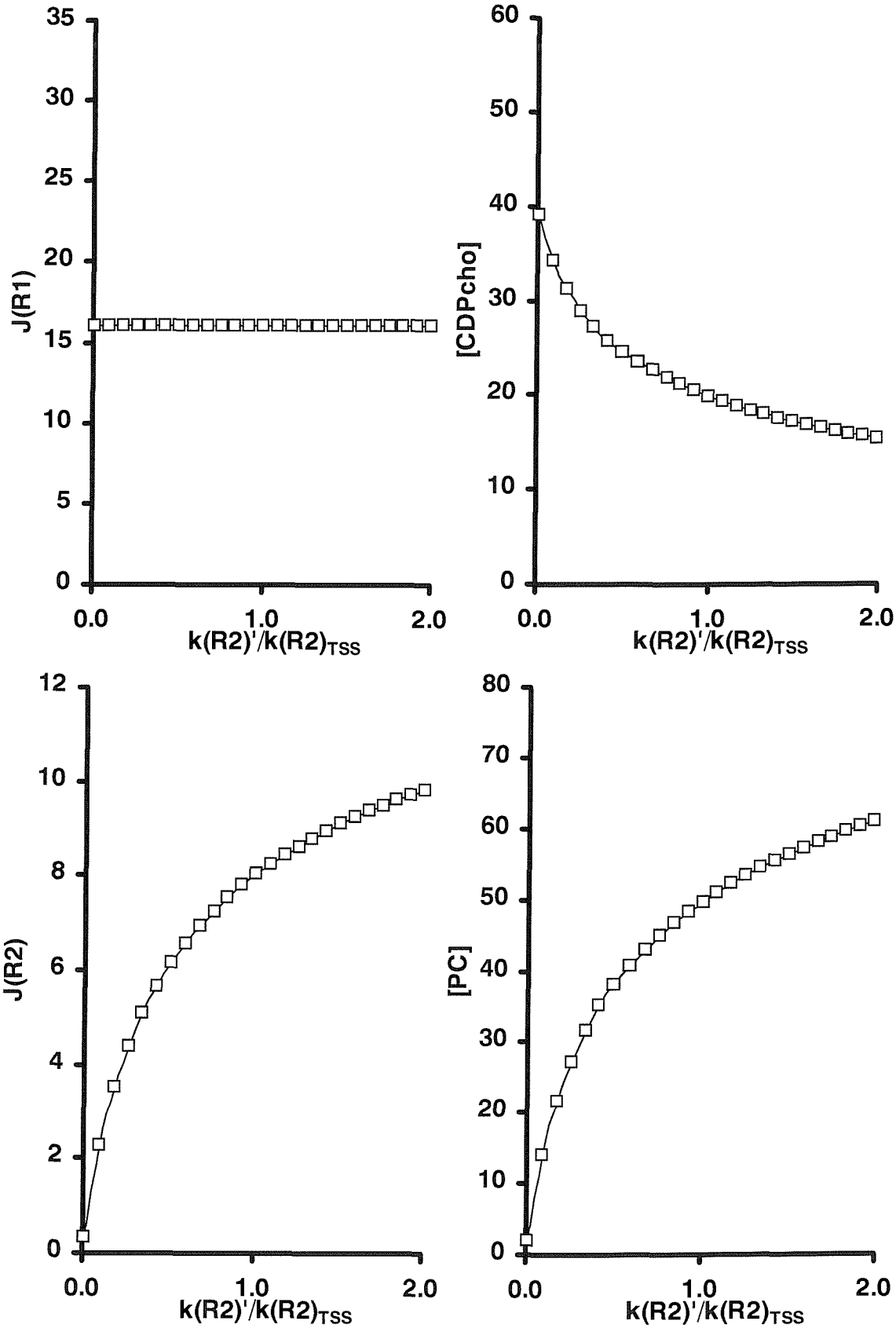

Figure 4.38: Effect of CPT activity upon the fluxes and products of R1 and R2.
The plots show how J(R1), J(R2) and the products of R1 and R2, CDPcho and PC, change as k(R2) is altered.

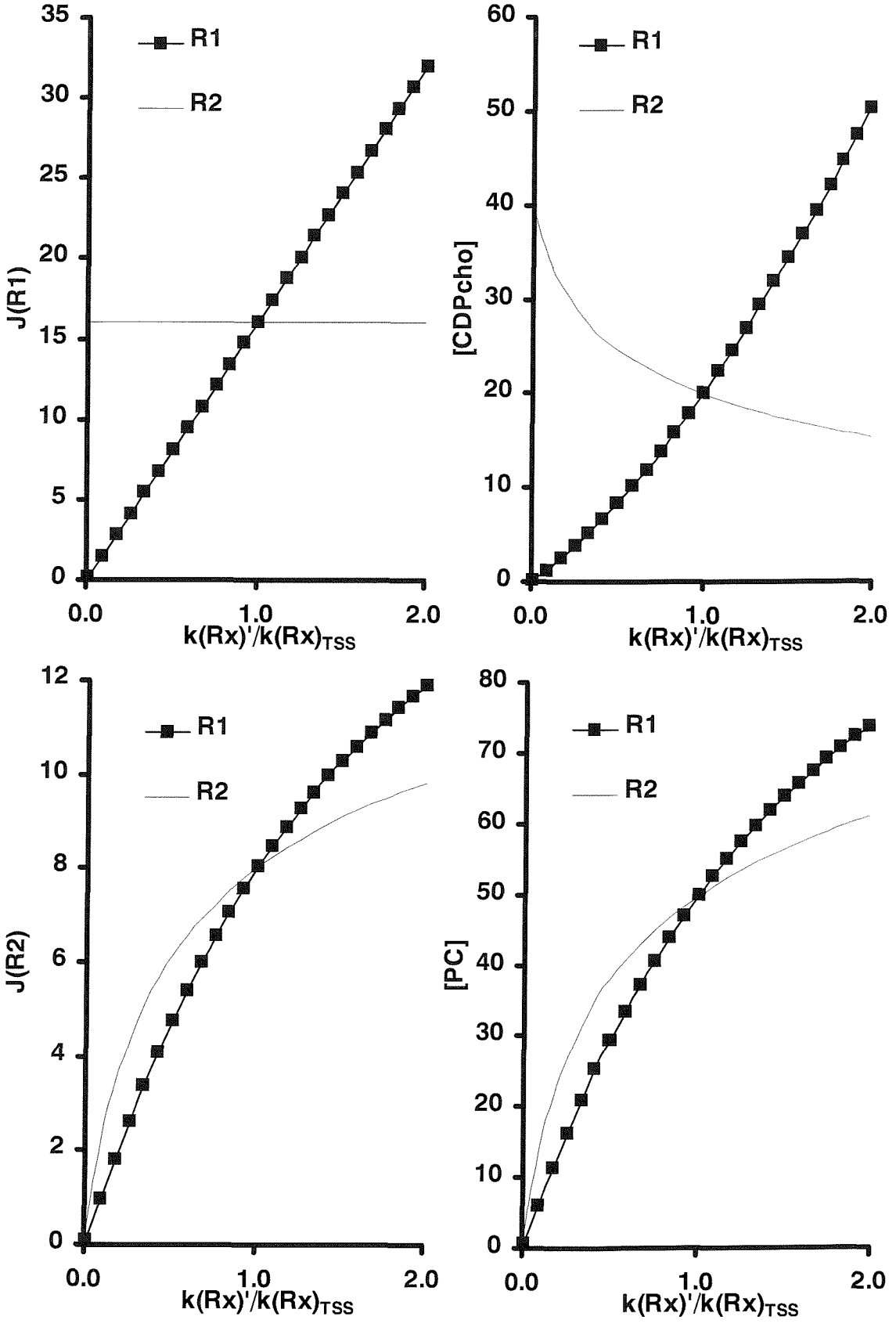

Figure 4.39: Effect of CCT activity upon the fluxes and products of R1 and R2.
The plots show how J(R1), J(R2) and the products of R1 and R2, CDPcho and PC, change as k(R1) is altered The plots for k(R2) are repeated for comparison. It is seen that PC concentration is more sensitive to the activity of CCT, than to the activity of CPT. This is due to the ability of CCT to provide CDPcho.

4.8 Key Result 2: Predict Feedback for CCT but not ECT

The analysis now moves to examine ethanolamine cytidylyltransferase (ECT). ECT catalyses the conversion of Peth to CDPeth: this is an analogous pathway to that for CCT, so common regulation of these enzymes might be expected. The sensitivity analysis predicted the system could be stabilised by inverse feedback at ECT. However, experiments show ECT activity is not affected by lipids (Vermuelen *et al.* 1993).

It will be shown that, compared to the subsystem model used for CCT, a larger ensemble of reactions must be considered to understand the effect of ECT on the torque parameter. Although the situation is rather more complex, the type of analysis presented previously for CCT may be extended. The analysis will also highlight the potential problems that can arise when considering isolated parts of the model, and the importance of carefully selecting and validating the subsystem model used.

4.8.1 Similarity of CCT and ECT

The CDP-choline and CDP-ethanolamine pathways are analogous pathways. The steps that precede the cytidylyltransferase step in each pathway (not included in model) are catalysed by one enzyme, choline/ethanolamine kinase. It has also been found that there are phosphotransferase enzymes which act on CDPcho *and* CDPeth (CEPT) (Henneberry & McMaster 1999). The specificity that allows independent control is therefore associated with the cytidylyltransferase step. The catalytic domain of ECT has significant similarities to the conserved domain of yeast and rat CCT, but ECT shows pronounced specificity for Peth (Bladergroen & Van Golde 1997).

CCT and ECT are important because in each pathway the synthesis of PC / PE is controlled through the cytidylyltransferase step. Compared with the literature on CCT and despite the fact that ECT was discovered at the same time, there is much less information on the control of the CDP-ethanolamine pathway (Vance 1996). However, under most conditions, ECT contributes significantly to the overall regulation of the CDP-ethanolamine pathway (Bladergroen & Van Golde 1997; Vermuelen *et al.* 1993). ECT, like CCT, is thought to exhibit a bimodal distribution between the RER and cytosolic space, suggesting a reversible interaction with the RER to bring ECT into close proximity to EPT (Bladergroen & Van Golde 1997).

4.8.2 CCT and ECT are under Independent Control

Based on the analogy of the CDP-choline and CDP-ethanolamine pathways it was initially thought that the regulation of PC and PE biosynthesis would be similar. It has however been shown that the pathways are under independent metabolic control. ECT displays no requirement for lipid and furthermore, ECT activity is not affected by the presence of various phospholipid preparations (Vermuelen *et al.* 1993). Crucially ECT lacks the membrane-binding domain seen in CCT (Dunne *et al.* 1996) and binding does not affect the activity of ECT. However, ECT does associate with the RER; it is thought that this may be necessary for metabolic channelling of PE synthesis, although this is difficult to prove experimentally (Bladergroen & Van Golde 1997).

In summary, studies have shown that CCT and ECT are functionally distinct enzymes as demonstrated by four key pieces of evidence (i) CCT and ECT are coded by different genes. (ii) There is no cross activity of ECT and CCT. (iii) The sub-cellular localisation of ECT and CCT is distinct. (iv) ECT, in contrast with CCT, is not markedly affected by exogenous lipids (Bladergroen & Van Golde 1997).

4.8.3 Treatment of CCT and ECT in the Model

In the model, CCT and ECT are treated the same, with equal kinetic constants and equal flux through CPT and EPT (in reality there may be more flux through CPT, however the solving of the model coefficients, using the equal flux branching assumption, results in equal treatment). Both are entry points to the model and have inexhaustible substrates. In addition, simulations were run with different ratios of PC and PE to eliminate factors resulting from the concentration differences. These features help ensure any differences do not occur as a result of the construction of the model, but stem from the structure of the network and the distribution of lipid types.

The equivalence of the modelling of CCT and ECT may be seen by examining the symmetry in the network. Looking at CCT and ECT in figure 4.22, a local symmetry about DAG may be noticed. If the layout of the model is modified, the high degree of global symmetry of the stoichiometric network can be more easily seen. The rearrangement requires the network to be set out in 3D; a projection of this is shown in figure 4.41, depicting the approximate mirror plane of symmetry through PS and DAG (strictly, the symmetry is valid only if the stoichiometric network is considered

as a network of reactions, ignoring the different lipid species). This representation clearly shows the similarities between the CDP-ethanolamine and CDP-choline pathways. CCT and ECT occupy equivalent positions with respect to the plane of symmetry and provide substrates for reactions that convert DAG to PC and PE respectively, species that also occupy equivalent positions on either side of the symmetry plane. Considering the similarities, the analysis of the behaviour of ECT was begun by considering ECT in the same way as for CCT, by the construction of a corresponding subsystem model.

4.8.4 The ECT-EPT Pair

Due to the similarities of CCT and ECT the first attempt to build a subsystem model for ECT was based on the CCT-CPT pair. The 'ECT-EPT pair' is shown in figure 4.40. In the figure, it can be seen that an increase in the activity of ECT will result in higher flux through R12. This conversion of DAG to PE would be expected to lead to a reduction in the torque parameter, since PE is less type II than DAG. The use of the ECT-EPT pair therefore leads to the conclusion that the stored elastic energy could be stabilised by normal type feedback acting on ECT. However, the sensitivity analysis using the full model showed that an increase in the activity of ECT causes an *increase* in the torque parameter (this result is repeated in figure 4.42 overleaf). Clearly, the ECT-EPT pair proves inadequate. It was therefore necessary to look in more detail at results from the model, both to explain the effect of ECT on the system and to construct a more successful subsystem model. The next section starts by reviewing the results of the sensitivity analysis for CCT and ECT.

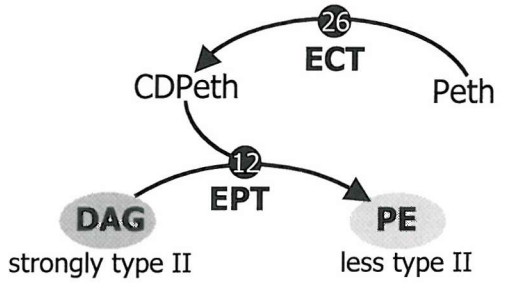

Figure 4.40: The 'ECT-EPT pair', a subsystem model to examine the action of ECT.
The two reactions must be considered together, as for the CCT-CPT pair, since ECT isolated would have no effect on the lipid concentrations, and therefore would not impact on the torque tension. This subsystem model however proves inadequate to explain the effect of ECT on the torque tension as it suggests ECT would lead to a reduction in the torque parameter, as discussed in the main text.

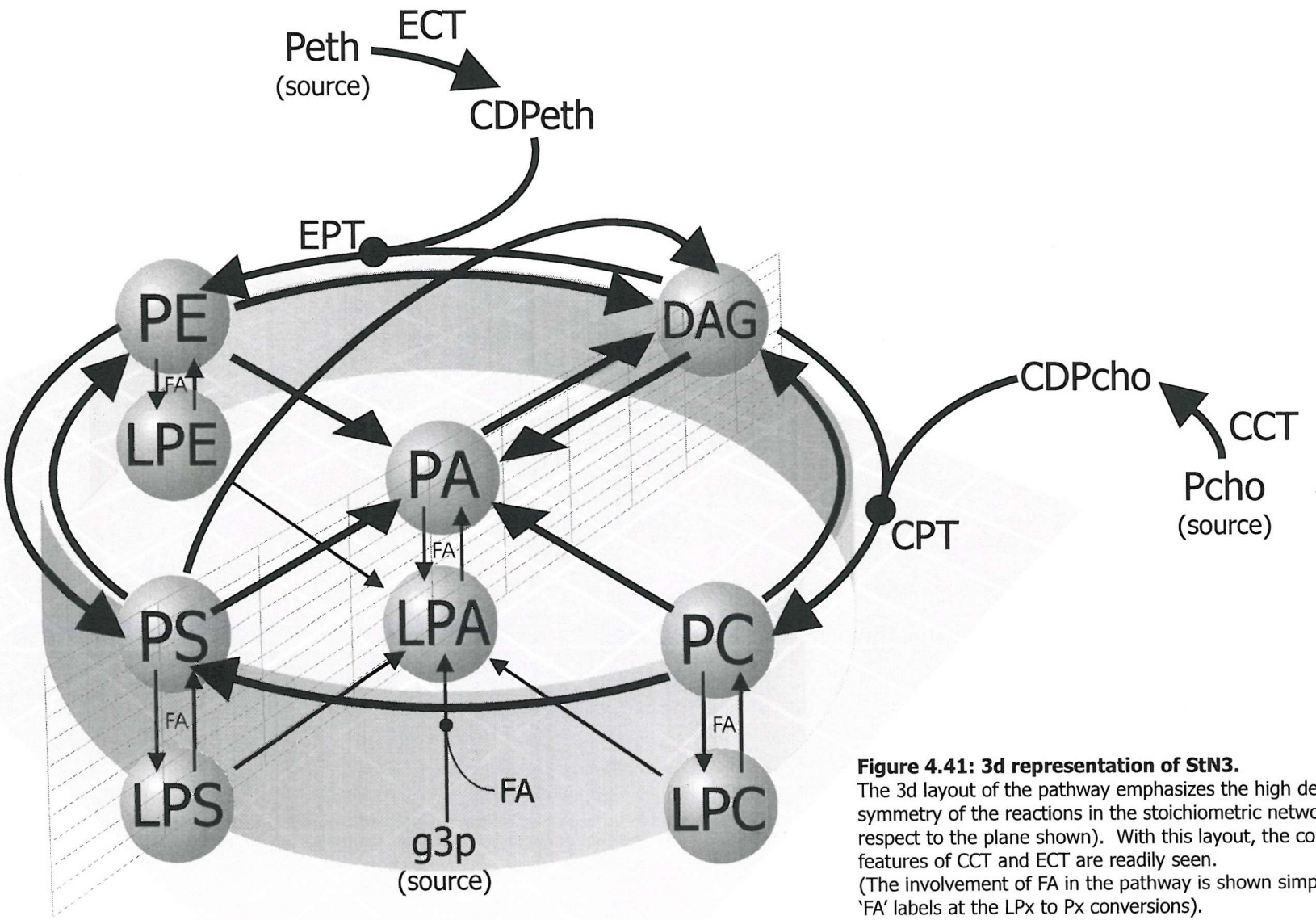

Figure 4.41: 3d representation of StN3.
The 3d layout of the pathway emphasizes the high degree of symmetry of the reactions in the stoichiometric network (with respect to the plane shown). With this layout, the common features of CCT and ECT are readily seen.
(The involvement of FA in the pathway is shown simply by the 'FA' labels at the LPx to Px conversions).

4.8.5 Sensitivity Results for ECT: Prediction of Inverse Control

Figure 4.42 shows that the model predicts that ECT will act to increase the torque parameter. This leads to the prediction that the stored elastic energy should be stabilised by inverse feedback at ECT. However, experimental results show ECT to be insensitive to the stored elastic energy in a membrane. In addition, the prediction of inverse control is counter-intuitive as was seen with the ECT-EPT pair. The conversion of DAG to PE, which is less type II, would always lead to a decrease of stored elastic energy and so λ would be stabilised by normal feedback. This therefore leads to the conclusion that the increase in stored elastic energy, observed upon a change in the activity of ECT, is the result of some other change in the reaction network caused by the action of ECT. This would explain why analysis of the ECT-EPT pair subsystem proves insufficient to understand the changes occurring. Justification of this required further investigation of (i) the effects of implementation feedback at ECT and (ii) the variation of the sensitivity of the torque parameter to the activity of ECT. These two analyses follow and are then explained, providing evidence ECT is not a candidate for feedback control.

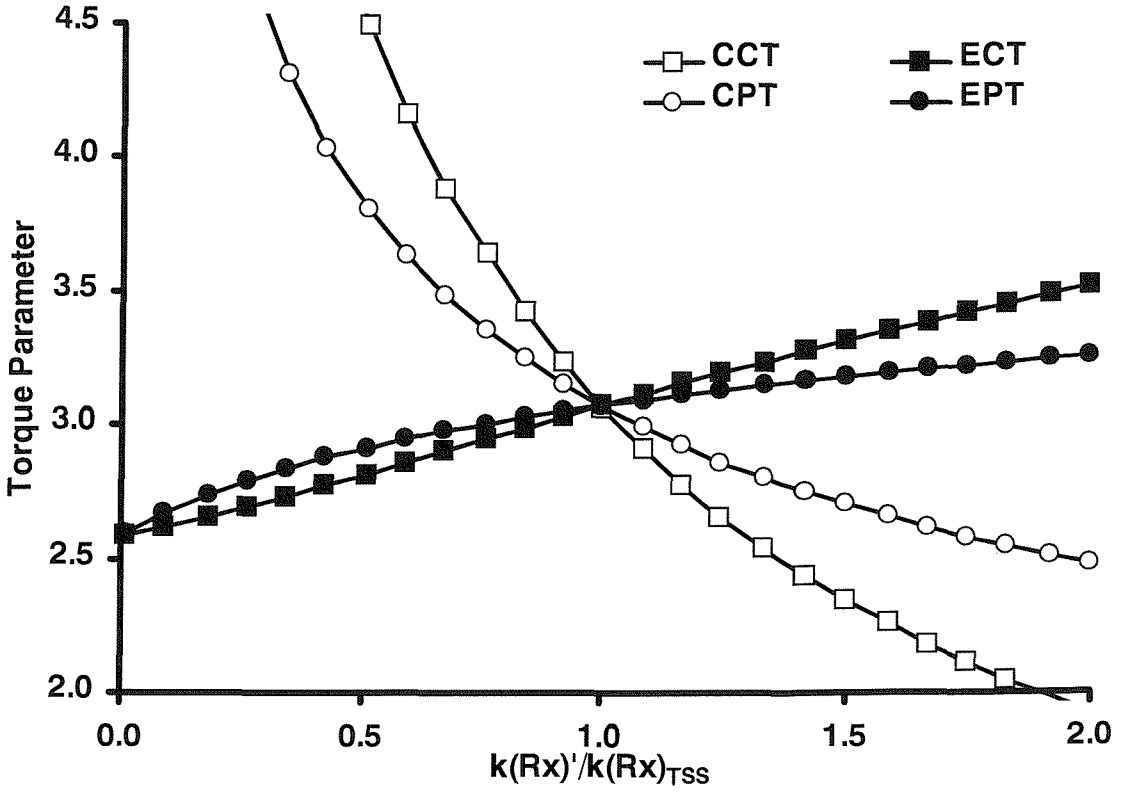

Figure 4.42: Sensitivity analysis of the torque parameter to CCT, CPT, ECT and EPT. The plots are repeated from the global sensitivity analysis in figure 4.19 to illustrate that the initial prediction of feedback at ECT is for inverse control (due to the positive gradient).

4.8.6 Effect of Feedback at ECT

Figure 4.43 shows how normal feedback at (a) CCT and (b) ECT affect the stability of the torque parameter. Normal feedback at CCT clearly stabilises the torque parameter relative to the uncontrolled model. Normal feedback at ECT is however not stabilising, in fact it is destabilising. This is as expected, since the model predicts inverse feedback will stabilise the torque parameter. However, the effect of inverse feedback is shown in figure 4.43 (c) and is not the simple stabilisation plot that would be expected. The plot passes through the shaded region and the discontinuity represents a regime where the system is unable to settle on a steady state and oscillates between states. The effect that ECT has on the system appears to prevent either type of feedback at ECT from providing stabilisation. This is consistent with literature reports that ECT not affected by lipid. In the final plot, in (d), both types of feedback at ECT are added to a system with normal feedback at CCT. Here the stabilisation of CCT prevents the conditions changing dramatically and destabilisation is not seen. However, neither type of feedback at ECT confers further stability on the system.

This was the first time it was noted for a reaction that neither type of feedback stabilised the torque parameter over the range used. Since the sensitivity plot for ECT showed an increase in ECT activity caused an increase in λ it had been expected that inverse feedback at ECT would stabilise the system. Inverse feedback at ECT does provide stabilisation over a certain range but causes destabilisation in other regimes. The initial conclusion drawn was that as the steady state changes (as the reaction coefficient is changed) the feedback changes from stabilising to non-stabilising. This type of behaviour was not observed previously when feedback was added at candidates for feedback. These results for ECT led to the first ideas about the possibility of varying behaviour, that the influence on the torque could change as the system changes, and was the initial reason for varying the conditions. In section 4.4.8, it was shown that the key control points selected, including CCT, did not show variation. The effect of these reactions on the torque parameter was not dependent on the arbitrarily set conditions of flux distribution or concentration. In the next section, it will be shown that the influence of ECT upon the torque parameter can vary dramatically, and a model will be presented to explain how this can occur, by comparing and contrasting the action of CCT and ECT.

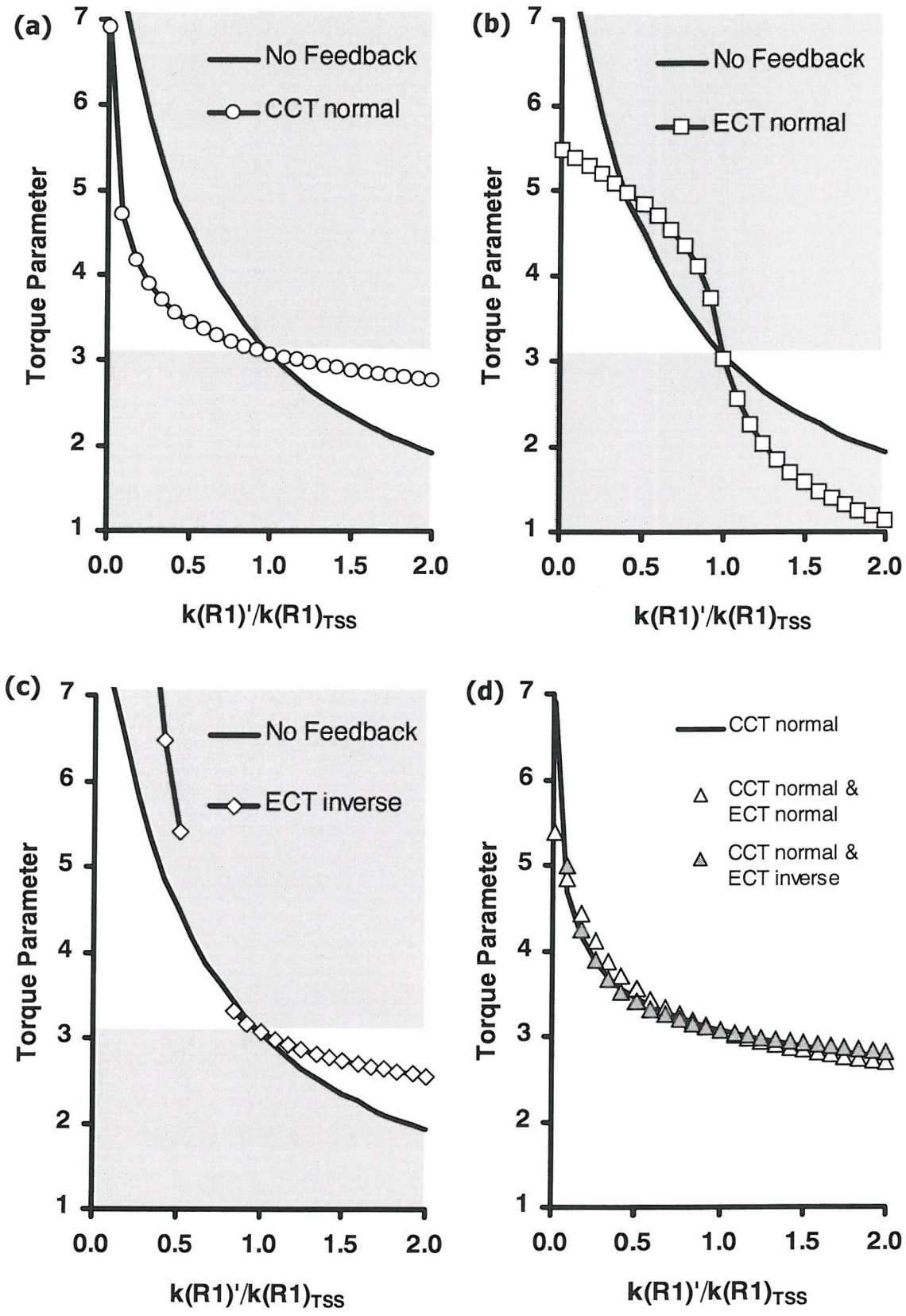

Figure 4.43: The effects of feedback at CCT and ECT.
(a) CCT(N), **(b)** ECT(N), **(c)** ECT(I) and **(d)** CCT(N),ECT(N) and CCT(N),ECT(I).
It is shown that normal feedback at ECT (b) does not stabilise the torque parameter. Inverse feedback at ECT (c) provides some stabilisation but also leads to chaotic behaviour (break in plot). Finally, with feedback at CCT, neither normal nor inverse feedback at ECT (d) confers extra stability.

4.8.7 Variation of the Sensitivity of the Torque Parameter to ECT

The sensitivity curves in figure 4.42 revealed ECT would be predicted to exhibit inverse behaviour. However, the results of adding feedback at ECT showed that the predicted inverse feedback at ECT was not stabilising. It was suggested that the feedback could change from a stabilising to a destabilising factor as the metabolite concentrations change (due to the alteration of the rate constant made in the sensitivity analysis). In order to investigate these effects, the variation of the influence of ECT on the torque parameter as the conditions change was examined.

λ vs. k(ECT) plots were generated for each of the model variations described in table 4.06 (section 4.4.8). The results for CCT and ECT, and also plots for CPT and EPT, are shown in figure 4.44. The plots for ECT clearly show more variation than those for CCT. One curve even has a negative gradient, which would lead to the prediction of normal feedback. An important point to note here is that the plot that has the negative gradient is variation 4, the variation with the most dramatic change in the steady state where the target concentration of each lipid is unity. This suggests that the effect of ECT on the torque parameter is dependent on the lipid concentrations. This variable behaviour of ECT is a key difference between CCT and ECT, and may be the origin of the difference in lipid regulation seen for CCT and ECT. The variable effect of ECT activity on the torque parameter is such that neither feedback would be stabilising over the range of conditions; this was seen when feedback was implemented in the model in section 4.8.6. The next step is to investigate the reasons for this, by looking at the concentration changes caused, in addition to the effect on the torque parameter. Comparison with CCT, which does not show variation, helps to reveal the origin of this difference in behaviour.

The plots for CPT and EPT, in figure 4.44, are similar to those for CCT and ECT respectively. This is because ECT has control of the flux through the EPT reaction, in the same way CCT was shown to drive the CPT reaction in the previous section. To explain the behaviour of ECT, the conversions mediated by CPT and EPT must be considered together, and compared and contrasted. The first stage in this was to examine how CCT and ECT affect the concentrations of the metabolites involved in the CPT and EPT reactions. These are DAG, PE and PC. The next section looks at how the concentrations of DAG, PE and PC are influenced by CCT and ECT.

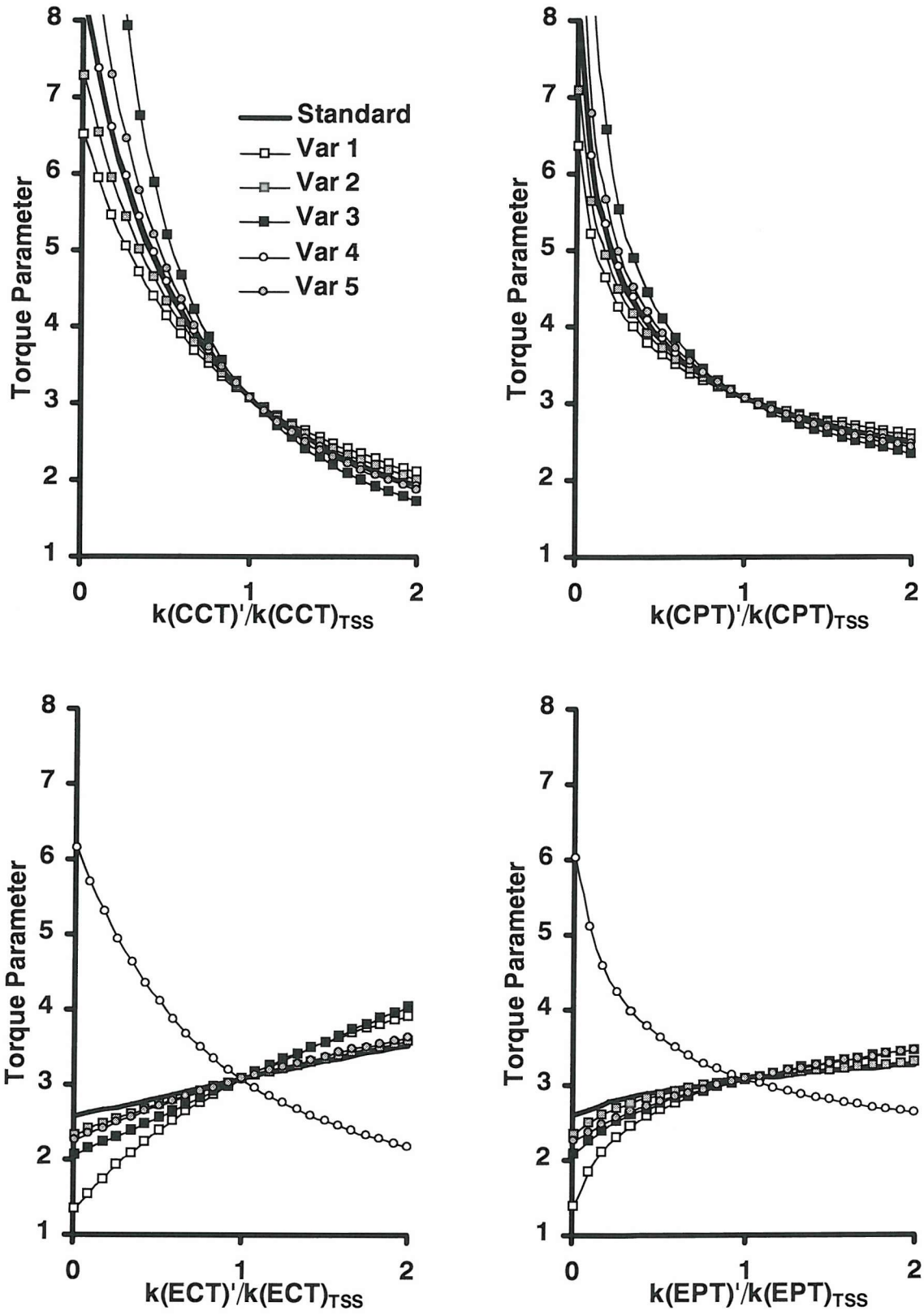

Figure 4.44: Scaled λ vs. k plots to examine changes, upon variation of the model, to the sensitivity of the torque parameter to CCT, CPT, ECT and EPT. The plots are for the five variations described previously without feedback. The crucial result is that the sensitivity of the torque parameter to ECT and EPT can change dramatically with the conditions. It is important that the plot with a negative gradient for ECT and EPT corresponds to the TSS with all concentrations set equal. This dramatic change in the concentrations has a large effect on the sensitivity of the torque.

4.8.8 Contrasting the Effect of ECT and CCT

It was shown in section 4.8.6 that neither feedback type at ECT stabilised the torque parameter. Furthermore, the sensitivity of the torque parameter to the activity of ECT in the uncontrolled network can be altered significantly and even reversed (from λ+ to λ-) if the conditions are changed. CCT does not exhibit either of these effects. Here, it is shown how the model can explain these differences by using sensitivity analysis of the model and rationalising the results in terms of the torque tension. The next step is an examination of the major lipid concentration changes that occur for each enzyme. Following this, the analysis continues with a detailed look at the structure of the pathway and the distribution of lipid types in the network.

A. Sensitivity of lipid concentrations to CCT and ECT

Experiments have found that the control of PC and PE biosynthesis depends on the supply of CDPcho/CDPeth and DAG (Bladergroen & Van Golde 1997; Vance 1996). Therefore, to compare the effect of CCT and ECT on the torque parameter, the lipid conversions mediated by CPT and EPT are considered. In figure 4.45 the concentration changes in PE, DAG and PC (the common substrate and the respective products of the CPT and EPT reactions) are shown as k(CCT) and k(ECT) are varied.

Figure 4.45 (a) shows the effect of an increase in the activity of CCT. The concentration of PC increases, whilst DAG decreases. These changes are both explained by use of the CCT-CPT pair model. However, a significant decrease in PE concentration is also seen (the shaded plot). Figure 4.45 (b) shows the effect of an increase in the activity of ECT. The concentration of PE increases, whilst DAG again decreases. These changes are also both explained by use of the ECT-EPT pair model. However, a significant decrease in PC concentration is also seen (the shaded plot).

Clearly, CCT significantly affects the concentration of PE in addition to that of DAG and PC. Similarly, the activity of ECT impacts on the amount of PC. The changes in concentration are similar, with the effects on PE and PC reversed. The further analysis considers this difference and the consequences of it. To do this CCT and ECT are considered together, by redefining the subsystem model to include PC, DAG and PE.

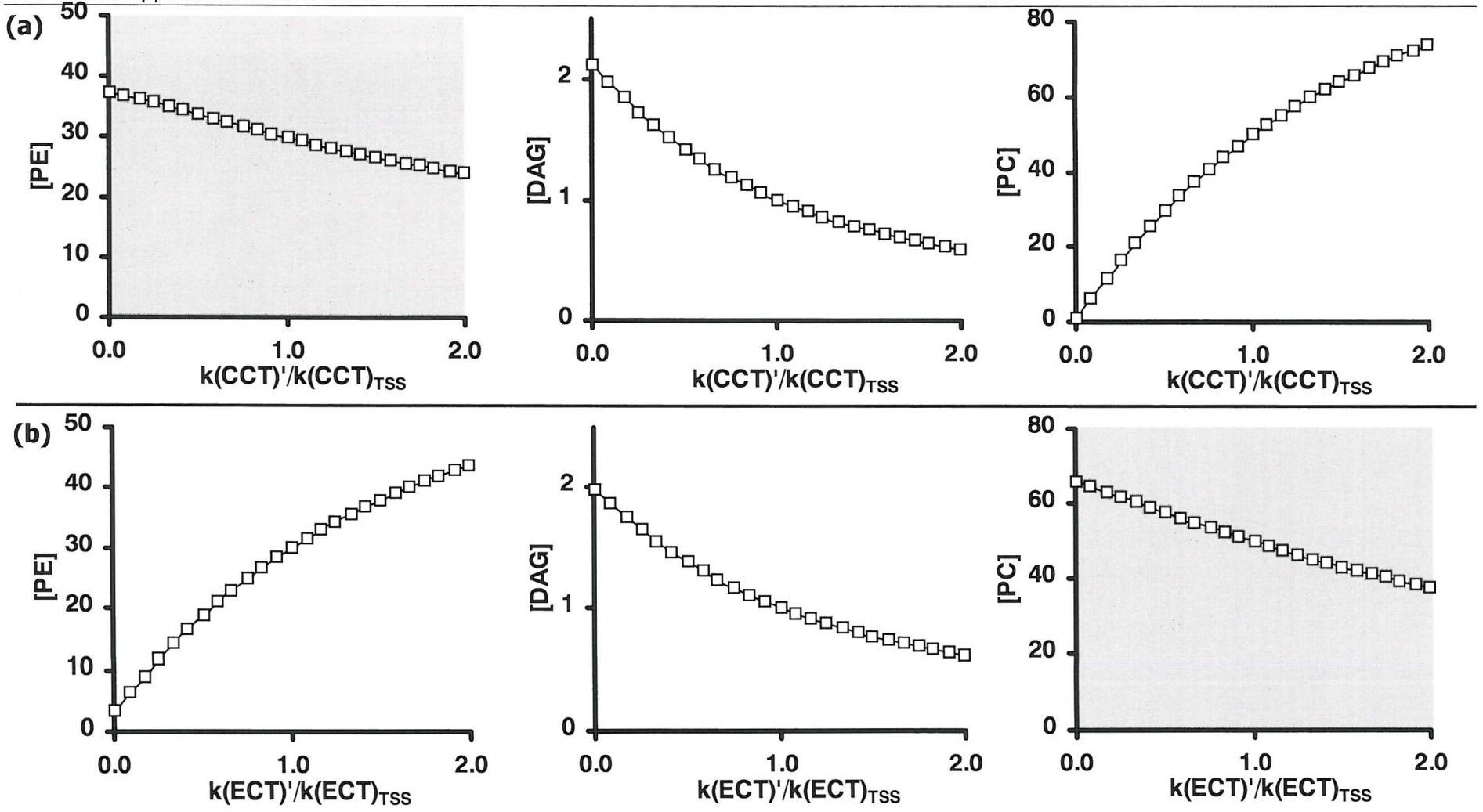

Figure 4.45: Concentration vs. k plots to show the effect of changes in CCT and ECT activity on concentrations of the lipid species PE, DAG and PC. **(a)** An increase in CCT activity directly causes a decrease in the concentration of DAG and an increase in the concentration of PC (as these are the substrate and product of R1). The change in CCT activity also gives rise to a decrease in PE concentration (shaded plot). **(b)** An increase in ECT activity directly causes a decrease in the concentration of DAG and an increase in the concentration of PE. The change in ECT activity also gives rise to a decrease in PC concentration (shaded plot). The significance of the concentration of PC means that the definition of a suitable subsystem model will require the inclusion of PE, DAG and PC.

B. Refined subsystem model: the 'CCT-CPT-ECT-EPT ensemble'

Figure 4.45 showed that an increase in ECT activity increases the amount of PE, but also depletes PC by competing with CCT for DAG. Due to the importance of PC concentration, it is prudent to consider the action of CCT and ECT together. The smallest subsystem model that includes, and links, CCT and ECT is the four-reaction combination of CCT, CPT, ECT and EPT as shown in figure 4.46.

A question that arises is, why does the CCT-CPT pair work for explaining CCT, whilst the ECT-EPT pair is insufficient for the effect of ECT? To answer this, it is necessary to look at the differences between PE and PC. The most significant is that PE is a type II lipid, whilst PC is a type 0 lipid. This is of course of central importance when considering effects on the stored elastic energy. This highlights the need to consider spontaneous curvature of the lipids of the system in more detail.

The next section looks again at the distribution of lipid types in the system. This examination reveals a key feature of the reaction network and the distribution of lipid types. It will be demonstrated how this can help explain the different impact on the system of the conversion of DAG to PC, and the conversion of DAG to PE. This difference will be used, with the subsystem model in figure 4.46, to explain the contrasting behaviour of CCT and ECT.

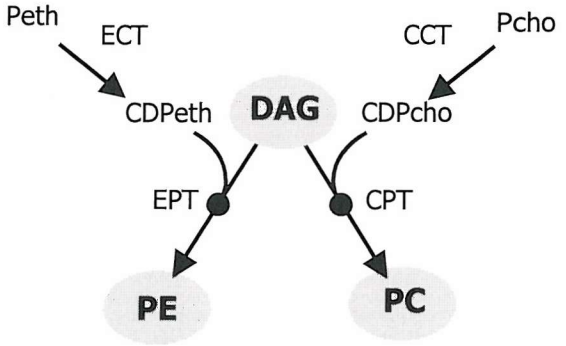

Figure 4.46: A refined subsystem model, the CCT-CPT-ECT-EPT ensemble to examine the action of ECT and the contrast with CCT. The use of this larger subsystem model is justified by examining the concentration changes that occur as CCT and ECT activity are changed. The model includes the three lipid species that are of significance: PE, DAG and PC.

C. Breakdown of symmetry

In figure 4.41 (section 4.8.3), it was noted that the stoichiometric network of the model showed a high degree of symmetry. The difference between the lipids, which would break down the symmetry of the network, is largely unimportant in this study since it has been shown how the concentration of individual lipids are not the important factors.

However, there is one factor that differentiates between the lipid species and is important when predicting feedback. The membrane property proposed to be under homeostatic control is the stored elastic energy. For this, only one physical property is important, the contribution to the torque tension as determined by the bending rigidity and the lipid spontaneous curvature. Figure 4.47 shows how labelling the lipids according to their favoured spontaneous curvatures, as type I, type 0 or type II lipids, breaks down the symmetry of the model.

The visualisation provided by figure 4.47 also highlights the importance of the conversion of DAG to PC, which was commented on in the analysis of CCT in section 4.7. Looking at the species which form a ring in the upper plane of the diagram, a general trend from PC as a type 0 lipid through PS and PE to DAG as a strongly type II lipid can be seen. There is then a 'discontinuity' between DAG and PC, as shown in the diagram. This discontinuity forms an important part of the explanation for why CCT shows strong lipid dependence but ECT in contrast does not.

With the lipid types considered, a refined subsystem model defined, results showing how the reactions impact on the concentrations and finally, knowledge of how the lipid concentrations impact on the torque parameter, it is possible to explain why CCT has a definite effect on the torque, and why, in contrast, ECT does not. The final section in the examination of the effects of CCT and ECT draws together these factors. This primarily involves comparing and contrasting the changes occurring in the system by considering how the concentration changes that occur result in the behaviour seen for the torque parameter.

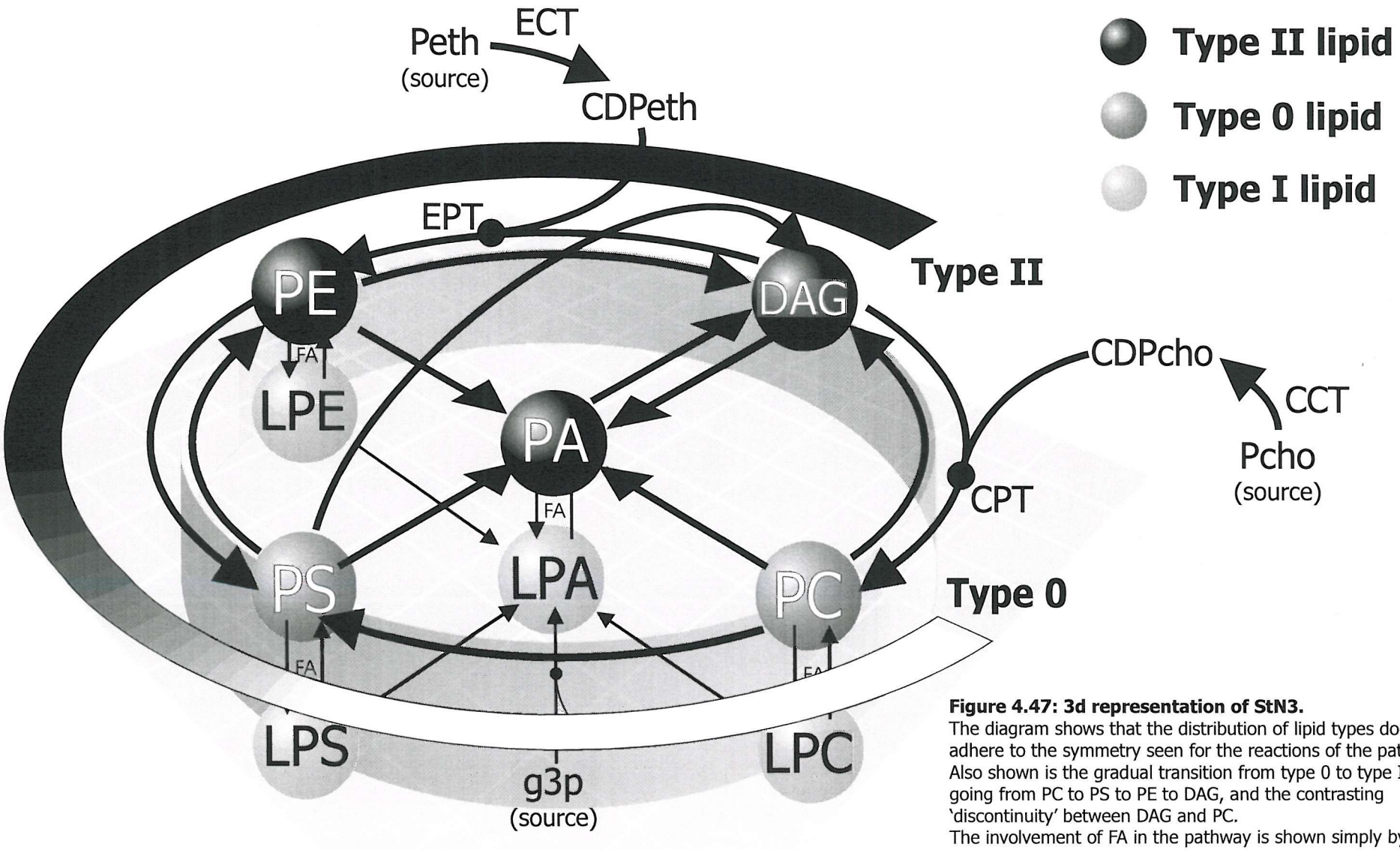

Figure 4.47: 3d representation of StN3.
The diagram shows that the distribution of lipid types does not adhere to the symmetry seen for the reactions of the pathway. Also shown is the gradual transition from type 0 to type II going from PC to PS to PE to DAG, and the contrasting 'discontinuity' between DAG and PC.
The involvement of FA in the pathway is shown simply by the 'FA' label.

D. How individual concentration changes contribute to changes in λ

In examining the behaviour of CCT and ECT, both the concentration changes and the lipid types have been examined. These details provide a framework to understand the behaviour seen for the torque parameter. The lipid types and the concentration changes will now be considered together to determine the changes in the torque. The key is to examine the correlation between the lipid types and the direction of the concentration changes caused by a change in the activity of each enzyme.

When considering the activity of CCT, the most important feature is the large difference in the spontaneous curvature favoured by DAG and PC lipids (shown in figure 4.47). CCT drives material across this 'discontinuity', by providing substrate for the conversion of DAG to PC, and therefore acts to reduce λ. Crucially, the depletion of PE, indirectly caused as DAG is converted to PC (see figure 4.45), also acts to decrease λ. For this reason, the contribution of PE can be ignored without affecting the prediction that CCT will act to decrease λ.

In a similar way, ECT indirectly reduces the concentration of PC in addition to driving the conversion of DAG to PE. Comparing to the effect of CCT, the difference is that the contributions to λ, resulting from each concentration change and the spontaneous curvature of each species, act against each other. The changes are more clearly illustrated in figure 4.48, where the changes in concentrations and contributions to the change in λ are summarised. These opposing contributions reveal that an increase in ECT activity could cause λ to increase or decrease, depending on which contribution dominates. Crucially the size of the contributions will depend on the concentrations. Therefore, the effect on λ will be concentration dependent (as was shown in section 4.8.7).

The analysis in figure 4.48 explains why the sensitivity plot for ECT varies as the conditions are changed and why neither feedback type stabilises the torque in a consistent manner over the sensitivity analysis ranges (since the concentrations change during the variation of $k(\mathrm{R}x)$, and this could be enough to make the feedback change from stabilising to destabilising). The results are consistent with the result that neither type of feedback acting at ECT would stabilise the torque parameter. It is therefore proposed that the reason that ECT exhibits no lipid dependence is that there would be no comprehensive benefit of feedback at ECT to system robustness.

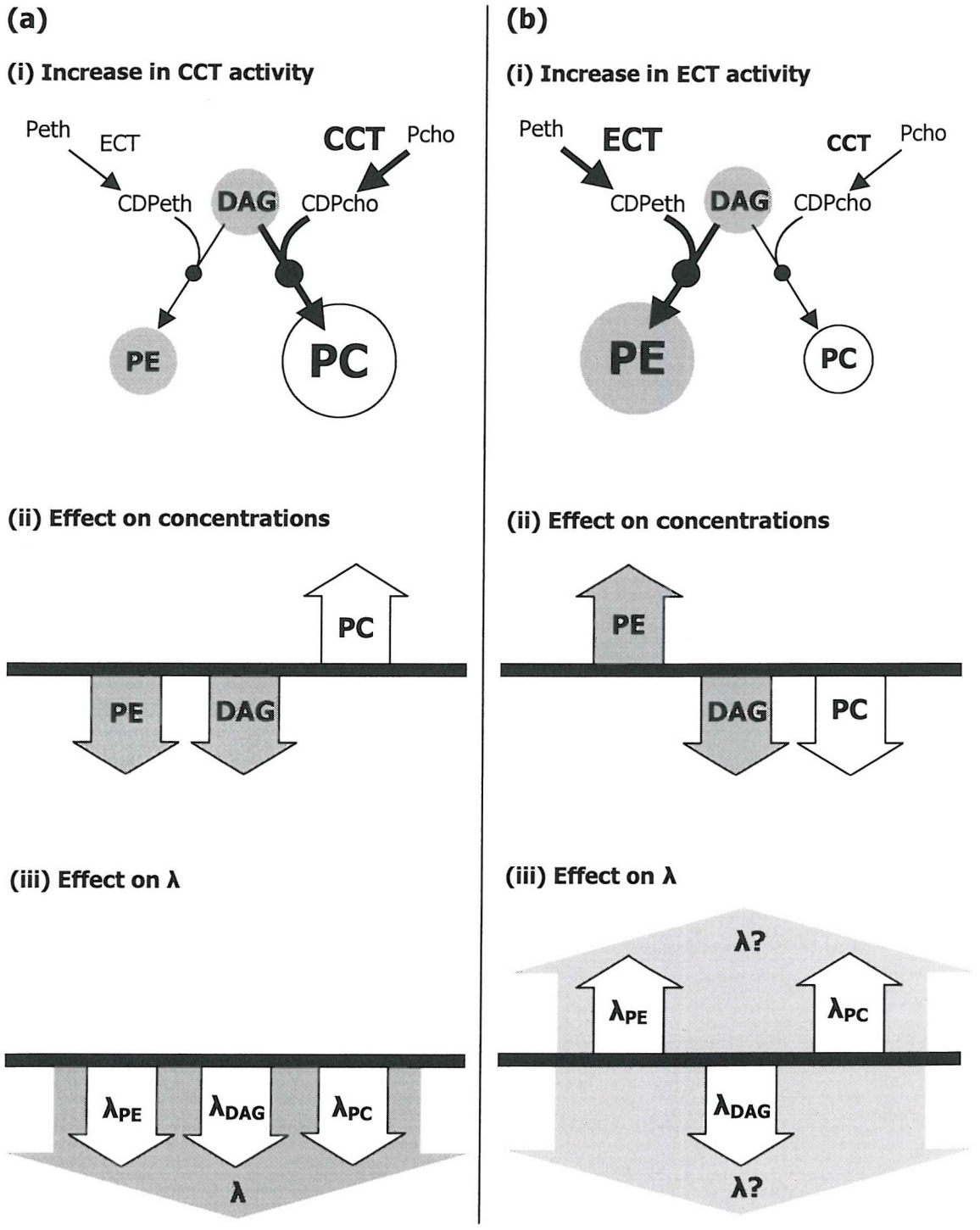

Figure 4.48: Comparing the difference in behaviour when CCT (a) and ECT (b) are increased. (i) The effect on the cytidylyltransferase and phosphotransferase network components. The effect of changing the rate of the cytidylyltransferase reaction is to increase the phosphotransferase step (DAG → PC for CCT and DAG → PE for ECT). **(ii) The concentration changes:** the arrows denote how the concentrations change from the previous steady state. The arrows do not show the size of the changes. Note that for CCT there is a correlation between the changes and the lipid spontaneous curvature (denoted by shading to indicate type II, unshaded represents type I/0).
(iii) The contribution to the torque parameter of each change is shown, along with the resultant overall change in λ. The important distinction is that for CCT the contributions to λ act in concert, whilst for ECT the effects oppose one another. The direction of the change in λ for ECT is therefore sensitive to the concentrations, fluxes and precise coefficients used.

The type of analysis applied here to ECT is important since it provides a method to eliminate a step as a candidate for feedback control. Looking at the sensitivity analysis results did not provide this since all the reactions in the sensitivity plot show some effect on the torque, and only a reaction that showed no effect could be eliminated by this method. However, the absence of a consistent effect on the torque could eliminate the reaction as a candidate. It is not a small effect on the torque which leads to the prediction that feedback will not act at ECT, it is the lack of a *consistent and large* effect as seen for CCT. This represents an important refinement of the method for choosing key candidates. With careful consideration, this analysis could be applied to the other points to improve the selection/elimination of candidates for feedback control (the challenges associated with this are detailed in section 4.10 which details further work).

The analysis also explains the variable effect of ECT and why the ECT-EPT pair is insufficient to explain the effect of ECT whilst the CCT-CPT pair is sufficient for CCT. The key is the examination of the effect of each contribution to λ. Since the CCT-CPT pair is valid for DAG → PC, one might assume that DAG → PC is more important than the alternative reaction, DAG → PE. However, this is not the reason. The important effect of the CCT reaction is the correlation of the changes, caused by the distribution of the lipid types. For CCT, ignoring DAG → PE does not matter since this secondary effect is reinforcing. However, DAG → PC is crucial when examining ECT as discussed and summarised in figure 4.48. This illustrates how oversimplifying the subsystem analysed (by looking at isolated reactions or too small a set of reactions as here) can render it invalid by neglecting important changes.

Discussion of this result highlights that knowledge of the torque tension hypothesis and the individual reaction stoichiometry is not always sufficient. The simulations and study of the network give an understanding of the system. The model identifies the concentration changes caused by each reaction. Examining the lipid types then reveals how the concentrations contribute to λ. The model is essential to show the concentrations would change in the manner presented and to show that these changes cause the response of λ to the activity of ECT to change, by looking at the variations and the effect of the implementation of feedback. This explanation could not have been arrived at without the system-wide analysis that the model provides.

4.9 Summary of Results

This work has yielded a model which tests the implications of the model presented by Attard *et al* for the interaction between CCT and an amphiphilic membrane. The results demonstrate that an incredibly simple model can help in the analysis of the behaviour of a complex system. Experiments with the model lead to a prediction of a set of feedback points (section 4.4). It is important to note that the model suggests control will be distributed (e.g. at CCT, CPT, g3pACT etc), rather than acting at one step. In addition, implementation of feedback shows the benefits of multiple feedback points (section 4.3 and section 4.6). This is consistent with evidence that lipid activation, that adheres to the type II to type I/0 classification, is a common feature of membrane synthesising enzymes. Furthermore, there is good correlation with experimental data on the effect of lipids on the enzyme activities (section 4.5).

Importantly, the integrative nature of the feedback provides a simple control to stabilise a complex system. One physical signal can act to regulate and maintain the biomembrane and provide robust control. Furthermore, the type of feedback control proposed does not render the system unresponsive. The type of multiple point MTT feedback investigated leads to an increase in the robustness of the torque parameter whilst facilitating lipid accumulation (section 4.6.4 and section 4.6.5). This is an example of robustness in some parameters with accompanying sensitivity in others.

The model can predict where feedback would be expected to act and, in addition, where it would not. For example, without looking at the details of CCT and ECT, the model can lead to an explanation of why lipid modulation for ECT would not provide a benefit in terms of MTT robustness. This is achieved by an analysis of the position in, and effect on, the pathway for each enzyme and applying the membrane torque tension hypothesis (section 4.8). It has previously been assumed that one may look at the isolated reaction's substrate and product to predict the enzymes lipid dependence. However, the model shows the need to look at system changes rather than local changes; this is because subsequent reactions, or reactions which compete for substrate may be more important with this type of feedback control. Clearly, we are a long way from a full understanding of the implications of feedback upon the system and the final section of this chapter examines ideas for further work using the model developed here.

4.10 Further Work

As a first piece of work in this area, there are many remaining long-term goals for the model. These targets are summarised by considering the possible development of the simulation procedures, the model itself and finally, methods the to test the model against experimental data.

4.10.1 Development of the Simulation Methods

The most straightforward development in the methods used in the simulation would be an improvement of the software used. At present, each sensitivity plot that forms part of the global sensitivity analysis must be generated separately by varying each rate coefficient. This requires up to 40 parameter settings and individual simulations for each global analysis run. These must be manually repeated each time a feature of the model is changed, making development of the model time consuming. The processing of data in these experiments is quite laborious and this could be more efficiently performed by modification of the software used. This improvement could be achieved by a change in the way GEPASI explores parameter space or by adaptation of the custom software to automate the parameter variation. Software development time will be worthwhile, now the methods for investigating and experimenting with the model are established, since these changes will facilitate the exploration of further variations, for example in the coefficients of the torque parameter or even the alteration of the network stoichiometry. Another area for attention is the adoption of more quantitative analysis. As stated in chapter 2 this will require development of measures of connectivity and robustness to further investigate the relationship between them. Work of this nature is currently underway in the Attard research group.

4.10.2 Enhancement of the Model

The improvement of the methods detailed above would facilitate development of the model itself. The model may be improved in several aspects. The first is a development and expansion of the stoichiometric network. This would involve inclusion of further lipid species, and attention to lipid degradation and the boundaries of the model. Refinement will also be possible with one goal being the modelling of the lipid chain diversity. Additionally an enhancement of the modelling

of cytosolic cofactors has been considered. Instead of simply clamping cytosolic metabolites, the model could be developed to include dual compartments, with one for the membrane and one for the cytosol. This would allow recreation of pool sizes and modelling of transfer between cytosol and membrane. Ultimately the model must address the spatial organisation of the cell membrane to a greater degree.

Another target is an improvement of the calculation of the stored elastic energy by refinement of the torque parameter function. This could be achieved through a number of routes. Testing against experimental data on lipid composition is one possibility. If the torque is homeostatically controlled it is reasonable to assume that the torque parameter calculated from experimental data should show a consistent range. Unfortunately, with existing literature data minor but important components, such as DAG, are often not measured. Another problem with testing the torque parameter is that it only includes a small number of species at present (those in the current model), so this will require attention. The calculation of λ may also be improved through molecular modelling of lipid species in a bilayer. Already, refinement of the values used in the torque parameter have been suggested, based on further studies of the effect of various lipid species on CCT (Attard, unpublished). A more significant challenge will be the inclusion of the enzymes themselves as amphipathic species within the model and the calculation of the torque parameter. This could possibly be achieved using stochastic simulations, which involve particles and probability. Currently, in the model λ is used to determine σ, the (enzyme activity) modulation parameter. However, with the proteins affecting λ, σ will also affect the value of λ. This is a further control loop and introduces the idea that the proteins will compete with each other to maintain the stored elastic energy.

Another area for modification is in the implementation of explicit feedback. This will primarily include experimentation with the relationship between σ and λ, that is how the enzymes are modulated by the stress. The introduction of a bell shaped curve (to model deactivation at very high stress) is expected to be the first stage in this. A further refinement would be different treatments for intrinsic and extrinsic membrane proteins since the physical effects will clearly be different. Another interesting area is consideration of how extrinsic membrane proteins may be inversely modulated by the MTT, as was briefly discussed for PLC in section 4.5.2.

4.10.3 Further Validation of the Model

Further testing against experimental data will also be important. The analysis performed for ECT and CCT could be extended to other enzymes as mentioned earlier. It would be interesting to determine if the model could identify other steps as not suitable for control of MTT or if ECT is unique? Progress in this area would depend on better experiments, specifically designed to look at membrane stress, to validate the model. The validation of an 'elimination' would require evidence that the reaction of interest is not controlled by the membrane torque tension. Such a 'negative' is harder to find than an effect, because of the criteria for ideal experiments. An effect may be seen even in a non-ideal experiment but in order to demonstrate there is no effect requires more careful investigation. Indeed, the experimental results for ECT are only available largely because of the contrasting behaviour seen with CCT. In addition, the comparison with CCT was crucial in the analysis presented here in explaining the reasons feedback at ECT could not confer stability. The model may however be useful in selecting an enzyme where this lack of modulation may subsequently be looked for experimentally.

Eventually, the model may be able to model other types of system responses. For example, experiments modelling of the exposure to ATLs, using comparison of model data with for example, mass spectrometry. It is possible to examine changes in lipid composition, lipid accumulation and spiking of metabolite concentrations. This would require a model suitable for examining transient behaviour as well as steady state behaviour and may require a different kinetic treatment. This may also allow more detailed work on CCT and PLA_2 and their roles in the maintenance of lipid content. Also, the important role of FA in the system was commented on and would warrant further research. Finally, experiments have been proposed to test the conclusions drawn about ECT from the model. It is possible to manipulate CCT and ECT, to experimentally test the CCT and ECT feedback results, by adding the CCT binding domain to ECT, and removing it from CCT. Will this cause instability? This could clarify whether feedback at ECT could be detrimental rather than simply not advantageous.

4.11 References

Arnold RS & Cornell RB (1996)
Lipid Regulation of CTP: Electrostatic, Hydrophobic, and Synergistic Interactions of Anionic Phospholipids and Diacylglycerol.
Biochemistry **35**: 9917-9924.

Attard GS, Smith WS, Templer RH, Hunt AN & Jackowski S (2000)
Modulation of CTP:phosphocholine cytidylyltransferase by membrane curvature elastic stress.
Proc. Natl. Acad. Sci. USA **97**: 9032-9036.

Barkai N & Leibler S (1997)
Robustness in Simple Biochemical Networks.
Nature **387**: 913-917.

Bladergroen BA & Van Golde LMG (1997)
CTP:phosphoethanolamine cytidylyltransferase.
Biochim. Biophys. Acta **1348**: 91-99.

Bladergroen BA, Wensing T, Van Golde LMG & Geelen MJH (1998)
Reversible translocation of CTP:phosphocholine cytidylyltransferase from cytosol to membranes in the adult bovine liver around parturition.
Biochim. Biophys. Acta **1391**: 233-240.

Boggs KP, Rock CO & Jackowski S (1995)
Lysophosphatidylcholine and 1-O-Octadecyl-2-O-Methyl-rac-Glycero-3-Phosphocholine Inhibit the CDP-Choline Pathway of Phosphatidylcholine Synthesis at the CTP Step.
J. Biol. Chem. **270**: 7757-7764.

Choy PC & Vance DE (1978)
Lipid Requirements for Activation of CTP:Phosphocholine Cytidylyltransferase from Rat Liver.
J. Biol. Chem. **253**: 5163-5167.

Clement JM & Kent C (1999)
CTP:Phosphocholine Cytidylyltransferase: Insights into Regulatory Mechanisms and Novel Functions.
Biochem. Biophys. Res. Commun. **257**: 643-650.

Coleman RA (1988)
Hepatic sn-glycerol-3-phosphate acyltransferases: effect of monoacylglycerol analogs on mitochondrial and microsomal activities.
Biochim. Biophys. Acta **963**: 367-374.

Cornell RB (1991a)
Regulation of CTP:Phosphocholine Cytidylyltransferase by Lipids. 1. Negative Surface Charge Dependence for Activation.
Biochemistry **30**: 5873-5880.

Cornell RB (1991b)
Regulation of CTP:Phosphocholine Cytidylyltransferase by Lipids. 2. Surface Curvature, Acyl Chain Length, and Lipid-Phase Dependence for activation.
Biochemistry **30**: 5881-5888.

Cornell RB & Arnold RS (1996)
Modulation of the activities of enzymes of membrane lipid metabolism by non-bilayer-forming lipids.
Chem. Phys. Lipids **81**: 215-227.

Dunne SJ, Cornell RB, Johnson JE, Glover NR & Tracey AS (1996)
Structure of the Membrane Binding Domain of CTP:Phosphocholine Cytidylyltransferase.
Biochemistry **35**: 11975-11984.

Fell DA (1992)
Metabolic Control Analysis: a survey of its theoretical and experimental development.
Biochem. J. **286**: 313-330.

Green PR & Bell RM (1984)
Asymmetric Reconstitution of Homogeneous Escherichia coli sn-Glycerol-3-phosphate Acyltransferase into Phospholipid Vesicles.
J. Biol. Chem. **259**: 14688-14694.

Green PR, Merrill AH & Bell RM (1981)
Membrane Phospholipid Synthesis in Escherichia coli. Purification, reconstitution and Characterization of sn-glycerol-3-phosphate acyltransferase.
J. Biol. Chem. **256**: 11151-11159.

Heinrich R, Rapoport SM & Rapaport TA (1977)
Metabolic Regulation and Mathematical Models.
Prog. Biophys. Molec. Biol. **32**: 1-82.

Henneberry AL & McMaster CR (1999)
Cloning and expression of human choline/ethanolaminephosphotransferase: synthesis of phosphatidylcholine and phosphatidylethanolamine.
Biochem. J. **339**: 291-298.

Henneberry AL, Wistow G & McMaster CR (2000)
Cloning, genomic organization and characterization of a human cholinephosphotransferase.
J. Biol. Chem **275**: 29808-29815.

Jackowski S (1994)
Co-ordination of membrane phospholipid synthesis with the cell cycle.
J. Biol. Chem. **269**: 3858-3867.

Jackowski S (1996)
Cell Cycle Regulation of Membrane Phospholipid Metabolism.
J. Biol. Chem. **271**: 20219-20222.

Jamil H, Hatch GM & Vance DE (1993)
Evidence that binding of CTP:phosphocholine cytidylyltransferase to membranes in rat hepatocytes is modulated by the ratio of bilayer- to non-bilayer-forming lipids.
Biochem. J. **291**: 419-427.

Jamil H, Yao Z & Vance DE (1990)
Feedback regulation of CTP:phosphocholine cytidylyltransferase Translocation between Cytosol and Endoplasmic Reticulum by Phosphatidylcholine.
J. Biol. Chem. **265**: 4332-4339.

Jelsema CL & Morre DJ (1978)
Distribution of phospholipid biosynthetic enzymes among cell components of rat liver.
J. Biol. Chem. **253**: 7960-7971.

Kanfer JN (1980)
The base exchange enzymes and phospholipase D of mammalian tissue.
Can. J. Biochem. **58**: 1370-1380.

Kent C (1997)
CTP:phosphocholine cytidylyltransferase.
Biochim. Biophys. Acta **1348**: 79-90.

Kessels JMM, Ousen H & Bosch HVD (1984)
Studies on reconstituted partially purified glycerophosphate acyltransferase from Escherichia coli.
Eur. J. Biochem. **138**: 543-549.

Killian JA & deKruijff B (1986)
The Influence of Proteins and Peptides on the Phase Properties of Lipids.
Chem. Phys. Lipids **40**: 259-284.

Kito M, Ishinaga M & Nishihara M (1978)
Function of phospholipids on the regulatory properties of solubilized and membrane bound sn-glycerol-3-phosphate acyltransferase of escherichia coli.
Bichim. Biophys. Acta **529**: 237-249.

Kuge O & Nishijima M (1997)
Phosphatidylserine synthase I and II of mammalian cells.
Biochim. Biophys. Acta **1348**: 151-156.

Lin Q, Higgs HN & Glomset JA (2000)
Membrane Lipids Have Multiple Effects on Interfacial Catalysis by a Phosphatidic Acid-Preferring Phospholipase A1 from Bovine Testis.
Biochemistry **39**: 9335-9344.

Lykidis A & Jackowski S (2001)
Regulation of Mammalian Cell Membrane Biosynthesis.
Prog. Nucleic Acid Re. **65**: 361-393.

McMaster CR & Bell RM (1997)
CDP-choline:1,2-diacylglycerol cholinephosphotransferase.
Biochim. Biophys. Acta **1348**: 100-110.

Morowitz HJ, Higinbotham WA, Matthysse SW & Quastler H (1964)
Passive Stability in a Metabolic Network.
J. Theor. Biol. **7**: 98-111.

Northwood IC, Tong AHY, Crawford B, Drobnies AE & Cornell RB (1999)
Shuttling of CTP: Phosphocholine Cytidylyltransferase between the Nucleus and Endoplasmic Reticulum Accompanies the Wave of Phosphatidylcholine Synthesis during the G0 to G1 Transition.
J. Biol. Chem. **274**: 26240-26248.

O K-m & Choy PC (1990)

Solubilization and Partial Purification of Cholinephosphotransferase in Hamster Tissues.
Lipids **25**: 122-124.

Rao NM & Sundaram CS (1993)
Sensitivity of Phospholipase C (Bacillus cereus) Activity to Lipid Packing in Sonicated Lipid Mixtures.
Biochemistry **32**: 8547-8552.

Scheideler MA & Bell RM (1989)
Phospholipid Dependence of Homogeneous, Reconstituted sn-Glycerol-3-phosphate Acyltransferase of Escherichia coli.
J. Biol. Chem. **264**: 12455-12461.

Scheideler MA & Bell RM (1992)
Glyerophosphate Acyltransferase from Escherichia coli.
Method. Enzymol. **209**: 55-63.

Sen A, Isac TV & Hui S-W (1991)
Bilayer Packing Stress and Defects in Mixed Dilinoleoylphoshatidylethanolamine and Palmitoyloleoylphosphatidylcholine and Their Susceptibility to Phospholipase A2.
Biochemistry **30**: 4516-4521.

Snider MD & Kennedy EP (1977)
Partial Purification of Glycerophosphate Acyltransferase from Escherichia coli.
J. Bacteriol. **130**: 1072-1083.

Thomas WE & Glomset JA (1999a)
Affinity Purification and Catalytic Properties of a Soluble, Ca2+-Independent, Diacylglyerol Kinase.
Biochemistry **38**: 3320-3326.

Thomas WE & Glomset JA (1999b)
Multiple Factors Influence the Binding of a Soluble Ca2+-Independent Diacylglycerol Kinase to Unilamellar Phosphoglyceride Vesicles.
Biochemistry **38**: 3310-3319.

Topham MK & Prescott SM (1999)
Mammalian Diacylglyerol Kinases, a Family of Lipid Kinases with Signaling Functions.
J. Biol. Chem. **274**: 11447-11450.

Tronchere H, Record M, Terce F & Chap H (1994)
Phosphatidylcholine Cycle and regulation of phosphatidylcholine biosynthesis by enzyme translocation.
Biochim. Biophys. Acta **1212**: 137-151.

Vance DE (1996) *Glycerolipid Biosynthesis in Eukaryotes*, p.153-181.
In *Biochemistry of Lipids, Lipoproteins and Membranes*
Edited by D. E. Vance & J. E. Vance. Elsevier Science.

Vermuelen PS, Tijburg LBM, Geelen MJH & Golde LMGv (1993)
Immunological Characterisation, Lipid Dependence, and Subcellular Localization of CTP: Phosphoethanolamine Cytidylyltransferase Purified from Rat Liver.
J. Biol. Chem. **268**: 7458-7464.

Wright MM & McMaster CR (2002)
PC and PE synthesis: Mixed micellar analysis of the cholinephosphotransferase and ethanolaminephosphotransferase activities of human choline/ethanolaminephosphotransferase 1 (CEPT1).
Lipids **37**: 663-672.

Yamashita S & Numa S (1972)
Partial Purification and Properties of Glycerophosphate Acyltransferase from Rat Liver.
Eur. J. Biochem. **31**: 565-573.

Yamashita S & Numa S (1981)
Glycerophosphate Acyltransferase from Rat Liver.
Method. Enzymol. **71**: 550-555.

Zhou X & Arthur G (1995)
Effect of 1-O-octadecyl-2-O-methyl-glycerophosphocholine on phosphatidylcholine and phosphatidylethanolamine synthesis in MCF-7 and A549 cells and its relationship to inhibition of cell proliferation.
Eur. J. Biochem. **232**: 881-888.

Zidovetski R, Laptalo L & Crawford J (1992)
Effect of Diacylglycerols on the Activity of Cobra Venom, Bee Venom, and Pig Pancreatic Phospholipases A2.
Biochemistry **31**: 7683-7691.

Appendices
code and data

A

Contents

Appendix 1: CNR1.0 Program Code

The c-code for the routine follows. The functions that define the model are shown separately. The functions that perform the simulation follow these.

```
//has 3sigfigs to match gepasi
//uncomment next line to track file values
//#define DEBUG

#define METNUM 16
#define REACTNUM 40

//define the species
#define PCHO 1
#define CDPCHO 2
#define PC 3
#define PA 4
#define DAG 5
#define PS 6
#define PE 7
#define FA 8
#define LPC 9
#define LPA 10
#define LPS 11
#define LPE 12
#define PETHA 13
#define CDPETHA 14
#define GLYC 15
#define FAPRE 16
//this way it is possible to rearrange
//but not have to redefine substrates and products


//header files=========================================================================//
#include <math.h>
#include <stdlib.h>
#include <stdio.h>
#include <time.h>
#include <string.h>

//CONSTANTS============================================================================//
#define MAX_SUBS 5
#define MAX_PROD 5
#define MAX_FLOW 20
//=====================================================================================//
//define structures
//a 'sigma'------------------------------------------------------------------------//
typedef struct
{
        int on;
        int type;
        double sigma;
        double c[12];
        double c1;      //pre exponential
        double c2;      //c1.exp(c2.sigma)
}controlstep;

//a 'reaction'---------------------------------------------------------------------//
typedef struct
{
        double rate;
        double k;
        controlstep control;
        int connect[METNUM+1];
        int subs[MAX_SUBS];
        int prod[MAX_PROD];
} reaction;

//a 'chemical species'-------------------------------------------------------------//
typedef struct
{
```

```
        char name[30];
        char fullname[50];
        double conc;
        double d_conc;
        int fixed;
        //need to initialise to zero
        //need to set and test for if on - if it is then dont update conc
        int flowin[MAX_FLOW];
        int flowout[MAX_FLOW];
} species;

//the parameters for the simulation-----------------------------------------//
typedef struct
{
        double endtime;  //end of sim
        double currtime; //tracks point in sim
        double dt;       //increment timestep
        int points;      //rows in data file
        double everynth; //frequency of data output
        double n;        //iteration counter
        int controlon[REACTNUM+1];
} parameters;

//=============================================================================//
//function prototypes
parameters get_parameters(void);
void get_mets(species []);
void init_var(reaction [], species[], int []);
void get_reacts(reaction []);
void get_connect(reaction []);
void initialise(reaction [], species[], int []);
void print_connect (reaction [], species [], FILE *);
void print_reacts (reaction [], species [], FILE *);
void calc_sigma(species [], reaction [], int[]);
void print_userdetails(FILE *);
void print_header(parameters ,FILE *);
void print_mets(species [], char [], FILE *);
void print_reacts(reaction [], FILE *);
void print_headings(species [], FILE *);
void print_currconc(species [], double time, FILE *);
void print_pos(parameters p, clock_t remain);
void print_fluxes(species [], reaction [], FILE *);
void print_ratios(species [], FILE *);
void print_sigma(species [], reaction [], FILE *);
double perform_RKstep (species spec[], reaction R[], double timestep);

//=============================================================================//
int main(void)
{
        parameters par;
        species met[METNUM + 1];
        reaction react[REACTNUM + 1];

        clock_t start;//,end; //variables for timing the sim

        //setup and open files
        FILE *datfp;
        if((datfp = fopen("jbdat.txt","w")) == NULL)
        {
                printf("Cannot Open Dat file");
                exit(0);
        }

        FILE *confp;
        if((confp = fopen("jbcon.txt","w")) == NULL)
        {
                printf("Cannot Open Con file");
                exit(0);
        }

        //call functions
        //get conditions for simulation
        par=get_parameters();                   //get runtime values for simulation
        init_var(react, met, par.controlon);    //initialise arrays
        get_mets(met);                          //get initial concentrations
        get_reacts(react);                      //get kinetic constants
        get_connect(react);
```

```
        //pre sim calculations
        initialise(react,met,par.controlon);
        //print_info (react, met,confp);
        calc_sigma(met, react, par.controlon);  //calculate initial sigmas

        print_userdetails(confp);
        print_header(par,confp);              //print date and parameters

        print_connect (react, met,confp);
        print_reacts(react,met,confp);
        print_mets(met, "Initial Concs", confp);//print concentrations to con file
        //print_reacts(react, confp);         //print kinetic data to con file

        print_headings(met, datfp);             //print data file headings
        print_currconc(met,par.currtime,datfp); //print first row in data file

        start = clock();                        //start timing the sim

        //perform this loop until the endtime is reached
        while (par.currtime<par.endtime)
        {
                //loop round this until its time for another data row
                for(par.n=0; par.n<par.everynth; par.n++)
                {
                        par.currtime +=perform_RKstep(met,react,par.dt);
                        calc_sigma(met, react, par.controlon);
                }
                //do necessary output
                print_currconc(met, par.currtime, datfp); //curr to row in data file
                print_pos(par,clock()-start); //print position in sim to screen
                //back to calculation loop
        }

        //final outputs to files
        print_mets(met, "Final Concs", confp);  //print final concs to con file
        print_fluxes(met, react, confp);
        //print_ratios(met, confp);
        print_sigma(met, react, confp);



        //close files
        fflush (confp);fclose (confp);
        fflush (datfp);fclose (datfp);
        //printf("\nfinished\nplease hit return\n");
        //getchar             ();
        return(0);
}
//============================================================================//
//These are the functions to modify to change the model                       //
//============================================================================//
void print_userdetails(FILE *fp)
{
        fprintf(fp, "Simulation Details\n");
        fprintf(fp, "\t****new simulation to verify******\n");
        fprintf(fp, "\t****insert important points here******\n");
        fprintf(fp, "\t****insert important points here************\n");
        fprintf(fp, "\n");
}


parameters get_parameters(void)
{
        parameters p;

        p.currtime=0;
        p.endtime=3000;
        p.dt=.0001;
        p.points=100;
        p.n=0;              //set the iterations counter to zero
        //calculate how often data should be output
        p.everynth=(p.endtime-p.currtime)/(p.dt*p.points) ;

        //return the parameters to the main routine
        return(p);
}
```

```
//=============================================================================//
void get_mets(species spec[])
{
        #define NAME(spc,lbl,fulllb)
        (strcpy(spec[spc].name,lbl));(strcpy(spec[spc].fullname,fulllb))
        #define CONC(spc,cnc) spec[spc].conc=(cnc)
        #define FIX(spc) spec[spc].fixed=1

        NAME(PCHO,"P-cho","P-choline");
        NAME(CDPCHO,"CDP-cho","CDP-choline");
        NAME(PC,"pc","phosphatidylcholine");
        NAME(PA,"pa","phosphatadic acid");
        NAME(DAG,"dag","diacylglycerol");
        NAME(PS,"ps","phosphatidylserine");
        NAME(PE,"pe","phosphatidylethanolamine");
        NAME(LPC,"l-pc","lyso-pc");
        NAME(LPA,"l-pa","lyso-pa");
        NAME(LPS,"l-ps","lyso-ps");
        NAME(LPE,"l-pe","lyso-pe");
        NAME(PETHA,"P-etha","P-ethanolamine");
        NAME(CDPETHA,"CDP-etha","CDP-ethanolamine");
        NAME(FA,"F-acid","Fatty Acid");
        NAME(GLYC,"gly3pho","glycerol 3-phosphate");
        NAME(FAPRE,"FApre","FA precursor");


        CONC(PCHO,1);    //concs are now set to zero as default
                FIX(PCHO);
        CONC(CDPCHO,19.96374);
        CONC(PC,49.68879);
        CONC(PA,1.002623);
        CONC(DAG,1.003633);
        CONC(PS,12.01316);
        CONC(PE,29.89593);
        CONC(PETHA,1);
                FIX(PETHA);
        CONC(CDPETHA,19.96374);
        CONC(LPC,0.5008787);
        CONC(LPA,0.5010472);
        CONC(LPS,0.5008091);
        CONC(LPE,0.5008160);
        CONC(FA,0.5001869);
        CONC(FAPRE,1);
                FIX(FAPRE);
        CONC(GLYC,1);
                FIX(GLYC);

        #undef NAME
        #undef CONC
        #undef FIX
}

//=============================================================================//
void get_connect(reaction r[])
{
        #define SUBS(reactn,subs,equiv) ((r[reactn]).connect[(subs)]=-(equiv))
        //macro for defining a substrate
        #define PROD(reactn,prod,equiv) ((r[reactn]).connect[(prod)]=(equiv))
        //macro for defining a product
         //in here describe the substrates and products of each reaction
       SUBS(1,PCHO,1);PROD(1,CDPCHO,1);
       SUBS(2,CDPCHO,1);SUBS(2,DAG,1);PROD(2,PC,1);
       SUBS(3,PC,1);PROD(3,DAG,1);
       SUBS(4,PC,1);PROD(4,PA,1);
       SUBS(5,PC,1);PROD(5,PS,1);
       SUBS(6,PA,1);PROD(6,DAG,1);
       SUBS(7,DAG,1);PROD(7,PA,1);
       SUBS(8,PS,1);PROD(8,PA,1);
       SUBS(9,PS,1);PROD(9,DAG,1);
       SUBS(10,PS,1);PROD(10,PE,1);
       SUBS(11,PE,1);PROD(11,PS,1);
       SUBS(12,CDPETHA,1);SUBS(12,DAG,1);PROD(12,PE,1);
       SUBS(13,PE,1);PROD(13,DAG,1);
       SUBS(14,PE,1);PROD(14,PA,1);
       SUBS(15,PA,1);PROD(15,LPA,1);PROD(15,FA,1);
       SUBS(16,LPA,1);SUBS(16,FA,1);PROD(16,PA,1);
```

```
        SUBS(17,PC,1);PROD(17,LPC,1);PROD(17,FA,1);
        SUBS(18,LPC,1);SUBS(18,FA,1);PROD(18,PC,1);
        SUBS(19,PS,1);PROD(19,LPS,1);PROD(19,FA,1);
        SUBS(20,LPS,1);SUBS(20,FA,1);PROD(20,PS,1);
        SUBS(21,PE,1);PROD(21,LPE,1);PROD(21,FA,1);
        SUBS(22,LPE,1);SUBS(22,FA,1);PROD(22,PE,1);
        SUBS(23,LPC,1);PROD(23,LPA,1);
        SUBS(24,LPS,1);PROD(24,LPA,1);
        SUBS(25,LPE,1);PROD(25,LPA,1);
        SUBS(26,PETHA,1);PROD(26,CDPETHA,1);
        SUBS(27,CDPETHA,1);
        SUBS(28,CDPCHO,1);
        SUBS(29,GLYC,1);SUBS(29,FA,1);PROD(29,LPA,1);
        SUBS(30,DAG,1);
        SUBS(31,PC,1);
        SUBS(32,PA,1);
        SUBS(33,PE,1);
        SUBS(34,PS,1);
        SUBS(35,LPA,1);
        SUBS(36,LPS,1);
        SUBS(37,LPC,1);
        SUBS(38,LPE,1);
        SUBS(39,FA,1);
        SUBS(40,FAPRE,1);PROD(40,FA,1);
        #undef PROD
        #undef SUBS

        //in here we may describe flowin and flowout for each species
        //(simply a different way of filling the matrix)
        #define FOUT(subs,reactn,equiv) ((r[reactn]).connect[(subs)]=-(equiv))
        #define FIN(prod,reactn,equiv) ((r[reactn]).connect[(prod)]=(equiv))
        /*FIN(PCHO,3,1);FIN(PCHO,9,1);FIN(PCHO,37,1);
        FOUT(PCHO,1,1);
        FIN(CDPCHO,1,1);
        FOUT(CDPCHO,2,1);FOUT(CDPCHO,42,1);
        */
        #undef FOUT
        #undef FIN
}
void get_reacts(reaction r[])
{
        #define RATE(rct,rte) r[rct].k=(rte)
        RATE(1,.16);
                r[1].control.on=1;
                        r[1].control.type=1;
                        r[1].control.c1=100;          r[1].control.c2=14.16;
                        r[1].control.c[1]=1;          r[1].control.c[2]=1;
                        r[1].control.c[3]=50;         r[1].control.c[4]=150;
                        r[1].control.c[5]=100;        r[1].control.c[6]=200;
                        r[1].control.c[7]=0;          r[1].control.c[8]=20;
                        r[1].control.c[9]=300;        r[1].control.c[10]=10;
                        r[1].control.c[11]=100;
        RATE(2,0.4);
                r[2].control.on=1;
                        r[2].control.type=1;
                        r[2].control.c1=100;          r[2].control.c2=14.16;
                        r[2].control.c[1]=1;          r[2].control.c[2]=1;
                        r[2].control.c[3]=50;         r[2].control.c[4]=150;
                        r[2].control.c[5]=100;        r[2].control.c[6]=200;
                        r[2].control.c[7]=0;          r[2].control.c[8]=20;
                        r[2].control.c[9]=300;        r[2].control.c[10]=10;
                        r[2].control.c[11]=100;
        RATE(3,0.046);
        RATE(4,0.046);
        RATE(5,0.046);
        RATE(6,17.628);
                r[6].control.on=1;
                        r[6].control.type=-1; //inverse feedback
                        r[6].control.c1=100;          r[6].control.c2=1.5;
                        r[6].control.c[1]=1;          r[6].control.c[2]=1;
                        r[6].control.c[3]=50;         r[6].control.c[4]=150;
                        r[6].control.c[5]=100;        r[6].control.c[6]=200;
                        r[6].control.c[7]=0;          r[6].control.c[8]=20;
                        r[6].control.c[9]=300;        r[6].control.c[10]=10;
                        r[6].control.c[11]=100;
        RATE(7,8);
        RATE(8,0.118);
```

```
        RATE(9,0.118);
        RATE(10,0.118);
        RATE(11,0.09);
        RATE(12,0.4);
        RATE(13,0.09);
        RATE(14,0.09);
        RATE(15,17.628);
        RATE(16,83.536);
                r[16].control.on=1;
                        r[16].control.type=-1; //inverse feedback
                        r[16].control.c1=100;           r[16].control.c2=1.5;
                        r[16].control.c[1]=1;           r[16].control.c[2]=1;
                        r[16].control.c[3]=50;          r[16].control.c[4]=150;
                        r[16].control.c[5]=100;         r[16].control.c[6]=200;
                        r[16].control.c[7]=0;           r[16].control.c[8]=20;
                        r[16].control.c[9]=300;         r[16].control.c[10]=10;
                        r[16].control.c[11]=100;
        RATE(17,0.046);
        RATE(18,4.543);
        RATE(19,0.118);
        RATE(20,2.81);
        RATE(21,0.09);
        RATE(22,5.351);
        RATE(23,2.271);
        RATE(24,1.405);
        RATE(25,2.676);
        RATE(26,16);
        RATE(27,0.4);
        RATE(28,0.4);
        RATE(29,0.18);
                r[29].control.on=1;
                        r[29].control.type=1;
                        r[29].control.c1=100;           r[29].control.c2=14.16;
                        r[29].control.c[1]=1;           r[29].control.c[2]=1;
                        r[29].control.c[3]=50;          r[29].control.c[4]=150;
                        r[29].control.c[5]=100;         r[29].control.c[6]=200;
                        r[29].control.c[7]=0;           r[29].control.c[8]=20;
                        r[29].control.c[9]=300;         r[29].control.c[10]=10;
                        r[29].control.c[11]=100;
        RATE(30,0.01);
        RATE(31,0.0002);
        RATE(32,0.01);
        RATE(33,0.000333);
        RATE(34,0.000833);
        RATE(35,0.02);
        RATE(36,0.02);
        RATE(37,0.02);
        RATE(38,0.02);
        RATE(39,0.02);
        RATE(40,0.15);
        #undef RATE
}

//=============================================================================//
//end of functions that require modification - the remainder process model     //
//=============================================================================//

double perform_RKstep (species spec[], reaction R[], double timestep)
{
        void calc_coeff(reaction R[], species spec[], double conc[], double dt, double
        c[]);

        static double conc[METNUM+1];
        static double coeff0[METNUM+1],coeff1[METNUM+1],coeff2[METNUM+1],
                coeff3[METNUM+1];
        int i;

        //step 0
        for (i=1;i<=METNUM;i++) conc[i]=spec[i].conc;
        //get the values to pass to function eval
        calc_coeff(R,spec,conc,timestep,coeff0);
        //step 1
        for (i=1;i<=METNUM;i++) conc[i]=(spec[i].conc+(coeff0[i]/2));
        calc_coeff(R,spec,conc,timestep,coeff1);
        //step 2
        for (i=1;i<=METNUM;i++) conc[i]=(spec[i].conc+(coeff1[i]/2));
        calc_coeff(R,spec,conc,timestep,coeff2);
```

```
        //step 3
        for (i=1;i<=METNUM;i++) conc[i]=(spec[i].conc+coeff2[i]);
        calc_coeff(R,spec,conc,timestep,coeff3);

        //for (i=1;i<=METNUM;i++)
        //
        printf("%lf\t%lf\t%lf\t%lf\n",coeff0[i],coeff1[i],coeff2[i],coeff3[i]);

        //final stage loop round and add up each for each reaction
        for (i=1;i<=METNUM;i++)
                if(spec[i].fixed==0)
                        spec[i].conc += ((coeff0[i] + 2*coeff1[i]+ 2*coeff2[i] +
                                coeff3[i])/6);

        return (timestep);
}


//=============================================================================//
void calc_coeff(reaction R[], species spec[], double conc[], double dt, double c[])
{
        void calc_rates(species spec[], reaction R[], double conc[]);
        int i,j;
        double net;
        //calculate each rate based on current concentrations
        calc_rates(spec,R,conc);

        //determine the reaction network by reading the flowin and flowout arrays
        for (i=1;i<=METNUM;i++)//loop round all metabolites
        {
                //printf("met %d",i);
                net=0; //net is zero
                for (j=0; spec[i].flowout[j]>0; j++)
                //while flowout element is positive (not sentinel)
                {
                        //printf("flowout %d " , spec[i].flowout[j]);
                        net -= R[ (spec[i].flowout[j]) ].rate;
                        //subtract R[x].rate (where x is the value in subs) from net
                }
                for (j=0; spec[i].flowin[j]>0; j++)//while flowin element is positive
                {
                        //printf("flowin %d " , spec[i].flowin[j]);
                        net += R[ (spec[i].flowin[j]) ].rate;
                        //add R[x].rate (where x is the value in subs) to net
                }
                //printf("\n");//getchar();
                spec[i].d_conc=net;//species flux
                c[i]=dt*net; //multiply netflow by dt to get coefficient for RK

        }
}

// old function which described the stoichiometry
// now calculated from the reactions using the function above
/*void calc_coeff(reaction R[], species spec[], double conc[], double dt, double c[])
{
        void calc_rates(species spec[], reaction R[], double conc[]);

        //calculate each rate based on current concentrations
        calc_rates(spec,R,conc);

        //here we describe the reaction network
        //ie which species are affected by which rates
        c[1] = dt * (R[4].rate - R[1].rate);
        c[2] = dt * (R[1].rate - R[2].rate);
        c[3] = dt * (R[2].rate - R[3].rate - R[5].rate - R[8].rate + R[9].rate);
        c[4] = dt * (R[3].rate + R[7].rate - R[4].rate);
        c[5] = dt * (R[5].rate - R[6].rate + R[10].rate);
        c[6] = dt * (R[6].rate - R[7].rate);
        c[7] = dt * (R[8].rate - R[9].rate - R[10].rate);
}*/

//=============================================================================//
void calc_rates(species spec[], reaction R[], double conc[])
{
        //read the reactions substrates to get the form of each rate equation
        int i,j;
```

```
        double multiplier;

        for(i=1;i<=REACTNUM;i++)
        {
                multiplier=1;//a multiplier which multiplies concs of subs together
                for(j=0;R[i].subs[j]>0;j++)
                        multiplier *= conc[(R[i].subs[j])];
                R[i].rate = R[i].control.sigma * R[i].k * multiplier;
                //note: times all by sigma - theyre set to 1 if not switched on
                //this allows control to be switched on without changing this
        }
}

//=============================================================================//
void print_pos(parameters p, clock_t remain)
{
  //this function prints the sim time, real time and a countdown bar
  int i;
  double stars;

  //print sim time remaining, sim time elapsed and real time since start
  printf("Sim t rem: %.1lf  elapsed: %.1lf  Real Time: %.2lf s\t",
                  p.endtime-p.currtime,p.currtime,(double)remain/CLK_TCK);
  //print the decreasing star bar
  stars=20*(p.endtime-p.currtime)/p.endtime;
  for(i=0 ;i<=stars;i++) printf("=");
  for(i=20;i>=stars;i--) printf("-");
  //return to beginning of the line
  printf("\r");
}

//=============================================================================//
void init_var(reaction r[], species spec[], int on[])
{
        int a,h,i;
        //empty the connectivity array
        for (h=1;h<=REACTNUM;h++)
                for(i=0;i<=METNUM;i++)
                        r[h].connect[i]=0;
        //effectively sets up a [REACTNUM][METNUM] zeroed array


        //empty each of the substrate  and product arrays
        for (h=1;h<=REACTNUM;h++)
        {
                for(i=0;i<MAX_SUBS;i++)r[h].subs[i]=-1;
                for(i=0;i<MAX_PROD;i++)r[h].prod[i]=-1;
        }
        //empty each of the flow arrays
        for (h=1;h<=METNUM;h++)
        {
                for(i=0;i<MAX_FLOW;i++)spec[h].flowin[i]=-1;
                for(i=0;i<MAX_FLOW;i++)spec[h].flowout[i]=-1;
        }
        //there last four statements are setting sentinel values for the arrays
        //the data are positive integers (a reaction or species index)

        //set all concentrations to 0 as default and not fixed
        for(h=1;h<=METNUM;h++)
        {
                spec[h].conc=0;
                spec[h].fixed=0;
        }
        //setup sigma storage
        for(i=0;i<=REACTNUM;i++) r[i].control.sigma=1; //set all sigmas to one
        for(i=0;i<=REACTNUM;i++) on[i]=0;
        //turn off sigmas
        for(i=1;i<=REACTNUM;i++)
        {
                r[i].control.on=0;          //set the control to be off for all steps
                r[i].control.type=1;        //set the control type to 1 (default)
                for (a=1;a<=6;a++)r[i].control.c[a]=0;
                //set coefficients to zero
        }

}
```

```
//=============================================================================//
void print_connect (reaction r[], species spec[], FILE *fp)
{
        int h,j;

        fprintf(fp,"Connectivity Matrix\n");
        //print out the connectivity matrix
        fprintf(fp,"\t spec\t");
        for (j=1;j<=METNUM;j++)
                fprintf(fp,"%2d ",j);
        fprintf(fp,"\n");
        for (h=1;h<=REACTNUM;h++)
        {
                fprintf(fp,"\tr[%2d]\t",h);//print reaction labels
                for (j=1;j<=METNUM;j++)
                {       fprintf(fp,"%2d ",r[h].connect[j]);
                }
                fprintf(fp,"\n");
        }
        fprintf(fp,"\n");

        fprintf(fp,"Flows from and to metabolites\n");
        //print out the FLOWINs and FLOWOUTs for each metabolite
        for(h=1;h<=METNUM;h++)//do for each met
        {       fprintf(fp,"\tmet:%2d (%-8s)  in:  ",h,spec[h].name);
                for(j=0;spec[h].flowin[j]>0;j++)
                        fprintf(fp,"%2d  ",spec[h].flowin[j]);
                fprintf(fp,"    out:  ");
                for(j=0;spec[h].flowout[j]>0;j++)
                        fprintf(fp,"%2d  ",spec[h].flowout[j]);
                fprintf(fp,"\n");
        }
        fprintf(fp,"\n");
}

//=============================================================================//
void print_reacts (reaction r[], species spec[], FILE *fp)
{
        //print out the rates and the reactions
        //remember to put in an if to print the sigmas (if on)
        int i,j;

        fprintf(fp,"Reactions and Rates\n");

        for(i=1;i<=REACTNUM;i++)//do for each reaction
        {       fprintf(fp,"\tR(%d) k  :%9.5lf ",i,r[i].k);
                for(j=0;r[i].subs[j]>0;j++)//scan for substrates
                {       fprintf(fp,"%5s ",spec[(r[i].subs[j])].name);//print species
                        if(r[i].subs[j+1]>0)fprintf(fp," + ");//if not last put plus
                }
                fprintf(fp," -> ");
                for(j=0;r[i].prod[j]>0;j++)
                {       fprintf(fp,"%-5s ",spec[(r[i].prod[j])].name);
                        if(r[i].prod[j+1]>0)fprintf(fp," + ");
                }
                fprintf(fp,"\n");
        }
        fprintf(fp,"\n");
}

//=============================================================================//
void initialise (reaction r[], species spec[], int on[])
{
        //generally this function is for doing 'do once' speed ups
        //ie stripping input data down to a quickly readable format
        //for example, building an index to the matrix
        int h,i,j,k,a,l;
        //fill the subs and product arrays
        for (i=1;i<=REACTNUM;i++)//do for EACH species
        {
                j=0;k=0;
                for(h=1;h<=METNUM;h++)
                {
                        if(r[i].connect[h]>0)
                                for(l=0;l<r[i].connect[h];l++)
                                //put in entries for equivalents
                                        r[i].prod[k++]=h;
```

```
                        else if(r[i].connect[h]<0)
                                for(l=0;l>r[i].connect[h];l--)
                                        r[i].subs[j++]=h;
                }
                r[i].subs[j++]=-1;
                r[i].prod[k++]=-1;
        }

        //fill the flowin and flowout arrays
        for(h=1;h<=METNUM;h++)//do for EACH species
        {
                j=0;k=0;
                for (i=1;i<=REACTNUM;i++)
                {
                        if(r[i].connect[h]>0)
                        {       for(l=0;l<r[i].connect[h];l++)
                                {       spec[h].flowin[j++]=i;
                                        //printf(" in: %d ",i);
                                        //j++;
                                }
                        }
                        else if(r[i].connect[h]<0)
                        {       for(l=0;l>r[i].connect[h];l--)
                                {       spec[h].flowout[k++]=i;
                                        //k++;
                                        //printf(" out: %d ",i);
                                }
                        }
                }
                spec[h].flowout[k]=-1;
                spec[h].flowin[j]=-1;
                //printf("\n");
        }


        //index which control steps are on
        j=1;
        for (i=1;i<=REACTNUM;i++)
        {
                if(r[i].control.on!=0)
                {
                        on[j]=i; //put number of step into index array
                        j++;     //move to next element of index array
                }
        }
        //this is to print out the index array
        printf("The Following Steps are on\n");
        for (a=1;on[a]!=0;a++) printf ("%d\t",on[a]);
        printf("\n\n");
}


//=============================================================================//
void calc_sigma(species spec[], reaction R[], int on[])
{
        int i;
        double ratio;
        //new calculation of sigma
        for (i=1;on[i]!=0;i++)  //eg read 4,3,2,0 means R4,3,2 are controlled
        {
                                if (R[on[i]].control.type==1)
                                        ratio=                  (
        (R[on[i]].control.c[1]*spec[PC].conc
                        +R[on[i]].control.c[2]*spec[PS].conc
                        +R[on[i]].control.c[3]*spec[LPA].conc
                        +R[on[i]].control.c[4]*spec[LPC].conc
                        +R[on[i]].control.c[5]*spec[LPE].conc
                        +R[on[i]].control.c[6]*spec[LPS].conc
                        +R[on[i]].control.c[7]*spec[0].conc)//AC!
        /
        (R[on[i]].control.c[8]*spec[PE].conc
                        +R[on[i]].control.c[9]*spec[DAG].conc
                        +R[on[i]].control.c[10]*spec[PA].conc
                        +R[on[i]].control.c[11]*spec[FA].conc)
                                        );

                                if (R[on[i]].control.type==-1)
```

```
                                        ratio=                  (
        (R[on[i]].control.c[8]*spec[PE].conc
                        +R[on[i]].control.c[9]*spec[DAG].conc
                        +R[on[i]].control.c[10]*spec[PA].conc
                        +R[on[i]].control.c[11]*spec[FA].conc)
        /
        (R[on[i]].control.c[1]*spec[PC].conc
                        +R[on[i]].control.c[2]*spec[PS].conc
                        +R[on[i]].control.c[3]*spec[LPA].conc
                        +R[on[i]].control.c[4]*spec[LPC].conc
                        +R[on[i]].control.c[5]*spec[LPE].conc
                        +R[on[i]].control.c[6]*spec[LPS].conc
                        +R[on[i]].control.c[7]*spec[0].conc)//AC
                                        );

        //R[on[i]].control.sigma=exp(-ratio);
        R[on[i]].control.sigma=R[on[i]].control.c1*exp(-R[on[i]].control.c2*ratio);
        //have added c1 and c2 coefficients
        }
}

//=============================================================================//
void print_header(parameters p,FILE *fp)
{
        time_t t;


        /*fprintf(fp, "Simulation Details\n");
        fprintf(fp, "****insert important points here******\n");
        fprintf(fp, "****insert important points here******\n");
        fprintf(fp, "****insert important points here******\n");
        fprintf(fp, "\n");*/

        time(&t);
        fprintf(fp, "Date and Time     : %s\n", ctime(&t));

        fprintf(fp, "Runtime Parameters\n");
        fprintf(fp, "\tEndtime           : %.0lf\n", p.endtime);
        fprintf(fp, "\tTime interval (dt): %lf\n", p.dt);
        fprintf(fp, "\t  (Iterations     : %.0lf)\n", (p.endtime/p.dt));
        fprintf(fp, "\n");
}

//=============================================================================//
void print_mets(species spec[], char heading[], FILE *fp)
{
        //this function prints concentrations to con file
        //it is also used at the start and the end
        int i;

        fprintf(fp, "%s\n", heading);

        for(i=0;i<=(METNUM);i++)
                fprintf(fp,"\t%d:%8s conc   :%10.7lf\n",
                        i,spec[i].name, spec[i].conc);

        fprintf(fp, "\n");
}

//=============================================================================//
void print_headings(species spec[], FILE *fp)
{
        //prints the headings in the data table
        int i;

        fprintf(fp,"%-11s\t","#Time");
        for (i=0;i<=(METNUM);i++) fprintf(fp,"%-11s\t",spec[i].name);
        fprintf(fp,"\n");
}

//=============================================================================//
void print_currconc(species spec[], double time, FILE *fp)
{
        //prints one row of the data table
        int i;

        fprintf(fp,"%11.6lf\t",time);
```

```
        for (i=0;i<=(METNUM);i++) fprintf(fp,"%11.7f\t",spec[i].conc);
        fprintf(fp,"\n");
}

//=============================================================================//
void print_fluxes(species spec[], reaction R[], FILE *fp)
{
        int i;

        fprintf(fp,"Species Fluxes\n");
        for (i=1;i<=(METNUM);i++)
                fprintf(fp,"\t%-8s %13.7lg\n",spec[i].name, spec[i].d_conc);
        fprintf(fp,"\n");

        fprintf(fp,"Reaction Fluxes\n");
        for (i=1;i<=(REACTNUM);i++)
                fprintf(fp,"\trate %2d  %.7lf\n",i, R[i].rate);
        fprintf(fp,"\n");
}

//=============================================================================//
void print_ratios(species spec[], FILE *fp)
{
        int i;
        double total;

        //note if if moeity conservations changed will give strange results
        fprintf(fp,"Lipid Percentages\n");
        for (i=3,total=0;i<=(METNUM);i++) //note i=3 not include Pcho & CDPcho
                total += spec[i].conc;
        for (i=3;i<=(METNUM);i++)
                fprintf(fp,"%-10s\t",spec[i].name);
        fprintf(fp,"\n");
        for (i=3;i<=(METNUM);i++)
                fprintf(fp,"%-10.11f\t",spec[i].conc*100/total);
        fprintf(fp,"\n");
}

//=============================================================================//
void print_sigma(species spec[], reaction R[], FILE *fp)
{

        //this is a function to calculate a sigma which is not related
        //to any particular reaction but is designed to see if modifying a rate
        //constant has any effect on the ratio of bilayer to non-bilayer
        double sigma;
        int i;

        i=1; //use the coefficients for the main control step
        sigma=                  (       (R[i].control.c[1]*spec[PC].conc
                                        +R[i].control.c[2]*spec[PS].conc
                                        +R[i].control.c[3]*spec[LPA].conc
                                        +R[i].control.c[4]*spec[LPC].conc
                                        +R[i].control.c[5]*spec[LPE].conc
                                        +R[i].control.c[6]*spec[LPS].conc
                                        +R[i].control.c[7]*spec[0].conc)//AC!
                                /
                                        (R[i].control.c[8]*spec[PE].conc
                                        +R[i].control.c[9]*spec[DAG].conc
                                        +R[i].control.c[10]*spec[PA].conc
                                        +R[i].control.c[11]*spec[FA].conc)
                                );
        fprintf(fp,"Lipid Ratio\n");
        fprintf(fp,"%lf\n",sigma);
}

//=============================================================================//

/*void print_reacts(reaction r[], FILE *fp)
{
        int i,j;

        for(i=1;i<=REACTNUM;i++)
        {
                //print each reaction coefficient
                fprintf(fp, "reaction %d:    k  :%9.5lf\n",i,r[i].k);
```

```
                //if control is on print the 'sigma coefficients'
                if (r[i].control.on==1)
                {
                        fprintf(fp, "\tcontrol on\ttype %d\n\t",r[i].control.type);

                        for(j=1;j<=6;j++)
                                fprintf(fp,"c%d=%.21f\t",j,r[i].control.c[j]);;

                        fprintf(fp,"\n");
                }
        }

        fprintf(fp, "\n");
}*/

//=============================================================================//
```

Appendix 2: Simulation Data

This appendix comprises the data tables for the sensitivity analysis. More details are given in the main text.

List of Tables

k´/k is used to represent $k(Rx)'/k(Rx)_{TSS}$ where space does not permit complete labelling

k'/k	R1	R2	R3	R4	R5	R6	R7	R8	R9	R10	R11	R12	R13	R14	R15	R16	R17	R18	R19	R20	R21	R22	R23	R24	R25	R26	R29
0.01	8.228	7.971	2.470	2.500	3.048	1.229	3.229	2.701	2.678	2.575	4.266	2.594	3.305	3.354	3.297	0.685	3.758	2.700	4.475	2.488	3.889	2.590	2.287	2.204	2.760	2.587	34.60
0.09	7.257	6.112	2.525	2.553	3.051	2.103	3.213	2.738	2.717	2.624	4.122	2.674	3.280	3.323	3.276	1.953	3.679	2.747	4.285	2.556	3.798	2.653	2.388	2.312	2.803	2.620	8.775
0.18	6.478	5.227	2.579	2.605	3.054	2.406	3.198	2.774	2.755	2.671	3.989	2.738	3.255	3.295	3.256	2.354	3.605	2.789	4.115	2.620	3.713	2.709	2.480	2.411	2.841	2.655	6.548
0.26	5.841	4.685	2.632	2.656	3.056	2.578	3.184	2.808	2.791	2.717	3.866	2.791	3.232	3.267	3.235	2.567	3.535	2.829	3.963	2.679	3.633	2.760	2.564	2.502	2.875	2.693	5.501
0.34	5.312	4.310	2.685	2.706	3.058	2.695	3.169	2.842	2.827	2.761	3.752	2.837	3.211	3.242	3.216	2.703	3.471	2.864	3.826	2.734	3.557	2.807	2.640	2.586	2.906	2.733	4.857
0.42	4.867	4.029	2.736	2.756	3.060	2.781	3.156	2.874	2.861	2.805	3.646	2.878	3.190	3.217	3.196	2.797	3.410	2.898	3.701	2.786	3.485	2.850	2.711	2.664	2.934	2.774	4.411
0.51	4.489	3.810	2.787	2.804	3.062	2.849	3.143	2.906	2.894	2.847	3.547	2.914	3.170	3.193	3.177	2.867	3.353	2.928	3.587	2.834	3.417	2.889	2.775	2.736	2.959	2.816	4.080
0.59	4.165	3.632	2.837	2.851	3.064	2.903	3.130	2.936	2.926	2.887	3.454	2.947	3.152	3.171	3.159	2.921	3.299	2.957	3.482	2.880	3.352	2.926	2.835	2.803	2.983	2.859	3.822
0.67	3.884	3.483	2.886	2.898	3.066	2.949	3.118	2.965	2.958	2.927	3.367	2.976	3.134	3.149	3.141	2.964	3.248	2.983	3.386	2.923	3.290	2.960	2.890	2.865	3.004	2.903	3.615
0.76	3.638	3.357	2.934	2.943	3.068	2.987	3.106	2.994	2.988	2.965	3.286	3.004	3.117	3.128	3.123	2.999	3.200	3.008	3.298	2.964	3.231	2.991	2.942	2.923	3.023	2.946	3.443
0.84	3.423	3.248	2.982	2.988	3.070	3.020	3.094	3.021	3.018	3.003	3.209	3.029	3.102	3.109	3.105	3.028	3.154	3.031	3.216	3.003	3.175	3.021	2.989	2.977	3.041	2.990	3.298
0.92	3.232	3.152	3.029	3.032	3.071	3.049	3.083	3.048	3.046	3.039	3.137	3.052	3.086	3.090	3.088	3.053	3.111	3.053	3.139	3.040	3.121	3.048	3.034	3.028	3.058	3.033	3.174
1.00	3.063	3.068	3.075	3.075	3.073	3.074	3.072	3.074	3.074	3.075	3.069	3.074	3.072	3.072	3.072	3.074	3.070	3.074	3.068	3.075	3.070	3.074	3.075	3.075	3.074	3.075	3.067
1.09	2.911	2.992	3.121	3.118	3.074	3.096	3.061	3.099	3.101	3.109	3.004	3.094	3.058	3.054	3.055	3.092	3.031	3.093	3.002	3.108	3.020	3.098	3.114	3.120	3.088	3.117	2.972
1.17	2.775	2.924	3.166	3.159	3.076	3.116	3.051	3.124	3.128	3.143	2.943	3.113	3.045	3.037	3.039	3.108	2.994	3.111	2.940	3.140	2.973	3.121	3.150	3.162	3.101	3.158	2.887
1.25	2.652	2.862	3.210	3.200	3.077	3.134	3.041	3.148	3.153	3.176	2.885	3.132	3.032	3.021	3.023	3.122	2.958	3.129	2.882	3.170	2.928	3.143	3.184	3.202	3.114	3.199	2.812
1.34	2.541	2.806	3.253	3.240	3.078	3.150	3.031	3.171	3.178	3.208	2.830	3.149	3.020	3.006	3.007	3.135	2.925	3.145	2.828	3.199	2.885	3.163	3.217	3.239	3.125	3.239	2.744
1.42	2.439	2.754	3.296	3.280	3.079	3.165	3.021	3.193	3.203	3.239	2.778	3.165	3.008	2.991	2.992	3.146	2.892	3.161	2.776	3.226	2.843	3.182	3.247	3.274	3.136	3.277	2.681
1.50	2.347	2.706	3.339	3.319	3.081	3.179	3.012	3.215	3.227	3.269	2.728	3.180	2.997	2.976	2.977	3.156	2.861	3.175	2.728	3.253	2.803	3.201	3.275	3.308	3.147	3.315	2.625
1.59	2.262	2.662	3.380	3.357	3.082	3.191	3.003	3.236	3.250	3.299	2.680	3.195	2.987	2.962	2.962	3.165	2.831	3.190	2.682	3.278	2.764	3.218	3.303	3.340	3.156	3.352	2.573
1.67	2.184	2.620	3.421	3.395	3.083	3.202	2.994	3.257	3.272	3.328	2.635	3.209	2.976	2.949	2.948	3.173	2.803	3.203	2.638	3.302	2.727	3.234	3.328	3.370	3.165	3.388	2.524
1.75	2.112	2.582	3.461	3.431	3.084	3.213	2.985	3.277	3.294	3.356	2.592	3.222	2.967	2.936	2.933	3.181	2.776	3.216	2.597	3.326	2.691	3.250	3.352	3.398	3.174	3.423	2.480
1.83	2.045	2.546	3.501	3.468	3.085	3.223	2.976	3.297	3.315	3.384	2.551	3.235	2.957	2.924	2.919	3.188	2.749	3.228	2.558	3.348	2.657	3.265	3.376	3.426	3.182	3.457	2.438
1.92	1.983	2.512	3.540	3.503	3.086	3.232	2.968	3.316	3.336	3.410	2.511	3.247	2.948	2.912	2.905	3.194	2.724	3.240	2.521	3.370	2.623	3.279	3.397	3.452	3.190	3.490	2.399
2.00	1.925	2.480	3.579	3.538	3.087	3.240	2.960	3.335	3.357	3.437	2.473	3.259	2.940	2.900	2.892	3.200	2.700	3.251	2.486	3.390	2.591	3.293	3.418	3.476	3.197	3.522	2.363

Table A1: Global Sensitivity Analysis of the torque parameter to reaction rates. Standard TSS conditions as given in chapter 3.

k'/k	R1 CCT	R2 CPT	R5 PSS I	R6 PAP	R7 DGK	R10 PSD	R11 PSS II	R12 EPT	R26 ECT	R29 g3pACT	PLA_2	PLC	PLD	ACT
0.01	8.228	7.971	3.048	1.229	3.229	2.575	4.266	2.594	2.587	34.600	14.641	2.467	1.446	0.523
0.09	7.257	6.112	3.051	2.103	3.213	2.624	4.122	2.674	2.620	8.775	10.688	2.509	1.560	1.372
0.18	6.478	5.227	3.054	2.406	3.198	2.671	3.989	2.738	2.655	6.548	8.484	2.552	1.679	1.704
0.26	5.841	4.685	3.056	2.578	3.184	2.717	3.866	2.791	2.693	5.501	7.075	2.598	1.804	1.929
0.34	5.312	4.310	3.058	2.695	3.169	2.761	3.752	2.837	2.733	4.857	6.095	2.645	1.933	2.109
0.42	4.867	4.029	3.060	2.781	3.156	2.805	3.646	2.878	2.774	4.411	5.372	2.694	2.066	2.264
0.51	4.489	3.810	3.062	2.849	3.143	2.847	3.547	2.914	2.816	4.080	4.816	2.744	2.203	2.403
0.59	4.165	3.632	3.064	2.903	3.130	2.887	3.454	2.947	2.859	3.822	4.375	2.796	2.343	2.531
0.67	3.884	3.483	3.066	2.949	3.118	2.927	3.367	2.976	2.903	3.615	4.015	2.849	2.486	2.652
0.76	3.638	3.357	3.068	2.987	3.106	2.965	3.286	3.004	2.946	3.443	3.717	2.904	2.632	2.765
0.84	3.423	3.248	3.070	3.020	3.094	3.003	3.209	3.029	2.990	3.298	3.465	2.960	2.780	2.874
0.92	3.232	3.152	3.071	3.049	3.083	3.039	3.137	3.052	3.033	3.174	3.249	3.017	2.930	2.978
1.00	3.063	3.068	3.073	3.074	3.072	3.075	3.069	3.074	3.075	3.067	3.062	3.076	3.082	3.079
1.09	2.911	2.992	3.074	3.096	3.061	3.109	3.004	3.094	3.117	2.972	2.898	3.136	3.234	3.176
1.17	2.775	2.924	3.076	3.116	3.051	3.143	2.943	3.113	3.158	2.887	2.754	3.197	3.388	3.270
1.25	2.652	2.862	3.077	3.134	3.041	3.176	2.885	3.132	3.199	2.812	2.625	3.259	3.542	3.362
1.34	2.541	2.806	3.078	3.150	3.031	3.208	2.830	3.149	3.239	2.744	2.510	3.323	3.696	3.451
1.42	2.439	2.754	3.079	3.165	3.021	3.239	2.778	3.165	3.277	2.681	2.406	3.387	3.850	3.538
1.50	2.347	2.706	3.081	3.179	3.012	3.269	2.728	3.180	3.315	2.625	2.312	3.452	4.004	3.623
1.59	2.262	2.662	3.082	3.191	3.003	3.299	2.680	3.195	3.352	2.573	2.226	3.518	4.157	3.706
1.67	2.184	2.620	3.083	3.202	2.994	3.328	2.635	3.209	3.388	2.524	2.148	3.584	4.310	3.788
1.75	2.112	2.582	3.084	3.213	2.985	3.356	2.592	3.222	3.423	2.480	2.076	3.652	4.461	3.868
1.83	2.045	2.546	3.085	3.223	2.976	3.384	2.551	3.235	3.457	2.438	2.009	3.720	4.612	3.946
1.92	1.983	2.512	3.086	3.232	2.968	3.410	2.511	3.247	3.490	2.399	1.948	3.788	4.761	4.023
2.00	1.925	2.480	3.087	3.240	2.960	3.437	2.473	3.259	3.522	2.363	1.891	3.857	4.909	4.098

Table A2: Global Sensitivity Analysis of the torque parameter to 'enzyme class' activities. Standard TSS conditions as given in chapter 3.

k'/k	R1	R2	R3	R4	R5	R6	R7	R8	R9	R10	R11	R12	R13	R14	R15	R16	R17	R18	R19	R20	R21	R22	R23	R24	R25	R26	R29
0.01	51.8	53.1	105.5	108.3	110.8	12.9	103.6	95.6	94.0	92.9	102.4	82.9	98.2	101.4	100.4	25.7	108.1	87.6	101.9	92.1	104.8	90.0	96.4	91.2	93.6	82.5	29.4
0.09	57.0	64.5	104.6	107.0	109.1	42.2	102.9	95.6	94.2	93.3	101.7	86.9	98.0	100.8	100.0	68.7	106.9	88.8	101.3	92.7	104.0	90.9	96.4	92.0	94.0	84.4	87.0
0.18	61.9	71.6	103.7	105.8	107.5	58.1	102.2	95.7	94.5	93.6	101.1	89.3	97.9	100.3	99.6	79.7	105.7	89.8	100.7	93.1	103.1	91.6	96.4	92.6	94.4	86.1	97.8
0.26	66.5	76.7	102.8	104.7	106.0	68.2	101.5	95.8	94.7	93.9	100.5	90.9	97.7	99.8	99.2	85.0	104.6	90.8	100.2	93.6	102.3	92.3	96.3	93.2	94.7	87.7	101.0
0.34	70.9	80.6	102.0	103.6	104.6	75.1	100.8	95.8	94.9	94.2	99.9	92.1	97.5	99.4	98.9	88.2	103.5	91.6	99.7	94.0	101.5	92.9	96.3	93.7	94.9	89.1	101.8
0.42	74.9	83.7	101.2	102.5	103.3	80.2	100.2	95.9	95.1	94.4	99.3	93.0	97.3	98.9	98.5	90.3	102.5	92.3	99.2	94.3	100.7	93.4	96.3	94.2	95.1	90.4	101.6
0.51	78.7	86.3	100.4	101.5	102.1	84.0	99.6	95.9	95.3	94.7	98.8	93.7	97.2	98.5	98.1	91.9	101.5	93.0	98.7	94.6	100.0	93.9	96.2	94.5	95.3	91.5	101.0
0.59	82.2	88.5	99.6	100.5	100.9	87.1	99.0	96.0	95.4	95.0	98.3	94.3	97.0	98.0	97.8	93.0	100.5	93.7	98.2	94.9	99.3	94.3	96.2	94.9	95.5	92.6	100.3
0.67	85.4	90.4	98.9	99.6	99.9	89.6	98.4	96.0	95.6	95.2	97.8	94.8	96.8	97.6	97.4	93.9	99.6	94.2	97.8	95.2	98.6	94.8	96.2	95.2	95.7	93.5	99.5
0.76	88.4	92.1	98.1	98.6	98.8	91.7	97.8	96.0	95.7	95.5	97.4	95.2	96.6	97.2	97.1	94.6	98.6	94.8	97.3	95.5	97.9	95.1	96.2	95.5	95.8	94.3	98.6
0.84	91.2	93.6	97.4	97.8	97.9	93.4	97.2	96.1	95.9	95.7	96.9	95.5	96.4	96.8	96.8	95.2	97.8	95.3	96.9	95.7	97.3	95.5	96.1	95.7	95.9	95.0	97.7
0.92	93.8	95.0	96.7	96.9	96.9	94.9	96.6	96.1	96.0	95.9	96.5	95.8	96.3	96.4	96.4	95.7	96.9	95.7	96.5	95.9	96.7	95.8	96.1	95.9	96.0	95.6	96.9
1.00	96.2	96.2	96.1	96.1	96.1	96.2	96.1	96.1	96.1	96.1	96.1	96.1	96.1	96.1	96.1	96.1	96.1	96.1	96.1	96.1	96.1	96.1	96.1	96.1	96.1	96.1	96.1
1.09	98.5	97.3	95.4	95.3	95.2	97.3	95.5	96.1	96.2	96.3	95.7	96.4	95.9	95.7	95.8	96.5	95.2	96.5	95.7	96.3	95.5	96.4	96.1	96.3	96.2	96.6	95.3
1.17	100.6	98.3	94.8	94.5	94.4	98.3	95.0	96.1	96.3	96.5	95.3	96.6	95.8	95.4	95.4	96.8	94.5	96.9	95.3	96.5	94.9	96.7	96.1	96.5	96.3	97.0	94.5
1.25	102.5	99.2	94.2	93.7	93.7	99.2	94.5	96.2	96.4	96.7	95.0	96.8	95.6	95.1	95.1	97.1	93.7	97.2	95.0	96.6	94.4	96.9	96.1	96.6	96.4	97.4	93.7
1.34	104.3	100.1	93.5	93.0	93.0	99.9	94.0	96.2	96.5	96.9	94.6	96.9	95.4	94.7	94.8	97.3	92.9	97.6	94.6	96.8	93.8	97.2	96.0	96.8	96.4	97.7	93.0
1.42	106.0	100.9	93.0	92.3	92.3	100.6	93.5	96.2	96.6	97.1	94.3	97.1	95.2	94.4	94.5	97.5	92.2	97.9	94.3	97.0	93.3	97.4	96.0	96.9	96.5	98.0	92.3
1.50	107.6	101.7	92.4	91.6	91.6	101.3	93.0	96.2	96.7	97.3	94.0	97.3	95.1	94.1	94.2	97.7	91.5	98.2	93.9	97.1	92.8	97.6	96.0	97.0	96.5	98.3	91.7
1.59	109.0	102.4	91.8	90.9	91.0	101.8	92.5	96.2	96.8	97.4	93.6	97.4	94.9	93.8	93.9	97.9	90.8	98.4	93.6	97.2	92.3	97.8	96.0	97.1	96.6	98.5	91.0
1.67	110.4	103.0	91.3	90.3	90.4	102.4	92.0	96.2	96.9	97.6	93.3	97.5	94.8	93.6	93.6	98.1	90.2	98.7	93.3	97.3	91.8	98.0	96.0	97.2	96.7	98.7	90.4
1.75	111.7	103.6	90.7	89.6	89.8	102.9	91.6	96.2	97.0	97.8	93.1	97.6	94.6	93.3	93.3	98.2	89.5	98.9	93.0	97.5	91.4	98.2	96.0	97.3	96.7	98.9	89.8
1.83	112.9	104.2	90.2	89.0	89.2	103.3	91.1	96.2	97.0	97.9	92.8	97.7	94.5	93.0	93.0	98.3	88.9	99.2	92.7	97.6	90.9	98.3	96.0	97.4	96.7	99.0	89.2
1.92	114.1	104.8	89.7	88.4	88.7	103.7	90.6	96.2	97.1	98.1	92.5	97.8	94.3	92.8	92.7	98.5	88.2	99.4	92.4	97.7	90.5	98.5	96.0	97.5	96.8	99.1	88.7
2.00	115.2	105.3	89.2	87.9	88.2	104.1	90.2	96.3	97.2	98.2	92.2	97.9	94.1	92.5	92.4	98.6	87.6	99.6	92.1	97.8	90.0	98.6	95.9	97.6	96.8	99.2	88.1

Table A3: Global sensitivity analysis of the total lipid to reaction rates. Standard TSS conditions as given in chapter 3.

k'/k	R1 CCT	R2 CPT	R5 PSS I	R6 PAP	R7 DGK	R10 PSD	R11 PSS II	R12 EPT	R26 ECT	R29 g3pACT	PLA_2	PLC	PLD	ACT
0.01	51.77	53.07	110.77	12.85	103.58	92.94	102.43	82.93	82.47	29.36	134.21	101.12	93.13	20.22
0.09	56.99	64.50	109.07	42.24	102.87	93.27	101.75	86.92	84.39	86.95	129.51	101.07	95.28	56.26
0.18	61.92	71.61	107.49	58.14	102.18	93.58	101.10	89.28	86.13	97.84	125.23	100.93	96.88	67.88
0.26	66.54	76.69	106.01	68.16	101.50	93.88	100.49	90.89	87.71	100.99	121.31	100.72	98.02	74.49
0.34	70.87	80.58	104.62	75.08	100.84	94.17	99.90	92.06	89.13	101.77	117.69	100.43	98.76	79.07
0.42	74.91	83.71	103.32	80.16	100.20	94.45	99.34	92.96	90.40	101.61	114.33	100.07	99.16	82.58
0.51	78.68	86.32	102.10	84.04	99.57	94.71	98.81	93.68	91.54	101.04	111.20	99.66	99.27	85.43
0.59	82.18	88.53	100.95	87.12	98.95	94.97	98.31	94.27	92.56	100.29	108.27	99.18	99.15	87.83
0.67	85.43	90.44	99.86	89.61	98.35	95.22	97.82	94.76	93.46	99.45	105.52	98.65	98.81	89.90
0.76	88.44	92.13	98.83	91.68	97.77	95.46	97.36	95.18	94.26	98.59	102.93	98.06	98.31	91.73
0.84	91.24	93.62	97.86	93.41	97.19	95.68	96.92	95.54	94.97	97.73	100.49	97.44	97.67	93.36
0.92	93.84	94.96	96.93	94.90	96.63	95.91	96.49	95.85	95.59	96.88	98.17	96.77	96.91	94.84
1.00	96.25	96.18	96.06	96.18	96.07	96.12	96.08	96.12	96.14	96.06	95.98	96.06	96.05	96.19
1.09	98.49	97.28	95.22	97.30	95.53	96.33	95.69	96.37	96.62	95.26	93.89	95.33	95.13	97.42
1.17	100.57	98.30	94.43	98.28	95.00	96.53	95.32	96.58	97.05	94.49	91.91	94.56	94.14	98.56
1.25	102.50	99.23	93.67	99.16	94.48	96.72	94.96	96.77	97.42	93.75	90.02	93.77	93.12	99.62
1.34	104.31	100.10	92.95	99.94	93.97	96.91	94.61	96.95	97.74	93.03	88.21	92.95	92.06	100.61
1.42	105.99	100.90	92.26	100.64	93.47	97.09	94.27	97.11	98.03	92.34	86.48	92.12	90.97	101.53
1.50	107.57	101.65	91.61	101.27	92.98	97.26	93.95	97.25	98.28	91.68	84.83	91.28	89.88	102.39
1.59	109.04	102.36	90.97	101.85	92.49	97.43	93.64	97.38	98.50	91.03	83.25	90.42	88.78	103.21
1.67	110.42	103.02	90.37	102.37	92.02	97.60	93.34	97.50	98.69	90.41	81.72	89.55	87.67	103.98
1.75	111.72	103.64	89.79	102.85	91.55	97.76	93.05	97.61	98.85	89.81	80.26	88.68	86.57	104.70
1.83	112.93	104.23	89.24	103.29	91.09	97.91	92.77	97.72	99.00	89.23	78.86	87.80	85.48	105.39
1.92	114.08	104.78	88.70	103.70	90.64	98.06	92.50	97.81	99.12	88.67	77.50	86.92	84.40	106.05
2.00	115.16	105.31	88.19	104.08	90.19	98.21	92.24	97.90	99.23	88.12	76.20	86.03	83.33	106.67

Table A4: Global sensitivity analysis of the total lipid to 'enzyme class' activities. Standard TSS conditions as given in chapter 3.

Variation1	$\mathcal{J}$(Rx)	k(Rx)	$k(Rx)_{lower}$	$k(Rx)_{upper}$
R1	16	**16**	0.16	32
R2	8	**0.4**	0.004	0.8
R3	2.281	**0.046**	0.00046	0.092
R4	2.281	**0.046**	0.00046	0.092
R5	2.281	**0.046**	0.00046	0.092
R6	17.628	**17.628**	0.17628	35.256
R7	8	**8**	0.08	16
R8	1.415	**0.118**	0.00118	0.236
R9	1.415	**0.118**	0.00118	0.236
R10	1.415	**0.118**	0.00118	0.236
R11	2.686	**0.09**	0.0009	0.18
R12	8	**0.4**	0.004	0.8
R13	2.686	**0.09**	0.0009	0.18
R14	2.686	**0.09**	0.0009	0.18
R15	17.628	**17.628**	0.17628	35.256
R16	20.884	**83.536**	0.83536	167.072
R17	2.281	**0.046**	0.00046	0.092
R18	1.136	**4.543**	0.04543	9.086
R19	1.415	**0.118**	0.00118	0.236
R20	0.702	**2.81**	0.0281	5.62
R21	2.686	**0.09**	0.0009	0.18
R22	1.338	**5.351**	0.05351	10.702
R23	1.136	**2.271**	0.02271	4.542
R24	0.702	**1.405**	0.01405	2.81
R25	1.338	**2.676**	0.02676	5.352
R26	16	**16**	0.16	32
R27	8	**0.4**	0.004	0.8
R28	8	**0.4**	0.004	0.8
R29	0.09	**0.18**	0.0018	0.36
R30	0.01	**0.01**	0.0001	0.02
R31	0.01	**0.0002**	0.000002	0.0004
R32	0.01	**0.01**	0.0001	0.02
R33	0.01	**0.000333**	3.33E-06	0.000666
R34	0.01	**0.000833**	8.33E-06	0.001667
R35	0.01	**0.02**	0.0002	0.04
R36	0.01	**0.02**	0.0002	0.04
R37	0.01	**0.02**	0.0002	0.04
R38	0.01	**0.02**	0.0002	0.04
R39	0.01	**0.02**	0.0002	0.04
R40	0.15	**0.15**	0.0015	0.3

Table A5: Variation1 Reaction coefficients and scan ranges.
for details of the conditions see main text (table 4.06).

Variation2	J(Rx)	k(Rx)	$k(Rx)_{lower}$	$k(Rx)_{upper}$
R1	16	**16**	0.16	32
R2	8	**0.4**	0.004	0.8
R3	2.281	**0.115**	0.00115	0.23
R4	2.281	**0.115**	0.00115	0.23
R5	2.281	**0.115**	0.00115	0.23
R6	17.628	**17.628**	0.17628	35.256
R7	8	**8**	0.08	16
R8	1.415	**0.118**	0.00118	0.236
R9	1.415	**0.118**	0.00118	0.236
R10	1.415	**0.118**	0.00118	0.236
R11	2.686	**0.0675**	0.000675	0.135
R12	8	**0.4**	0.004	0.8
R13	2.686	**0.0675**	0.000675	0.135
R14	2.686	**0.0675**	0.000675	0.135
R15	17.628	**17.628**	0.17628	35.256
R16	20.884	**83.536**	0.83536	167.072
R17	2.281	**0.115**	0.00115	0.23
R18	1.136	**4.543**	0.04543	9.086
R19	1.415	**0.118**	0.00118	0.236
R20	0.702	**2.81**	0.0281	5.62
R21	2.686	**0.0675**	0.000675	0.135
R22	1.338	**5.351**	0.05351	10.702
R23	1.136	**2.271**	0.02271	4.542
R24	0.702	**1.405**	0.01405	2.81
R25	1.338	**2.676**	0.02676	5.352
R26	16	**16**	0.16	32
R27	8	**0.4**	0.004	0.8
R28	8	**0.4**	0.004	0.8
R29	0.09	**0.18**	0.0018	0.36
R30	0.01	**0.01**	0.0001	0.02
R31	0.01	**0.0005**	0.000005	0.001
R32	0.01	**0.01**	0.0001	0.02
R33	0.01	**0.00025**	2.5E-06	0.0005
R34	0.01	**0.000833**	8.33E-06	0.001667
R35	0.01	**0.02**	0.0002	0.04
R36	0.01	**0.02**	0.0002	0.04
R37	0.01	**0.02**	0.0002	0.04
R38	0.01	**0.02**	0.0002	0.04
R39	0.01	**0.02**	0.0002	0.04
R40	0.15	**0.15**	0.0015	0.3

Table A6: Variation 2 Reaction coefficients and scan ranges.
for details of the conditions see main text (table 4.06).

Variation3	J(Rx)	k(Rx)	$k(Rx)_{lower}$	$k(Rx)_{upper}$
R1	16	**16**	0.16	32
R2	8	**0.4**	0.004	0.8
R3	2.281	**0.046**	0.00046	0.092
R4	2.281	**0.046**	0.00046	0.092
R5	2.281	**0.046**	0.00046	0.092
R6	17.628	**17.628**	0.17628	35.256
R7	8	**8**	0.08	16
R8	1.415	**0.118**	0.00118	0.236
R9	1.415	**0.118**	0.00118	0.236
R10	1.415	**0.118**	0.00118	0.236
R11	2.686	**0.09**	0.0009	0.18
R12	8	**0.4**	0.004	0.8
R13	2.686	**0.09**	0.0009	0.18
R14	2.686	**0.09**	0.0009	0.18
R15	17.628	**17.628**	0.17628	35.256
R16	20.884	**83.536**	0.83536	167.072
R17	2.281	**0.046**	0.00046	0.092
R18	1.136	**0.9086**	0.009086	1.8172
R19	1.415	**0.118**	0.00118	0.236
R20	0.702	**2.81**	0.0281	5.62
R21	2.686	**0.09**	0.0009	0.18
R22	1.338	**5.351**	0.05351	10.702
R23	1.136	**0.4542**	0.004542	0.9084
R24	0.702	**1.405**	0.01405	2.81
R25	1.338	**2.676**	0.02676	5.352
R26	16	**16**	0.16	32
R27	8	**0.4**	0.004	0.8
R28	8	**0.4**	0.004	0.8
R29	0.09	**0.18**	0.0018	0.36
R30	0.01	**0.01**	0.0001	0.02
R31	0.01	**0.0002**	0.000002	0.0004
R32	0.01	**0.01**	0.0001	0.02
R33	0.01	**0.000333**	3.33E-06	0.000666
R34	0.01	**0.000833**	8.33E-06	0.001667
R35	0.01	**0.02**	0.0002	0.04
R36	0.01	**0.02**	0.0002	0.04
R37	0.01	**0.004**	0.00004	0.008
R38	0.01	**0.02**	0.0002	0.04
R39	0.01	**0.02**	0.0002	0.04
R40	0.15	**0.15**	0.0015	0.3

Table A7: Variation 3 Reaction coefficients and scan ranges.
for details of the conditions see main text (table 4.06).

Variation4	$\mathcal{J}$(Rx)	k(Rx)	$k(Rx)_{lower}$	$k(Rx)_{upper}$
R1	16	**16**	0.16	32
R2	8	**8**	0.08	16
R3	2.281	**2.281**	0.02281	4.562
R4	2.281	**2.281**	0.02281	4.562
R5	2.281	**2.281**	0.02281	4.562
R6	17.628	**17.628**	0.17628	35.256
R7	8	**8**	0.08	16
R8	1.415	**1.415**	0.01415	2.83
R9	1.415	**1.415**	0.01415	2.83
R10	1.415	**1.415**	0.01415	2.83
R11	2.686	**2.686**	0.02686	5.372
R12	8	**8**	0.08	16
R13	2.686	**2.686**	0.02686	5.372
R14	2.686	**2.686**	0.02686	5.372
R15	17.628	**17.628**	0.17628	35.256
R16	20.884	**20.884**	0.20884	41.768
R17	2.281	**2.281**	0.02281	4.562
R18	1.136	**1.136**	0.01136	2.272
R19	1.415	**1.415**	0.01415	2.83
R20	0.702	**0.702**	0.00702	1.404
R21	2.686	**2.686**	0.02686	5.372
R22	1.338	**1.338**	0.01338	2.676
R23	1.136	**1.136**	0.01136	2.272
R24	0.702	**0.702**	0.00702	1.404
R25	1.338	**1.338**	0.01338	2.676
R26	16	**16**	0.16	32
R27	8	**8**	0.08	16
R28	8	**8**	0.08	16
R29	0.09	**0.09**	0.0009	0.18
R30	0.01	**0.01**	0.0001	0.02
R31	0.01	**0.01**	0.0001	0.02
R32	0.01	**0.01**	0.0001	0.02
R33	0.01	**0.01**	0.0001	0.02
R34	0.01	**0.01**	0.0001	0.02
R35	0.01	**0.01**	0.0001	0.02
R36	0.01	**0.01**	0.0001	0.02
R37	0.01	**0.01**	0.0001	0.02
R38	0.01	**0.01**	0.0001	0.02
R39	0.01	**0.01**	0.0001	0.02
R40	0.15	**0.15**	0.0015	0.3

Table A8: Variation 4 Reaction coefficients and scan ranges.
for details of the conditions see main text (table 4.06).

Variation5	$\mathcal{J}$(Rx)	k(Rx)	$k(Rx)_{lower}$	$k(Rx)_{upper}$
R1	**16**	16	0.16	32
R2	**8**	0.4	0.004	0.8
R3	**2.457**	0.0491	0.000491	0.0982
R4	**1.228**	0.0246	0.000246	0.0492
R5	**3.685**	0.0737	0.000737	0.1474
R6	**18.491**	18.491	0.18491	36.982
R7	**12**	12	0.12	24
R8	**1.496**	0.1247	0.001247	0.2494
R9	**1.496**	0.1247	0.001247	0.2494
R10	**1.496**	0.1247	0.001247	0.2494
R11	**1.566**	0.0522	0.000522	0.1044
R12	**4**	0.2	0.002	0.4
R13	**1.566**	0.0522	0.000522	0.1044
R14	**1.566**	0.0522	0.000522	0.1044
R15	**18.491**	18.491	0.18491	36.982
R16	**20.701**	82.805	0.82805	165.61
R17	**1.228**	0.02457	0.000246	0.04914
R18	**0.609**	2.437	0.02437	4.874
R19	**1.496**	0.1247	0.001247	0.2494
R20	**0.743**	2.972	0.02972	5.944
R21	**1.566**	0.0522	0.000522	0.1044
R22	**0.778**	3.112	0.03112	6.224
R23	**0.609**	1.218	0.01218	2.436
R24	**0.743**	1.486	0.01486	2.972
R25	**0.778**	1.556	0.01556	3.112
R26	**16**	16	0.16	32
R27	**12**	0.6	0.006	1.2
R28	**8**	0.4	0.004	0.8
R29	**0.09**	0.18	0.0018	0.36
R30	**0.01**	0.01	0.0001	0.02
R31	**0.01**	0.0002	0.000002	0.0004
R32	**0.01**	0.01	0.0001	0.02
R33	**0.01**	0.000333	3.33E-06	0.000667
R34	**0.01**	0.000833	8.33E-06	0.001667
R35	**0.01**	0.02	0.0002	0.04
R36	**0.01**	0.02	0.0002	0.04
R37	**0.01**	0.02	0.0002	0.04
R38	**0.01**	0.02	0.0002	0.04
R39	**0.1**	0.2	0.002	0.4
R40	**0.15**	0.15	0.0015	0.3

Table A9: Variation 5 Reaction coefficients and scan ranges.
for details of the conditions see main text (table 4.06).

k'/k	R1	R2	R3	R4	R5	R6	R7	R8	R9	R10	R11	R12	R13	R14	R15	R16	R17	R18	R19	R20	R21	R22	R23	R24	R25	R26	R29
0.01	6.519	6.367	2.577	2.597	3.262	1.297	3.164	2.677	2.663	2.437	4.723	1.394	3.541	3.577	3.253	0.741	3.778	2.691	4.353	2.516	3.956	2.538	2.345	2.224	2.875	1.344	33.90
0.09	5.939	5.220	2.623	2.642	3.238	2.275	3.154	2.715	2.703	2.498	4.513	1.838	3.494	3.526	3.236	2.056	3.695	2.739	4.183	2.582	3.859	2.608	2.439	2.329	2.901	1.554	8.929
0.18	5.455	4.636	2.669	2.686	3.216	2.567	3.146	2.753	2.741	2.557	4.321	2.111	3.448	3.476	3.219	2.434	3.618	2.782	4.030	2.642	3.767	2.670	2.525	2.425	2.925	1.748	6.633
0.26	5.046	4.265	2.713	2.729	3.196	2.716	3.137	2.789	2.779	2.614	4.147	2.306	3.403	3.428	3.203	2.628	3.547	2.822	3.893	2.699	3.681	2.727	2.602	2.514	2.946	1.926	5.550
0.34	4.695	3.999	2.756	2.771	3.177	2.809	3.129	2.824	2.815	2.671	3.987	2.456	3.361	3.382	3.187	2.748	3.480	2.858	3.767	2.751	3.598	2.778	2.673	2.596	2.965	2.092	4.887
0.42	4.392	3.797	2.799	2.811	3.160	2.874	3.121	2.859	2.850	2.725	3.839	2.578	3.320	3.338	3.172	2.831	3.417	2.892	3.653	2.800	3.520	2.826	2.738	2.672	2.983	2.246	4.429
0.51	4.128	3.635	2.841	2.851	3.144	2.923	3.113	2.892	2.885	2.779	3.703	2.680	3.280	3.295	3.156	2.891	3.358	2.923	3.548	2.846	3.446	2.869	2.798	2.742	2.999	2.389	4.091
0.59	3.896	3.502	2.881	2.890	3.130	2.961	3.106	2.924	2.918	2.831	3.577	2.767	3.242	3.254	3.141	2.938	3.303	2.952	3.452	2.889	3.375	2.909	2.853	2.807	3.014	2.523	3.828
0.67	3.691	3.390	2.921	2.928	3.116	2.991	3.098	2.955	2.951	2.882	3.460	2.843	3.205	3.214	3.126	2.974	3.250	2.979	3.363	2.930	3.308	2.947	2.904	2.868	3.027	2.648	3.617
0.76	3.508	3.293	2.960	2.966	3.103	3.016	3.091	2.986	2.982	2.931	3.351	2.910	3.169	3.176	3.112	3.004	3.201	3.005	3.281	2.969	3.244	2.981	2.951	2.924	3.039	2.765	3.444
0.84	3.344	3.208	2.998	3.002	3.092	3.038	3.084	3.015	3.013	2.980	3.250	2.970	3.134	3.139	3.098	3.028	3.154	3.029	3.204	3.005	3.182	3.014	2.994	2.977	3.051	2.875	3.298
0.92	3.196	3.134	3.036	3.038	3.080	3.056	3.077	3.044	3.043	3.027	3.155	3.024	3.101	3.103	3.084	3.049	3.110	3.051	3.133	3.040	3.124	3.044	3.035	3.027	3.061	2.979	3.173
1.00	3.063	3.067	3.073	3.073	3.070	3.071	3.070	3.072	3.072	3.073	3.065	3.073	3.069	3.068	3.070	3.067	3.068	3.072	3.067	3.072	3.067	3.072	3.073	3.073	3.071	3.076	3.064
1.09	2.942	3.007	3.109	3.107	3.060	3.085	3.064	3.100	3.101	3.118	2.981	3.119	3.037	3.035	3.056	3.082	3.028	3.092	3.004	3.104	3.013	3.099	3.108	3.117	3.080	3.168	2.969
1.17	2.831	2.952	3.144	3.140	3.051	3.097	3.057	3.126	3.129	3.163	2.903	3.160	3.007	3.002	3.043	3.096	2.990	3.110	2.946	3.133	2.961	3.124	3.141	3.158	3.089	3.255	2.885
1.25	2.730	2.902	3.179	3.173	3.042	3.108	3.051	3.152	3.156	3.206	2.828	3.199	2.977	2.971	3.030	3.107	2.954	3.128	2.891	3.162	2.912	3.147	3.172	3.197	3.097	3.338	2.810
1.34	2.637	2.856	3.213	3.205	3.034	3.118	3.044	3.177	3.182	3.248	2.758	3.235	2.949	2.940	3.017	3.118	2.919	3.145	2.840	3.189	2.864	3.170	3.202	3.234	3.104	3.416	2.742
1.42	2.551	2.814	3.246	3.236	3.026	3.126	3.038	3.202	3.208	3.289	2.691	3.268	2.921	2.911	3.004	3.127	2.886	3.161	2.791	3.214	2.818	3.191	3.229	3.269	3.111	3.490	2.680
1.50	2.472	2.774	3.279	3.267	3.019	3.134	3.032	3.226	3.233	3.329	2.628	3.300	2.894	2.882	2.991	3.135	2.855	3.176	2.745	3.239	2.774	3.211	3.255	3.301	3.118	3.560	2.624
1.59	2.398	2.738	3.311	3.297	3.012	3.142	3.026	3.249	3.258	3.369	2.568	3.329	2.868	2.854	2.979	3.143	2.825	3.190	2.701	3.263	2.731	3.230	3.280	3.333	3.124	3.626	2.573
1.67	2.330	2.704	3.342	3.327	3.005	3.148	3.021	3.272	3.282	3.408	2.512	3.357	2.843	2.827	2.967	3.150	2.796	3.204	2.660	3.285	2.690	3.248	3.303	3.362	3.129	3.690	2.525
1.75	2.266	2.672	3.373	3.355	2.998	3.154	3.015	3.295	3.305	3.445	2.458	3.383	2.818	2.801	2.955	3.156	2.768	3.217	2.621	3.307	2.650	3.265	3.325	3.391	3.135	3.750	2.481
1.83	2.207	2.642	3.404	3.384	2.992	3.160	3.009	3.316	3.328	3.482	2.406	3.408	2.794	2.775	2.943	3.162	2.741	3.230	2.583	3.328	2.612	3.281	3.346	3.417	3.140	3.808	2.440
1.92	2.151	2.613	3.433	3.412	2.987	3.165	3.004	3.338	3.350	3.519	2.357	3.432	2.771	2.751	2.931	3.167	2.716	3.242	2.548	3.348	2.575	3.297	3.366	3.443	3.145	3.863	2.402
2.00	2.099	2.586	3.463	3.439	2.981	3.170	2.998	3.358	3.372	3.554	2.310	3.455	2.748	2.726	2.920	3.172	2.691	3.253	2.514	3.367	2.539	3.312	3.385	3.467	3.150	3.916	2.366

Table A10: Variation 1: Global Sensitivity Analysis of the torque parameter to reaction rates.

k'/k	R1	R2	R3	R4	R5	R6	R7	R8	R9	R10	R11	R12	R13	R14	R15	R16	R17	R18	R19	R20	R21	R22	R23	R24	R25	R26	R29
0.01	9.711	9.456	3.370	3.413	4.249	1.374	4.316	3.585	3.555	3.387	5.891	3.140	4.473	4.540	4.422	0.823	5.255	3.529	6.272	3.267	5.326	3.408	3.030	2.876	3.674	3.117	52.16
0.09	8.738	7.543	3.439	3.478	4.232	2.710	4.296	3.637	3.610	3.457	5.673	3.352	4.435	4.495	4.392	2.538	5.117	3.601	5.968	3.364	5.190	3.498	3.168	3.025	3.733	3.213	13.19
0.18	7.932	6.588	3.506	3.542	4.216	3.169	4.276	3.688	3.662	3.526	5.472	3.497	4.398	4.452	4.364	3.095	4.990	3.667	5.699	3.454	5.062	3.580	3.293	3.164	3.785	3.306	9.532
0.26	7.257	5.986	3.572	3.605	4.202	3.423	4.257	3.736	3.714	3.592	5.287	3.608	4.363	4.411	4.336	3.394	4.873	3.727	5.461	3.539	4.942	3.654	3.408	3.292	3.833	3.397	7.833
0.34	6.683	5.561	3.637	3.667	4.189	3.591	4.239	3.783	3.763	3.657	5.117	3.699	4.330	4.372	4.309	3.584	4.763	3.783	5.247	3.618	4.828	3.722	3.513	3.411	3.876	3.486	6.810
0.42	6.192	5.240	3.700	3.727	4.177	3.713	4.221	3.829	3.812	3.719	4.958	3.775	4.298	4.334	4.282	3.716	4.661	3.835	5.055	3.693	4.721	3.785	3.609	3.522	3.915	3.573	6.115
0.51	5.767	4.985	3.763	3.786	4.165	3.807	4.204	3.873	3.858	3.781	4.811	3.841	4.267	4.298	4.256	3.814	4.567	3.883	4.880	3.763	4.619	3.843	3.699	3.624	3.951	3.657	5.607
0.59	5.397	4.777	3.824	3.843	4.154	3.883	4.187	3.916	3.904	3.840	4.673	3.898	4.238	4.263	4.230	3.890	4.478	3.927	4.722	3.829	4.523	3.896	3.781	3.720	3.984	3.740	5.217
0.67	5.072	4.602	3.884	3.900	4.145	3.945	4.171	3.958	3.948	3.898	4.545	3.950	4.210	4.230	4.205	3.950	4.394	3.969	4.577	3.892	4.431	3.946	3.858	3.810	4.014	3.820	4.906
0.76	4.786	4.452	3.943	3.955	4.135	3.997	4.155	3.999	3.991	3.954	4.424	3.996	4.183	4.198	4.181	4.000	4.316	4.009	4.445	3.952	4.344	3.992	3.929	3.893	4.041	3.897	4.652
0.84	4.531	4.322	4.001	4.009	4.126	4.041	4.140	4.038	4.033	4.009	4.311	4.039	4.158	4.167	4.156	4.040	4.242	4.045	4.322	4.009	4.261	4.035	3.995	3.972	4.067	3.972	4.440
0.92	4.303	4.207	4.058	4.062	4.118	4.079	4.125	4.076	4.074	4.062	4.205	4.077	4.133	4.138	4.133	4.075	4.173	4.080	4.209	4.063	4.182	4.075	4.057	4.046	4.090	4.045	4.258
1.00	4.099	4.105	4.114	4.114	4.110	4.113	4.110	4.113	4.113	4.114	4.105	4.113	4.110	4.109	4.110	4.105	4.107	4.113	4.105	4.114	4.106	4.113	4.114	4.115	4.112	4.115	4.102
1.09	3.915	4.013	4.169	4.165	4.103	4.142	4.096	4.149	4.152	4.165	4.011	4.146	4.087	4.082	4.087	4.130	4.045	4.144	4.008	4.163	4.034	4.149	4.168	4.180	4.133	4.183	3.965
1.17	3.748	3.931	4.223	4.215	4.096	4.169	4.082	4.184	4.189	4.214	3.921	4.177	4.065	4.055	4.064	4.153	3.986	4.173	3.917	4.210	3.965	4.182	4.219	4.242	4.151	4.249	3.844
1.25	3.597	3.855	4.276	4.264	4.090	4.192	4.068	4.218	4.226	4.262	3.837	4.206	4.044	4.030	4.042	4.173	3.930	4.201	3.832	4.254	3.899	4.214	4.267	4.300	4.169	4.312	3.736
1.34	3.458	3.786	4.329	4.312	4.083	4.214	4.055	4.251	4.262	4.309	3.757	4.233	4.024	4.005	4.021	4.190	3.877	4.227	3.753	4.297	3.836	4.244	4.312	4.355	4.186	4.373	3.639
1.42	3.332	3.722	4.380	4.359	4.078	4.233	4.042	4.284	4.296	4.355	3.680	4.258	4.004	3.981	4.000	4.206	3.826	4.252	3.679	4.338	3.775	4.272	4.354	4.408	4.201	4.432	3.552
1.50	3.215	3.664	4.430	4.405	4.072	4.251	4.030	4.315	4.330	4.400	3.608	4.282	3.985	3.958	3.979	4.220	3.778	4.276	3.609	4.378	3.716	4.299	4.395	4.457	4.216	4.488	3.472
1.59	3.108	3.609	4.480	4.450	4.067	4.267	4.017	4.346	4.363	4.444	3.539	4.305	3.967	3.936	3.958	4.233	3.731	4.299	3.543	4.415	3.660	4.325	4.433	4.505	4.230	4.543	3.398
1.67	3.009	3.558	4.529	4.494	4.062	4.282	4.005	4.376	4.396	4.486	3.474	4.327	3.950	3.914	3.938	4.245	3.687	4.321	3.480	4.452	3.606	4.349	4.469	4.549	4.243	4.596	3.331
1.75	2.917	3.510	4.576	4.538	4.057	4.295	3.993	4.405	4.427	4.528	3.411	4.348	3.933	3.893	3.918	4.256	3.645	4.341	3.422	4.486	3.554	4.373	4.503	4.592	4.255	4.647	3.268
1.83	2.831	3.466	4.624	4.580	4.052	4.308	3.982	4.433	4.458	4.569	3.351	4.367	3.917	3.873	3.899	4.265	3.605	4.361	3.366	4.520	3.504	4.395	4.535	4.633	4.267	4.696	3.210
1.92	2.751	3.424	4.670	4.622	4.048	4.320	3.970	4.461	4.488	4.609	3.294	4.386	3.901	3.853	3.879	4.274	3.566	4.380	3.313	4.552	3.455	4.416	4.566	4.672	4.278	4.743	3.156
2.00	2.677	3.384	4.715	4.663	4.043	4.331	3.959	4.487	4.517	4.648	3.239	4.404	3.886	3.834	3.860	4.283	3.529	4.399	3.263	4.584	3.409	4.436	4.596	4.709	4.288	4.788	3.105

Table A11: Variation 2: Global Sensitivity Analysis of the torque parameter to reaction rates.

k'/k	R1	R2	R3	R4	R5	R6	R7	R8	R9	R10	R11	R12	R13	R14	R15	R16	R17	R18	R19	R20	R21	R22	R23	R24	R25	R26	R29
0.01	8.038	7.455	1.186	1.195	1.278	1.064	1.620	1.480	1.472	1.359	2.006	1.064	1.811	1.827	1.619	0.594	3.707	1.090	1.867	1.396	1.843	1.381	0.880	1.312	1.550	1.056	24.11
0.09	6.067	4.363	1.219	1.228	1.306	1.292	1.614	1.489	1.481	1.380	1.956	1.155	1.783	1.798	1.614	1.232	3.272	1.139	1.833	1.417	1.814	1.406	0.948	1.348	1.551	1.095	5.357
0.18	4.852	3.349	1.252	1.260	1.334	1.366	1.609	1.497	1.490	1.400	1.910	1.224	1.757	1.770	1.609	1.367	2.938	1.186	1.801	1.437	1.787	1.428	1.015	1.379	1.553	1.135	3.764
0.26	4.029	2.823	1.284	1.292	1.360	1.412	1.604	1.505	1.499	1.420	1.866	1.279	1.732	1.744	1.605	1.431	2.673	1.230	1.771	1.455	1.760	1.448	1.079	1.408	1.554	1.177	3.053
0.34	3.438	2.493	1.317	1.323	1.385	1.445	1.599	1.513	1.508	1.438	1.825	1.326	1.709	1.720	1.600	1.469	2.457	1.273	1.742	1.471	1.735	1.466	1.141	1.433	1.556	1.219	2.634
0.42	2.993	2.263	1.349	1.355	1.410	1.471	1.594	1.521	1.516	1.456	1.786	1.367	1.688	1.697	1.595	1.495	2.278	1.315	1.716	1.486	1.711	1.482	1.201	1.455	1.557	1.261	2.353
0.51	2.648	2.091	1.380	1.386	1.435	1.492	1.590	1.528	1.524	1.474	1.749	1.404	1.667	1.675	1.591	1.513	2.128	1.355	1.690	1.500	1.687	1.497	1.259	1.476	1.559	1.305	2.150
0.59	2.372	1.957	1.412	1.417	1.458	1.509	1.585	1.535	1.531	1.490	1.714	1.437	1.648	1.654	1.586	1.527	1.999	1.393	1.667	1.513	1.665	1.511	1.315	1.494	1.560	1.348	1.995
0.67	2.148	1.849	1.444	1.447	1.481	1.524	1.581	1.541	1.539	1.507	1.681	1.467	1.629	1.634	1.582	1.538	1.888	1.430	1.644	1.525	1.643	1.524	1.369	1.511	1.561	1.392	1.873
0.76	1.962	1.759	1.475	1.478	1.503	1.537	1.577	1.548	1.546	1.522	1.649	1.495	1.612	1.615	1.578	1.547	1.791	1.466	1.623	1.536	1.623	1.535	1.422	1.527	1.562	1.436	1.774
0.84	1.806	1.684	1.506	1.508	1.525	1.548	1.573	1.554	1.553	1.537	1.619	1.520	1.595	1.598	1.573	1.554	1.705	1.501	1.602	1.547	1.602	1.546	1.472	1.541	1.563	1.480	1.692
0.92	1.673	1.619	1.537	1.538	1.546	1.557	1.569	1.560	1.559	1.552	1.591	1.544	1.579	1.581	1.569	1.560	1.629	1.535	1.583	1.557	1.583	1.556	1.521	1.554	1.564	1.524	1.622
1.00	1.559	1.562	1.567	1.567	1.567	1.566	1.565	1.566	1.566	1.566	1.564	1.567	1.565	1.564	1.565	1.566	1.562	1.567	1.564	1.566	1.564	1.566	1.568	1.566	1.565	1.568	1.562
1.09	1.460	1.512	1.598	1.597	1.587	1.574	1.562	1.571	1.572	1.580	1.538	1.588	1.550	1.549	1.561	1.570	1.501	1.599	1.547	1.575	1.546	1.575	1.614	1.577	1.566	1.611	1.510
1.17	1.373	1.468	1.628	1.626	1.606	1.580	1.558	1.577	1.578	1.593	1.513	1.608	1.537	1.534	1.557	1.574	1.445	1.630	1.530	1.583	1.529	1.583	1.658	1.588	1.567	1.654	1.464
1.25	1.297	1.428	1.658	1.654	1.625	1.587	1.555	1.582	1.584	1.606	1.489	1.626	1.524	1.520	1.553	1.578	1.395	1.659	1.514	1.591	1.512	1.591	1.701	1.597	1.568	1.697	1.423
1.34	1.229	1.392	1.688	1.683	1.644	1.592	1.551	1.587	1.589	1.619	1.467	1.644	1.511	1.507	1.549	1.581	1.350	1.688	1.498	1.598	1.495	1.598	1.742	1.606	1.569	1.739	1.387
1.42	1.168	1.360	1.717	1.711	1.662	1.597	1.548	1.592	1.595	1.631	1.445	1.661	1.500	1.494	1.545	1.583	1.308	1.717	1.484	1.605	1.480	1.605	1.783	1.615	1.570	1.781	1.354
1.50	1.114	1.330	1.746	1.739	1.680	1.602	1.545	1.596	1.600	1.643	1.424	1.677	1.488	1.481	1.541	1.586	1.269	1.744	1.469	1.611	1.464	1.612	1.822	1.622	1.570	1.822	1.325
1.59	1.065	1.302	1.776	1.767	1.697	1.606	1.542	1.601	1.605	1.654	1.404	1.693	1.478	1.469	1.538	1.588	1.234	1.770	1.456	1.618	1.449	1.618	1.859	1.630	1.571	1.862	1.298
1.67	1.020	1.277	1.805	1.795	1.714	1.610	1.539	1.605	1.610	1.666	1.385	1.708	1.467	1.458	1.534	1.590	1.201	1.796	1.443	1.624	1.435	1.624	1.896	1.637	1.572	1.902	1.273
1.75	0.980	1.254	1.833	1.822	1.731	1.614	1.536	1.609	1.615	1.676	1.367	1.722	1.457	1.447	1.530	1.592	1.170	1.822	1.430	1.629	1.421	1.629	1.932	1.643	1.572	1.941	1.250
1.83	0.943	1.232	1.862	1.849	1.747	1.618	1.533	1.614	1.620	1.687	1.349	1.735	1.448	1.436	1.527	1.593	1.142	1.846	1.418	1.635	1.407	1.635	1.966	1.649	1.573	1.979	1.229
1.92	0.909	1.212	1.890	1.876	1.762	1.621	1.530	1.618	1.624	1.697	1.332	1.749	1.439	1.426	1.523	1.595	1.115	1.870	1.406	1.640	1.394	1.640	2.000	1.655	1.573	2.017	1.209
2.00	0.877	1.193	1.918	1.903	1.778	1.624	1.528	1.621	1.629	1.707	1.315	1.761	1.430	1.416	1.520	1.596	1.091	1.893	1.395	1.645	1.381	1.645	2.032	1.661	1.574	2.054	1.191

Table A12: Variation 3: Global Sensitivity Analysis of the torque parameter to reaction rates.

k'/k	R1	R2	R3	R4	R5	R6	R7	R8	R9	R10	R11	R12	R13	R14	R15	R16	R17	R18	R19	R20	R21	R22	R23	R24	R25	R26	R29
0.01	2.300	2.234	0.683	0.693	0.954	0.703	0.920	0.703	0.696	0.779	1.049	1.679	0.704	0.717	0.940	0.280	1.149	0.720	1.389	0.669	1.017	0.767	0.607	0.564	0.666	1.709	73.78
0.09	2.048	1.737	0.698	0.708	0.942	0.665	0.913	0.718	0.712	0.786	1.026	1.421	0.718	0.730	0.932	0.519	1.112	0.736	1.309	0.690	0.999	0.778	0.637	0.599	0.691	1.582	6.344
0.18	1.838	1.487	0.714	0.723	0.931	0.686	0.907	0.733	0.727	0.793	1.004	1.276	0.732	0.743	0.924	0.625	1.078	0.752	1.240	0.710	0.982	0.789	0.666	0.630	0.714	1.471	3.313
0.26	1.661	1.330	0.729	0.737	0.921	0.712	0.901	0.747	0.741	0.801	0.984	1.179	0.745	0.756	0.916	0.688	1.047	0.766	1.179	0.728	0.966	0.798	0.692	0.660	0.735	1.372	2.320
0.34	1.511	1.221	0.744	0.752	0.911	0.737	0.895	0.760	0.755	0.808	0.965	1.108	0.759	0.768	0.909	0.731	1.019	0.779	1.126	0.746	0.950	0.807	0.716	0.688	0.754	1.285	1.830
0.42	1.383	1.138	0.759	0.766	0.903	0.760	0.889	0.774	0.769	0.814	0.948	1.053	0.772	0.780	0.902	0.761	0.993	0.791	1.079	0.762	0.936	0.815	0.738	0.714	0.771	1.207	1.539
0.51	1.273	1.073	0.773	0.780	0.894	0.779	0.884	0.787	0.783	0.821	0.932	1.009	0.785	0.792	0.895	0.785	0.969	0.802	1.037	0.778	0.923	0.822	0.759	0.739	0.786	1.139	1.346
0.59	1.178	1.021	0.788	0.793	0.887	0.796	0.879	0.799	0.796	0.827	0.917	0.973	0.797	0.804	0.888	0.803	0.947	0.813	0.999	0.793	0.910	0.829	0.778	0.761	0.801	1.077	1.207
0.67	1.095	0.977	0.802	0.806	0.880	0.812	0.874	0.811	0.809	0.833	0.903	0.943	0.810	0.815	0.881	0.818	0.926	0.822	0.965	0.807	0.898	0.835	0.796	0.783	0.814	1.023	1.102
0.76	1.023	0.940	0.816	0.819	0.873	0.825	0.869	0.823	0.821	0.840	0.890	0.916	0.822	0.826	0.875	0.830	0.906	0.832	0.933	0.820	0.887	0.841	0.813	0.803	0.826	0.974	1.020
0.84	0.959	0.908	0.830	0.832	0.867	0.837	0.865	0.835	0.833	0.845	0.878	0.894	0.834	0.836	0.868	0.841	0.888	0.841	0.905	0.833	0.876	0.847	0.829	0.822	0.837	0.930	0.954
0.92	0.903	0.880	0.844	0.845	0.862	0.847	0.860	0.846	0.845	0.851	0.867	0.873	0.846	0.847	0.862	0.849	0.871	0.849	0.879	0.845	0.866	0.852	0.843	0.840	0.847	0.890	0.900
1.00	0.854	0.855	0.857	0.857	0.856	0.857	0.856	0.857	0.857	0.857	0.856	0.855	0.857	0.857	0.856	0.857	0.856	0.857	0.855	0.857	0.856	0.857	0.857	0.857	0.857	0.854	0.854
1.09	0.810	0.833	0.871	0.869	0.851	0.866	0.852	0.868	0.869	0.862	0.846	0.839	0.868	0.867	0.850	0.863	0.841	0.864	0.833	0.868	0.847	0.861	0.870	0.874	0.866	0.822	0.815
1.17	0.770	0.813	0.884	0.881	0.846	0.873	0.848	0.878	0.880	0.868	0.836	0.825	0.880	0.877	0.844	0.869	0.826	0.871	0.812	0.879	0.838	0.866	0.882	0.889	0.874	0.793	0.780
1.25	0.735	0.795	0.897	0.893	0.842	0.881	0.844	0.888	0.891	0.873	0.827	0.812	0.891	0.886	0.839	0.874	0.813	0.878	0.793	0.889	0.829	0.870	0.894	0.903	0.882	0.766	0.750
1.34	0.703	0.779	0.909	0.904	0.837	0.887	0.841	0.898	0.901	0.878	0.818	0.799	0.901	0.895	0.833	0.879	0.801	0.885	0.776	0.899	0.821	0.874	0.905	0.917	0.890	0.742	0.724
1.42	0.674	0.764	0.922	0.916	0.833	0.893	0.837	0.908	0.912	0.883	0.810	0.788	0.912	0.904	0.828	0.883	0.789	0.891	0.759	0.909	0.813	0.877	0.915	0.930	0.896	0.719	0.700
1.50	0.648	0.750	0.934	0.927	0.829	0.899	0.834	0.917	0.922	0.888	0.802	0.778	0.922	0.913	0.823	0.887	0.777	0.897	0.744	0.918	0.806	0.881	0.925	0.943	0.903	0.699	0.679
1.59	0.624	0.737	0.947	0.937	0.826	0.904	0.830	0.927	0.932	0.892	0.795	0.768	0.932	0.922	0.817	0.890	0.767	0.902	0.729	0.927	0.799	0.884	0.934	0.954	0.909	0.680	0.659
1.67	0.603	0.725	0.959	0.948	0.822	0.909	0.827	0.935	0.942	0.897	0.788	0.760	0.942	0.930	0.812	0.893	0.756	0.908	0.716	0.935	0.792	0.887	0.943	0.966	0.915	0.663	0.642
1.75	0.583	0.714	0.970	0.958	0.819	0.913	0.824	0.944	0.951	0.901	0.781	0.751	0.952	0.939	0.807	0.896	0.747	0.913	0.703	0.943	0.785	0.890	0.951	0.977	0.920	0.647	0.626
1.83	0.564	0.704	0.982	0.969	0.816	0.917	0.821	0.953	0.961	0.906	0.775	0.744	0.962	0.947	0.802	0.899	0.737	0.918	0.691	0.951	0.779	0.893	0.959	0.987	0.925	0.632	0.611
1.92	0.548	0.694	0.994	0.979	0.813	0.921	0.818	0.961	0.970	0.910	0.769	0.736	0.971	0.955	0.798	0.901	0.728	0.922	0.679	0.959	0.773	0.896	0.967	0.997	0.930	0.619	0.597
2.00	0.532	0.685	1.005	0.989	0.810	0.925	0.815	0.969	0.979	0.914	0.763	0.729	0.981	0.962	0.793	0.903	0.720	0.927	0.669	0.966	0.767	0.899	0.974	1.006	0.935	0.606	0.584

Table A13: Variation 4: Global Sensitivity Analysis of the torque parameter to reaction rates.

k'/k	R1	R2	R3	R4	R5	R6	R7	R8	R9	R10	R11	R12	R13	R14	R15	R16	R17	R18	R19	R20	R21	R22	R23	R24	R25	R26	R29
0.01	9.717	9.348	2.370	2.755	2.628	1.160	3.352	2.751	2.723	2.418	3.854	2.260	3.413	3.449	3.327	0.665	3.869	2.608	4.521	2.470	3.970	2.570	2.381	2.214	2.783	2.255	33.36
0.09	8.337	6.791	2.432	2.783	2.690	1.970	3.323	2.783	2.757	2.484	3.767	2.378	3.377	3.409	3.304	1.913	3.782	2.669	4.327	2.541	3.869	2.635	2.469	2.321	2.823	2.340	8.951
0.18	7.276	5.649	2.494	2.811	2.746	2.293	3.296	2.814	2.791	2.547	3.686	2.479	3.343	3.371	3.281	2.326	3.700	2.724	4.153	2.607	3.774	2.693	2.549	2.419	2.858	2.422	6.736
0.26	6.437	4.974	2.556	2.838	2.795	2.489	3.270	2.844	2.823	2.608	3.610	2.568	3.310	3.335	3.258	2.548	3.622	2.773	3.996	2.668	3.685	2.747	2.622	2.510	2.891	2.500	5.654
0.34	5.759	4.516	2.617	2.866	2.839	2.626	3.245	2.873	2.855	2.668	3.537	2.646	3.279	3.301	3.236	2.690	3.548	2.819	3.855	2.725	3.602	2.796	2.690	2.593	2.920	2.575	4.977
0.42	5.202	4.181	2.677	2.893	2.879	2.729	3.221	2.902	2.886	2.725	3.468	2.716	3.250	3.268	3.214	2.789	3.478	2.860	3.726	2.779	3.523	2.841	2.752	2.671	2.946	2.646	4.504
0.51	4.737	3.922	2.737	2.920	2.916	2.810	3.198	2.929	2.915	2.781	3.403	2.781	3.221	3.237	3.193	2.862	3.412	2.899	3.608	2.830	3.448	2.883	2.809	2.742	2.970	2.715	4.152
0.59	4.344	3.714	2.795	2.947	2.949	2.875	3.175	2.956	2.944	2.834	3.342	2.840	3.194	3.207	3.173	2.918	3.349	2.934	3.501	2.877	3.377	2.921	2.863	2.809	2.992	2.782	3.877
0.67	4.010	3.543	2.854	2.974	2.979	2.929	3.154	2.982	2.973	2.886	3.283	2.894	3.169	3.179	3.152	2.963	3.289	2.967	3.401	2.922	3.310	2.957	2.912	2.870	3.012	2.846	3.655
0.76	3.723	3.398	2.911	3.000	3.007	2.975	3.133	3.007	3.000	2.937	3.227	2.945	3.144	3.151	3.133	3.000	3.231	2.998	3.310	2.964	3.247	2.990	2.958	2.928	3.030	2.907	3.472
0.84	3.474	3.274	2.968	3.026	3.032	3.015	3.114	3.031	3.027	2.986	3.173	2.992	3.120	3.125	3.113	3.030	3.176	3.026	3.225	3.005	3.186	3.022	3.001	2.982	3.047	2.967	3.317
0.92	3.257	3.166	3.025	3.052	3.056	3.049	3.094	3.055	3.053	3.033	3.123	3.037	3.097	3.100	3.094	3.056	3.124	3.053	3.146	3.043	3.129	3.051	3.041	3.032	3.063	3.024	3.185
1.00	3.066	3.071	3.080	3.078	3.078	3.078	3.076	3.078	3.078	3.080	3.074	3.079	3.076	3.075	3.076	3.078	3.074	3.078	3.073	3.079	3.074	3.078	3.079	3.080	3.078	3.080	3.070
1.09	2.898	2.987	3.135	3.104	3.098	3.105	3.058	3.101	3.103	3.124	3.027	3.119	3.055	3.052	3.057	3.097	3.026	3.102	3.004	3.113	3.021	3.104	3.114	3.124	3.091	3.134	2.969
1.17	2.749	2.911	3.189	3.130	3.117	3.128	3.040	3.122	3.127	3.168	2.983	3.157	3.034	3.030	3.040	3.114	2.980	3.124	2.940	3.146	2.971	3.129	3.147	3.166	3.104	3.186	2.880
1.25	2.616	2.843	3.243	3.155	3.135	3.150	3.023	3.144	3.150	3.210	2.940	3.193	3.015	3.008	3.022	3.129	2.936	3.145	2.879	3.177	2.923	3.152	3.179	3.205	3.116	3.237	2.800
1.34	2.497	2.781	3.296	3.180	3.152	3.169	3.007	3.164	3.173	3.251	2.899	3.227	2.996	2.987	3.005	3.142	2.893	3.165	2.823	3.207	2.877	3.174	3.208	3.242	3.127	3.285	2.727
1.42	2.390	2.724	3.348	3.205	3.168	3.186	2.991	3.184	3.196	3.291	2.860	3.260	2.978	2.967	2.988	3.153	2.852	3.183	2.769	3.236	2.833	3.194	3.236	3.278	3.137	3.333	2.662
1.50	2.294	2.671	3.399	3.230	3.182	3.202	2.975	3.204	3.217	3.330	2.822	3.292	2.961	2.948	2.971	3.164	2.813	3.201	2.719	3.263	2.790	3.214	3.262	3.311	3.147	3.379	2.602
1.59	2.207	2.623	3.450	3.254	3.196	3.216	2.960	3.223	3.239	3.368	2.786	3.322	2.944	2.929	2.955	3.174	2.775	3.218	2.671	3.290	2.750	3.233	3.287	3.342	3.156	3.424	2.547
1.67	2.128	2.578	3.500	3.279	3.209	3.229	2.946	3.241	3.259	3.405	2.751	3.351	2.928	2.911	2.939	3.182	2.739	3.234	2.626	3.315	2.711	3.250	3.311	3.372	3.165	3.468	2.496
1.75	2.056	2.537	3.550	3.303	3.221	3.242	2.931	3.260	3.279	3.441	2.718	3.379	2.912	2.893	2.923	3.190	2.704	3.249	2.583	3.339	2.673	3.267	3.333	3.401	3.173	3.510	2.449
1.83	1.990	2.498	3.598	3.327	3.233	3.253	2.917	3.277	3.299	3.476	2.685	3.406	2.897	2.876	2.908	3.197	2.670	3.264	2.543	3.362	2.637	3.283	3.355	3.428	3.181	3.551	2.405
1.92	1.929	2.461	3.647	3.351	3.244	3.263	2.904	3.294	3.318	3.511	2.654	3.432	2.882	2.860	2.892	3.204	2.637	3.278	2.504	3.384	2.602	3.299	3.375	3.454	3.188	3.592	2.364
2.00	1.874	2.427	3.694	3.375	3.255	3.273	2.890	3.311	3.337	3.544	2.624	3.457	2.868	2.844	2.877	3.210	2.606	3.291	2.467	3.406	2.568	3.314	3.395	3.479	3.195	3.631	2.326

Table A14: variation 5: Global Sensitivity Analysis of the torque parameter to reaction rates.

$k(R1)'/k(R1)_{TSS}$	Stdrd	Var1	Var2	Var3	Var4	Var5
0.01	8.26	6.52	7.27	15.78	8.26	9.72
0.09	7.29	5.94	6.54	11.91	7.36	8.34
0.18	6.50	5.45	5.94	9.52	6.60	7.28
0.26	5.86	5.05	5.43	7.91	5.97	6.44
0.34	5.33	4.70	5.00	6.75	5.43	5.76
0.42	4.88	4.39	4.63	5.88	4.97	5.20
0.51	4.50	4.13	4.32	5.20	4.57	4.74
0.59	4.17	3.90	4.04	4.66	4.23	4.34
0.67	3.89	3.69	3.80	4.22	3.93	4.01
0.76	3.65	3.51	3.58	3.85	3.67	3.72
0.84	3.43	3.34	3.39	3.55	3.45	3.47
0.92	3.24	3.20	3.22	3.28	3.24	3.26
1.00	3.07	3.06	3.07	3.06	3.07	3.07
1.09	2.92	2.94	2.93	2.87	2.91	2.90
1.17	2.78	2.83	2.81	2.70	2.77	2.75
1.25	2.66	2.73	2.69	2.55	2.64	2.62
1.34	2.54	2.64	2.59	2.41	2.52	2.50
1.42	2.44	2.55	2.49	2.29	2.42	2.39
1.50	2.35	2.47	2.41	2.19	2.33	2.29
1.59	2.26	2.40	2.33	2.09	2.24	2.21
1.67	2.19	2.33	2.25	2.00	2.16	2.13
1.75	2.11	2.27	2.18	1.92	2.09	2.06
1.83	2.05	2.21	2.12	1.85	2.03	1.99
1.92	1.99	2.15	2.06	1.78	1.97	1.93
2.00	1.93	2.10	2.00	1.72	1.91	1.87

$k(R2)'/k(R2)_{TSS}$	Stdrd	Var1	Var2	Var3	Var4	Var5
0.01	8.00	6.37	7.08	14.63	8.02	9.35
0.09	6.13	5.22	5.65	8.56	6.24	6.79
0.18	5.24	4.64	4.93	6.57	5.34	5.65
0.26	4.70	4.26	4.48	5.54	4.78	4.97
0.34	4.32	4.00	4.16	4.89	4.38	4.52
0.42	4.04	3.80	3.92	4.44	4.09	4.18
0.51	3.82	3.64	3.73	4.10	3.86	3.92
0.59	3.64	3.50	3.58	3.84	3.67	3.71
0.67	3.49	3.39	3.44	3.63	3.51	3.54
0.76	3.36	3.29	3.33	3.45	3.38	3.40
0.84	3.25	3.21	3.23	3.31	3.26	3.27
0.92	3.16	3.13	3.15	3.18	3.16	3.17
1.00	3.07	3.07	3.07	3.07	3.07	3.07
1.09	3.00	3.01	3.00	2.97	2.99	2.99
1.17	2.93	2.95	2.94	2.88	2.92	2.91
1.25	2.87	2.90	2.89	2.80	2.86	2.84
1.34	2.81	2.86	2.83	2.73	2.80	2.78
1.42	2.76	2.81	2.79	2.67	2.74	2.72
1.50	2.71	2.77	2.74	2.61	2.69	2.67
1.59	2.67	2.74	2.70	2.56	2.65	2.62
1.67	2.63	2.70	2.66	2.51	2.61	2.58
1.75	2.59	2.67	2.63	2.46	2.57	2.54
1.83	2.55	2.64	2.59	2.42	2.53	2.50
1.92	2.52	2.61	2.56	2.38	2.49	2.46
2.00	2.48	2.59	2.53	2.34	2.46	2.43

Table A15: Scaled Variations. Torque parameter sensitivity to CCT and CPT.

(for tables A15-A18 the data is sourced from tables A10-A14. The values for Variation 2, 3 and 4 are scaled so $\lambda_{TSS}=3.1$, as for the standard conditions)

$k(g3pACT)'/k(g3pACT)_{TSS}$	Stdrd	Var1	Var2	Var3	Var4	Var5
0.01	34.60	33.91	39.05	47.35	265.03	33.37
0.09	8.78	8.93	9.88	10.52	22.79	8.95
0.18	6.55	6.63	7.13	7.39	11.90	6.74
0.26	5.50	5.55	5.86	5.99	8.33	5.65
0.34	4.86	4.89	5.10	5.17	6.58	4.98
0.42	4.42	4.43	4.58	4.62	5.53	4.50
0.51	4.08	4.09	4.20	4.22	4.83	4.15
0.59	3.83	3.83	3.90	3.92	4.34	3.88
0.67	3.62	3.62	3.67	3.68	3.96	3.65
0.76	3.45	3.44	3.48	3.48	3.67	3.47
0.84	3.30	3.30	3.32	3.32	3.43	3.32
0.92	3.18	3.17	3.19	3.18	3.23	3.19
1.00	3.07	3.06	3.07	3.07	3.07	3.07
1.09	2.98	2.97	2.97	2.96	2.93	2.97
1.17	2.89	2.89	2.88	2.87	2.80	2.88
1.25	2.82	2.81	2.80	2.79	2.70	2.80
1.34	2.75	2.74	2.72	2.72	2.60	2.73
1.42	2.69	2.68	2.66	2.66	2.52	2.66
1.50	2.63	2.62	2.60	2.60	2.44	2.60
1.59	2.58	2.57	2.54	2.55	2.37	2.55
1.67	2.53	2.53	2.49	2.50	2.31	2.50
1.75	2.49	2.48	2.45	2.45	2.25	2.45
1.83	2.44	2.44	2.40	2.41	2.19	2.41
1.92	2.41	2.40	2.36	2.37	2.14	2.36
2.00	2.37	2.37	2.32	2.34	2.10	2.33

$k(PLA_2)'/k(PLA_2)_{TSS}$	Stdrd	Var1	Var2	Var3	Var4	Var5
0.01	14.71	13.42	23.90	27.38	169.46	16.44
0.09	10.64	10.10	14.41	15.72	24.94	11.72
0.18	8.47	8.16	10.42	11.12	13.79	9.17
0.26	7.09	6.89	8.22	8.64	9.68	7.55
0.34	6.10	5.98	6.82	7.10	7.54	6.44
0.42	5.38	5.30	5.85	6.04	6.22	5.63
0.51	4.81	4.77	5.14	5.27	5.34	5.01
0.59	4.37	4.34	4.60	4.69	4.69	4.51
0.67	4.02	4.00	4.16	4.22	4.21	4.12
0.76	3.72	3.71	3.81	3.85	3.83	3.79
0.84	3.46	3.46	3.52	3.54	3.53	3.51
0.92	3.25	3.25	3.28	3.28	3.27	3.27
1.00	3.06	3.06	3.07	3.06	3.06	3.07
1.09	2.90	2.90	2.88	2.87	2.89	2.89
1.17	2.75	2.75	2.72	2.70	2.73	2.73
1.25	2.62	2.62	2.58	2.56	2.60	2.59
1.34	2.51	2.51	2.46	2.43	2.48	2.46
1.42	2.40	2.40	2.35	2.31	2.38	2.35
1.50	2.31	2.31	2.25	2.21	2.29	2.25
1.59	2.23	2.22	2.16	2.11	2.21	2.16
1.67	2.15	2.14	2.07	2.03	2.13	2.07
1.75	2.07	2.07	2.00	1.95	2.07	1.99
1.83	2.01	2.00	1.93	1.88	2.00	1.92
1.92	1.95	1.94	1.86	1.81	1.95	1.86
2.00	1.89	1.88	1.81	1.75	1.90	1.80

Table A16: Scaled Variations. Torque parameter sensitivity to g3pACT and PLA_2.

$k(PLC)'/k(PLC)_{TSS}$	Stdrd	Var1	Var2	Var3	Var4	Var5
0.01	2.47	2.69	2.51	2.70	1.77	2.51
0.09	2.51	2.72	2.55	2.72	1.85	2.54
0.18	2.55	2.75	2.60	2.74	1.95	2.58
0.26	2.60	2.78	2.64	2.76	2.05	2.62
0.34	2.64	2.81	2.68	2.79	2.15	2.66
0.42	2.69	2.84	2.73	2.81	2.25	2.71
0.51	2.74	2.87	2.78	2.85	2.36	2.75
0.59	2.80	2.91	2.82	2.88	2.47	2.80
0.67	2.85	2.94	2.87	2.91	2.59	2.86
0.76	2.90	2.97	2.92	2.95	2.71	2.91
0.84	2.96	3.01	2.97	2.99	2.83	2.97
0.92	3.02	3.04	3.03	3.03	2.95	3.02
1.00	3.08	3.07	3.08	3.08	3.08	3.08
1.09	3.14	3.11	3.13	3.12	3.22	3.14
1.17	3.20	3.14	3.19	3.17	3.35	3.20
1.25	3.26	3.17	3.24	3.21	3.49	3.26
1.34	3.32	3.21	3.30	3.26	3.63	3.32
1.42	3.39	3.24	3.36	3.31	3.78	3.39
1.50	3.45	3.27	3.42	3.36	3.92	3.45
1.59	3.52	3.31	3.47	3.42	4.07	3.51
1.67	3.58	3.34	3.53	3.47	4.22	3.58
1.75	3.65	3.38	3.59	3.52	4.38	3.64
1.83	3.72	3.41	3.65	3.58	4.53	3.71
1.92	3.79	3.44	3.71	3.63	4.69	3.77
2.00	3.86	3.48	3.77	3.69	4.85	3.84

Table A17: Scaled Variations. Torque parameter sensitivity to PLC.

$k(ECT)'/k(ECT)_{TSS}$	Stdrd	Var1	Var2	Var3	Var4	Var5
0.01	2.60	1.34	2.33	2.07	6.15	2.25
0.09	2.63	1.55	2.40	2.15	5.70	2.34
0.18	2.66	1.75	2.47	2.23	5.29	2.42
0.26	2.70	1.93	2.54	2.31	4.94	2.50
0.34	2.74	2.09	2.61	2.39	4.63	2.57
0.42	2.78	2.25	2.67	2.48	4.35	2.65
0.51	2.82	2.39	2.73	2.56	4.10	2.72
0.59	2.87	2.52	2.80	2.65	3.88	2.78
0.67	2.91	2.65	2.86	2.73	3.68	2.85
0.76	2.95	2.76	2.91	2.82	3.51	2.91
0.84	3.00	2.88	2.97	2.91	3.35	2.97
0.92	3.04	2.98	3.02	2.99	3.20	3.02
1.00	3.08	3.08	3.08	3.08	3.08	3.08
1.09	3.12	3.17	3.13	3.16	2.96	3.13
1.17	3.16	3.26	3.18	3.25	2.85	3.19
1.25	3.20	3.34	3.22	3.33	2.76	3.24
1.34	3.24	3.42	3.27	3.41	2.67	3.29
1.42	3.28	3.49	3.31	3.50	2.59	3.33
1.50	3.32	3.56	3.36	3.58	2.52	3.38
1.59	3.36	3.63	3.40	3.66	2.45	3.42
1.67	3.39	3.69	3.44	3.73	2.39	3.47
1.75	3.43	3.75	3.47	3.81	2.33	3.51
1.83	3.46	3.81	3.51	3.89	2.28	3.55
1.92	3.49	3.86	3.55	3.96	2.23	3.59
2.00	3.53	3.92	3.58	4.03	2.18	3.63

$k(EPT)'/k(EPT)_{TSS}$	Stdrd	Var1	Var2	Var3	Var4	Var5
0.01	2.60	1.39	2.35	2.09	6.03	2.26
0.09	2.68	1.84	2.51	2.27	5.10	2.38
0.18	2.75	2.11	2.62	2.40	4.58	2.48
0.26	2.80	2.31	2.70	2.51	4.23	2.57
0.34	2.84	2.46	2.77	2.60	3.98	2.65
0.42	2.88	2.58	2.83	2.68	3.78	2.72
0.51	2.92	2.68	2.87	2.76	3.63	2.78
0.59	2.95	2.77	2.92	2.82	3.50	2.84
0.67	2.98	2.84	2.96	2.88	3.39	2.89
0.76	3.01	2.91	2.99	2.93	3.29	2.94
0.84	3.03	2.97	3.02	2.98	3.21	2.99
0.92	3.06	3.02	3.05	3.03	3.14	3.04
1.00	3.08	3.07	3.08	3.08	3.07	3.08
1.09	3.10	3.12	3.10	3.12	3.01	3.12
1.17	3.12	3.16	3.13	3.16	2.96	3.16
1.25	3.14	3.20	3.15	3.19	2.91	3.19
1.34	3.15	3.23	3.17	3.23	2.87	3.23
1.42	3.17	3.27	3.19	3.26	2.83	3.26
1.50	3.19	3.30	3.21	3.29	2.79	3.29
1.59	3.20	3.33	3.22	3.32	2.76	3.32
1.67	3.21	3.36	3.24	3.35	2.73	3.35
1.75	3.23	3.38	3.25	3.38	2.70	3.38
1.83	3.24	3.41	3.27	3.41	2.67	3.41
1.92	3.25	3.43	3.28	3.43	2.64	3.43
2.00	3.26	3.45	3.30	3.46	2.62	3.46

Table A18: Scaled variations. Torque parameter sensitivity to ECT and EPT.

	No feedback						
k'/k	**R1**	**R2**	**R6**	**R7**	**R16**	**R26**	**R29**
0.01	8.228	7.971	1.229	3.229	0.685	2.587	34.600
0.09	7.257	6.112	2.103	3.213	1.953	2.620	8.775
0.18	6.478	5.227	2.406	3.198	2.354	2.655	6.548
0.26	5.841	4.685	2.578	3.184	2.567	2.693	5.501
0.34	5.312	4.310	2.695	3.169	2.703	2.733	4.857
0.42	4.867	4.029	2.781	3.156	2.797	2.774	4.411
0.51	4.489	3.810	2.849	3.143	2.867	2.816	4.080
0.59	4.165	3.632	2.903	3.130	2.921	2.859	3.822
0.67	3.884	3.483	2.949	3.118	2.964	2.903	3.615
0.76	3.638	3.357	2.987	3.106	2.999	2.946	3.443
0.84	3.423	3.248	3.020	3.094	3.028	2.990	3.298
0.92	3.232	3.152	3.049	3.083	3.053	3.033	3.174
1.00	3.063	3.068	3.074	3.072	3.074	3.075	3.067
1.09	2.911	2.992	3.096	3.061	3.092	3.117	2.972
1.17	2.775	2.924	3.116	3.051	3.108	3.158	2.887
1.25	2.652	2.862	3.134	3.041	3.122	3.199	2.812
1.34	2.541	2.806	3.150	3.031	3.135	3.239	2.744
1.42	2.439	2.754	3.165	3.021	3.146	3.277	2.681
1.50	2.347	2.706	3.179	3.012	3.156	3.315	2.625
1.59	2.262	2.662	3.191	3.003	3.165	3.352	2.573
1.67	2.184	2.620	3.202	2.994	3.173	3.388	2.524
1.75	2.112	2.582	3.213	2.985	3.181	3.423	2.480
1.83	2.045	2.546	3.223	2.976	3.188	3.457	2.438
1.92	1.983	2.512	3.232	2.968	3.194	3.490	2.399
2.00	1.925	2.480	3.240	2.960	3.200	3.522	2.363

	Feedback R1(N,c_1=100), R2(N,c_1=100), R29(N,c_1=100), R16(I,c_1=100), R6(I,c_1=100)						
k'/k	**R1**	**R2**	**R6**	**R7**	**R16**	**R26**	**R29**
0.01	3.570	3.551	2.814	3.093	2.690	3.030	5.036
0.09	3.489	3.396	2.952	3.091	2.935	3.032	3.532
0.18	3.421	3.313	2.990	3.090	2.986	3.034	3.385
0.26	3.364	3.258	3.012	3.088	3.012	3.036	3.307
0.34	3.315	3.219	3.026	3.086	3.029	3.039	3.255
0.42	3.271	3.188	3.037	3.084	3.040	3.042	3.216
0.51	3.233	3.163	3.046	3.083	3.049	3.046	3.185
0.59	3.199	3.142	3.053	3.081	3.055	3.050	3.159
0.67	3.169	3.124	3.058	3.080	3.061	3.054	3.137
0.76	3.141	3.109	3.063	3.078	3.065	3.059	3.118
0.84	3.116	3.096	3.067	3.077	3.068	3.064	3.101
0.92	3.094	3.084	3.071	3.075	3.072	3.069	3.087
1.00	3.073	3.073	3.074	3.074	3.074	3.074	3.073
1.09	3.054	3.064	3.077	3.073	3.077	3.080	3.061
1.17	3.036	3.055	3.080	3.071	3.079	3.085	3.050
1.25	3.019	3.047	3.082	3.070	3.080	3.091	3.040
1.34	3.004	3.040	3.084	3.069	3.082	3.096	3.031
1.42	2.989	3.034	3.086	3.068	3.083	3.101	3.022
1.50	2.976	3.027	3.087	3.066	3.085	3.107	3.014
1.59	2.963	3.022	3.089	3.065	3.086	3.112	3.006
1.67	2.951	3.016	3.090	3.064	3.087	3.117	2.999
1.75	2.940	3.011	3.092	3.063	3.088	3.122	2.992
1.83	2.929	3.007	3.093	3.062	3.089	3.127	2.986
1.92	2.918	3.002	3.094	3.061	3.090	3.132	2.980
2.00	2.909	2.998	3.095	3.060	3.090	3.137	2.974

Table A19: Torque sensitivity analysis (selected reactions) with and without feedback.

	No feedback						
k'/k	**R1**	**R2**	**R6**	**R7**	**R16**	**R26**	**R29**
0.01	51.77	53.07	12.85	103.58	25.75	82.47	29.36
0.09	56.99	64.50	42.24	102.87	68.65	84.39	86.95
0.18	61.92	71.61	58.14	102.18	79.69	86.13	97.84
0.26	66.54	76.69	68.16	101.50	85.03	87.71	100.99
0.34	70.87	80.58	75.08	100.84	88.21	89.13	101.77
0.42	74.91	83.71	80.16	100.20	90.34	90.40	101.61
0.51	78.68	86.32	84.04	99.57	91.86	91.54	101.04
0.59	82.18	88.53	87.12	98.95	93.01	92.56	100.29
0.67	85.43	90.44	89.61	98.35	93.91	93.46	99.45
0.76	88.44	92.13	91.68	97.77	94.63	94.26	98.59
0.84	91.24	93.62	93.41	97.19	95.22	94.97	97.73
0.92	93.84	94.96	94.90	96.63	95.71	95.59	96.88
1.00	96.25	96.18	96.18	96.07	96.13	96.14	96.06
1.09	98.49	97.28	97.30	95.53	96.49	96.62	95.26
1.17	100.57	98.30	98.28	95.00	96.81	97.05	94.49
1.25	102.50	99.23	99.16	94.48	97.08	97.42	93.75
1.34	104.31	100.10	99.94	93.97	97.32	97.74	93.03
1.42	105.99	100.90	100.64	93.47	97.54	98.03	92.34
1.50	107.57	101.65	101.27	92.98	97.73	98.28	91.68
1.59	109.04	102.36	101.85	92.49	97.91	98.50	91.03
1.67	110.42	103.02	102.37	92.02	98.07	98.69	90.41
1.75	111.72	103.64	102.85	91.55	98.21	98.85	89.81
1.83	112.93	104.23	103.29	91.09	98.34	99.00	89.23
1.92	114.08	104.78	103.70	90.64	98.46	99.12	88.67
2.00	115.16	105.31	104.08	90.19	98.57	99.23	88.12

	Feedback R1(N,c_1=100), R2(N,c_1=100), R29(N,c_1=100), R16(I,c_1=100), R6(I,c_1=100)						
k'/k	**R1**	**R2**	**R6**	**R7**	**R16**	**R26**	**R29**
0.01	39.37	41.82	14.70	103.91	46.04	78.78	26.13
0.09	49.75	61.15	45.01	103.15	73.63	81.05	106.40
0.18	58.11	70.87	59.69	102.40	81.29	83.18	109.86
0.26	64.99	77.00	68.88	101.68	85.45	85.15	109.09
0.34	70.72	81.32	75.30	100.97	88.15	86.96	107.46
0.42	75.58	84.58	80.08	100.29	90.07	88.61	105.68
0.51	79.75	87.16	83.82	99.62	91.52	90.10	103.95
0.59	83.36	89.27	86.82	98.97	92.66	91.43	102.33
0.67	86.52	91.03	89.30	98.33	93.57	92.61	100.83
0.76	89.32	92.54	91.38	97.71	94.33	93.64	99.45
0.84	91.81	93.85	93.16	97.10	94.97	94.55	98.17
0.92	94.05	95.00	94.69	96.50	95.51	95.33	96.99
1.00	96.07	96.02	96.03	95.92	95.98	96.00	95.89
1.09	97.91	96.93	97.22	95.35	96.40	96.56	94.87
1.17	99.60	97.75	98.27	94.80	96.76	97.04	93.92
1.25	101.14	98.50	99.21	94.25	97.08	97.43	93.03
1.34	102.57	99.18	100.06	93.72	97.37	97.76	92.20
1.42	103.89	99.81	100.83	93.19	97.62	98.02	91.41
1.50	105.12	100.38	101.53	92.68	97.86	98.22	90.67
1.59	106.27	100.92	102.17	92.17	98.07	98.38	89.96
1.67	107.35	101.41	102.76	91.68	98.27	98.49	89.30
1.75	108.36	101.87	103.30	91.19	98.44	98.57	88.67
1.83	109.31	102.31	103.81	90.71	98.61	98.61	88.06
1.92	110.21	102.71	104.27	90.24	98.76	98.63	87.49
2.00	111.06	103.09	104.70	89.78	98.90	98.62	86.94

Table A20: Total lipid sensitivity analysis (selected reactions) with and without feedback.